Impact of CO_2 and humidified air on micro gas turbine performance for carbon capture

Thom Munro Gray Best

Submitted in accordance with the requirements for the degree of Doctor of Philosophy

The University of Leeds

Doctoral Training Centre in Low Carbon Technology

Energy Research Institute

School of Chemical and Process Engineering

September 2016

The candidate confirms that the work submitted is his own, except where work which has formed part of jointly authored publications has been included. The contribution of the candidate and the other authors to this work has been explicitly indicated below. The candidate confirms that appropriate credit has been given within the thesis where reference has been made to the work of others.

Parts of Chapters 3, and 4 in the thesis are based on work as follows which has either been published in academic journals or was presented as part of conference proceedings:

Best, T., et al., *Gas-CCS: Experimental impact of CO_2 enhanced air on combustion characteristics and Microturbine performance,* Oral presentation to the CCS International Forum in Athens, CO2QUEST, March 2015.

Best, T., et al., *Impact of CO_2-enriched combustion air on micro-gas turbine performance for carbon capture.* Energy, 2016. Tbc (Accepted Awaiting Publication date). [1]

Best, T., et al., *Exhaust gas recirculation and selective Exhaust gas recirculation on a micro-gas turbine for enhanced CO_2 Capture performance.* The Future of Gas Turbine Technology 8th International Gas Turbine Conference, 2016.[2]

In each of the jointly authored publications the candidate was the lead author and responsible for all experimental data collection, processing, analysis and evaluation. Dr Karen Finney was also involved for data collection, other co-authors provided modelling processing, results and analysis. Or supervisory support.

As co-author the candidate also provided experimental data collection, processing, analysis and evaluation for the following papers:

Agbonghae, E.O., et al., *Experimental and Process Modelling Study of Integration of a Micro-turbine with an Amine Plant.* Energy Procedia, 2014. 63: p. 1064-1073 [3]

Ali, U., et al., *Process Simulation and Thermodynamic Analysis of a Micro Turbine with Post-combustion CO_2 Capture and Exhaust Gas Recirculation.* Energy Procedia, 2014. 63: p. 986-996. [4]

Akram, M., et al., *Performance evaluation of PACT Pilot-plant for CO_2 capture from gas turbines with Exhaust Gas Recycle.* International Journal of Greenhouse Gas Control, 2016. 47: p. 137-150. [5]

Ali, U., et al., *Benchmarking of a micro gas turbine model integrated with post-combustion CO_2 capture.* Energy, 2016. Submitted In Review. [6]

Finney, K.N., et al., *CFD of Selective Exhaust Gas Recirculation On Micro-Gas Turbines For Enhanced CO_2 Capture Performance* ASME, 2016. Turbo Expo 2017 [7]

ACKNOWLEDGEMENTS

This work was carried out thanks to funding from the Engineering and Physical Sciences Research Council (EPSRC) via the Doctoral Training Centre in Low Carbon Technologies at the University of Leeds.

Thanks to my supervisors, Dr. Karen Finney, Professor Mohamed Pourkashanian, and Professor Derek Ingham for their guidance and support. Karen, thanks for your enthusiasm, structure and guidance; Mohamed, for your in depth knowledge and opportunities you provided, and Derek for your patience.

Thanks to Martin Murphy for all his technical support making the experiments possible.

Thanks to my colleagues of the Doctoral Training Centre in Low Carbon Technologies – for support writing up Ray Edmonds, Zarashpe Kapadia, Ramzi Cherad, Katrina Adams, and Clare Linton, and to all my colleagues for making the DTC a memorable time. Thanks to a friend many of us will miss, for all the good memories.

Thanks to the Management Committee of the Doctoral Training Centre, Professor Paul Williams, James McKay, Rachael Brown and Emily Bryan-Kinns.

Most importantly thanks to all of my ***family*** whose ongoing support I will never be able to express how much I appreciate.

ABSTRACT

There is overwhelming evidence for anthropogenically driven climate change and as such it is critical to reduce the emissions of greenhouse gases. A large source of these is combustion for energy.

Combined Cycle Gas Turbine (CCGT) power generation is going to be a significant part of the future of base power load generation in the UK and internationally. The CO_2 emissions of gas turbines are significantly lower than coal, but must still be addressed.

Gas exhaust emissions also present a challenge due to the low volume percentage of CO_2 in the exhaust, as the current most mature technology for carbon capture is post combustion capture using solvents, which is significantly more efficient with higher CO_2 partial pressures.

This thesis looks at potential ways to increase CO_2 partial pressure in the gas turbine exhaust for improved capture efficiency. To do this exhaust gas recirculation (EGR), and humidified air (HAT) or a combination could be beneficial. There is a lack of bench and pilot scale experimental research into this area. A Turbec T100 Microturbine was used to investigate the impacts of EGR and HAT, through the addition of CO_2 and Steam before the combustor.

In addition the turbine particulate emissions were analysed. This is as gas combustion has high emissions of fine particulate matter. Particulates are of increasing consideration as an environmental pollutant, and may contribute to solvent degradation.

The investigations found that the performance of the turbine is largely dependant upon ambient temperature. The results matched with the literature showing impact on the combustion process reducing peak temperatures, and an increase in unburned hydrocarbons, and carbon monoxide. This resulted in a slightly reduced generation efficiency. However this loss in turbine efficiency is potentially superseded by a gain in capture efficiency and net CCGT low carbon generation with carbon capture and storage.

1 TABLE OF CONTENTS

LIST OF TABLES

LIST OF FIGURES

NOMENCLATURE

CCS	Carbon Capture & Storage
CHP	Combined Heat & Power
EGR	Exhaust gas recirculation
FEED	Front End Engineering Design
HAT	Humidified Air Turbine
HHV	Higher Heating Values
LHV	Lower Heating Value
MEA	Monoethanolamine
NOx	Oxides of nitrogen (NO and NO_2)
PACT	Pilot-scale Advanced Capture Technology
PT	Pressure transducer
RPM	Revolutions Per Minute
TC	Thermocouple
TIT	Turbine Inlet Temperature
TOC	Total organic carbon
TOT	Turbine Outlet Temperature
UHC	Unburnt Hydrocarbon
UKCCSRC	UK Carbon Capture Storage Research Council

1 Introduction

1.1 Climate Change

Since the industrial revolution human activities have been releasing greenhouse gas emissions and removing natural carbon sinks but the pace of which has increased from the mid twentieth century. At this point, atmospheric concentration increases became more apparent, and a related change in climate has been recorded. The rise in the average global temperatures is an anthropogenic climate change.

The greenhouse gases released cause an increase in the radiative forcing in the Earth‘s atmosphere, an increase in the amount of radiative energy absorbed from the sun, this is the balance of energy coming in and leaving, with a positive effect on the radiative forcing leading to warming. Different gases released by human activities, such as CO_2 and methane, cause varying degrees of radiative forcing, and remain in the atmosphere for different periods of time. For these reasons, greenhouse gases are rated according to their Global Warming Potential (GWP) which takes account of these variations. Carbon dioxide does not have a particularly high global warming potential but due to the quantity emitted, and the difficulty in providing alternatives to its source, it is vastly the most significant GHG, and hence the focus of much attention, the significant increase in atmospheric concentration and corresponding radiative forcing is clear in Figure 1-1 Radiative forcing of CO2 7,995 BC – 2005AD [8].

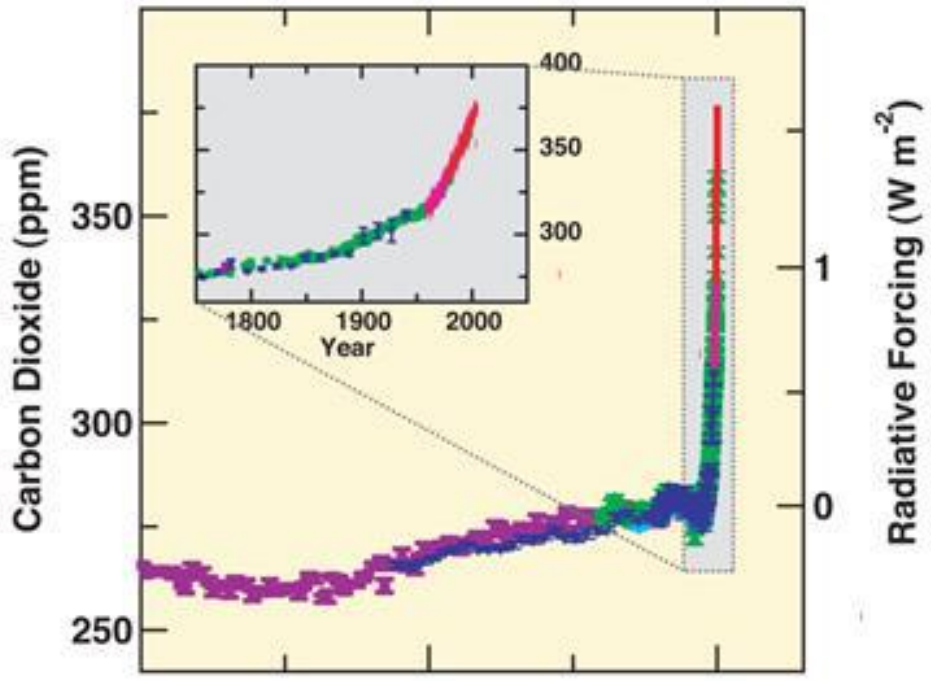

Figure 1-1 Radiative forcing of CO_2 7,995 BC – 2005AD [8].

The atmospheric concentration of CO_2 recently peaked at over 400ppm, [9] the highest recorded in over 650,000 years, as evidenced through ice cores, the levels have been increasing at an ever higher rate, only slowing since the middle of the last century through periods of economic recession [8].

The high levels of greenhouse gas and positive impact on radiative forcing, it is believed, with a very high certainty, to have contributed to most of the increase in the rate of warming in the last 4 decades. Global average temperatures have risen on average by 0.074°C per decade between 1901 and 2010, but at even more than double that of the average between 1979 to 2010 at 0.169°C per decade, with the northern hemisphere warming at a rate of 0.241°C per decade during this period[10].

This increasing temperature is a major concern due to the potential impact on sea levels, fresh water, crops and extreme weather events. This increases the pressures on plants and animals adaptability to temperature rise mean that 20-30% of the species assessed are at increased risk of extinction [11].

There is, and will be an increasingly significant human cost to the anthropogenic alteration of climate. The World Health Organisation in particular has highlighted concerns with heat-related mortality, coastal flood, diarrhoeal disease, malaria, denghue and malnutrition causing increased fatalities. [12]

All of these affects are as a result of the current warming up of the earth to what is very likely to exceed a 2°C rise this century, on the pre-industrial average global temperatures.

Currently, the rate of greenhouse gases being released in to the atmosphere, and hence the increase in the radiative forcing, puts the probable temperature rise of the Earth by the end of the century to be closer to 6°C over pre-industrial averages. The impacts of this could be catastrophic, with up to one third of Africa experiencing huge crop reductions, and sea levels threatening cities such as Shanghai, New York, London, Tokyo, Hong Kong etc. Partial collapse of the Amazonian rainforest, up to 50% of species are facing extinction, increased risk of extreme weather, in the form of hurricanes, fires, flooding drought etc. As well as a significantly higher risk of sudden change in key climate systems, such as the Atlantic thermohaline circulation [13].

1.2 Emission Sources

The significance of energy supply emissions can be seen in the Greenhouse gas emissions statistics released by DECC [14]. Seen in Table 1-1 UK GHG emissions 1990-2012 energy supply is the primary contributor, with transport being a noteworthy second, a sector that along with others could be more easily decarbonised using alternative low carbon technologies, the legitimacy of which depends upon the provision of electricity from a decarbonised grid.

Table 1-1 UK GHG emissions 1990-2012 [15]

							$MtCO_2e$
	1990	1995	2000	2005	2010	2013	2014
Energy Supply	277.9	237.9	220.9	231.0	206.7	189.5	163.8
Transport	121.9	122.2	126.7	130.4	120.1	116.6	117.9
Business	115.4	113.4	116.8	109.9	94.9	90.9	88.5
Residential	80.1	81.7	88.7	85.7	87.6	77.3	64.2
Agriculture	58.7	58.1	54.6	50.9	48.3	48.1	49.1
Waste Management	68.8	71.0	66.5	52.1	29.9	21.1	18.8
Industrial Process	60.0	50.9	27.2	20.6	12.7	13.0	13.0
Public	13.5	13.3	12.1	11.2	9.7	9.5	8.1
LULUCF	0.3	-0.1	-2.9	-5.5	-7.8	-8.6	-9.0
Total	**796.6**	**748.5**	**710.6**	**686.3**	**602.1**	**557.3**	**514.4**

With 31% of the GHG emissions coming from supply, and an additional 23% from transport that could be electrified, it is clear that it is impossible to reduce greenhouse gas emissions 80% from 1990 levels by 2050, as mandated by the UK 2008 Climate Change Act, without making huge reductions in the energy supply of emissions.

The National Grid facilitates and coordinate energy supplies in the UK; looking at the Gone Green 2011 report from the same year as the emission figures gives the carbon intensity of the grid as 500gCO_2/kWh, with projections that this will be 48gCO_2/kWh by 2030. This is approximately in line with the fourth carbon budget, set in 2011 for the period 2023 – 2027, which states that the grids carbon intensity should be 50gCO_2/kWh in order for the budgets overall greenhouse gas emissions target, which has been voted into law, is to be met [16] [17]. It is estimated that an increase in generating capacity of 30 – 40GW of low carbon generation will allow the carbon intensity target and the increases in demand to be met as Figure 1-2 National Grid predicted energy mix to 2030 [16][18].

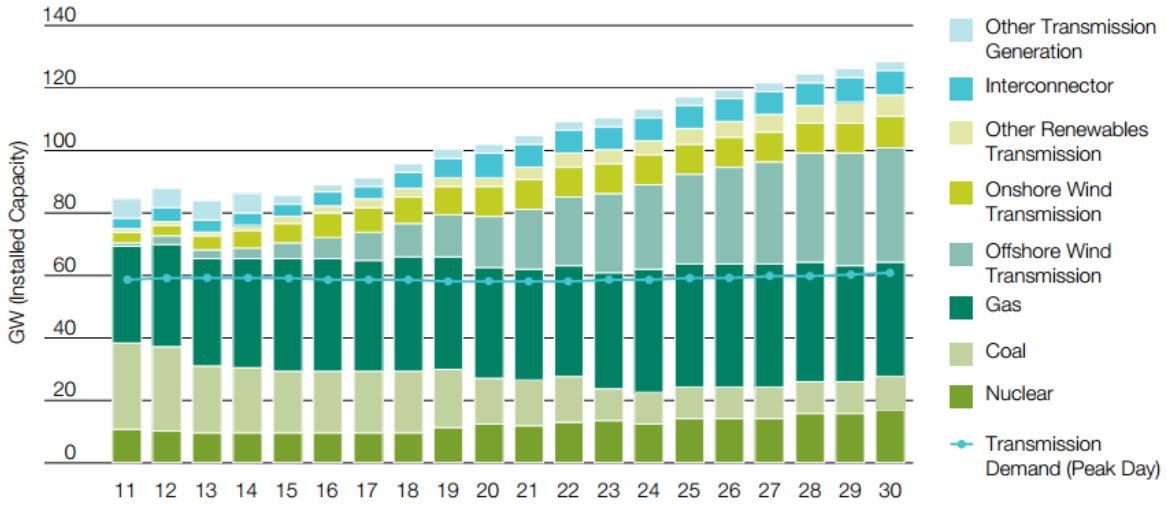

Figure 1-2 National Grid predicted energy mix to 2030 [16]

This reduction in carbon intensity of power generation must be met with alternative technologies. Stringent European legislation, in the form of the Industrial Emissions Directive, which encompasses Medium Combustion Plants, already makes many current coal plants less economically competitive due to penalties on SO_x, NO_x and particulate emissions, that new plants would have to have expensive facilities to treat, that gas does not require [19]. The carbon intensity of unabated coal is also much too high at 920gCO_2/kWh, and even gas at 400gCO_2/kWh means that they cannot play a large part in a decarbonised grid with a carbon intensity of 0-50gCO_2/kWh, to make up the shortfall with lower emission technologies such as Carbon Capture storage must be employed [20].

1.3 Emissions Reduction

For these reasons it is critical to reduce the global emissions of greenhouse gases, and this was recognised internationally at the Rio Earth Summit in 1992, the outcome of which was further discussions and the drawing up of an agreement in 1997, namely with the Kyoto Protocol. Although successful as a starting point, with the aim to reduce emissions to 95% of what they were in 1990 which was established as the baseline year. Moreover the protocol wasn‘t ratified

until 2005, and has now expired, it had a number of key exemptions, particularly with no targets for developing nations, whose emissions have grown at the fastest rates, and it was never ratified by the largest emitter, the United States. Unfortunately the targets were also insufficiently ambitious in their levels of reduction, with the aim to reduce global emissions by 5% not being sufficient to avoid warming of 2°C by 2100 [21].

In 2008, the UK introduced the first legally binding framework to reduce domestic GHG emissions by 80% by 2050 on a territorial basis This is a significant piece of legislation, and impacts heavily on the future direction of UK power generation due to the carbon intensive nature of the energy supply [22].

1.4 Electrification

In conjunction with the need to decarbonise the current generating power in the UK, there is also a significant additional requirement to meet an increased energy demand attributable not only to economic growth but also to the electrification of transport, industry, and properties. If these areas are not electrified then it is impossible to meet the UK‘s climate change act GHG with a reduction of 80% by 2050 as they currently account for nearly half of the UKs emissions [22].

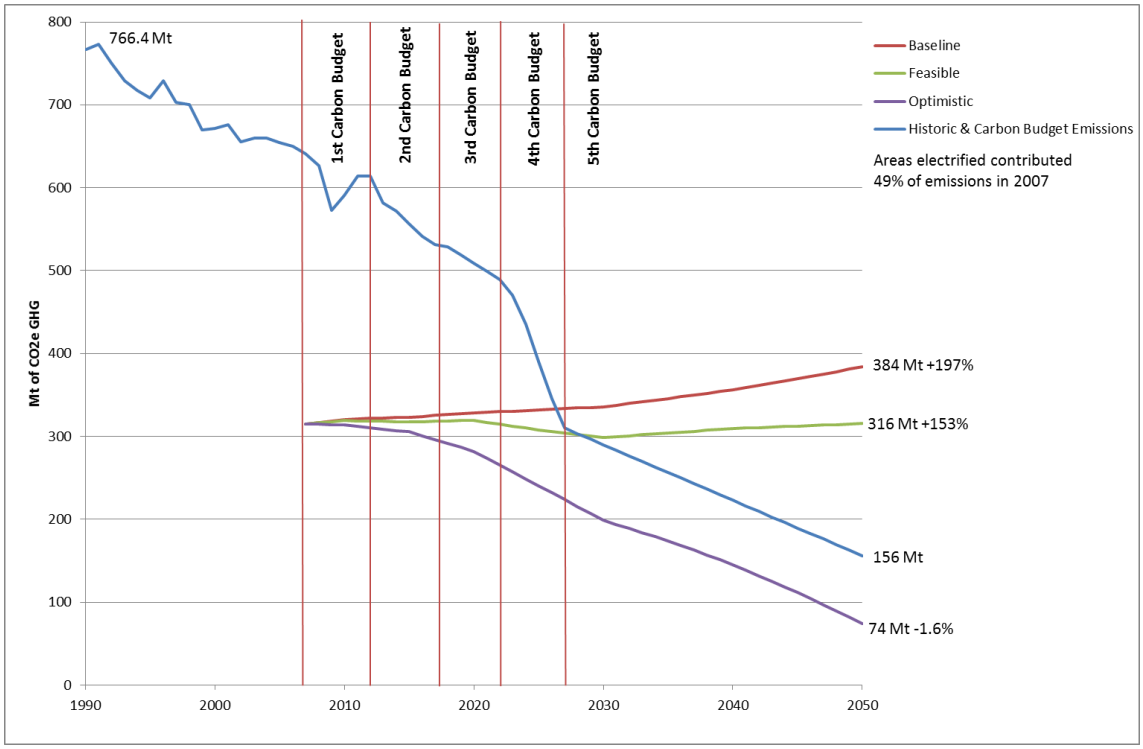

Figure 1-3 Current UK emissions total, and areas that could be electrified in context of the Climate Change Act and Carbon Budgets.

Looking at the emissions trends in Figure 1-3 Current UK emissions total, and areas that could be electrified in context of the Climate Change Act and Carbon Budgets.from the DECC 2050 Pathways Calculator, under the Governments baseline scenario under which no action is taken, and the country carries on as normal, then the GHG emissions rise and the reduction targets will all be missed. Ignoring changes in peoples behaviour and focusing on industry adapting to meet changes in demand in a carbon constrained manner, then only the most optimistic of assumptions allows the GHG reduction targets to be met. These assumptions rely on the national grid being decarbonised, thus necessitating Carbon Capture Storage roll out, and this shows that without it, then the targets are unachievable.

A decarbonised grid, with CCS playing a significant role, would have the potential to further significantly increase the capacity to meet the higher demands that could be expected from electrification of other sectors to assist in the net reduction in GHG emissions. Providing that the

capacity for the further electrification of heating, cooling, cooking and electric transport, will make them genuine low carbon alternatives. This increased low carbon generation is particularly important for decarbonising transport. Global CO_2 produced from transport is 6,755.8 $MtCO_2$, which is more than 20% of the total global emissions, a number similar in scale to all the heat and electricity CO_2 emissions from developing nations. The potential for decarbonising this sector is huge, whether this is achieved through electrification or the use of hydrogen, the source of this energy will be stationary, the increase in electricity demand that this will create is likely to still come from carbonaceous fuels creating a potential increase in the emissions, or the potential additional opportunity for a growth in CCS to decarbonise other sectors indirectly [23].

1.5 Accumulated Emissions

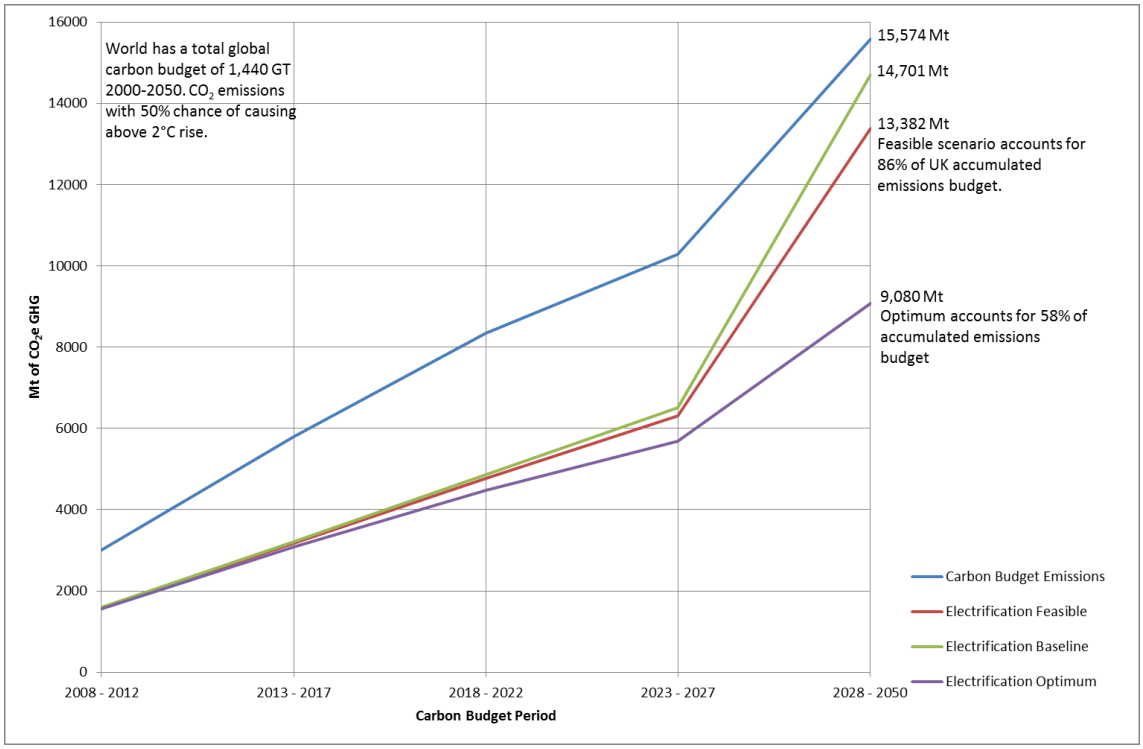

Figure 1-4 Accumulated UK emissions pathways

Beyond the climate change acts legislated reduction, it is the necessary to consider where these reduction targets come from.

The UK aims to contribute its share of emissions cuts as part of a global attempt to reduce them and give a 50% chance of avoiding an average global temperature rise of 2°C by 2100, this in truth is probably optimistic. [24]

However to do this, the global concentration of CO_2 must be controlled with consideration to its atmospheric lifespan and the amount of time it would take for sinks, such as the oceans and plant growth, to consume carbon dioxide and there will be net reductions in the atmospheric concentration. This means simply providing a step change in GHG emissions close to 2050 to meet the target in the manner in which it has been legislated, would not have contributed the net reduction of 42 years‘ worth of consistent cuts.

If it is assumed that the UK can continue to take a global share of the net emissions that it did in 1990, the baseline for most targets originating from the Kyoto agreement, this would give an allowance of 15,574MT of CO_2 equivalent emissions when taken in conjunction with the carbon budgets as recommended by the climate change committee [25, 26].

In 2007, power generation, and all possible sectors with potential to be electrified accounted for 47% of the UKs GHG emission total. However these emissions can be avoided, as Figure 1-4 Accumulated UK emissions pathways using DECCs pathway analysis even with the most optimistic roll out of all low carbon technologies, and with CCS playing a more significant part than it is projected by any current body then the sectors would still consume 58% of this allowance.

1.6 Low Carbon Technologies

The realistic alternatives for zero carbon generation are nuclear and wind power, with significant contributions possible from solar and tidal sources.

On the microscale decentralised generation front there has been significant uptake of solar over the last 5 years, having seen costs drop dramatically the technology has become very competitive. In 2013 DECC forecast there would be 10GW of installed capacity by 2020, this

was already achieved in early 2016, with 20GW now a realistic possibility by that date, despite reductions in subsidies. [27] The true TWh generated per year though is variable and not flexible to meeting demand due to its nature.

The UK has the best wind resource in Europe, and this could potentially generate up to 26% of its power from wind farms both on and offshore, with a manageable installation rate of 2GW by 2024. The actual power potential offshore is huge, with more than 4,500 TWh; the annual UK power consumption is approximately 360TWh. The main issue with wind power is that the intermittent nature of the supply does not match the patterns of demand [28] [29].

In addition to the best wind resources in Europe, the UK also has the largest available potential tidal energy sources, capable of providing large scale reliable, predictable generation competitively with other low carbon technologies such as nuclear agreed strike prices over the long term. [30, 31] A number of large potential generation sites are spread throughout the UK from the Orkney Isle's to the Severn Estruary, both potentially over 1GW each, DECC estimates up that the UK has potential to have up to 27GW of installed capacity by 2050. [27]

Nuclear can supply large power demands reliably. However it is extremely controversial, and depending on which account you read the costs range from between comparatively economic with coal and gas, and many multiples more. Also it is difficult for traditional nuclear to be flexible in its output to meet the peaks in the national power demand.

Coal and gas have the advantage of being able to meet demands as and when necessary and to ramp up supply at relatively short notice. This is a significant advantage, and although gas has been traditionally volatile in price, the prospect of increased energy supply from shale may result in more consistent pricing of energy.

There are also additional political energy security issues surrounding supply. Currently coal and gas is imported. Having the capacity to generate energy from domestic supplies of coal or gas,

if necessary, is advantageous as power stations take years to build and last decades, it is difficult to predict political situations this far in advance.

Beyond the UK it must be considered that coal and gas provide the majority of the world's energy, and climate change is a global issue that cannot be simply tackled by one nations actions. Altering domestic supply to nuclear and wind would not resolve the emissions made in developing nations such as China, Brazil, India, etc. whose power supply is dominated by coal, and this is increasingly so.

Already developing (Non-Annex I Parties exempt from emissions control) produce more CO_2 for electricity and heat than developed nations, namely 6.954GtCO_2 of global total of 12.48GtCO_2. Coal and gas accounts for 43% and 36% of the fuel emissions, and there was a growth in coal CO_2 emissions of 4.9% to 13.1Gt globally. This is predicted to rise to 15.3Gt by 2035 if the energy mix is not diversified and abatement measurements are not introduced. However the potential outlook with CCS is much brighter, with a predicted reduction to 5.6GtCO_2 [20, 23].

There needs to be a solution to mitigate the emissions of power stations where there is a certain carbon lock in once they are built due to their life span, and the economic value meaning they are extremely unlikely to be closed before the end of their useful life.

This breakdown of emissions sources and the important consideration of the impact of accumulation is intended to depict the critical need for CCS [14]. It also highlights that with large scale implementation other emission sectors could be electrified allowing the UK to achieve a national reduction of 80%. Without CCS it will simply not be possible to meet national or global emissions targets which are based on the premise of avoiding a 2C global temperature rise or more that would cause avoidable long term and catastrophic impacts for people and the environment.

1.7 Capital Driven Fossil Fuel Consumption

The challenges of decarbonisation are not just technical, physical, and policy based but financial. Meinshausen et al.[25] in 2009 estimated that the planet could absorb an additional 1,440$GtCO_2$ between 2000 and 2050 and still have a 50% chance of not exceeding a 2°C warming this century above pre industrial temperatures. Between 2000 and 2011, an estimated 321$GtCO_2e$ emissions were released with emissions growing year on year. If it is considered that there are believed to be fossil fuel reserves equivalent to at least 2,795 $GtCO_2$, it is clear that they cannot all be extracted and used either without almost certainly causing unacceptable warming or without being mitigated with technologies, such as carbon capture storage [25, 32].

In 2004, Shell announced to the market it had overestimated its reserves by 20%, and within days the companies‘ shares fell by 10%, or £3billion.

The largest 100 coal, oil and gas companies have a combined net worth of over $7.42 trillion, a price based on their proven and partially unproven reserves. If only 1,119$GtCO_2e$ of the known 2,795$GtCO_2$ were used then this would be a loss of 60% of their assets, and if this was reflected on the markets it would be a loss of $4.452 trillion. This would be a significant loss that would severely affect the market, pensions and jobs, and is a huge pressure and incentive for countries and economies to continue to extract the value that they can from fossil fuels [32]. This kind of pressure may necessitate a pragmatic solution, such as that which can be offered by carbon capture and storage.

Carbon Capture and Storage is an energy solution that can potentially abate the installed capacity of emissions, allow developing nation‘s power needs and new infra-structure, and allow for the utilisation of carbonaceous fuel assets whose economic value means it is unlikely they will not be utilised, without contributing to climate change.

This all means strong incentive and pressure groups against abandoning fossil fuels.

1.8 Research Objectives

Due to the critical need for CCS highlighted, this research aims to contribute to overcoming some of the barriers for combined cycle gas turbines with post combustion amine capture due to the energy intensive process of solvent regeneration. The intention is to build upon the understanding of Exhaust Gas Recirculation (EGR) and Humidified Air Turbines (HAT), so it may be applied to improve the net process efficiency of Combined Cycle Gas Turbine (CCGT) systems through demonstration of the enhancement technologies at a pilot scale. This was done through adaptation and experimentation with micro gas turbines.

The study aims to:-

1. Establish the base performance of the turbines for relative comparison
2. Investigate what impact does EGR have on turbine combustion emissions
3. Determine what the EGR emissions indicate about combustion performance
4. Determine the impact of EGR on the mechanical performance of the turbine and net efficiency
5. Investigate what impact HAT has on the turbine combustion emissions
6. Determine what the HAT emissions indicate combustion performance
7. Determine the impact of HAT on the mechanical performance of the turbine and net efficiency
8. How these changes may impact post combustion capture efficiency through increased exhaust CO_2 partial pressures
9. Investigate what particulate emissions can be expected from gas turbine combustion
10. Determine the impact of EGR on particulate distribution

Of particular focus throughout is the emissions increase in CO_2 vol% for improved capture efficiency.

1.9 Thesis Structure

The research in the thesis is presented as below:

Chapter One is an introduction to climate change, emission sources, fossil fuel dependence, and the therefore critical importance of CCS to address the issues.

Chapter Two reviews the literature of experimental & modelling studies into EGR, HAT and particulate emissions. It then highlights the areas for further research that the thesis explores.

Chapter Three explains the experimental set up for the gas turbine investigations, measurement with FTIR and paramagnetic analysers, and establishes a base performance for comparison of results.

Chapter Four covers the adaptation of Low Carbon Combustion Centre facilities and turbine for additional measurement and alteration of oxidising air composition. EGR is then simulated using CO_2 fed into the compressor. The results from changes in mechanical performance, emissions, and specific fuel combustion are then analysed.

Chapter Five covers further adaptation to allow humidification of the air post compression using steam rendered from a separate boiler. The results from changes in mechanical performance, emissions, and specific fuel combustion are then analysed.

Chapter Six covers the need for further investigation into particulates impact on post combustion capture, and how particulate size distribution, measured using a DMS500 analyser, may be altered by the addition of technologies designed to improve CCS such as EGR.

Chapter Seven is a discussion and summary of findings.

Chapter Eight discusses experimental limitations and makes recommendations for future work

2 Carbon Capture and Storage

2.1 What is Carbon Capture and Storage

There has been significant investigation into developing a commercial carbon capture and storage project.

Until late 2015 there were two commercial UK bids for £1 billion of grant funding to demonstrate CCS on a large plant. The preferred bid project in Peterehead was to capture emissions from a combined cycle gas turbine power plant using post combustion capture. This would have been a very similar process to that researched in this thesis, with the potential of exhaust gas recirculation (EGR) and humidified air (HAT) technologies being applied to the system.

2.1.1 Peterhead

The SSEs combined cycle gas power plant is based at Peterhead, and is in collaboration with Shell was named as a preferred bidder for the government grant to develop a CCS demonstration project. The project is to use post combustion capture to prevent 90% of one of the 385MW turbines emissions and transport them to the Goldeneye gas field operated by Shell in the Northern basin. [33]

The Goldeneye project pipes gas to St Fergus, 7.5km north of the SSE plant, and the Goldeneye site itself is connected to the shore via a 105km pipeline. If the plant produces emissions of 400gCO2/kWh [20] then the plant emissions per annum may be assumed to be 1,349,040 TCO2, at 90% capture this is 1.21MTCO_2. The *Element Energy* and the European Commission Directate-General Energy, studies show significant suitable storage capacity. [34, 35]

2.1.2 White Rose

The White Rose project was a proposed 426MW oxyfuel coal power plant based at the Drax power station with the ability to cofire with biomass and the plant would capture about 90% of the emissions approximately 2 $MTCO_2$ per annum. The Inside Drax 2011 annual report reports emissions of 760 tonnes per GWh in 2011, extrapolating 426MW is approximately 3,731 GWh therefore 2.835MT and at 90% capture 2.55$MTCO_2$ per annum would be captured. The lower estimated figure from the White Rose project site may be accounted for due to a higher biomass mix, or energy dense quality of coal. [36, 37]

The project lies 80km from the coast, looking at the projected pipelines and storage sites there are a number of possible injection sites for the depleted gas reservoirs in the Southern North Sea basin.

2.2 Capture Techniques

There are a number of potential carbon capture and storage technologies. The focus of this thesis, EGR and HAT technologies is for the development of post combustion capture systems.

2.2.1 Pre Combustion Capture

Pre-combustion capture is the removal of CO_2 before combustion takes place. This can be achieved by creating a syngas with the carbon removed and then burning this fuel in a nitrogen atmosphere or with steam.

In comparison to a conventional gas or coal plant, a pre-combustion plant has the additional energy impingements of an air separation unit (ASU), the reformation of fuel to a syngas and then to hydrogen, and CO_2 separation and compression for storage.

The natural gas is pressurised and preheated and it is introduced in to a pre-reformer where long chain hydrocarbons are reduced down to methane with the introduction of steam and this creates H and CO, then CH_4 H_2O. After this the off gases are then cooled for steam reformation to create CO_2 from the CO, and pressurised for transport ***[38].***

The process of pre combustion can also be applied to coal in Integrated Gasification Combined Cycle plants where the coal is gasified to create a syngas for combustion.

2.2.2 Oxyfuel

Oxy-fuel substitutes some of the air with oxygen for combustion. It is derived from an air separation unit, with the remaining mass flow made up from flue gas being recirculated which also assists in the control of the temperature to within metallurgical constraints due to the higher combustion temperature of the pure oxygen than air. Using oxygen to oxidize the fuel for combustion, instead of air, results in a huge increase in the CO_2 concentration in the exhaust flue gases. This results in exhaust CO_2 being easier to separate, compress without absorption as post combustion capture, and hence there is no high energy penalty for the solvent regeneration. [39, 40]

2.2.3 Post Combustion Capture

Post combustion capture of CO_2 is seen with oxyfuel as the most promising technology for the commercial role out of CCS, and it is likely to be the most flexible option for retrofitting to existing power stations in order to assist in `negating “carbon lock in”.

2.2.3.1 Adsorption

Adsorption is the physical process of CO_2 attaching to a solid surface. Once the adsorbent is saturated with CO_2, it is then regenerated either through heating or a shift in the pressure, called the pressure swing adsorption, PSA [41].

Activated carbon and zeolites are the ideal mediums for CO_2 capture. However they are not sufficiently selective to treat low partial pressures of CO_2, or achieve high capture rates [41].

2.2.3.2 Cryogenic Separation

Cryogenic separation of CO_2 from the flu gas is also a possible method of capture. Chilling to -56.6C at which point the CO_2 would condense, then the required refrigeration would need much energy due to the large mass of the exhaust flow that is required to be treated, if the mass flow were reduced and the CO_2 concentration was significantly higher, for example from oxygen enriched processes it may be more economic [41].

2.2.3.3 Membrane Separation

Due to the limited pressure drop required for membrane separation, it could prove to be an energy efficient method of CO_2 separation, with polymer membranes potentially achieving CO_2 separation near to 60% [42]. Selectively permeable membranes could be used for CO_2 separation. Membranes face significant selectivity challenges with the higher the selectivity than the purer is the CO_2 separated but thus less percentage volume unless it is driven by significant pressures then requiring higher energy for pumping, or multiple membrane stages that require increased capital expenditure. Alternatively, less selective membranes may be cheaper to build and operate. However they are less selective and the CO_2 purity would be a reflection of that [41].

2.2.3.4 Absorption

The most mature process from industry is chemical absorption, and it is the basis upon which most large scale capture plants, such as at Ferrybridge, West Yorkshire UK, have been built. CO_2 forms a weak bond with a chemical solvent, which is then broken when the solvent is regenerated under heat and pressure releasing pure CO_2, and allowing the solvent to be reused for capture [41].

If the contaminants into the capture process, such as SO_2 and O_2, are kept low, the solvent can be highly selective, with relatively low levels of degradation [41].

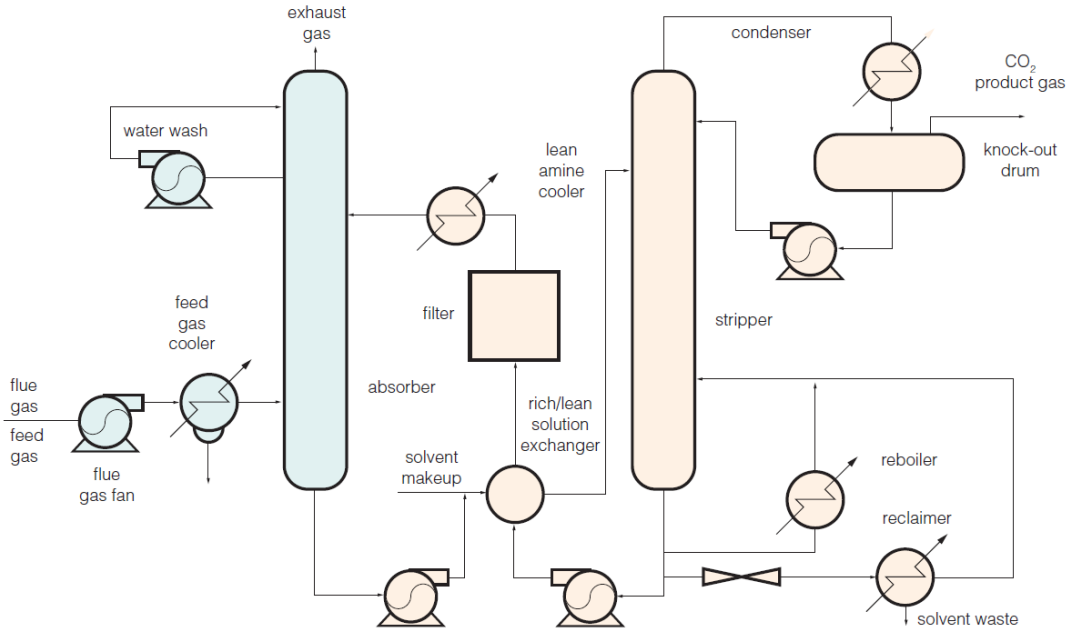

Figure 2-1 A schematic of the amine absorption process [43].

2.2.3.4.1 Pretreatment

SO_2 must be removed as efficiently as possible from the exhaust gas before passing through the capture solvent in the absorber otherwise they form heat stable salts. The SO_2 is reduced by a flue gas desulpherisation unit and the NOx is removed with selective catalytic reduction [41].

2.2.3.4.2 Absorption Column

The exhaust flue gas temperature into the absorber must also be controlled. Since high temperatures damage the amine and result in the solvent evaporating. Cooling of the exhaust gases is achieved through direct contact cooling, which is essentially a water wash system. At Beighton this phase is combined with the Flue Gas desulperisation [41].

Solvent is normally at a temperature of 40-60C in the absorber column for CO_2 scrubbing. After the exhaust flue is scrubbed it goes through a water wash which re-entrains solvent vapour and this reduces the losses. Increased capture can be achieved with larger absorption columns, with an increased energy penalty and capital expenditure requirements [43].

The absorption reaction of the amine and CO_2 is exothermic. This means that as the CO_2 is captured then the temperature in the absorber increases, and at the top of the absorber tower the exhausted gas should have significantly reduced CO_2 concentrations, by 70% to 90%, depending on the capture levels being operated.

2.2.3.4.3 Desorption Stripper

Rich CO_2 is pumped via a heat exchanger to the top of the stripper to be heated by the reboiler to a temperature of 100-140C, thus liberating the CO_2. The hotter lean solvent passes through a heat exchanger with the rich loaded warming it before entering the stripper, and cooling the lean solvent before entering the absorber to help reduce losses that would come from the heating and cooling and improve the overall capture efficiency process [43].

The reboiler is the main energy penalty of post combustion carbon capture, with heat being provided by steam bled from before the station turbines, meaning a loss in the potentially generated energy [41].

2.2.3.4.4 Solvents

Ideal solvent properties are ones which have a low heat of reaction with CO_2 which means the energy requirement for regeneration is low. The solvent should also have a high absorption capacity, which means a reduced mass flow. Further, it must be stable under high temperature variations.

Amines are the most popular solvents, and there is significant industrial experience using them. Monoethanolamine MEA has been used extensively and is able to capture CO_2 at low partial pressures which is ideal for the combustion exhaust gases.

Amine solutions are weak base that react, binding with acidic CO_2 or H_2S, making ionic molecules. This is an exothermic reaction, with the amine solution heating up until saturation at which point temperature rises slow.

Numerous reaction mechanisms are considered to be occurring, including two step reactions where carbamic acid is formed, then carbamate through the transfer of a proton to the amine base. [44]

$$CO_2 + RNH_2 \rightleftharpoons \mathrm{RNHCOOH} \qquad 2\text{-}1$$

$$RNHCOOH + B \rightleftharpoons \mathrm{RNHCOO^-} + \mathrm{BH^+} \qquad 2\text{-}2$$

Zwitterion mechanism has also been suggested as another two-step process:

$$CO_2 + RNH_2 \rightleftharpoons RNH_2 + \mathrm{COO^-} \qquad 2\text{-}3$$

$$RNH_2 + \mathrm{COO^-} + B \rightleftharpoons \mathrm{RNHCOO^-} + \mathrm{BH^+} \qquad 2\text{-}4$$

CO_2 and amine have formed a zwitterion, from which a carbamate is produced from deprotonation to a base.

A single step simultaneous CO_2 and base reaction has also been suggested where the amine bonds with the CO_2.

$$CO_2 + RNH_2 + \mathrm{B} \rightleftharpoons \mathrm{RNHCOO^-} + \mathrm{BH^+} \qquad 2\text{-}5$$

This reaction is believed to be weak and temporary. [44]

Different amines have different reaction processes, and absorption and desorption rates. For these reason mixes of different amine solution are being investigate more efficient capture, and solvent regeneration.

Unfortunately it has draw backs in the degradation due to oxidisation, and the energy intensity of regeneration.

Oxidation occurs in the absorber where the amine capture solutions first comes into contact with the exhaust gas, which from gas turbines has a large mol% of O_2. Oxidation has been found to be the most significant degradation method of amines, signifantly higher than thermal heat cycling from regeneration and the exothermic capture reaction. Oxygen causes demethylation reactions, forming acids, which further degrade the amine solution, and reduced its capture functionality. [45] Oxidisation can be reduced through the addition of metal inhibitors such as iron and copper to catalyse the oxidation process. [46]

Also the MEA can thermally degrade over 205°C. However this is significantly below the operational temperatures. At 135°C Davis [47] found that the amine degraded at a rate of about 2.5 – 6% per week, and this is within the operational temperatures [41].

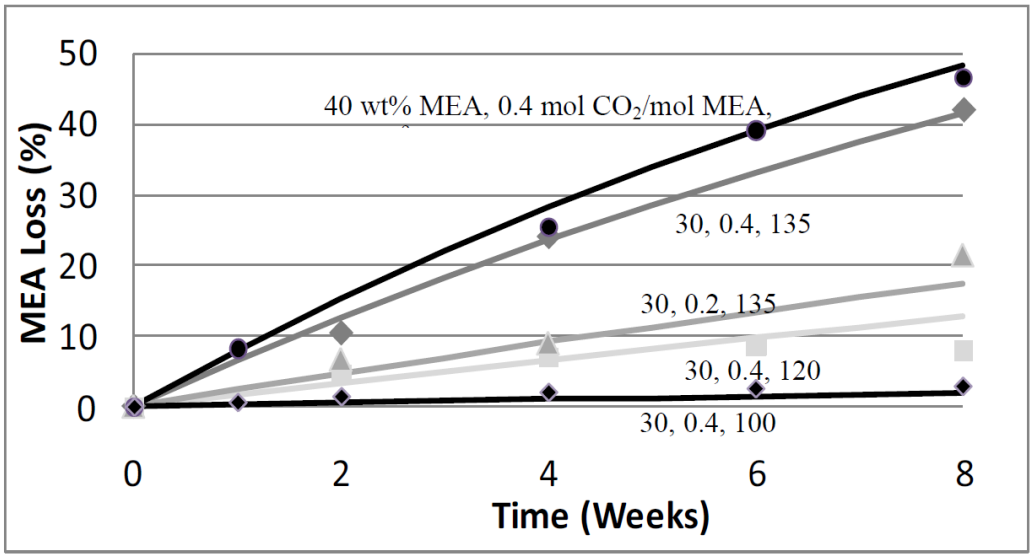

Figure 2-2 MEA losses as a function of time [47]

Davis and Rochelle (2009)[47] investigated the monoethanolamine losses due to thermal degradation under temperatures similar to those experienced in the stripper column. Their findings were that the majority of solvent degradation was thermal, with losses of 2.5-6% per week at 135C [47].

2.2.4 Retrofitting

Retrofitting combustion plants has the potential to produce a step change in the emissions from what would be considered locked in carbon emissions. Studies have suggested that retrofitting would result in a 11% overall reduction in plant efficiency which would cost about 675/kW Euro, but with a significant potential cost reduction with a capture ready plant design [42].

2.3 Combustion

2.3.1 Gas Power

Gas power offers lower cost construction, a smaller site footprint, and lower emissions than coal power. The public perception of gas is also considerably more positive than for coal, as it is a cleaner fuel that people are more accepting of and tend to oppose less.

For these reasons, as well as the now levelling in the gas prices, gas turbines have been gaining increasingly more popularity among private sector generators due to the lower capital investment, and the relative ease of meeting legislated emissions targets.

The expansion of shale gas use in the US has also driven some new activities, with the possibility of an increasing amount of exploitable reserves in the UK, Europe and Asia. As gas generation is more efficient than coal, potentially higher fuel costs can be offset by the improved efficiency in the plants.

2.3.1.1 Gas Turbines

Gas turbine cycles can be considered in terms of the Brayton cycle, with a compression, combustion and expansion phase. Strictly speaking, the Brayton cycle is for working fluids in a closed system which is not possible with combustion requirement for additional air for combustion. However it is assumed that energy is recovered from the exhaust gases, as it is in most turbines.

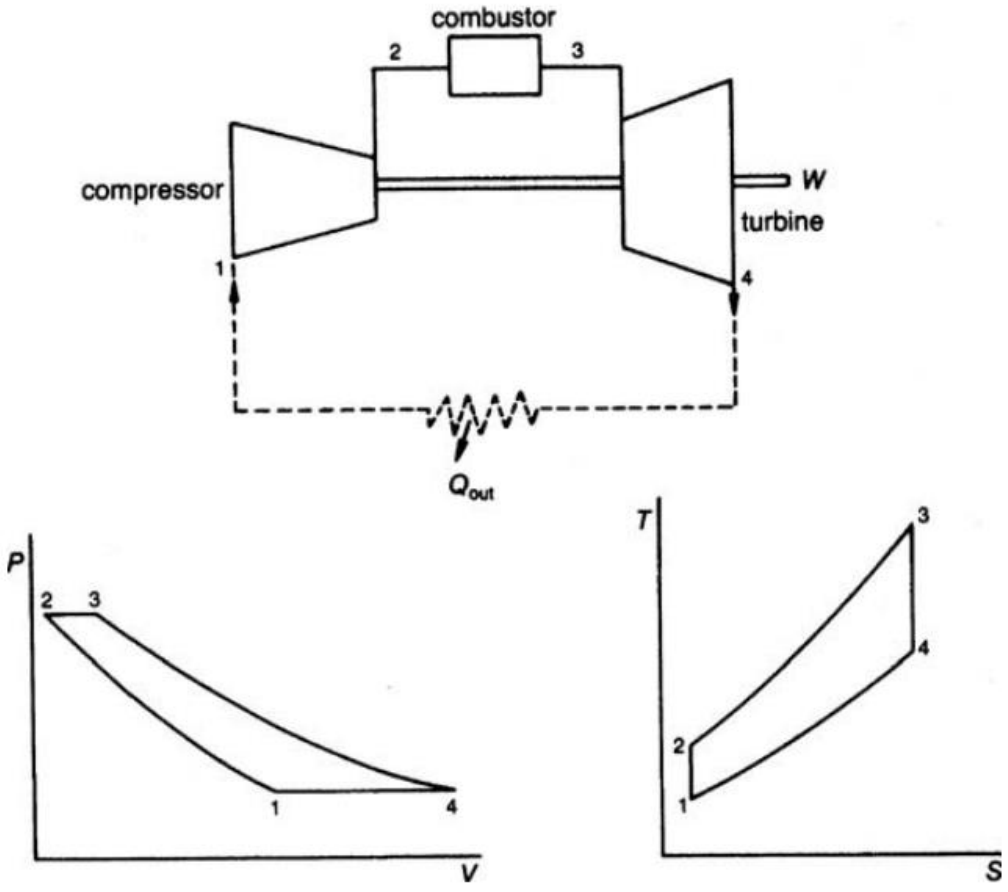

Figure 2-3 Theoretical Brayton cycle for simple gas turbines [48].

The Brayton cycle is considered as an ideal model of the gas turbine combustion process, the compression of air for combustion and the expansion over the turbine are considered to be adiabatic as in ***Figure 2-3*** Theoretical Brayton cycle for simple gas turbines [48]., with no change

in the heat of the working fluid, and isentropic, with no change in entropy. The combustor is considered isobaric, with no change in pressure.

Boyce (2012) splits the combustion in a gas turbine down into the first law of thermodynamics. [48]

Compressors work: The work done by the compressor is the mass flow rate of the air times the change in specific enthalpy.

Compressor work:

$$W_c = \dot{m}_a(h_2 - h_1) \qquad \textit{2-6}$$

h = enthalpy = Cp*T (Specific heat * temperature)

Turbine work: The total work done by the turbine is assumed to be the total mass flow through it multiplied by the change in the specific enthalpy across it.

Turbine work:

$$W_t = (\dot{m}_a + \dot{m}_f)(h_3 - h_4) \qquad \textit{2-7}$$

Cycle output: The total work done by the cycle is the work produced by the turbine less the impingement of the compressor.

Cycle output:

$$W_{cyc} = W_t - W_c \qquad \textit{2-8}$$

Heat energy added from the fuel: The heat energy is added over the combustor, and it is equivalent to the flow rate of the fuel multiplied by its lower heating value (lower calorific value).

Heat energy from fuel:

$$Q_{2-3} = \dot{m}_f * LHV_f \qquad 2\text{-}9$$
$$= (\dot{m}_a + \dot{m}_f)(h_3) - \dot{m}_a h_2$$

This is equivalent to the total mass flow rate multiplied by the specific exit enthalpy of the combustor, less the mass flow rate of the air multiplied by the specific enthalpy at entry of the combustor.

Overall cycle efficiency: The cycle efficiency is the cycles work output over the fuel energy put into the system at the combustor.

Cycle efficiency:

$$\eta_{cyc} = \frac{W_{cyc}}{Q_{2-3}} \qquad 2\text{-}10$$

The efficiencies of the turbine are generally limited by the temperature and pressure restraints of the working materials. Improvements may be made through heat recovery in the heat exchangers, integrated combined cycle and combined heat and power (CHP) applications.

The actual cycle differs to that of Brayton for numerous reasons. In reality no system is adiabatic, all elements of the turbine cause losses and none are 100% efficient. Further, the working fluid is not truly incompressible and the specific heat is not constant.

The result is the actual cycle is less efficient than that, this is seen in ***Figure 2-4 Schematic of the theoretical and actual Brayton*** cycle [48].

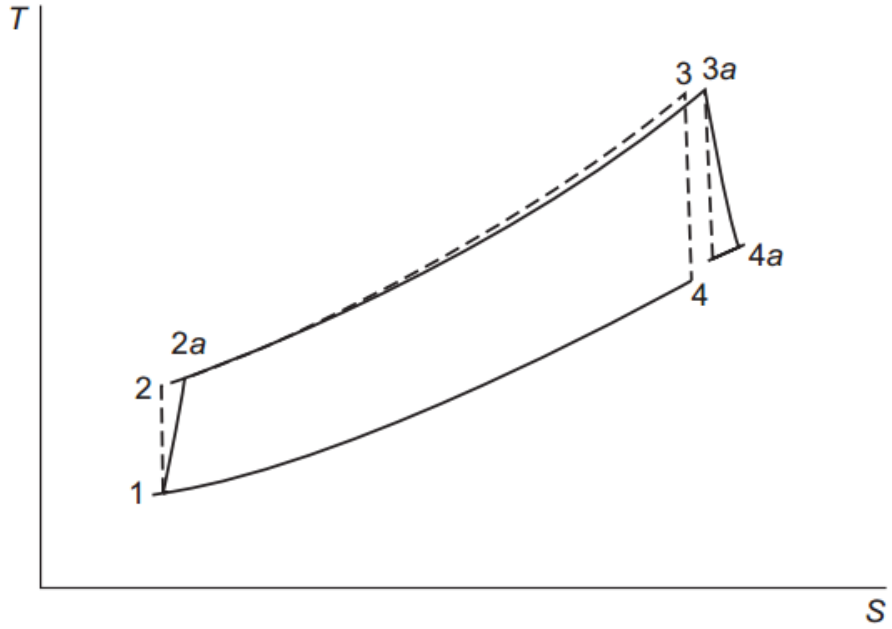

Figure 2-4 Schematic of the theoretical and actual Brayton cycle [48]

The “a” values on the graph indicate the expectations of a real cycle that are different to the dotted line of the ideal cycle.

The design principle of a gas turbine at its most basic level is relatively simple with a single shaft driven by the turbine also driving the generator and the compressor.

2.3.2 Combined Cycle Gas Turbines

Large gas combustion power plants use combined cycle turbines. These Combine cycle turbines have a higher efficiency than “single” or “simple” cycle turbines, as not only do they drive a turbine directly from gas combustion, but using heat recovery steam is generated to drive additional turbine(s) through the Rankine cycle, making more efficient use of the fuel. A plant is considered to be a combined cycle when the hot exhaust gas from the initial turbine is used to power a steam plant and turbine, or multiple steam turbines. This combines both the Brayton cycle for a gas, and the Rankine for a steam.

The reported performance of manufacturers turbines is under standard conditions. The air intake is designed for ISO conditions of 60% relative humidity, 15C and 1.017 bar. Any alterations to these conditions will impact upon the performance as the density of the air will alter and thus the mass flow through the turbine will change, and the oxygen for stoichiometric combustion will be affected. Higher temperatures result in less dense air, as well as an elevation in the humidity [49].

Combined cycle efficiencies are most enhanced by higher firing temperatures, due to the heat recovered in the second steam cycle. This is different to simple cycles that benefit from increases in the pressure ratio [49].

2.3.2.1 Turbine Classes

Modern turbines and development are broadly classed into different series according to their operating turbine inlet temperature at a given pressure ratio. This is not the maximum temperature in the unit which can be significantly higher in the flame of the combustor, than when exiting the combustor the temperature and hitting the turbine blades. This delineation is made as the higher the operating temperature and pressure that the turbine can operate then the more efficient is the turbine [49].

The delineation is not strict between each series or classes, as manufacturers have developed and improved upon their original designs. Changes have allowed older designs to be run at higher temperatures, or allowing the choice to run turbines that can operate at higher temperatures lower in a trade-off for greater flexible efficiency which may be required for different customer needs. For example, instead of being used in steady state operation, the turbine may be expected to be used as and when, ramping up and down its output to meet more volatile intermittent market demands.

2.3.2.2 Gas Turbine Series Examples of Development

D class turbines have dominated the market from the 1980's onwards when legislation demanded lower NOx emissions from stationary power sources. Much of the current UK fleet use D class turbines due to the round of investment and the "dash for gas" in the early 1990's. The turbines were the first with Dry Low NOx burners, that reduced production of Nitrogen Oxides (NOx) through peak flame temperature control and reduction for environmental reasons, and have turbine inlet temperatures in the 1,150-1,200C range [50].

H system gas turbines were developed to have a 1400C turbine inlet temperature, and tend to be part of a combined-cycle system using heat recovery steam generation from the exhaust gases [51] [52].

The GE H system utilises steam for cooling instead of chargeable air from the compressor and this improves the turbines overall efficiency. This steam that is used for cooling is taken from before the intermediate pressure steam turbine and is effectively "reheated" by the cooling process to be reused in the IP turbine [51].

The compressor pressure ratio is 23:1 with an air flow of 558-685kg/s feeding into a can-annular combustor, comprising fourteen lean combustion chambers. The fuel is injected into the combustor via a swirling nozzle, or swozzle, using vanes within the combustor to induce a swirl which also acts as points for fuel injection, before going through a further diffuser into the combustor chamber. The combusted gas expands into a four stage turbine which itself is cooled by both steam in a closed-loop system and air by the third stage, with no cooling required or used in the final stage [51].

The J Series turbines, developed by Mitsubishi, achieve 1,600C turbine inlet temperatures for higher efficiency operation. This is achieved through more efficient lower compression ratios of

23:1, down from 25:1 in H – class turbines. Also it is managed through more efficient cooling and better Thermal Barrier Coatings (TBC) [53].

The combustor in the J series turbine uses Exhaust Gas Recirculation to help reduce NOx emissions that are propagated by higher combustion temperatures. Steam cooling of the combustor also contributes to keep emissions below about 15ppm[53].

1700C Contemporary Inlet Temperature Target

There are also many joint government and industrial research projects that aim at driving forward the development of ever more efficient gas turbines, a significant contemporary target is the development of a 1,700C turbine inlet temperature, within the American Department of Energy Advanced Turbine System development program with GE, and a Japanese national project with Mitsubishi.

2.3.3 Gas Combustion

2.3.3.1 Exhaust Gas Recirculation

Exhaust gas recirculation has the potential to make the CCS process more efficient and reducing the energy impingement and the capital costs associated with large absorber columns and reboiler duty. The largest energy penalty in the post combustion capture system is the energy required to regenerate a CO_2 loaded solvent in the stripper column, by increasing the CO_2 volume percentage of the mass flow through the system this can be reduced. This would make the unit cost of capture cheaper and hence the unit cost of CCS low carbon electricity for the consumer [54].

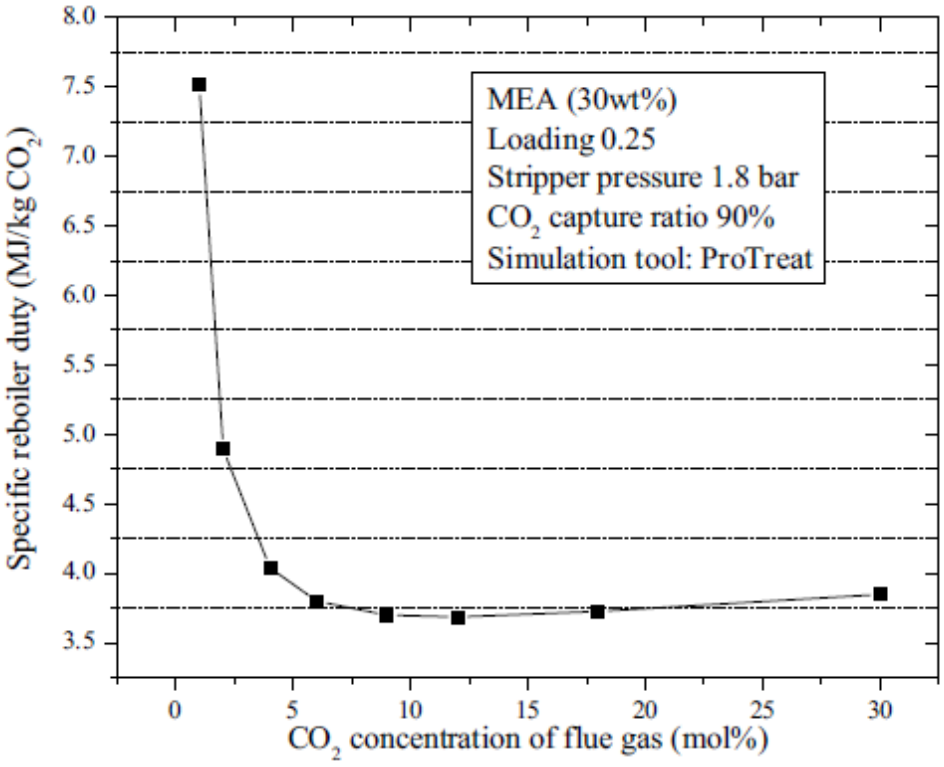

Figure 2-5 Stripper energy demand as a function of CO_2% [55]

As can be seen in ***Figure 2-5*** Stripper energy demand as a function of CO2% [55] the energy demand of the reboiler can be significantly reduced. If the percentage of CO_2 goes too high then a negative affect can be seen due to the heat released during absorption no longer being counter acted by the water vapourisation as the gas liquid ratios are smaller [54].

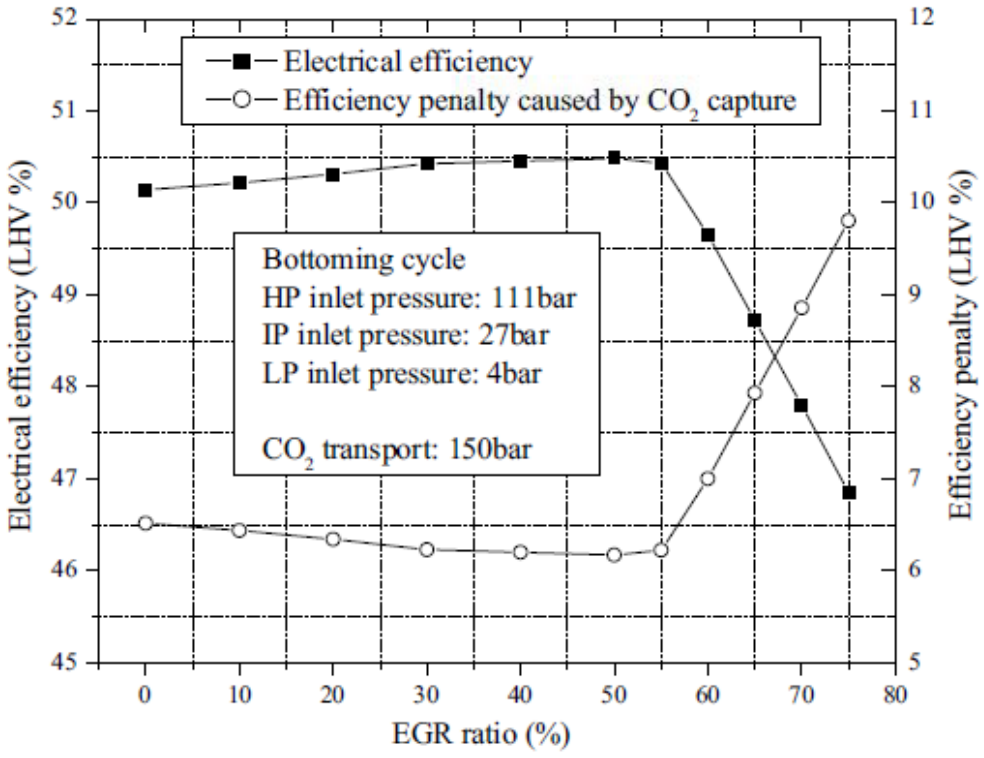

Figure 2-6 EGR efficiency penalties [55].

Enriching the CO_2 content and decreasing accordingly the O_2 content with EGR could also result in less solvent degradation due to the oxidation by the oxygen of the solvent, or alternatively removing or reducing the need for process alterations or chemical inhibitor additives that would have otherwise been used to address the issue [56].

Reducing the efficiency penalty and plant capture requirements results in significant economic savings. Rokke and Hostad, (2010) showed 50% EGR could reduce the capital expenditure for capture by more than a fifth.[56]

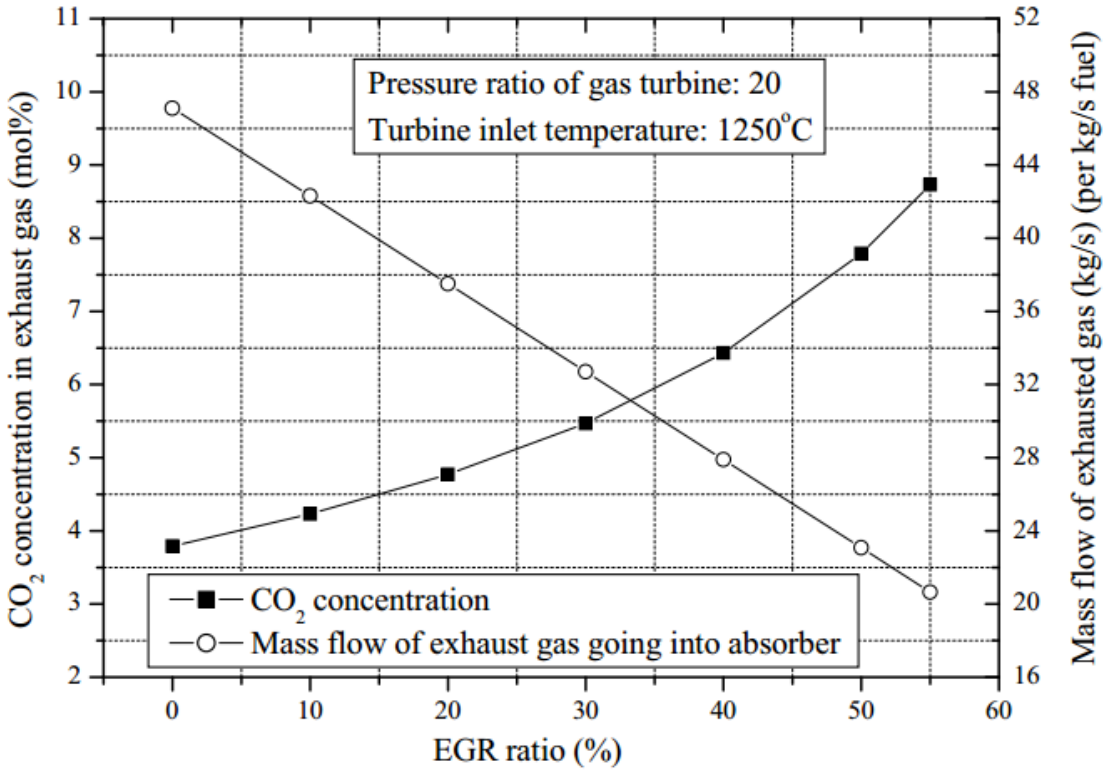

Figure 2-7 EGR reducing total exhaust mass flow [56]

2.3.3.1.1 Impact of EGR on Combustion

There are three major impacts of implementing EGR on combustion, namely thermal, radiation and kinetic. The heat capacity of the CO_2, along with dissociation, reduces the flame speeds and the increased radiativity of CO_2 also means radiation losses increase linearly with CO_2 dilution [57].

2.3.3.1.2 Flame speed

The recirculation of exhaust gas has been shown to reduce the flame speed of combustion. The increase in N_2 and CO_2 fractions result in lower laminar flame velocities due to the reduced rates of reaction which also contribute to increasing the flame instability over a range of equivalence ratios [58].

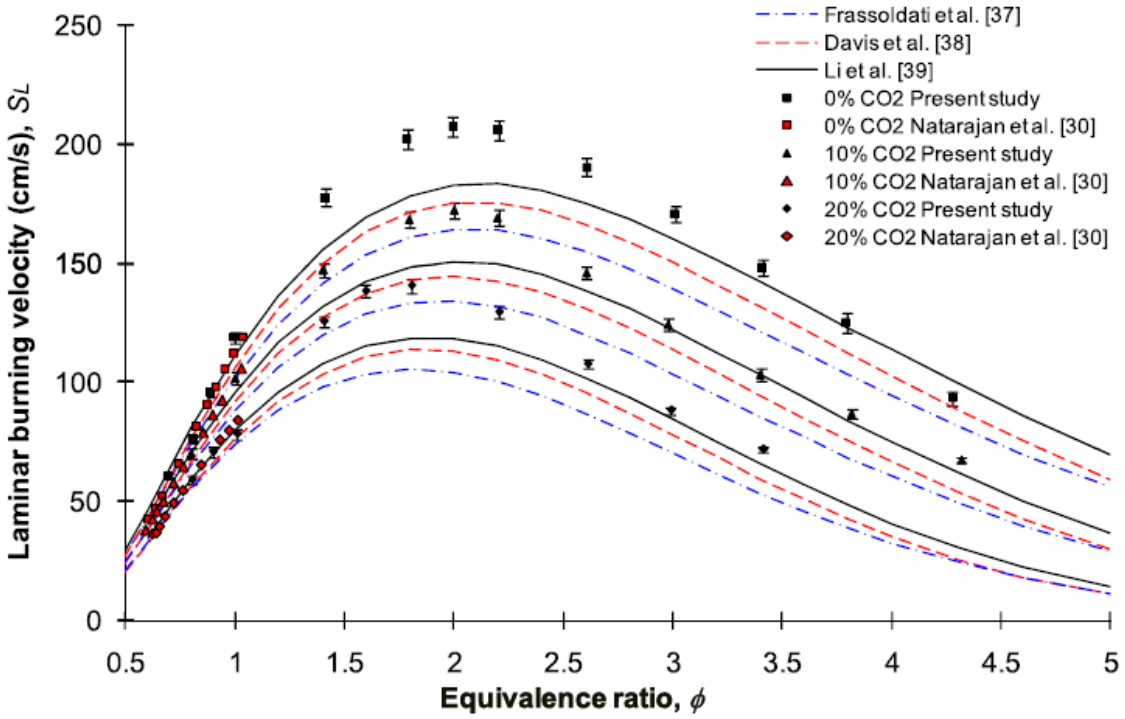

Figure 2-8 CO_2 flame speed relationship [58]

Burbano et al. (2011), demonstrated, through experimental data, the impact that increasing CO_2 concentrations has on reducing the flame speed. [58] The reduction in speed is increasingly more of an issue at lean, and particularly rich, equivalence ratios compared to normal combustion due to the impact it has on flame stability [58]. This is caused by an increase in the heat capacity of the CO_2 product, and a reduction in the heat released reducing the reaction rates. This effect is compounded by the recirculation, in the comparison to air.

2.3.3.1.3 Radiative and heat capacity changes

The higher specific heat of CO_2 (Table 2-1 Specific heat of working of the fluid species [59] means that more energy is required to increase its temperature. This means, with increasing CO_2 and reducing O_2 in the oxidisier, more fuel energy is required to raise the temperature the same amount as would be required for combustion with air, which is mainly comprised of nitrogen. This means lower combustion temperatures for the same fuel flow [59].

Table 2-1 Specific heat of working of the fluid species [59]

	H_2O	CO_2	N_2	O_2
T (K)	kJ/kg.K			
250	Liquid	0.782	1.044	0.910
1000	2.267	1.232	1.167	1.085
2000	2.832	1.371	1.287	1.180

CO_2 is also more radiative than nitrogen, increasing the rate of the heat loss, as compared to air, from the combustor before the combustion products even reach the turbine, thus resulting in lower turbine inlet temperatures [57].

2.3.3.1.4 Flame temperature

Recirculating CO_2 significantly reduces the flame temperature. As discussed in the literature, increases in CO_2 volumes to the combustor causes a reduction in the flame intensity. This results in decreasing the flame temperature and consequentially NOx emissions through a reduction in the production of thermal NOX, the primary source of NOx, particularly in gas combustion [57].

Not only are there heat reductions due to the higher heat capacity and increased radiativity of CO_2 but this in turn also causes slower combustion reactions and more diffuse flames [57].

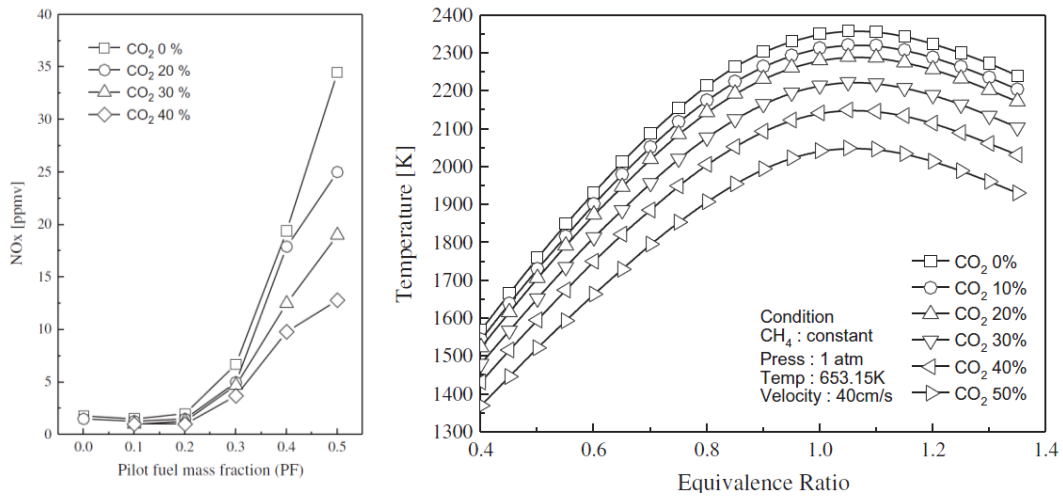

Figure 2-9 Temperature, CO_2, NOx relationship [57].

Lee et al, (2013), have demonstrated the correlation of increasing CO_2 in the oxidiser, lowers the temperature and hence lowers the NOx emissions as ***Figure 2-9*** Temperature, CO2, NOx relationship [57].

2.3.3.1.5 NOx

To tackle environmentally damaging NOx emissions, peak flame temperature began to be controlled in gas turbines to reduce the formation. Initially this was done using steam and water cooling. However during the 1980's gas turbine manufactures started to introduce "Dry Low NOx" burners. These burners recycled a proportion of the exhaust gases back into the combustor as a diluent, reducing flame temperature and hence NOx formation. [49]

This technology was then considered for application to CCS, as it increased mol% of CO2, the principle cause of temperature reduction. ElKady et al. (2009) and others have noted a marked reduction in NOx emissions with EGR, with a 50% reduction with EGR at 35%. [60] This can be attributed to the reduced combustion temperatures, which they then countered with higher equivalence ratios. This resulted in a restoration of the desired combustion temperatures but with higher UHC and CO levels then being observed.

Rokke and Hostad (2010) similarly showed the practical impact of EGR through the addition of CO_2, N_2 and O_2 to a 65kW gas turbine combustor. With the results showing the expected trends of CO_2 and N_2 causing a reduction in NOx emissions due to the reduced temperatures. They were able to restore these temperatures with oxygen vitiaition, but this again caused increases in NOx [59].

Apart from the reduced temperature impact on NOx emissions, the reburning of the species, such as NO and CO due to their recycling, can reduce their quantities in the final emissions [56]. This also contributes to the observed reductions.

Flame stability/ lean blow out

The general necessity to attain high efficiency and legislated low NOx emissions, which have negative environmental and health impacts, results in the design of fuel lean combustion systems. This fuel lean combustion can then be particularly sensitive to changes in the oxidizer with the lower stability of the flame than fuel rich systems [57],

Flame instability and lean conditions ultimately result in blow out. Recycling the exhaust gas results in relatively lower O_2 concentrations in the oxidiser for combustion. Bolland et al. (1997) found that lean blow out occurred below 13.5% O_2, and that 16-18% is required for flame stability. Li Hailong et al. (2011) looked at the vitiation of the oxidiser and found that with EGR a flame could be sustainable at 14%mol O_2. However CO levels were high and there was significant unburned hydrocarbons and they considered that this indicated EGR without O_2 enrichment would probably be limited to 40% for these reasons [56].

Experiments were carried out by El Kady et al. (2009) looking at the combustion characteristics of a commercially used dry low NOx combustor from an GE F-Class turbine. Flame stability was highlighted as a concern due to a reduction in the band of equivalence ratios that stable combustion would be achievable. Lean blow out was a concern and this was made worse by increasing the levels of EGR on the premixture of the oxidiser and fuel, and to avoid lean blow out in the tests they utilised a pilot fuel [61].

Premixed combustion is more dependent on a good flame velocity for stability, consequently the turbine flames are at greater risk of instability than conventional diffusion flames. However diffusion flames have much higher NOx emissions and so are not an acceptable alternative for stable efficient combustion with EGR [59].

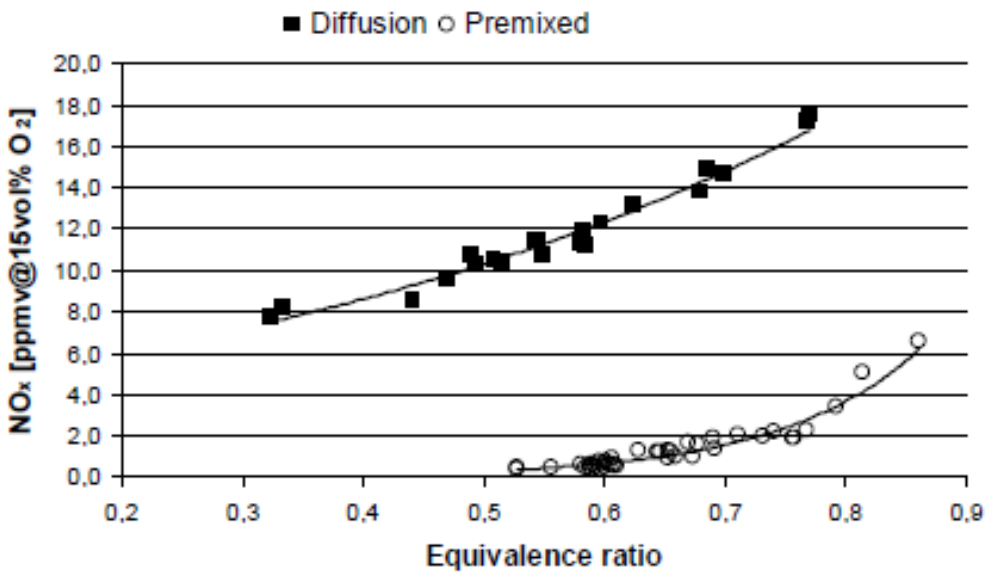

Figure 2-10 Comparison of diffusion and premixed flame NOx emissions with the equivalence ratio [59].

Rokke and Hustad (2010) found the instability from EGR caused lean blow out at equivalence ratios below about 0.6, and this is significantly higher than for a diffusion flame which occurs at about 0.25. The equivalence ratio is the fuel air ratio divided by the stoichiometric fuel air ratio requirement [59].

Increasing EGR levels increases the CO_2 concentration, reduces the NOx and reduces the total mass flow for post combustion capture.

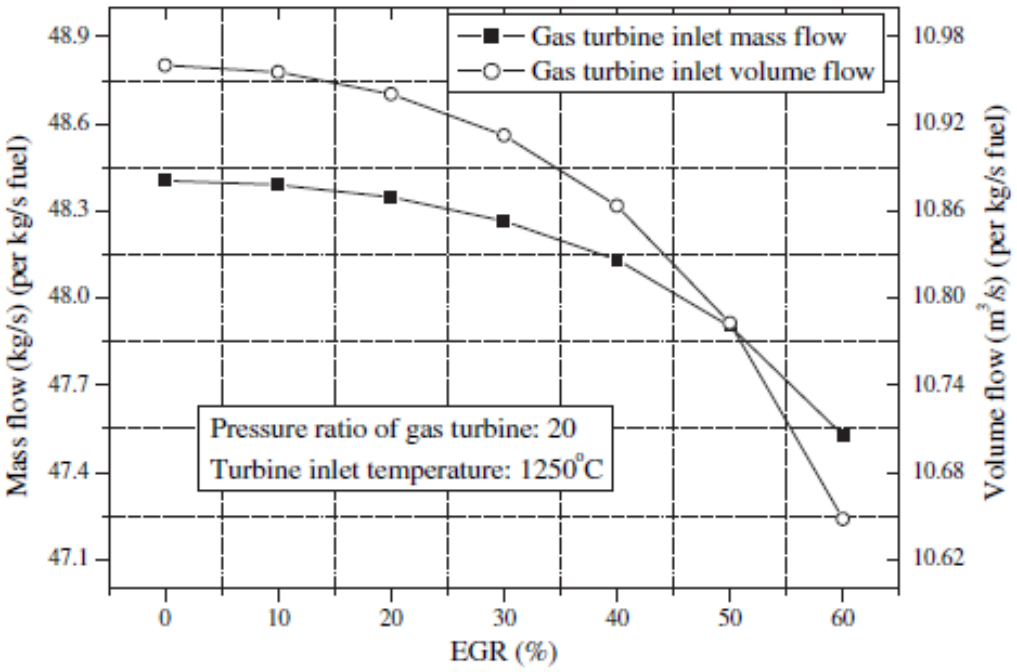

Figure 2-11 Inlet mass and volume flow with EGR [56].

In most studies, a level of 35% recirculation is considered the higher end of practically feasible exhaust gas recirculation. The level of 35% causes CO_2 to increase to as much as 8% by volume in the turbine exhaust [61].

However, higher EGR levels have been modelled. H Lie et al. (2011) showed an EGR of 55% would more than double CO_2 from 3.8mol% to 8.7% and reduces the gas mass flow to the absorber by 56.2%. The reduction in volume reduces the duty on the reboiler by 60%. This is slightly more optimistic than some other studies such as El Kady et al. (2009), but still in fairly reasonable agreement [56].

In a second study by Hailong et al. (2011) they simulated exhaust gas recirculation ratios up to 50%, again finding similar results, increasing CO_2 exhaust mol% from 3.8% to 7.9% in doing, and reducing the mass flow of the exhaust gases by more than half. The study found that these high levels of recirculation could reduce the reboiler duty by 8.1% and create a net efficiency improvement of 0.4% for a natural gas combined cycle plant [54].

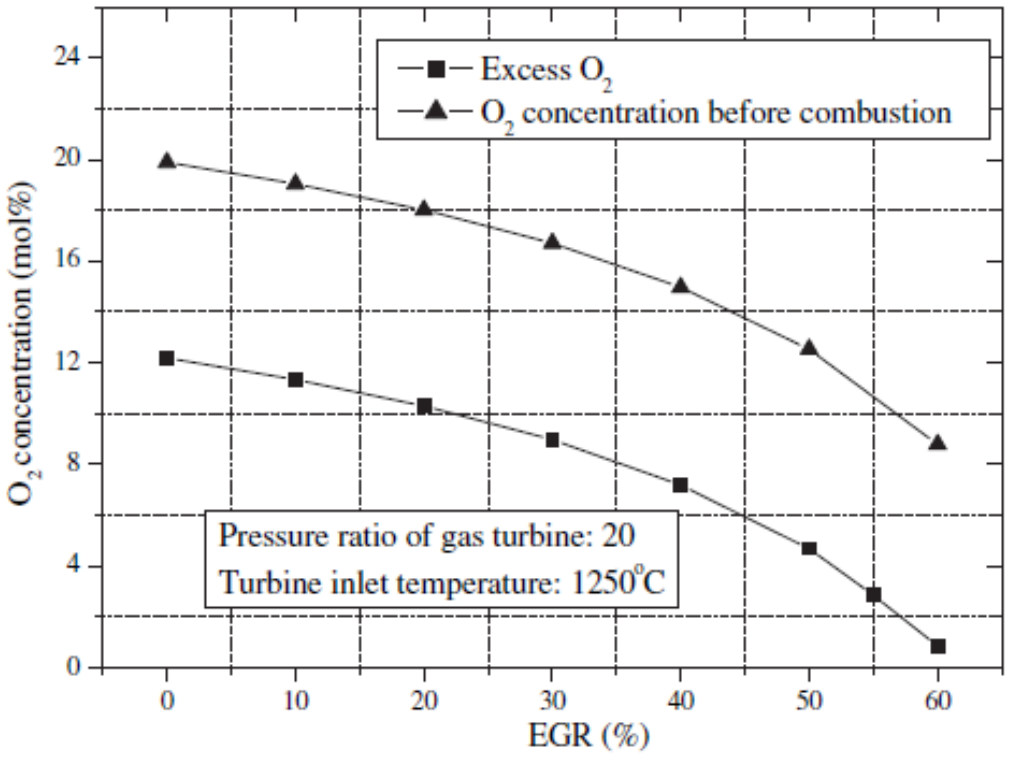

Figure 2-12 O_2 concentrations before and after combustion with EGR [55]

As discussed in this review, increasing EGR causes a higher CO_2 concentration that can lead to quenching, flame instability and blow out. In addition a very low O_2 levels the flame can be extinguished, as Figure 2-12 O_2 concentrations before and after combustion with EGR [55] Therefore although the increasing EGR levels to 55% has been investigated, other practical studies would indicate that the reduction in O_2 mol% to 11% would most likely blowout. It would certainly impact upon the combustion performance and flame stability due to the associated reduction in the flame speed, and increased residence time. There would be a reduction in the reaction rates, and combustion would be more spread out and the peak flame temperatures reduced, with the resultant increases in CO from reduced oxidation and dissociation [54]

2.3.4 Microturbines

Microturbines can provide distributed and back-up power economically and even more so when used for combined heat and power applications providing total energy efficiencies of up to 77%

and thus giving a short pay back period. The practical and economic advantages in tandem with the improved ability to remotely control and monitor the turbines has led to increased deployment [62].

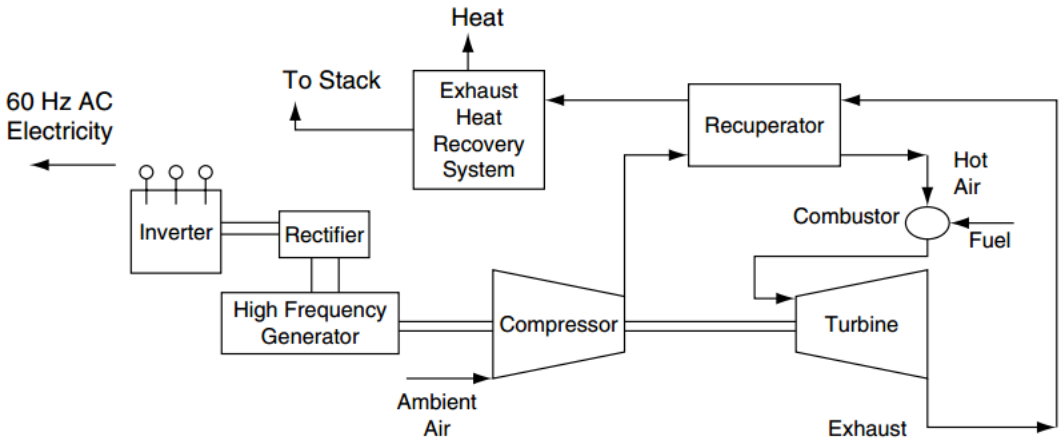

Figure 2-13 Schematic of a simple cycle microturbine process [62].

Recuperators are heat exchangers between the compressed air for combustion and the combusted exhaust gas. This means they must withstand the pressures and a large temperature differential between the inlet and exhaust gases that they come in contact with, the effect of which may be worsened through thermal work fatigue if the turbine experiences numerous switch offs and start ups.

Moisture evaporation in the inlet air may also contribute to corrosion as well as contaminants in the hot exhaust air from the feed gas.

The recuperator can create significant improvements in the gas turbines efficiency and make the cycles behaviour more closely follow that of the Brayton cycle. However in the effective exchange of enthalpy there will be pressure losses incurred that affect the pressure in the turbine and impinge upon the cycle efficiency and hence this becomes a balancing process.

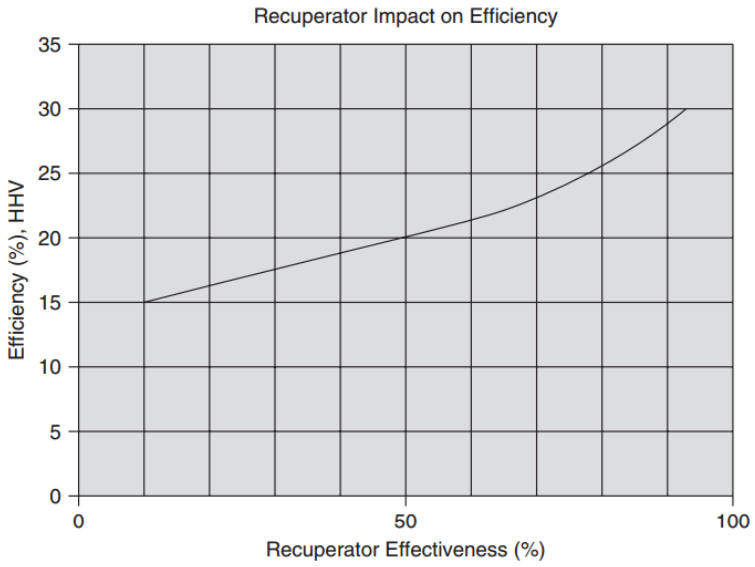

Figure 2-14 Efficiency improvement possible from the recuperator [62]

The effectiveness shown in ***Figure 2-14*** Efficiency improvement possible from the recuperator [62] it is the ratio up to the potential maximum heat transfer in the exchanger. Although effectiveness of 90% are not feasible, it can still be seen that effectiveness values in the 70% range can contribute significant cycle efficiency improvements.

This effectiveness relationship is also described by in ***Figure 2-15 Recuperator performance [48]***.

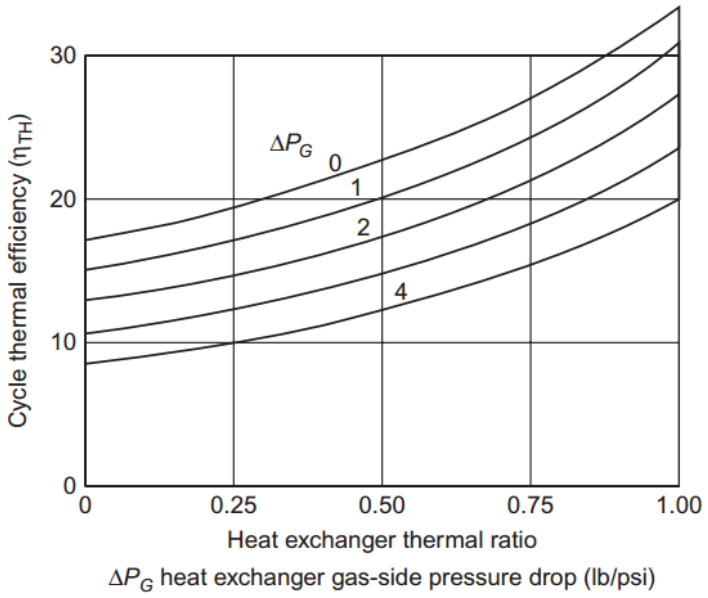

Figure 2-15 Recuperator performance [48].

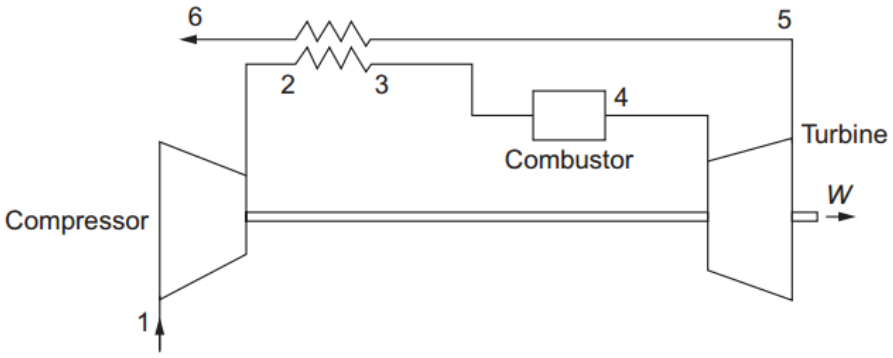

Figure 2-16 Schematic of a simple cycle gas turbine [48].

The effectiveness of the recuperator is the percentage of energy that it recovers.

Recuperator effectiveness

$$\varepsilon_{recup} = \frac{T_3 - T_2}{T_5 - T_2} \qquad 2\text{-}11$$

The effectiveness relates to the temperatures shown in ***Recuperator effectiveness***, particularly the temperature of the exhaust gas T5 entering the recuperator, and the temperature of the air for the combustion leaving the recuperator T3.

The improvement in theoretical efficiency, ignoring pressure losses, can then be calculated as:

Efficiency improvement from the recuperator [48]:

$$\eta_{RCYC} = \frac{(T_4 - T_{5)} - (T_2 - T_1)}{(T_4 - T_3)} \qquad 2\text{-}12$$

The pressure ratio has a significant impact on the expected efficiency performance and hence also the specific power of a gas turbine. This can be seen in ***Figure 2-17 Impact of the pressure ratio on the turbine performance*** [62].

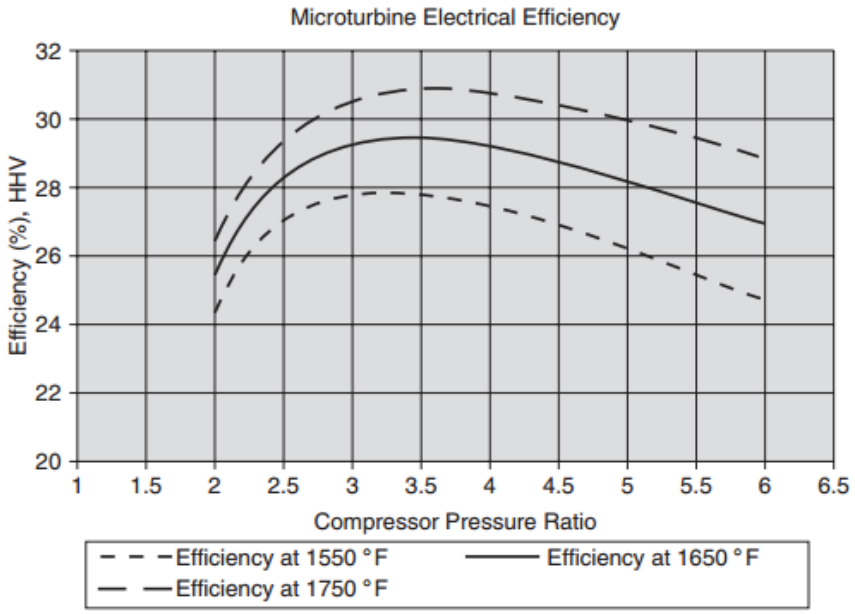

Figure 2-17 Impact of the pressure ratio on the turbine performance [62].

Reduction in the turbine output can be achieved through a reduction in the rotational speed which then reduces the air feed, compression and fuel feed in turn. However these alterations result in a decrease in the efficiency due to the turbine design load being higher.

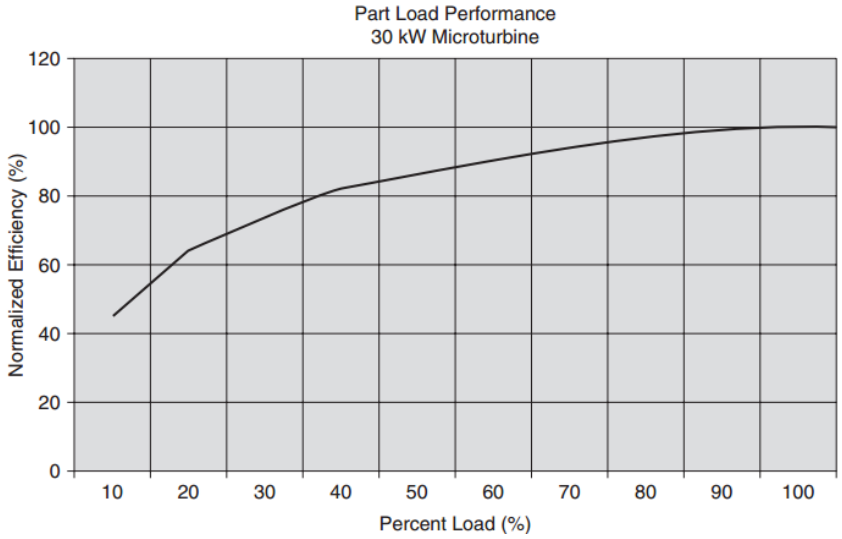

Figure 2-18 Reduced performance below the optimum design load [62].

The ambient conditions of the turbine can severely effect the performance. The pressure and temperature changes result in varying air densities from the designed parameters.

If the ambient temperature is high, or the altitude and hence pressure is high, then this will result in a reduced density, which means that for the same fuel air mix and pressure ratios, the compressor has to work harder, or alternatively it does not provide the desired pressure or mix.

2.3.5 Humidified Air Turbines

Humidified Air Turbines (HAT), where steam is injected before combustion to improve the turbine efficiency, reduces NO_x emissions and after being condensed out increases the volume percentage of CO_2 found in the exhaust. Humidified Air Turbines has been used historically to improve turbine efficiency and reduce emissions. Also it has the benefit that after being condensed out of the exhaust gases that the volume percentage of CO_2 is increased, meaning more efficient capture is possible with higher partial pressure. [63]

In a conventional gas turbine the pressure ratio and turbine inlet temperature are the biggest factors driving the performance of a turbine. With HAT, the rate of steam injection post

compression becomes a strong influencing factor. Steam injection increases the specific power output of the turbine and steam injection reduces NO_x formation. The addition of steam increases the mass flow through the turbine. [63] If this steam is added post compression (as it is in the experimental set up) it means additional mass flow through the turbine for which the compressor has not had to do work for. This is indicated in the experiment by the constant compressor pressure at vary steam injection rates. The addition of steam also increases the specific heat capacity of the oxidising working fluid, implying that a greater heat transfer through the recuperator can be achieved by increasing its efficiency [64]. The steam also cools the flame temperature and reduce NO_x formation. Older lower NOx combustors used water for peak flame temperature control[63].

The residence time and temperature are the factors that influence the thermal NO_x formation. Steam acts as a diluent reducing temperature. Although the addition of steam may appear to augment the power output of the microturbine, this is not taking into account the energy of rendering the steam which is done by an external unit. [65] If water was added instead of steam to the post compression phase then efficiency gains would be reduced due to the energy required to generate that into steam.

The addition of steam to create humidified air can cause poor combustion and this would be shown by higher levels of UHC and CO [66]. It is possible to reduce NO_x without increasing CO and incomplete combustion significantly. However it has been shown when HAT is used the higher concentrations of CO_2 can be achieved in the exhaust gas on condensing out the air [67]. Ward De Paepe [68], used a spray saturation tower and found humidification of the compressed air post compression in a T100 micro gas turbine had an impact of improving the efficiency by 1.2 – 2.4%, however their humidification percentage was not quantified, and emissions were not published [69]. Mohammed Mansouri [70] looked at both HAT, they found an improvement in efficiency from 23% to 25.8% with 30g/s steam, equivalent to 108kg/h with HAT[70].

2.4 CO_2 Transportation

The key energy penalties that are associated with the running costs and capital expenditure for any form of CCS are the separation, compression, and transportation for sequestration.

Transport poses a number of challenges, in simple engineering terms designing a pipe to meet the flow rates, and the liquid properties of the CO_2.

Beyond these key issues are the collaboration of stake holders, from the public, to land owners to private investment, for the installation and operation, the key issue for all of these is the distance from the site of CO_2 production to the storage site.

Aside from the ability and permissions to provide a CCS transport network is the probable necessity to be able to buffer the CO_2 delivery at both point of source, and the point of storage to allow for varying flows to be made consistent from a CO_2 source and to allow for steady state injection into the sequestration sites, or the temporary storage when the site sequestration site or injection facilities may require maintenance.

An issue particularly in terms of public safety and perception is the often close proximity of power plants to the populous and industry due to the demand they have created.

The release of liquid CO_2 could be potentially fatal, although dispersion may be rapid, high concentrations and the displacement of CO_2 can result in asphyxiation.

The economics of the CO_2 transport process are dominated by the volume of CO_2 to be transported, and the distance for it to be transported.

This will also affect the appropriate economics of the mode of transportation, pipelines and ships. With pipeline transport generally proving to be more economic for large quantities, but it is shipping for small quantities over large distances that is more economic.

Beyond economic appropriate scenarios shipping could be utilised for priming storage sites and the early stages of commissioning of CCS networks.

Another key issue with mobile transmission of CO_2, whether rail or shipping, is the inability to capture the CO_2 emissions released by the processes, however with pipeline transport pumping stations could be powered by decarbonised grid generation.

There are several CO_2 pipeline network proposals in Europe, the US and Australia. A particularly promising idea is the concept for a European network due to the relative proximity of a large number of emitters in different countries to good quality storage sites.

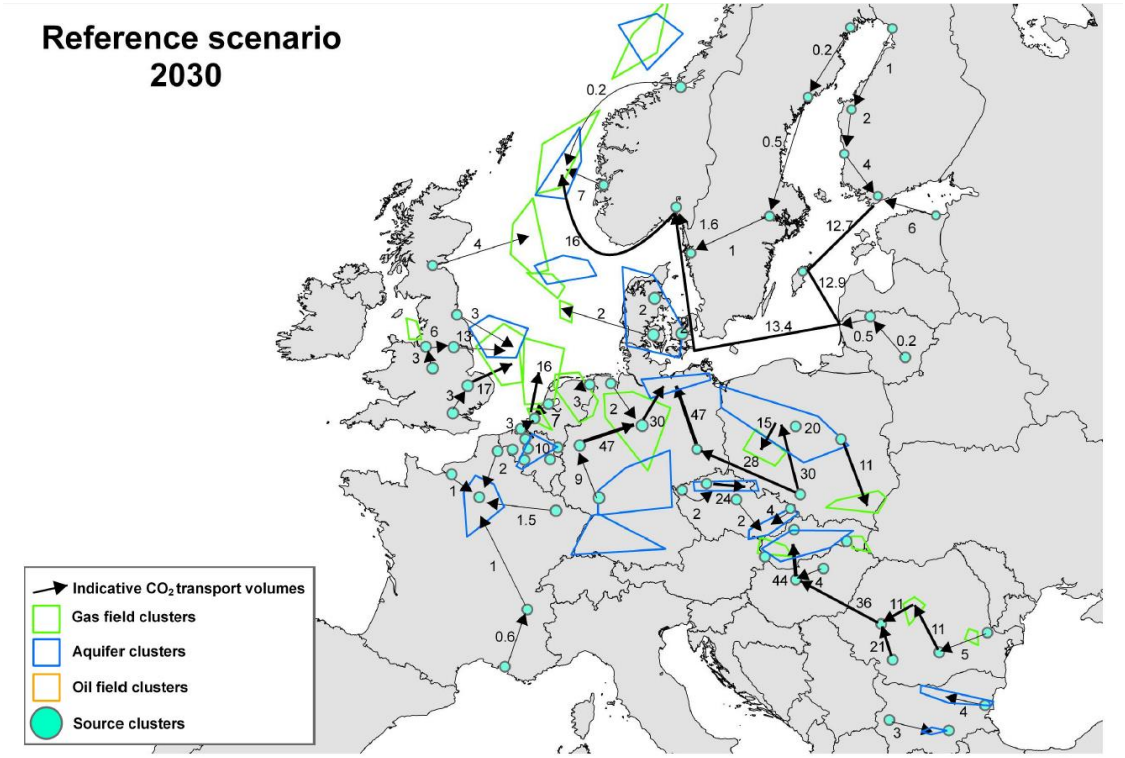

Figure 2-19 Potential CO_2 Europipe Network [71]

A European CO_2 pipeline network has been the focus of significant work over the last 5 years or so, and this is mainly in anticipation of a faster and greater uptake of demonstration and commercial CCS projects.

The EU has a number of projects, the on-going Zero Emissions Platform (ZEP), the CO_2 Euro pipe project and the EC feasibility study for Europe-wide CO_2 infrastructure [72].

Unfortunately all of these studies projections have been significantly affected by the regression in Germanys CCS policy, but they do provide the best basis for the analysis of the potential and feasible capacity.

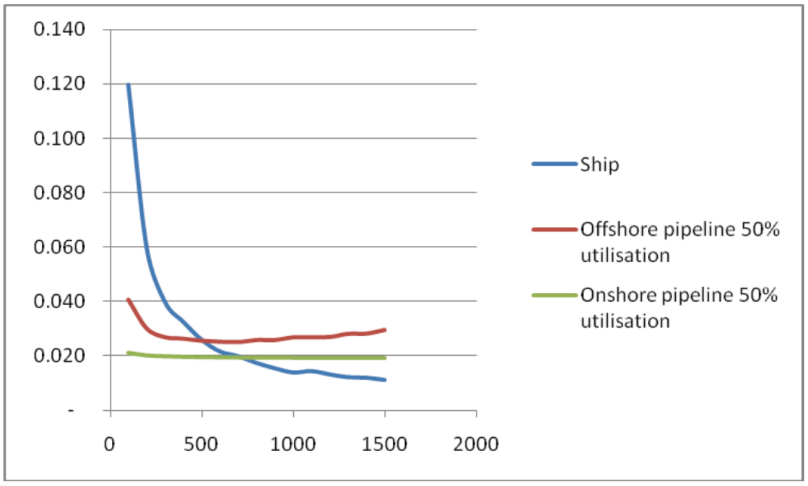

Figure 2-20 Transport to distance cost comparisons [72]

For the purposes of comparison of the transportation costs, it is useful to look at the Peterhead and White Rose projects.

2.4.1 CO_2 Usage and Storage

2.4.1.1 Enhanced Oil Recovery

Since the 1980's, CO_2 has been used for the enhanced oil recovery (EOR) to extract previously unrecoverable resources. Potentially carbon capture could be subsidised by providing this CO_2

for oil recovery and then storage [42]. Though the motive for using CO_2 is for increased oil extraction, not all of the CO_2 is recovered for recirculation and a proportion is sequestered during the process. This could be self defeating dependant on how much CO_2 would be released from the combustion of recovered oil and gas, compared to how much CO_2 is stored by the process.

2.4.1.2 Storage

The cost of avoided CO_2 is different to the cost of capture.
Cost of avoidance is

2-13

$$Cost = Capture\ cost * \frac{fraction\ of\ CO2\ captured}{efficiency\ of\ plant\ with\ capture / efficiency\ of\ plant\ without\ capture - (1 - fraction\ of\ CO2\ captured)}$$

Economically capture from smaller more carbon intensive plants is significantly more expensive.

2.5 Particulate Matter

Particulate matter is a field of increasing research interest. Traditionally the particulate emissions from large static power generation such as coal power plants has been identified as an environmental pollutant, with legislation and corresponding emissions control technologies implemented. Both legislation and technology focused on reducing larger particulate size emissions. However with CCGT generation smaller particles dominate the emissions spectrum and in much greater number, this requires research as to the potential environmental impact, and possible requirement for improved legislation.

The particulate size and number can also be impacted by the addition of CCS technologies, such as EGR and HAT. With EGR affecting flame temperature, and hence particulate formation, and type. HAT may also effect the nature of nucleation particles, with increased moisture able

increasing the likely hood of acidic particle formation with uncombusted fuel. In addition the increased humidity may increase particle agglomeration, affecting particle size and hence number.

The impact of particulates on the post combustion capture process has also received limited research. There is a potential for increased amine solvent degradation, depending on the nature of the particulate emissions. It is a necessary step in the research process to start quantifying and identifying the particulates and modes emitted from gas turbine combustion to provide data for further research.

2.5.1 Different PM categories PM10, 2.5, 1

There are currently three key particulate size ranges generally defined for consideration, namely PM10, PM2.5 and PM1. PM10 are particulate matter up to the range of 10µm, this can include debris from volcanoes or anthropogenic activities such as mining or combustion of carbonaceous fuels. Coal ash would fall into this category. Although it can have a serious impact on health when inhaled, or the environment as a pollutant if allowed to escape into the atmosphere, most emission sources can be dealt with relatively easily. Although its lifespan may be more significant than smaller particles, it also settles within a relatively short period of time. [73]

Above 10 micrometers particles tend to settle to the ground, below is the aerosol issue that may stay in atmosphere for weeks.

PM2.5 can be more difficult to deal with than PM10. They are particles of diameter 2.5 µm and below. Although they are smaller in size, they are significantly more abundant, and much can be removed by physical filters, but some cannot. PM2.5 can include sources such as in mining, but combustion emissions tend to make up a significant proportion of this category, including soot. These emissions can be carcinogenic in nature containing oxidants, and heavy metals. However

even the size of the particles, inert or not, can cause issues. They may also form the nucleation of larger particles and smogs. Further it is possible for particles of this size to be more easily inhaled, not trapped in the nose or by mucus, or removable by the body through coughing, etc. [73]

PM1 particles are particles of size up to a diameter 1 μm. Anthropogenic sources of these small particles are significantly different from combustion, and are difficult to physically filter due to their small size. Although volatile organic compounds of this size may have relatively short atmospheric lifespans before oxidising or settling they are large in volume from combustion sources, and after accumulation can coagulate to form larger particles. Particles of this size can pass into cells and physically disrupt the replication of DNA which can lead to cancers. [74] Also they contribute to smogs, environmental pollution and acid rain.[73]

Within the PM1 category are ultra fine particles, sub 0.1 μm (100nm) in diameter [75] these particles are a significant proportion of the particulates created by “cleaner” combustion fuels such as petroleum and gas.

Particles of this size can pass through the air blood barrier and the blood brain barrier [76] and are thought to be a significant risk factor for Alzheimer’s, [77] as well as being potentially carcinogenic.

2.5.2 Why is particulate matter of concern?

Particulate matter can be a serious environmental pollutant. Particulates can cause direct harm to humans through inhalation, in addition they can cause environmental damage through polluting with their contents which can contain heavy metals, thus causing contamination. Particulates also contribute to acid rain and smog, through the creation of sulphuric and nitric acid nucleation particles originating from NO_x and SO_x emissions. [78] Also this has significant impact on human health.

Particulates have been recognised to impact on the climate and historically volcanic eruptions have caused global cooling. Dependant on the particle size and nature, they can reflect radiation and scatter it thus causing cooling, or they can absorb and reflect it thus causing warming.

Depending on the nature of the particulate emissions, size, distribution, number, composition it is possible that they may be of concern for solvent degradation in post combustion capture. One of the first steps to investigating this is to quantify the emissions on a pilot scale, as well as the impact that the addition of CCS technologies such as HAT and EGR have on those particulate compositions and distributions. This is as EGR can cause lower flame temperatures, affecting complete combustion of fuel and the formation of particles. Humidification may also cause increased particle agglomeration and effect particle number and size distribution.

2.5.2.1 Impact on human health

Particularly dangerous can be thoracic particles. These are respirable particles that can pass the larynx and through the lining of the respiratory tract. Thoracic and respirable particle definitions for human health risk assessment

Currently much legislation of particulates is on the basis of total emitted mass. However this may be an increasingly inappropriate mechanism for legislative limits due to particles size be the key factor that can effect human health, and with modern power generation, such as that with CCGT, large numbers of Ultra Fine particulate being produced, the total mass of which can be a fraction of larger particulate matter, such as soot that can be produced by generation from coal and biomass.

2.5.3 Particulate Matter Sources

The principal components of the particulates are smoke, ash, ambient noncombustibles, trace metals may also be present in particles and erosion and corrosion products. [73] Two additional components that could be considered particulate matter in some localities are sulfuric acid and

unburned hydrocarbons that are liquid at standard conditions, and these can go on to form nucleation particles.

Particles tend to be comprised of sulphates, nitrates, and ammonia but also black carbon, organic carbon, minerals and water. [73]

2.5.4 PM1 analysed

Within PM1 there are numerous sub categories of particle sizes. Ultrafine particles are considered to have a diameter less than 100nm, and nanoparticles are those with a diameter below 50nm. These size ranges account for the majority in number, of airborne particles. Particles over 1µm in diameter are considered coarse mode. [73]

Most studies consider two particulate modes within PM1, defined as nucleation up to 30nm, and accumulation 30nm -500nm. [75] Some authors also consider a 3rd "Aitken" mode between 10-50nm, and this occurs through the condensation of the nucleation mode particles.

2.5.4.1 Nucleation

Nucleation mode particles are the smallest, they are newly formed from chemical reactions and condensation processes and they are the potential start of larger particles collecting. [73]

Nucleation particles are generally considered to be sub 10nm in diameter, [73] these particles have relatively short atmospheric life spans with VOCs disappearing, and particles being atmospherically oxidised.

There are two types of nucleation processes for particles to be formed. Heterogeneous nucleation where substances condense on particles and grow and homogenous nucleation is the other process with low vapour pressure molecules condensing and forming new particles. [73]

A common nucleation combustion particle is the formation of sulphuric acid, H_2SO_4 from sulphur dioxide emissions which can occur in combustion is an example of homogenous nucleation. [73]

2.5.4.2 Accumulation

The accumulation mode is where particles have started to join together to form larger particles, and can have a longer atmospheric life span. Coagulation of particles slowly causes an increase in particle size, and a reduction in their total number. [73] Significant reductions in nucleation particle numbers may be mirrored by only small growth in accumulation particles. With vapour condensation and coagulation nucleation mode particles grow into accumulation mode particles. These have a significantly longer atmospheric life. [73]

Accumulation mode particles may also comprise of metals and polycyclic aromatic hydrocarbons PAH, rather than from a slow agglomeration.

EGR also has the potential to increase the number of accumulation mode particles, with smaller nucleation particles having longer residence times and possibly recycle several times in the combustor before being exhausted, and growing in size.

2.5.5 Atmospheric particulate distribution

Atmospheric particulates tend to be dominated by nucleation particles, with less accumulation mode. Kumar et al [79] reported nucleation mode particles between $3 – 6 \times 10^4$ dN/dlog Dp (cm^3), and accumulation at 1×10^4 dN/dlog Dp (cm^3). [79]

Similarly Cernuschi et al [80] reported similar size range peaks in the PM1 range, but also with a peak in the larger PM10 range. [81] These ranges and number are consider in the results reported here ambiently, and for those in the gas turbines.

2.5.6 Expected Gas Turbine Particulate Matter

Often combustion emissions will contain more than one peak in particle size. Standard combustion emissions would be considered bimodal with nucleation and accumulation particulate matter being observed.

Eli Brewer et al [75] also found that higher concentrations of nano particles in exhaust gas air concluding further research as to the nature and volatility of particles below 10nm in diameter being observed is required to determine their potential impact on health. They found particles of diameter 2-3nm this being four orders of magnitude higher than ambient conditions. [75]

Combustion of natural gas has been found to produce high numbers of particles of diameters 2-3nm. [75, 82] This is the particle mode that we will expect to be observed in the results for GT1 and GT3. Minutolo et al [82] found that increasingly fuel rich combustion resulted in larger particle size emissions. [82] This will probably be less apparent for the Turbec 100 turbines, due to the lean nature of the combustion.

However with CO_2 addition through EGR, an increase in aromatic compounds can occur when there is insufficient oxygen for complete combustion. These compounds are then involved in condensation reactions that form particles. [82, 83] This increase in UHC is observed with EGR.

Fuel rich mixes create more fine particles as seen in Minutolo [82] who also found inefficient fuel mixing resulted in more emissions of ultrafine particles below a diameter 100nm. They also presented particles over in diameter 10nm being already present in the air before combustion, and not a product of it. [82] The origin of the ultra fine particles was found to be aromatic compounds that were incompletely condensed, and not oxidised. This could be Aitken zone particles.

If particles are significant enough in number, it may be expected that they would coagulate and create a bimodal trend. [84]

2.5.7 Particulate matter legislation

Most legislation of particulates is on a mass basis, however this may not be an appropriate form of legislation for gas turbines due to the ultrafine nature of most of the particulate emissions from them. [75] The link between health, and anthropogenic ultrafine particle sources needs further investigation to determine possible appropriate future legislative measures. [80]

2.5.8 Particulate emissions control technology

There are many effective particulate control technologies for large combustion power plants that prevent and reduce significant particulate release that can contribute to environmental contamination, damage to human health and smog. [73]

The first primary emission control technology that has been used in combustion plant and cement works, etc is bag houses, these are coarse fabric filters through which exhaust emissions pass, with particulate matter being trapped and building up on one side of a fabric filter. These can be shaken out to collect sedimented coagulated particulates and allow the continuing use of the filter without blockage of exhaust emissions, and this can be highly efficient, as shown in Figure 2-21 A typical fabric filter capture efficiency [85].

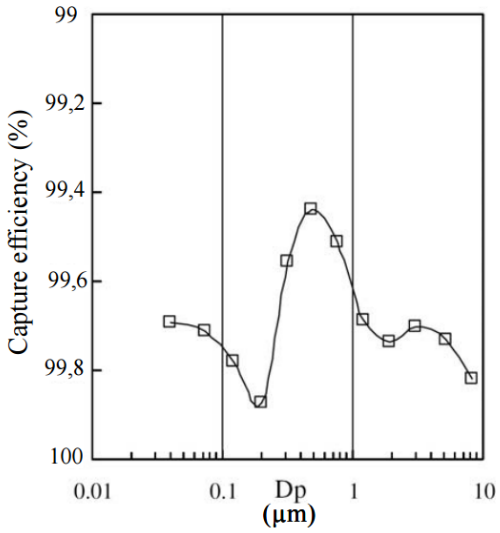

Figure 2-21 A typical fabric filter capture efficiency [85]

There are also static electro precipitators. These are electrically charged thin metal structures or frames of wires where there is a large total surface area with positively charged particles attracted to them and conglomerating. These electro static precipitators are then banged, or shaken to release the particulate for collection. [85]

Cyclones can be utilised to remove particulates and they can be sized accordingly to the expected distribution of size and mass of the particulates emitted. Friable materials will coagulate in them and drop from the bottom of the cyclone, and cleaner exhaust gases will be emitted. [86]

Wet and humid particulate emissions treatment is also available, wet scrubbers can shower, and charge, exhaust gases counter current, and remove entrained particulate emissions. [85]

2.6 Summary

From review it is evident that post combustion capture and storage from a combined cycle gas turbine power plant is a feasible possibility, with all individual elements of the process proven, from combustion, to capture, to transportation to sequestration. However the technology is

currently comparatively expensive, and the highest cost step of the process is the solvent regeneration. This is due to its high energy intensity, however there is potential to reduce the impact of this through the application EGR and HAT, with further pilot scale demonstration of this being useful.

From the literature review it can be seen that there has been a significant number of modelling papers researching the potential exhaust gas recirculation on gas turbines for increasing CO_2 emissions for improved capture efficiency. Modelled work has also looked at the probable impact on turbine performance, and hence the likely net process efficiency changes through the addition of more extensive EGR application beyond the traditional flame temperature an NOx control. However experimentally there has been very little EGR turbine research.

Interesting research has been carried out on combustors alone, altering the oxidising air mix to investigate the emissions impact of higher recirculation ratios, and the impact on flame temperature as an indicator of potential efficiency change. [60] However this did not look at the complete turbine system, or post combustion capture potential.

One paper investigate the effect of uncontrolled accidental recirculation of exhaust emissions into the turbine inlet, noting changes in inlet temperature and hence turbine frequency. This was not a controlled experiment though, and did not include any emissions analysis, or quantification of recirculation percentage. [87]

There is also a significant number of papers which model the impact of humidified air on turbine performance, power augmentation, and increases in CO_2 vol% in the exhaust emissions for capture. The use of HAT for power augmentation and flame temperature control is not novel, however there is not currently any experimental pilot scale studies that have investigated the potential impact of combining both HAT and EGR technologies.

This thesis will aim to address some of the knowledge gaps as to the impact on turbine performance, and efficiency with experimental application of EGR on a pilot scale to a microturbine. It will also assess the impact of combining HAT and EGR on turbine performance, and address the potential process gains from increased exhaust CO_2 vol% and net energy gains.

The thesis will also asses and report the particulate distribution from the gas turbine, both before and after adaptation with simulated EGR, due to the potential for particulates to contribute to solvent degradation in the post combustion capture process. As currently there is no experimental literature on the subject, and the issue of ultra fine particulate emissions is receiving increasing attention due to their potential impact on human health.

3 Micro gas turbine operation baseline conditions

There extensive pilot scale test facilities housed at Low Carbon Combustion Centre in Beighton near Sheffield. Providing flexible combustion, process, and treatment options shown in Figure 3-1 Schematic of UKCCSRC PACT facilities this thesis investigates the performance and adaptation of the two microturbines on site.

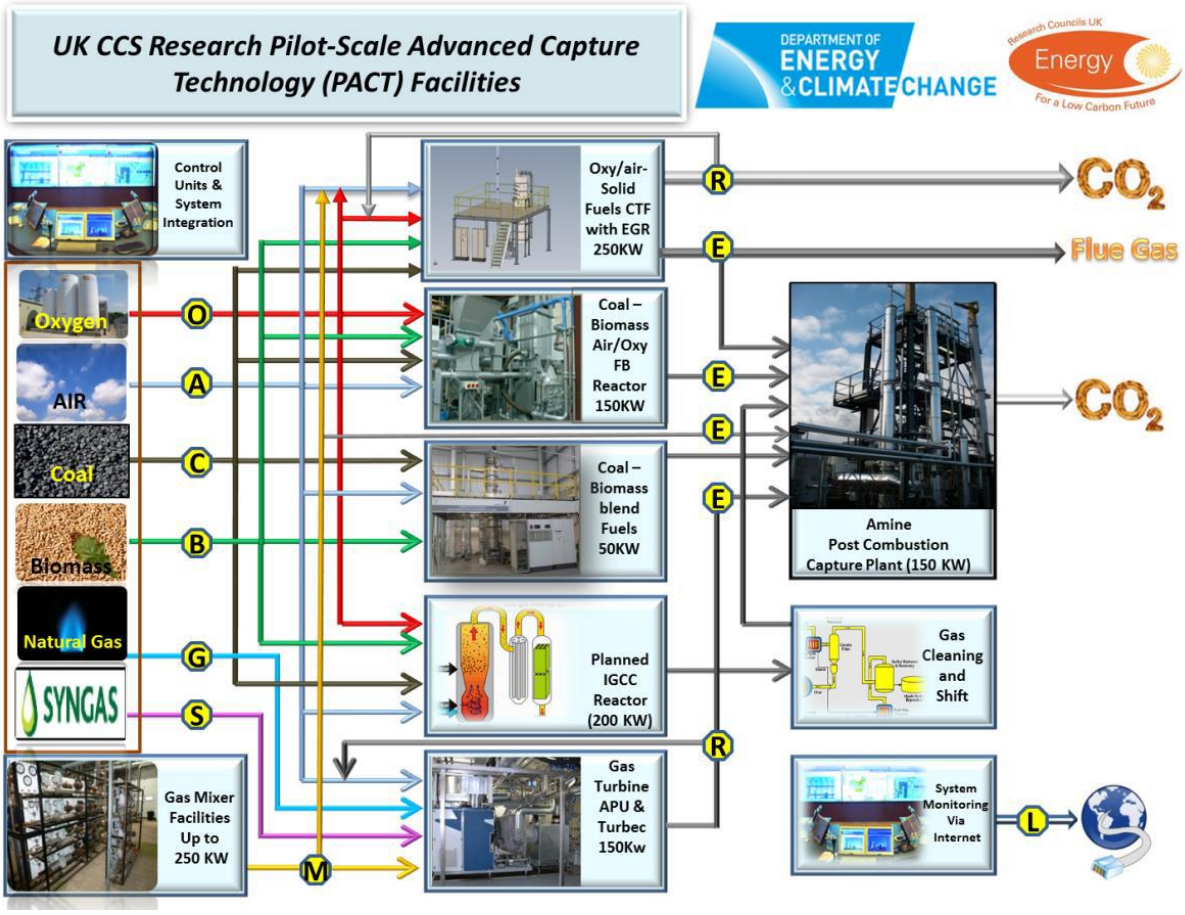

Figure 3-1 Schematic of UKCCSRC PACT facilities

The turbines are the same model but different series. They are rated at 100kW electrical output, and have a Combined Heat Power unit attached with 165kW output, and it consumes 333kW of fuel per hour. Both are second-hand reconditioned units and so the performance may not be up to the manufacturer's specification, particularly the older Series 1 model.

The base performance of both Turbec 100 microturbines must be established before adaptation for enriching CO_2 exhaust content, and for comparison. For this the emissions performance and efficiency of the turbines have been established across all turn down ratios and compared in combination with the capture process so it can accurately be determined as to what impact the alterations to the turbines have upon on the energy intensity of carbon capture for the whole process and its efficiency.

Initial experimentation will establish their current performance, in regards to maximum and minimum power output and their associated emissions. This data was collected across the range of both turbines minimum and maximum power output.

The turbines will be run at steady state for 15 minutes, 3 times at each power rating, 40 – 100kW in accordance with ISO 2314 to determine emissions performance. Steady state was determined through a number of factors, the first was ensuring warm up and consistent temperature that could impact emissions. This was done using the turbine outlet temperature stabilising close to 645°C, and with the addition of more thermocouples TC4 was also a reliable indicator of steady temperature when it rose above 615°C. In addition to this constant power generation and engine speed being achieved, with minimal variation during test runs. Of highest importance are the CO, CO_2 and NO_x emission levels. The data was analysed and outliers were investigated and if insignificant dismissed before the remaining data will be combined that's finding a mean average emissions for each turbine at each power rating and the efficiency of the turbine.

The turbines ran with the absorption capture plant in order to calculate the overall efficiency of the process without an enriched level of CO_2 in the exhaust, or the Humid Air Turbine process.

This initial data was used to determine the base performance of the turbines that can be then used for comparison with new data from simulated EGR and the HAT process. Looking at the effect the processes have on the turbines emissions, efficiency, and the total processes

efficiency. This data will provide a relative comparison that indicates the relative positive or negative changes in the efficiency and emissions performance.

Each test base performance test received multiple runs at several power outputs on each turbine in order to ensure consistency in the results. Time constraints meant that 3 runs were unachievable since 15 minutes running at each power, with allowances for 5 minutes ramping up or down is 20 minutes per test. This would be a total of 360 hrs, or 45 working days, which is towards the upper limit of the budget testing.

3.1 Beighton Facilities

There are two micro gas turbines at the PACT CORE facility. Both are Turbec T100 PH, provided by NewEnco. The turbines are rated to provide 100kW of electrical power, with combined heat units providing an additional 165kW of thermal power from hot water distribution. The supplied as new efficiency is 30% electrically, and up to 77% with the combined heat units included. Figure 3-2 Photograph of Turbec series 1 gas turbine. shows the turbine for which most of the testing was conducted.

Figure 3-2 Photograph of Turbec series 1 gas turbine.

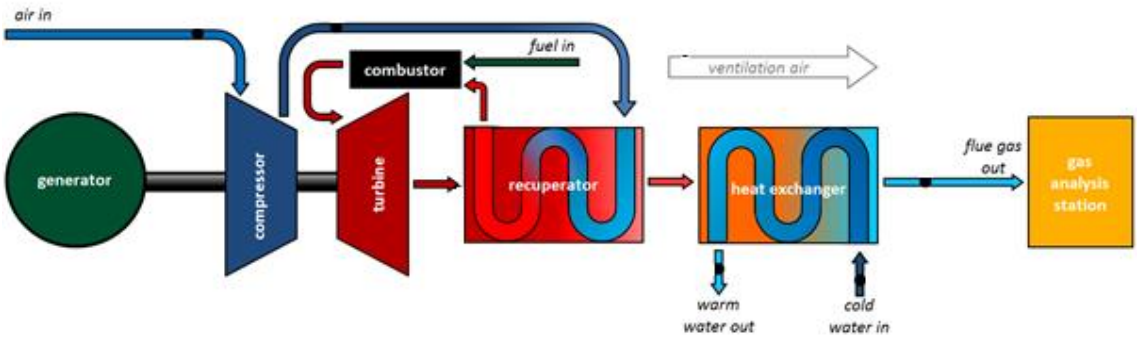

Figure 3-3 Turbec T100 PH component schematic

The turbine components are depicted in Figure 3-3 Turbec T100 PH component schematic. The turbine is a single shaft, where the compressor is driven by the turbine, and to which the generator is also attached to one end. Ambient air is compressed by the centrifugal compressor to the correct pressure ratio for the turbine at the desired power output. The maximum designed pressure ratio is 4.5:1 (3.5BarG). This pressurised air passes through the recuperator heat exchanger, where heat is recovered from the exhaust gases of the turbine outlet. After recuperation, the air enters the combustion chamber. This heat recovery significantly increases the overall turbine efficiency, above that of a simple cycle turbine. In the combustion chamber, neutral gas mixes with the swirled oxidising air, and there is electrical ignition. The combustion mix is air rich, and fuel lean, thus ensuring complete combustion and reduced emissions, such as NO_x, without post combustion treatment. However this does mean additional unnecessary work has to be done by the compressor.

The combusted gas passes through the radial turbine, thus driving further compression and the generator. The combustion gases enter the turbine at up to 950°C and 4.5 bar, this expands through the turbine, with the pressure decreasing to almost atmospheric and the temperature 650°C, at which point it passes through the hot side of the recuperator heat exchanger, thus heating the compressed oxidising air. After recuperation in the combined heat power units, the gas enters the water heat exchanger at 300°C, this improving the net efficiency of the turbine, before passing through the building exhaust pipe at 90°C. The turbine auxiliary systems include

lubrication, cooling, externally housed coarse inlet and fine internal air filtration, of which the pressure drop is monitored on the Series 3. There is also a natural gas compressor on both units, raising the fuel pressure up to 6.5 bar, in the series this is incorporated in the unit, and is external to the Series 1.

One of the turbines is an older Series 1 100kW model, however its peak power generation is slightly below this due to age and work fatigue, although it was reconditioned before the PACT facility received delivery of it. The newer turbine is a Series 3 and also rated at 100kW although capable of generating slightly more than this in reality.

Currently the two turbines ancillary equipment set up only allows for one turbine at a time to run. This is due to shared flue gas, water cooling. During establishment of baseline performance generated power could not be dumped to the national grid, and instead was used to power an electrical heater that was in turn cooled by a fan. This means the Standard Operating Procedure must be extra vigilantly followed when switching between use of one turbine and another, to ensure adequate air provision, exhaust and cooling to avoid the turbines tripping, the dynamic loading of which is not ideal for ensuring the turbines enduring performance.

After the ancillary equipment is correctly set up for the chosen turbine to run and the isolator switches on the turbines are at an on position the start up, load generation and shut down can be controlled remotely.

The newer Series 3 turbine has a connection that allows its control and performance to be controlled by the manufacturer's software. The older Series 1 has slightly more limited remote control and performance monitoring functionality through a computer browser, however the browser does not provide data collection options

The WinNap software connected directly to the turbine via LAN connection allows more thorough observation of parameters through multiple inspection windows, with the ability to also log this data. The WinNap software also allows some control of the turbine, changing power reference, and turbine alarm signals.

3.2 Methodology

3.2.1 Data Acquisition

The performance of the microturbines was monitored by their power output, fuel consumption and the monitoring of species changes in the exhaust gas as an indication of the efficiency of the combustion occurring and the impact that EGR has upon the process. The turbine performance data will be monitored and recorded through Turbecs own software. The Turbec software allows the monitoring of fuel and air inlet temperature, turbine exit temperature, exhaust gas temperature. Initially data from the Horiba analysers was logged, monitoring SO_2, CO_2, O_2, NO_x, and CO in the exhaust gases. Unburned hydrocarbons will also be analysed and logged. This was later upgraded to FTIR monitoring using Calcmet libraries and software for recording of results.

Flow meter readings and data from National Grid on natural gas composition is used to calculate the energy input.

There is provision to monitor or calculate most aspects of the turbine performance. However during the baseline testing, pressure and temperature measurements were more limited with no measurements before and after the compressor, in the combustor and at the turbine inlet point.

At the start of all testing days the analysers where necessary were zeroed and calibrated, and at the end the calibration was checked.

For the Signal and Servoflex analysers used this was done by zeroing with a nitrogen purge, and known calibration cylinder gases of analysed species being used to set a point on the analyser ranges, with the analyser then using proportional extrapolation to give readings within its range.

For the FTIR zeroing was done using a nitrogen purge for a “zero” spectrum to be generated, and then an air “background” spectrum was taken. The ranges of the spectrum are taken from a library, and do not require individual calibration.

To effectively determine the combustion and turbine efficiency, as well as the impact of EGR, on all the tests days the following were recorded:

The atmospheric pressure and humidity.

The combustion gas pressure into the turbine and into the combustor.

The ambient air temperature and the inlet air temperature which will be affected by the recuperation and EGR.

The turbines inlet temperature which is usually considered a key indication of potential efficiency, and the turbines exhaust temperature.

The fuel flow rate from metering and heating value from twice daily regionally reported National Grid data.

Electrical power output, and net power output.

The shaft speed of the turbine.

Figure 3-4 Horiba gas analyser.

The Horiba analysers Figure 3-4 Horiba gas analyser. were replaced by the FTIR due to calibration difficulties since it was not possible to attain accurate readings with the analysers during the initial independent testing. It was evident that the readings were incorrect since even using sample gases, such as air with known O_2 and N_2 concentrations values, were significantly different. The CO_2 readings were also known to be incorrect due the analysers being set up for CO_2 ranges above 50% due to the analyser being a repeat of a previous order for an oxyfuel rig with significantly higher CO_2 exhaust gas concentrations.

3.2.2 FTIR

The FTIR, Fourier transform infrared spectroscopy, measures the absorbance of infra-red to determine the gas species within a sample. It achieves this by measuring the absorbance and thus creating multiple data points using multiple frequencies directed at an interferometer which splits the light source that is not absorbed and directs it at a photoelectric sensor. From

all the samples collected, the absorption at each wavelength is known, and using a Fourier transform the species within the sample can be calculated.

Figure 3-5 Photograph of FTIR gas analysis setup.

The FTIR is connected as shown in Figure 3-5 Photograph of FTIR gas analysis setup. as standard, all sample lines of the exhaust flue gases are heated to prevent condensation in the line from the sample point or in the analyser. In addition filters seen in Figure 3-6 Photographs of the complete heated sample filter for the FTIR, and dissembled., prevent large debris from contaminating the cells interferometer which is very sensitive.

Figure 3-6 Photographs of the complete heated sample filter for the FTIR, and dissembled.

Multiple spectrums are created over multiple ranges of infra-red, then the Fourier transfer analysis is used by the computer program to create a spectrum of the absorption for the sample. The spectra must be compared to the background absorption and transmittance to determine the difference that a sample gas creates on it. The background spectrum is taken before sampling and should be replicable, significant deviation from the shape shown in Figure 3-7 Example of optimum FTIR background reading shape, is a strong indicator of potential fault that needs resolving.

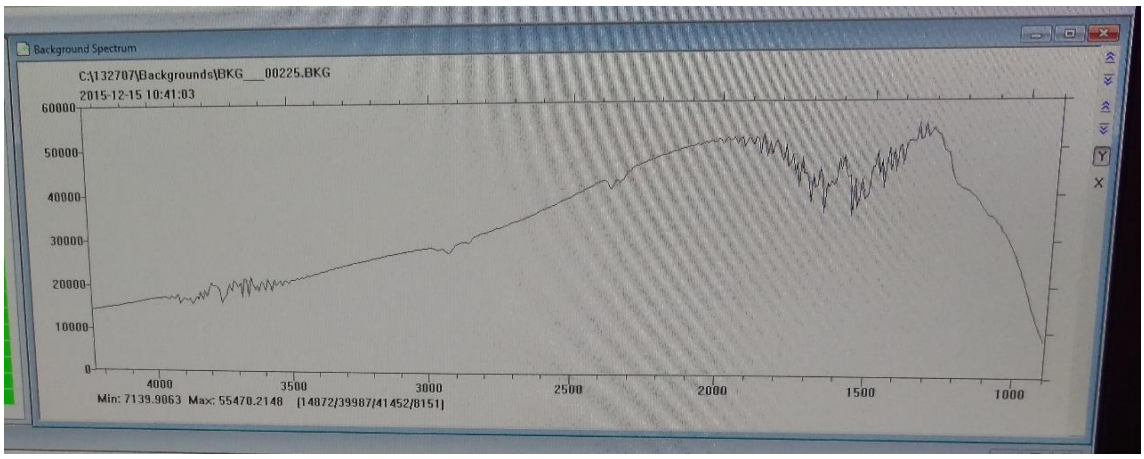

Figure 3-7 Example of optimum FTIR background reading shape.

The instrument must also be zero checked. Nitrogen is a diatomic molecule and does not absorb infrared radiation, and hence will not interfere with the FTIR sample readings. It is used to purge the cell interferometer between samples, and is used as a zero check gas to ensure that there is not any unexpected absorbance. The optimum zero shape will be relatively flat as Figure 3-8 FTIR zero

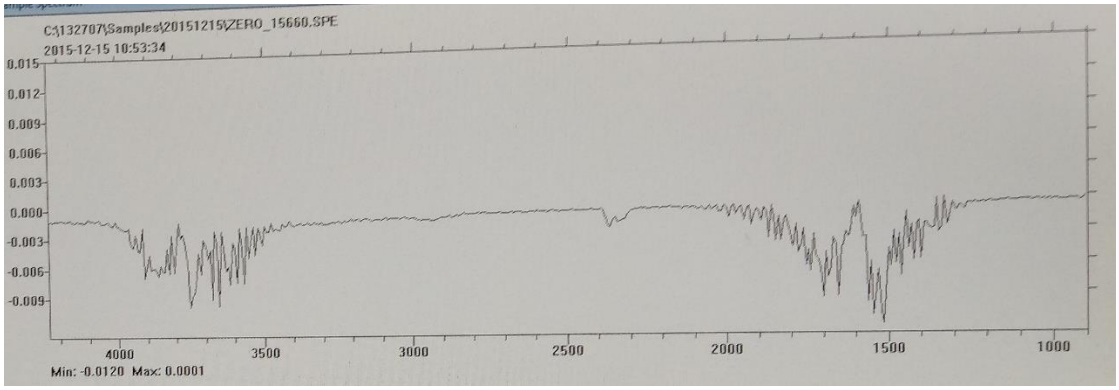

Figure 3-8 FTIR zero example.

The Calcmet software for the FTIR contains a significant volume of intellectual property in the form of spectrum libraries. These libraries contain the standard expect spectrum for different gas species and concentrations. From this library, a selection was made to scan for relevant expected gas species. As in Figure 3-9 Highlighted gas species in FTIR are plotted during testing, but all values are recorded. Even if a species has not be selected, if required old sample spectrum can be analysed to see if they contain any gas species within the library. It is the advantage of

the Fourier transformation of the results that makes the FTIR relatively quick, with the ability to detect multiple species in single samples.

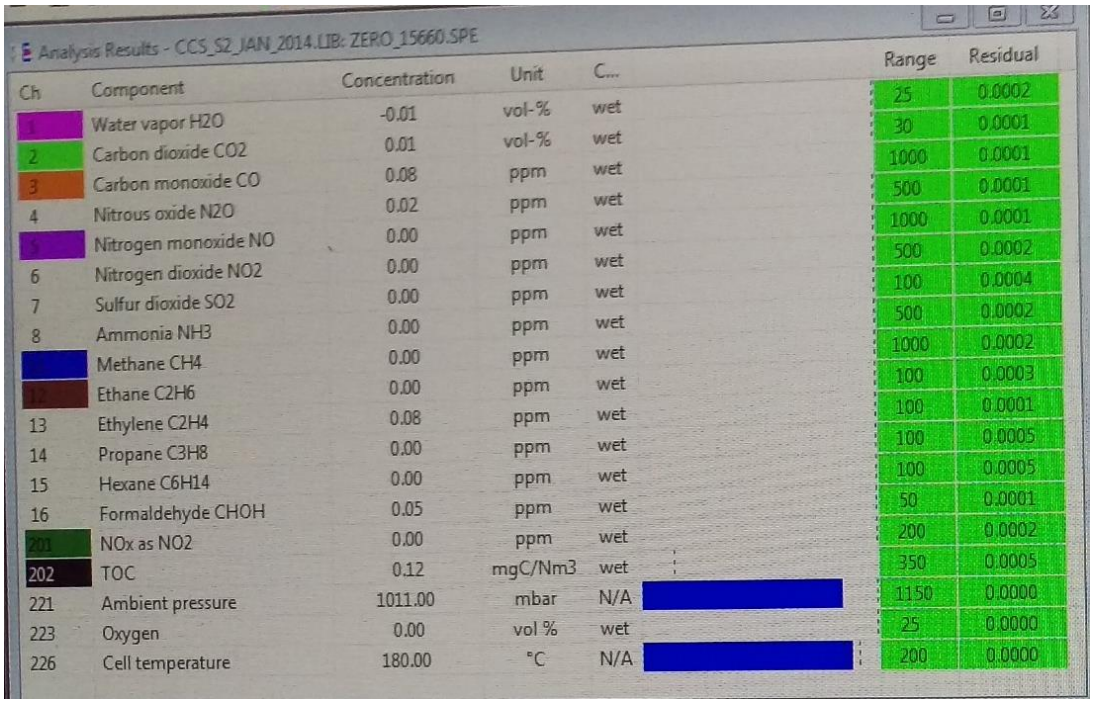

Figure 3-9 Highlighted gas species in FTIR library.

3.2.2.1 Accuracy of the Results

The FTIR uses absorption units, the ratio of incident light to absorbed light. The residual values visible are effectively measures of the "error" in terms of the residual absorption units. The known sample spectrum is added to the library, the sample may then present peaks at 1.2um and this is then used to identify CO_2, the amplitude of absorbance, or the amount absorbed at this frequency is then used to indicate the concentration of the sample. This means that if a 5% CO_2 sample would be expected to have x absorption units, and the sample actually reads x-0.001, then the 0.001 is the residual from the expected value for that concentration and the actual sample reading. For all samples, there is a residual value recorded in the raw data, so the residual is a measurement of the discrepancy, however it is not necessarily a linear functional representation of the error as a sample can contain multiple gas species with overlapping spectra that could interfere with the expected absorption. It is however an indicator of how accurate the sample is. Calibration gases of CO, and CO_2 were passed through the FTIR, showing

the results of CO to be within 1ppm of the cylinder certificates, and providing the exact volume percentage of CO_2. These results are reassuring, however this cannot be taken to be indicative of the accuracy of all gases due to the nature of the FTIR sampling technique.

3.2.3 Servomex

Oxygen for baseline measurements was measured using a Servomex Mini MP 5200. The oxygen was sampled from the same point as the FTIR sample was drawn.

Figure 3-10 Photograph of the Servomex MP 5200 & sample condensing unit.

The Servomex Servoflex MiniMP 5200 analyser can monitor O_2 and CO_2 and this is done using a nondispersive infrared sensor, where infrared light is passed through the sample gas where the species specific wavelengths are absorbed by the CO_2, a filter that blocks all frequencies outside the CO_2 range covers an infra-red sensor which is used to measure the difference between the IR emitted and absorbed, this corresponds to the concentration of CO_2 in the sample. The O_2 analysis is paramagnetic as O_2 is attracted to strong magnetic fields it fills two glass spheres that have a mirror mounted between, the field causes the suspension to rotate, a light reflects off the mirror and photocells detect the change caused by the movement thus generating a signal

that is linked to a feedback signal with a current going through the rotating suspension and this current is proportional to the concentration of oxygen.

3.2.4 Fuel Meter

Both the Series 1 and 3 gas turbines at the Low Carbon Combustion Centre Beighton, share a Quantometer turbine flow meter, with the supplier certification claiming a less than 1% relative error at calibration for the flow rates measured, however this is a suspiciously accurate figure and there are concerns as to the potential error this introduces. As much as possible this is mitigated through long test lengths, at minimum of 15 minutes each, and multiple runs of many tests. The gas flow rotates an axial turbine in its path, which in turn drives a meter display.

Figure 3-11 Photograph of the Quantometer gas meter.

The meter is designed and calibrated for flows of between 10 – 100m^3/h. However as the meter only sends signals every 0.1m^3 then readings are taken manually for improved accuracy to 2 decimal places.

Common S.A manufactured and supplied the Quantometer, with calibration certificates showing the relative error for readings. The maximum relative error is 0.63% at 25m^3/h, dropping to 0.36% at 40m^3/h. The meter causes minimal disruption to the gas flow, thus causing a maximum

pressure drop of 5.85mbar (fuel is combusted at 5-6bar). This is depicted in Figure 3-12 The error and pressure drop of the Quantometer.

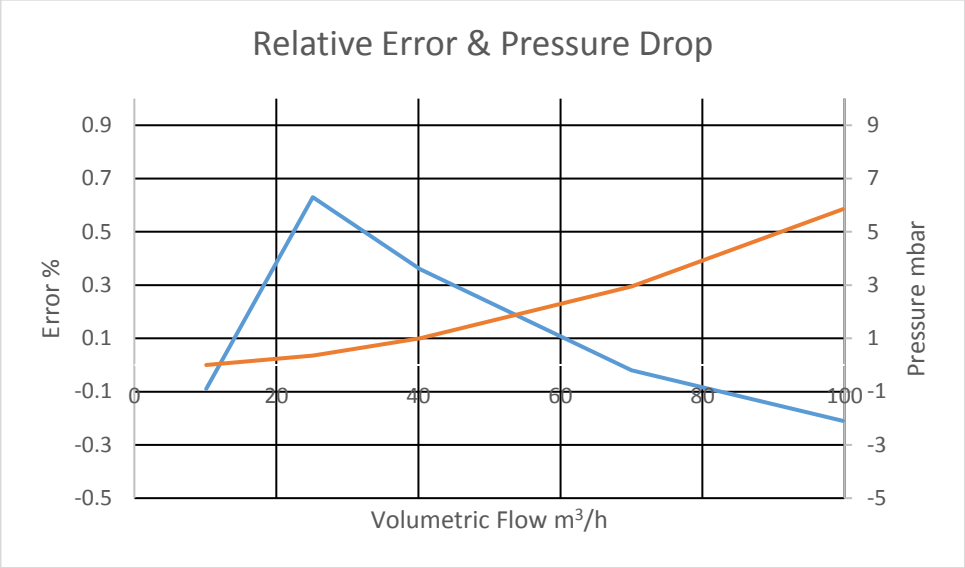

Figure 3-12 The error and pressure drop of the Quantometer.

3.2.4.1 Fuel Composition

Energy data is provided online by the National Grid in terms of calorific value. Further details of the composition was supplied on request for each day tested.

National Grid provides twice daily reports, available online, of post code specific gas calorific values. Though it is possible there may be dead spots, and lag in supply, the values reported by National Grid were very consistent. In addition composition can be requested, this data was similarly consistent.

The calorific value of any fuel is the amount of heat energy available when it is fully combusted, hence it is critical for determining turbine performance and efficiency. The natural gas supply is regulated to keep within 37.5MJ/m^3 to 43 MJ/m^3.

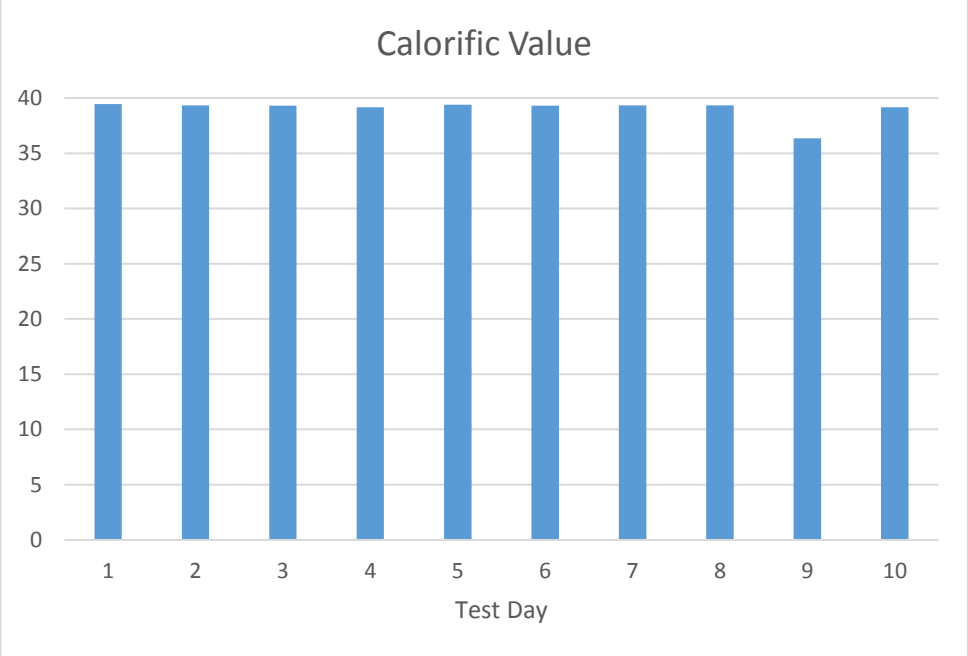

Figure 3-13 Natural gas calorific value.

The average CV for all the test days was 39.3MJ/m^3, with a standard deviation of 0.1MJ/m^3. This is with the exception of test day 9, when there was a significant drop in the average fuel CV to 36.35MJ/m^3. This is shown in Figure 3-13 Natural gas calorific value.

The National Grid determines the calorific value of the gas supplied through chromatography at multiple reception terminals throughout the UK. The calorific value for gas supplied to PACT is from the "Exit Zone" EM, Blyborough. The CV is calculated from the chromatographs, summing the CV stated in ISO-6976, Natural gas —Calculation of calorific values, density, relative density and Wobbe index from composition. All calorific values are gross, high heating values (HHV), turbine electrical efficiency is calculated on a Lower Heating Value basis, which is a lower net value, as the latent heat of vaporisation of water is not recoverable for this process.

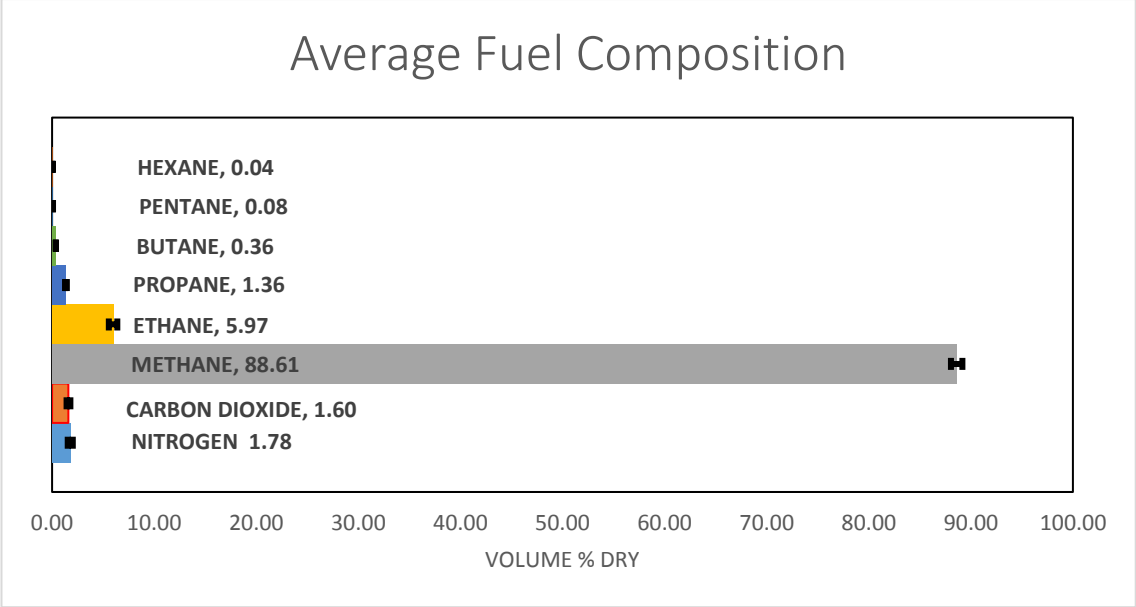

Figure 3-14 Natural gas fuel composition.

Using Figure 3-14 Natural gas fuel composition, and ISO 6976 the Higher Heating Value was calculated to be the same as the stated values for each test days, and to calculate the turbine electrical efficiency then a lower heating value was determined in Table 3-1 Gas calorific value calculation.

Table 3-1 Gas calorific value calculation.

	Typical Analysis (mole %)	Density g/L	Molar Mass g/mol	Molecular Weight	Litres/ Mole of Natural Gas	% Volume Composition	Mole/ m3	Moles in m3 Gas	CV Superior kJ/mol	HHV MJ/mn3	Gas Specific Enthalpy HHV MJ/mn3	CV Inferior kJ/mol	Gas Specific Enthalpy LHV MJ/mn3
Methane	88.610	0.6556	16.04	14.21	20.94	88.61	42.31	37.49	891.56	37.73	33.43	802.69	30.10
Ethane	5.970	0.5440	30.07	1.80	1.41	5.97	42.31	2.53	1562.14	66.10	3.95	1428.84	3.61
Propane	1.360	2.0090	44.1	0.60	0.32	1.36	42.31	0.58	2221.10	93.98	1.28	2043.37	1.18
Butane	0.360	2.4800	58.12	0.21	0.09	0.36	42.31	0.15	2879.76	121.86	0.44	2657.6	0.40
Pentane	0.080	0.6260	72.15	0.06	0.02	0.08	42.31	0.03	3538.60	149.73	0.12	3272	0.11
Hexanes	0.040	0.6548	86.18	0.03	0.01	0.04	42.31	0.02	4198.24	177.65	0.07	3887.21	0.07
Nitrogen	1.780	1.2510	14	0.25	0.42	1.78	42.31	0.75			0.00		0.00
Carbon Dioxide	1.600	1.5620	44	0.70	0.38	1.60	42.31	0.68			0.00		0.00
Oxygen	0	1.4290	16	0.00	0.00	0.00	42.31	0.00			0.00		0.00
Hydrogen	0	0.07	1	0.00	0.00	0.00	42.31	0.00			0.00		0.00
				17.86	23.59	99.80		42.23		Total	**39.28**		35.46
			Density kg/m	**0.80**									

Using the fuel data from the composition, it is possible to determine the moles of oxygen required for stoichiometric combustion of the gas. This is the minimum amount required for complete combustion of all gas species to form CO_2 and H_2O. From the moles of oxygen the corresponding volume can be found, and with air comprising 29% nitrogen and 21% oxygen, the volume of air for combustion can be accurately estimated as Table 3-2 Stoichiometric calculation.

Table 3-2 Stoichiometric calculation.

	No Carbon	Molecular Weight Carbon	Molecular Weight Hydrogen	No CO2	Molecular Weight CO2	No H2O	Molecular Weight H2O	O2 Req	Molecular mass of O2 Req	Moles O2 req /m3 fuel	Moles of H2O exhaust/m3 fuel	Moles of Exhaust CO2/ m3	Volume of Exhaust CO2/m3 fuel
Methane	1	12	4	1	44	2	36	2	64	74.99	74.99	37.49	0.84
Ethane	2	24	6	2	88	3	54	3.5	112	8.84	7.58	5.05	0.11
Propane	3	36	8	3	132	4	72	5	160	2.88	2.30	1.73	0.04
Butane	4	48	10	4	176	5	90	6.5	208	0.99	0.76	0.61	0.01
Pentane	5	60	12	5	220	6	108	8	256	0.27	0.20	0.17	0.00
Hexanes	6	72	14	6	264	7	126	9.5	304	0.16	0.12	0.10	0.00
Nitrogen					0			0	0			0.00	0.00
Carbon Dioxide	1	***12***		1	44			1	32			0.68	0.02
Oxygen					0			0	0	0.00	0.00	0.00	0.00
Hydrogen			***1***		0	0.5		0.25	8	0.00	0.00	0.00	0.00
										88.13	85.95	45.83	1.03

Below in Table 3-3 Air volume for combustion, is the air required for complete combustion per m^3 of fuel, this is not the total volume of air used. With the volumes of air and fuel, and with measured CO_2 volume percentage data, it is possible to determine the total volume of the exhaust gas, and the air:fuel ratio used for combustion in the turbine. This data can then be used to plan future experiments by altering the combustion air composition.

Table 3-3 Air volume for combustion.

		Air for combustion	
	Moles	kg o2/m3 fuel	m3 air/ m3 fuel
Total O2 from air (21%)	88.13	2.82	1.97
N2 (79%)	331.54	9.28	7.42
Air total	419.67	12.10	9.39
Combustion CO2	45.83	2.02	1.29

3.2.5 WinNap Data

The WinNap program monitors and controls the performance of the Series 1 turbine.

During the operation “watch windows” the key parameters are opened and monitored from the control room to ensure that there is no significant variation during a test run that may require a rerun. These parameters are also recorded for later review and test averaging. The parameters monitored by the program are as follows shown in Figure 3-15 WinNap monitored values

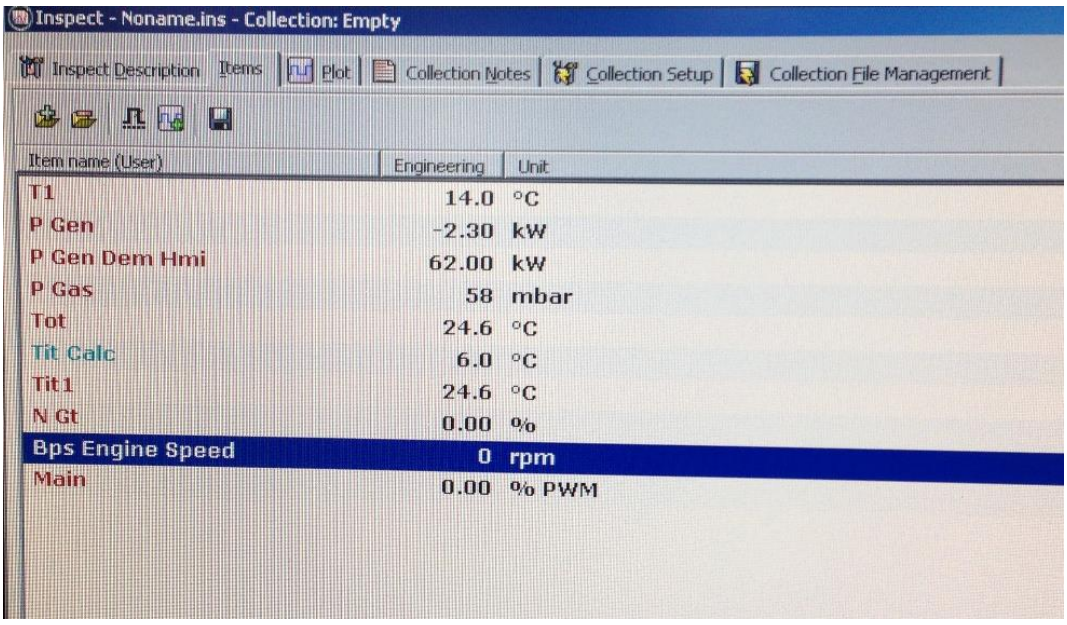

Figure 3-15 WinNap monitored values.

- PGen Dem HMI: The set power point
- PGen: The actual generated power
- BPS Engine: The speed of the engine (rpm)
- T1: The measured inlet air temperature
- TIT Calc: The calculated value for turbine inlet temperature
- TOT: The measured turbine outlet temperature
- NGt: The current running percentage of the maximum engine speed
- PGas: The natural gas fuel combustor inlet pressure
- Pilot: The percentage open that the pilot fuel valve is
- Main: The percentage open that the main fuel valve is

Figure 3-16 WinNap test view.

The inspected values plot can then be viewed live, and are saved at 1Hz to match the frequency of collection by the developed LabView program.

Within the WinNap program, it is possible to view the basis for some turbine calculation and subsequent operations. This varies from altering alarms from being a warning or preventing start up, to showing the matrix for the fuel flow from which the mass of fuel through each valve delivered into the turbine can be calculated.

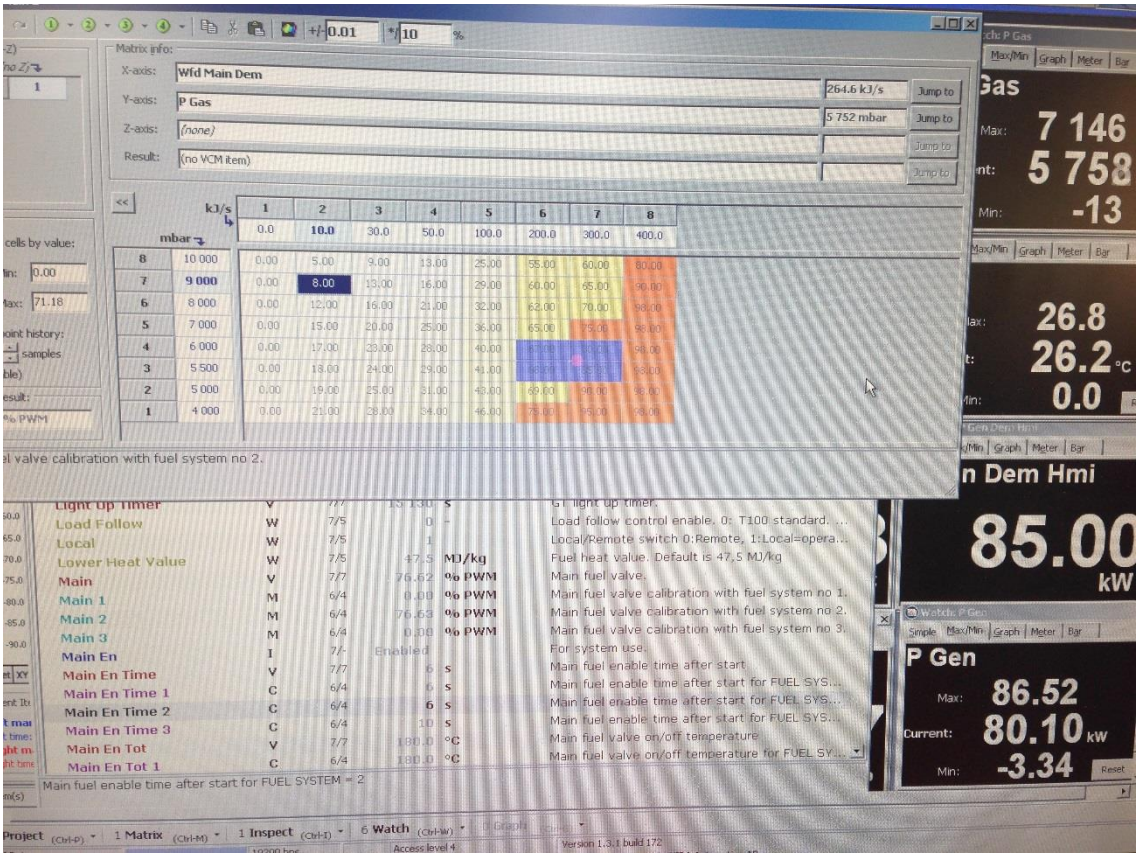

Figure 3-17 WinNap calculation matrices example.

Unfortunately, due to the age of the WinNap program it would not run stably on operating systems newer than Windows 2000, and due to conflicts with other monitoring programs for the FTIR, required an additional standalone computer.

3.3 Standard Operation Performance

To determine relative changes in performance upon the modifications and further testing of the turbine, a full performance evaluation of the turbines base performance across all turn down ratios was carried out.

As all tests were carried out once steady state was achieved, with data analysed before being used to form averages, the standard deviations of the results are relatively small and difficult to depict visually on the plotted figures, the maximum deviation of any result can be seen in Table 3-4 Instrumental errors.

Table 3-4 Instrumental errors.

Instrument	Instrumental Error		Measured	Results Max Deviation
	%	Unit		Baseline
Gasmet DX4000 FTIR	-	-	CO ppm	17.32
	-	-	CH4 ppm	3.91
	-	-	CO2 vol %	0.02
	-	-	NOx ppm	1.27
Quantometer	0.63%	0.19 m3	-	-
Turbec T100	-	-	Speed RPM	58.59
	-	-	Power kW	0.464

3.3.1 Mechanical Performance

3.3.1.1 Speed

The speed of the turbine determines the amount of power generated by the generator. Higher speeds correspond to higher mass flows, higher torque, higher frequency turning the generator magnet, moving the electrons and improving electrical current generation.

As expected the turbine speed increases with power generation to meet the demand. This behaviour can be seen with the Series 1 gas turbine in Figure 3-18 Turbine speed & power output.

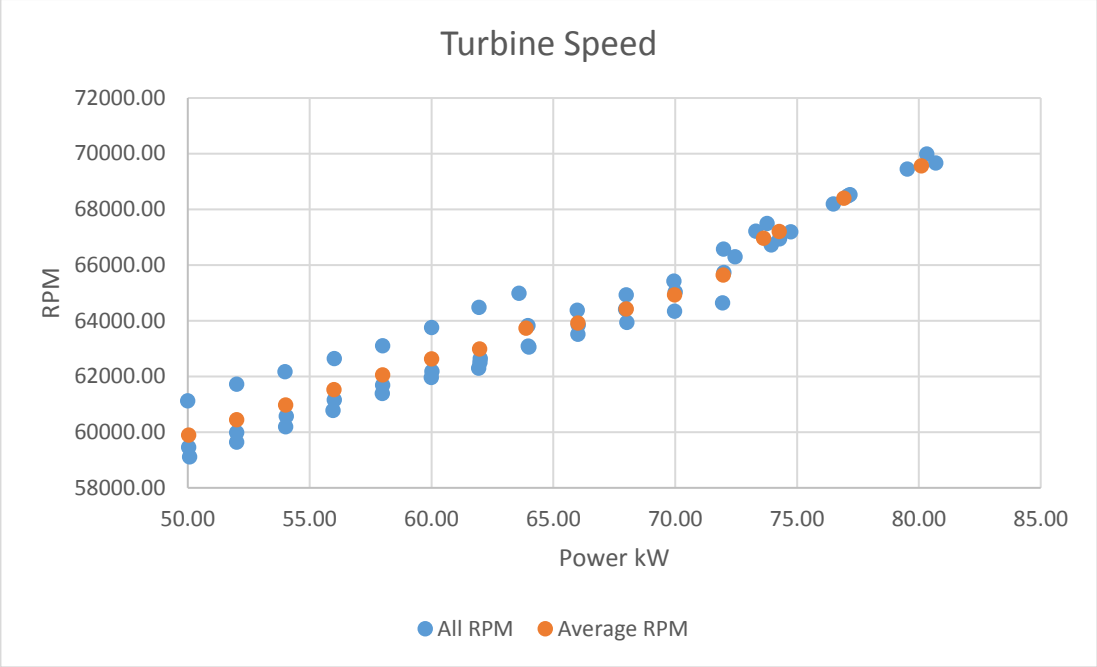

Figure 3-18 Turbine speed & power output.

There are multiple plots of speed for each power setting. The average is depicted in orange. The top of the trend showing that higher speeds were conducted on the warmest test day.

3.3.1.2 Impact of Ambient Temperature

The ambient temperature has been found to be the most critical factor in dictating turbine efficiency. Figure 3-19 Turbine speed and RPM, shows all of the baseline results over a broad range of turn down ratios that correlate the ambient temperature with the turbine speed. This relationship also correlates strongly with efficiency.

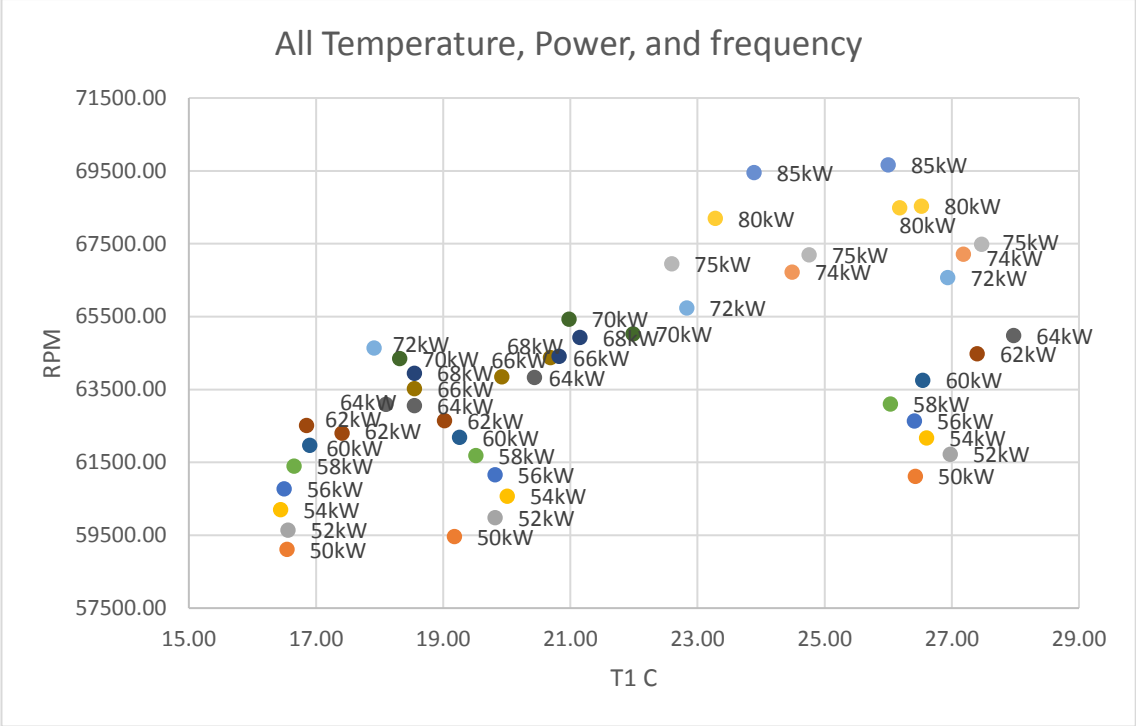

Figure 3-19 Turbine speed and RPM.

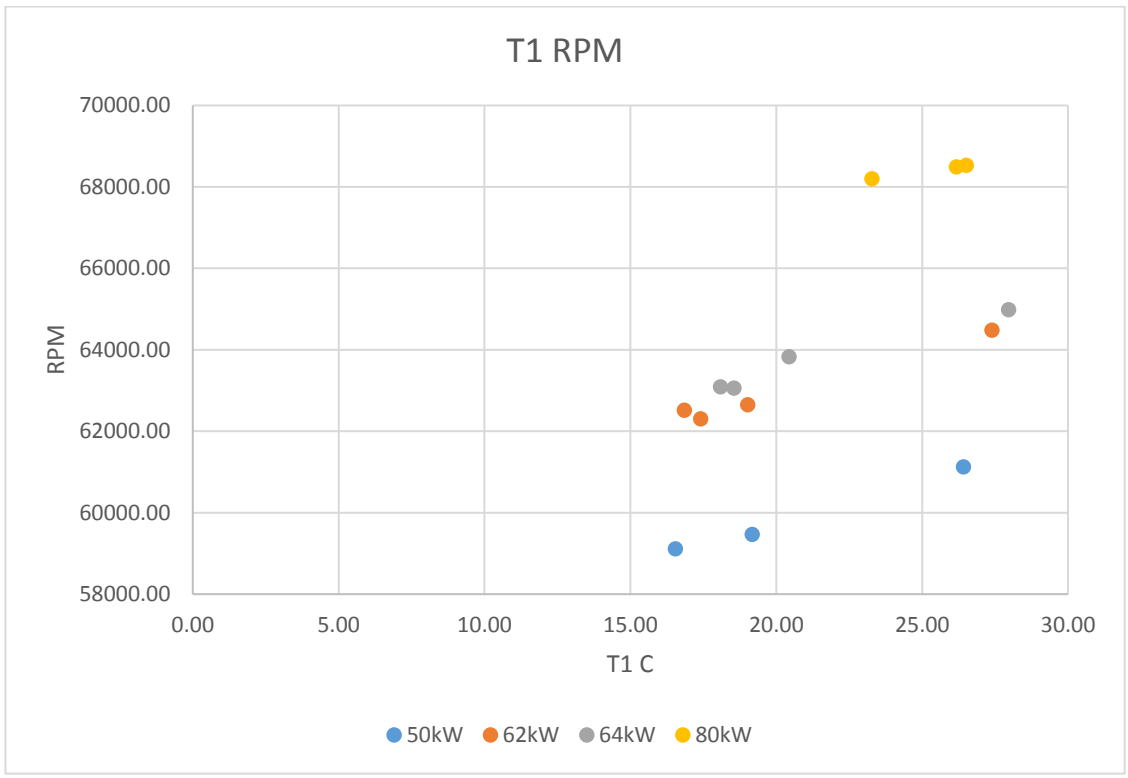

Figure 3-20 Turbine speed and ambient temperatures.

Figure 3-20 Turbine speed and ambient temperatures mirrors the traditionally observed trend of temperature and gas turbine performance efficiency drops, and the turbine speed increases

as the ambient temperature increases. This is due to the change in volume, as the Brayton cycle efficiency.

3.3.2 Emissions Analysis

As discussed where all the results for the baseline testing obtained using the FTIR and Servomex oxygen analyser.

3.3.2.1 Emissions reporting and corrections

All the reported gas species (with the exception of H_2O) are on a dry basis for comparison to industrial standards and the literature of gas turbine emission reporting. The dry basis is calculated as 3-1 follows.

$$\text{Dry Basis Volume Concentration} = \frac{Wet\ Basis\ Concentration}{1 - H_2O\ Volume} \quad \textbf{3-1}$$

Of key importance is the reporting of the NOx emissions due to their impact on the atmosphere, causing acid rain and smog which impacts on human health. The industry standard is for NOx to be reported on a dry basis corrected to 15% oxygen. This is seen in legislation such as that the EU Large Combustion Plants Regulation 2012, where it is specified that the emissions are to be reported at 273.15K, 101.3kPa. Oxygen correction is made using the equation 3-2:

$$NO_{x\ O_2\ Corrected} = NO_x \left(\frac{20.9 - O_{2_{Ref}}}{20.9 - O_{2_{Measure\ Exhaust}}} \right) \quad \textbf{3-2}$$

The EU Large Combustion Plant Directive (LCP) includes large single cycle gas turbines, and those with an efficiency above 35%, giving NOx limitations of 50η/35, where η is the efficiency of the turbine, and for the Turbec T100 Series 1 this would be equivalent to 34mg/Nm^3.

This means that the two microturbines at PACT do not fall within the stipulated emissions limits [88]. There are other applicable regional authority guidelines for air quality that are applicable, with the Greater London Authority proposing 5g/kWh for compression ignition gas engines [89].

With ordinary steady operating conditions, the Series 1 turbine is compliant with significantly lower emissions.

3.3.2.2 Combustion Performance

The largest volume percentage of emissions, other than nitrogen, are CO_2 and H_2O from complete combustion of the fuel.

The other key indicators of the combustion performance is CO from incomplete combustion, and Unburnt Hydro Carbons (UHC) which is a mixture of species, though dominated by the most prevalent in the fuel. For supplied natural gas, it can be seen that it is dominated by methane, at over 88% by volume of the supply.

3.3.2.3 CO_2

The CO_2 volume percentage steadily increases with power output. However the true CO_2 mass increase is hidden by the higher mass flow through the turbine at higher power output where the turbine frequency and pressure is significantly increased as seen in Figure 3-21 CO2 Emissions at varying power outputs.

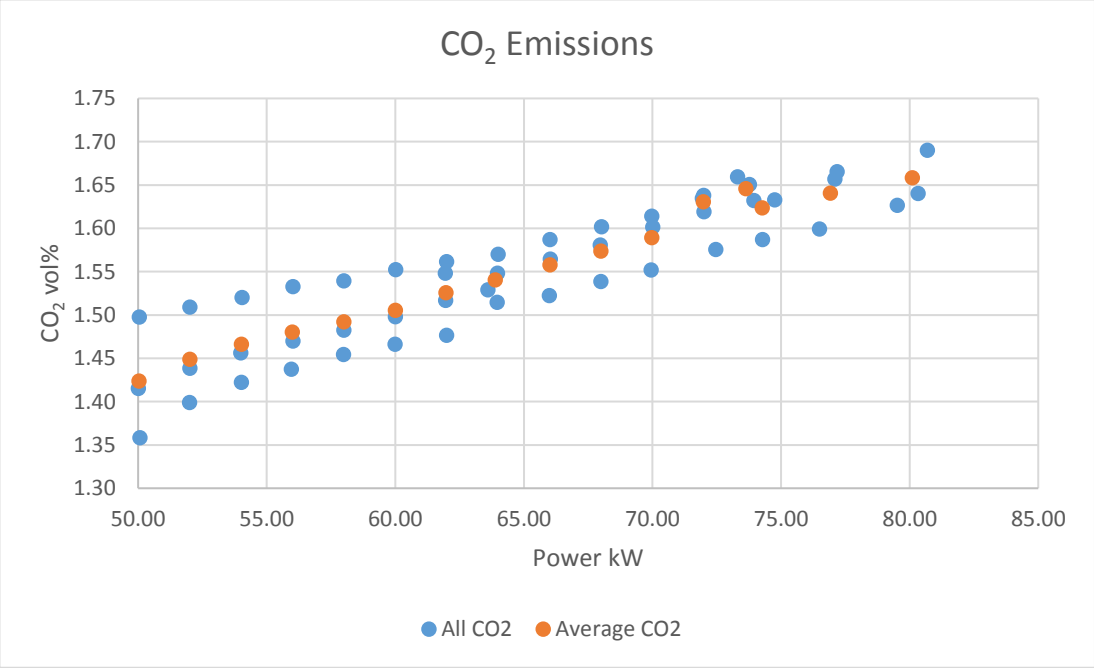

Figure 3-21 CO2 Emissions at varying power outputs.

Water vapour follows a similar pattern to that of the CO_2, as Figure 3-22 Water emissions relationship to fuel consumption shows, increasing with increasing power output, corresponding to the complete combustion of the increased fuel volume to create that power output.

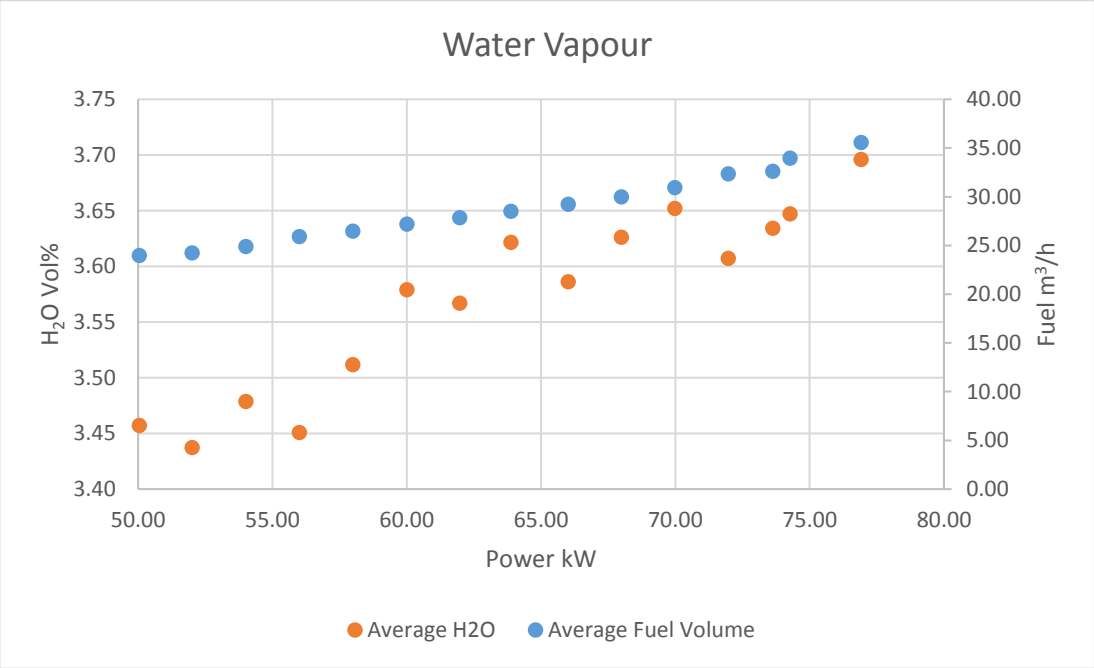

Figure 3-22 Water emissions relationship to fuel consumption.

3.3.2.4 UHC

The dominant species in the natural gas supplied is methane, higher methane in the exhaust is an indication of uncombusted fuel and poor combustion conditions and possibly insufficient residency time, poor mixing, or reduced flame speed.

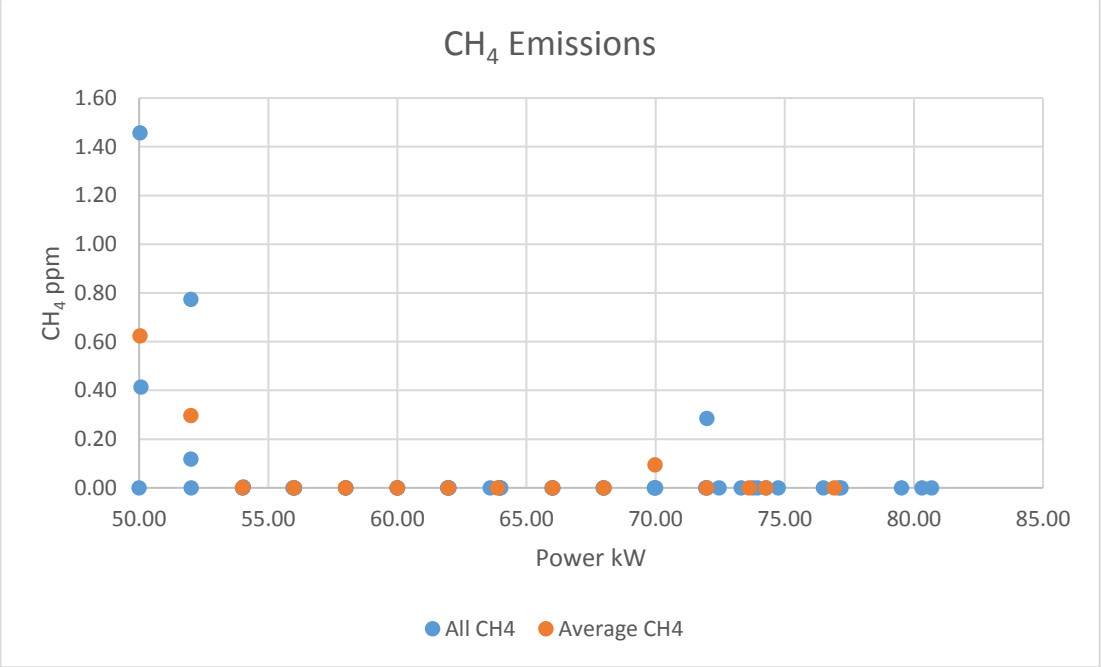

Figure 3-23 Unburnt CH4 at varying power outputs.

3.3.2.5 CO

The turbine has diminished combustion performance at lower power outputs, at the bottom of the turn down ratios. The increased CO emissions are a product of incomplete combustion, inadequate mixing and residence turbine, the reduced flame speed and temperature.

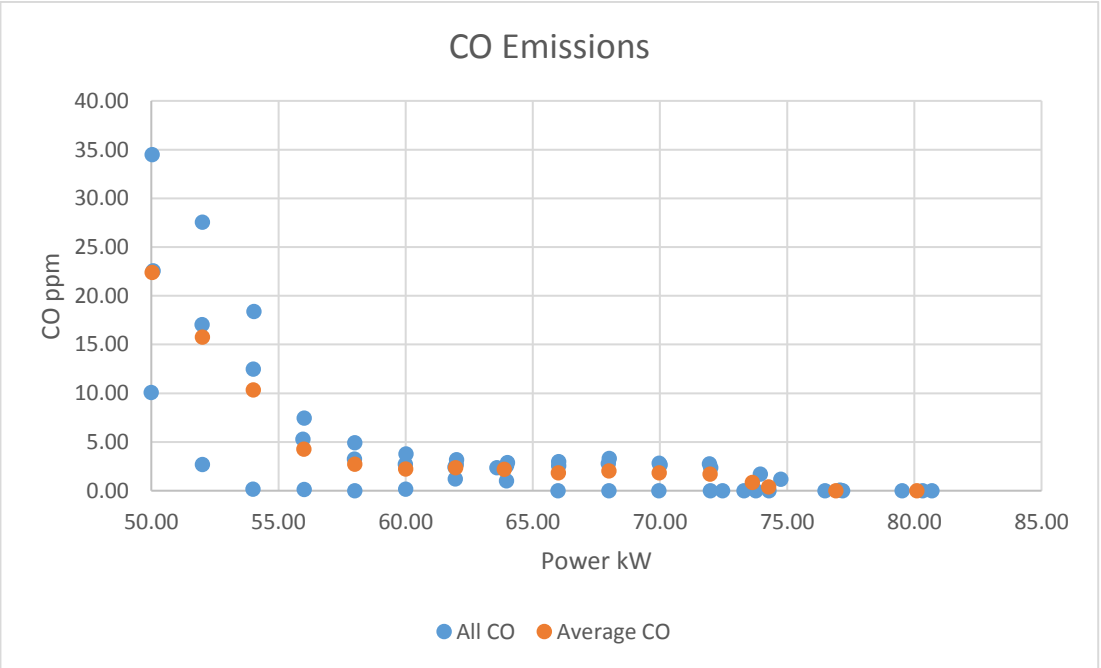

Figure 3-24 CO emissions at various power outputs.

The higher levels of CO and CH_4 at the bottom of the turbines turn down ratios provide a consistent trend. Though the ppm values may be low, they represent significant changes due to the lean fuel nature of the turbines combustion, and this means the fuel, and combustion products, will be a small part of the total exhaust.

3.3.2.6 NO_x

The NO_x is usually reported on a dry basis corrected to 15% O_2. For the purposes of comparison with the exhaust gas recirculation and enhanced oxidising mixtures, or humidified air, there are better metrics for changes in the NOx levels. This is because oxygen is displaced by the substitution of species in the air. Hence the NOx results reported corrected to 15% O_2 appear disproportionately lower..

For the purposes of comparison dry NO_x ppm results have been presented.

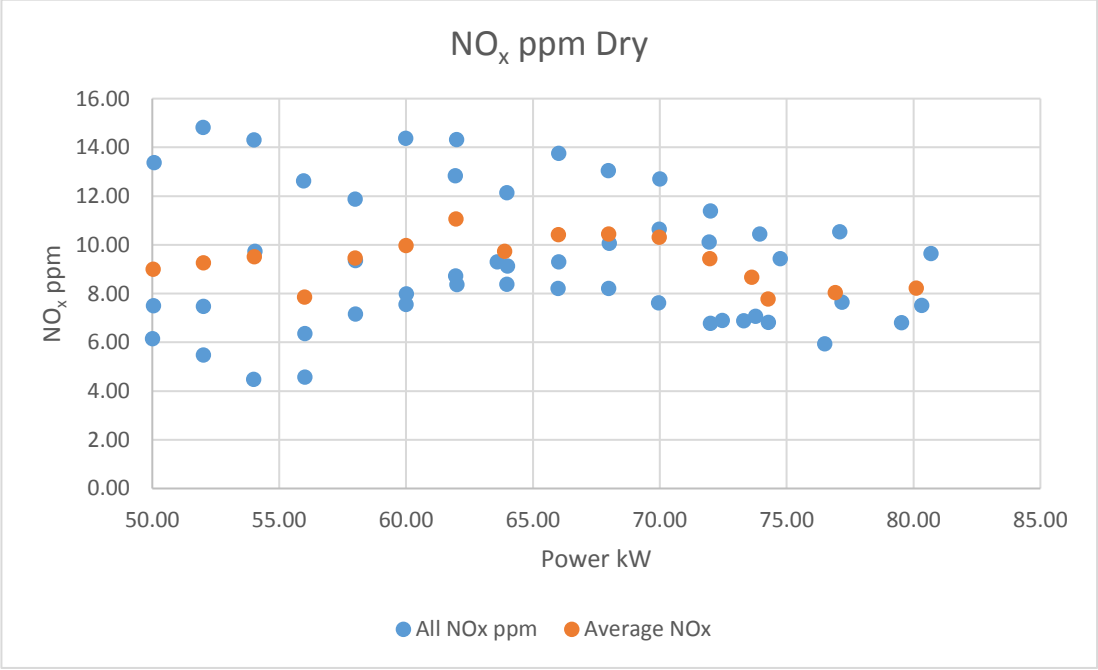

Figure 3-25 NOx ppm (dry) at 50kW – 85kW.

The more appropriate metrics for comparison are the NO_x production on a basis of fuel consumption, and turbine power output.

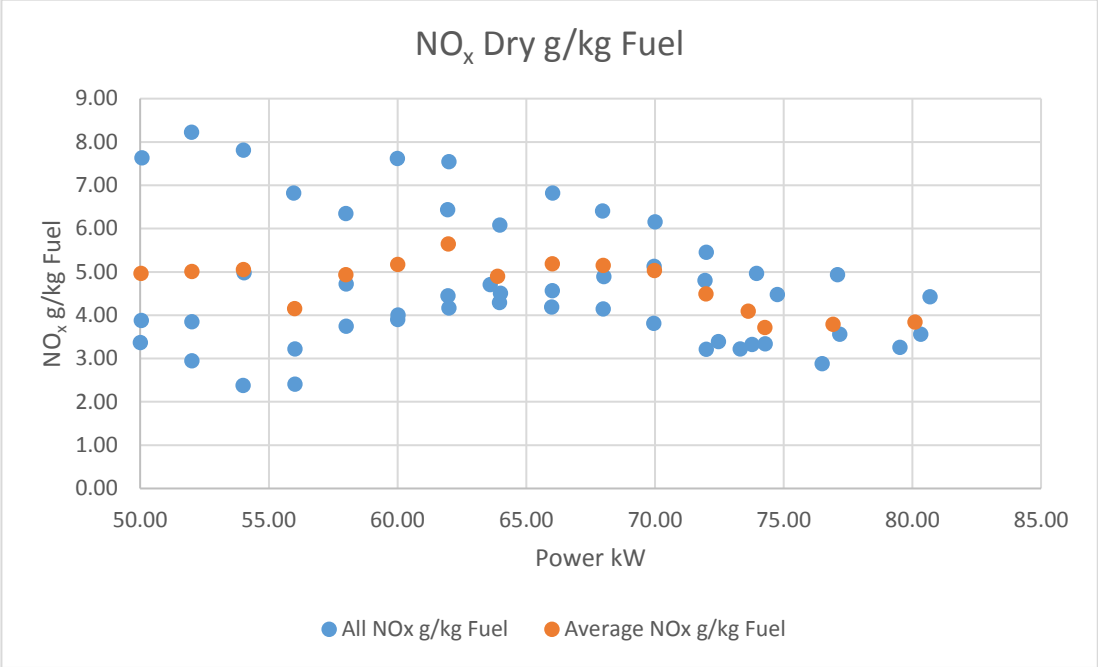

Figure 3-26 NOx reported on fuel consumption basis.

Reporting the NO_x on the basis of fuel combusted does remove the bias of changing exhaust volumes and reduced oxygen content. However it does not reflect upon the output or efficiency. Hence a lower efficiency combustion may produce less NO_x per kg of fuel due to lower combustion temperatures, but as the primary purpose of the fuel combustion is to generate power then this is not a useful bench mark. This is where the measurements, in terms of power output, is advantageous and unaffected by the changing O_2 levels.

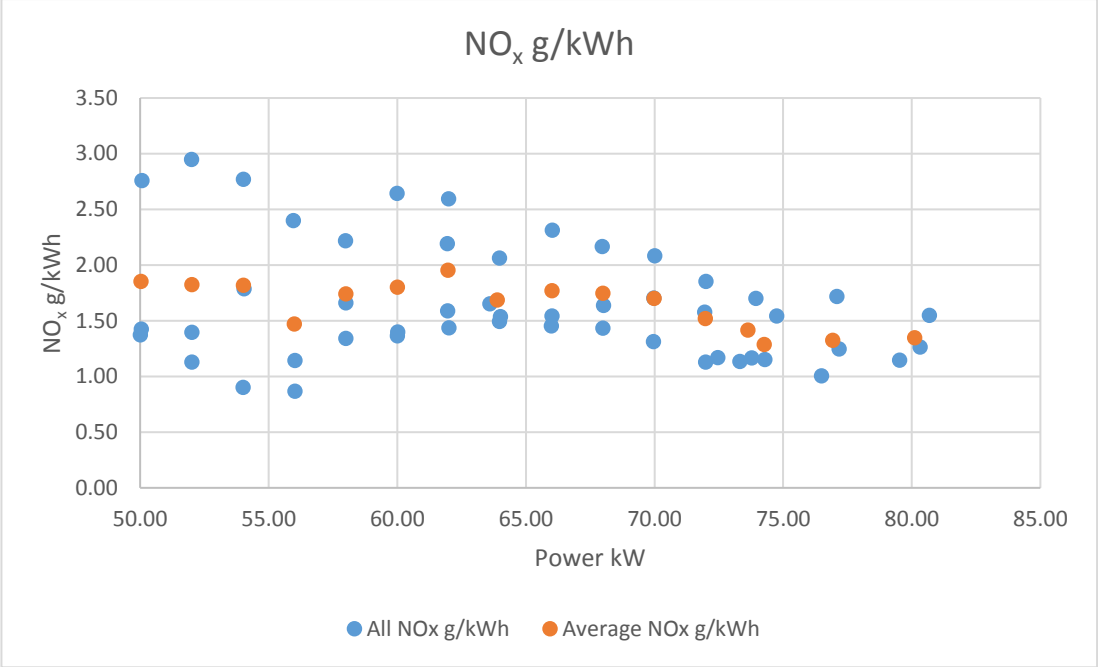

Figure 3-27 NOx reported on power output basis.

The advantage of reporting NO_x not in PPM corrected to 15% oxygen is that the exhaust gas recirculation's emissions are not unfairly judged by apparently lower emissions. This is since it is to be expected that it would produce higher emissions on that basis. Reporting the NOx emissions in terms of fuel mass flow or power generated resolves this apparent skewing of the figures, meaning all gas turbines can be judged on the same and pertinent metric.

3.3.3 Efficiency

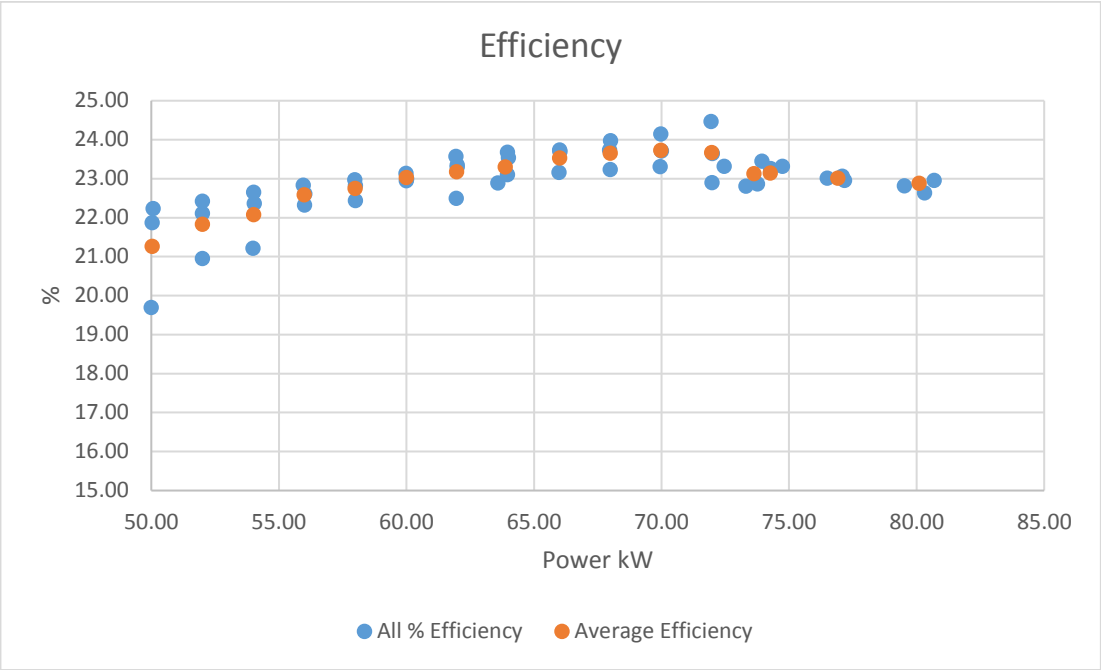

Figure 3-28 Turbine electrical efficiency.

The efficiency is plotted against power output. In Figure 3-28 Turbine electrical efficiency where the efficiency is calculated from the Kilowatts generated converted to joules. This is divided by the Lower Heating Value of the gas to give the net efficiency of the process. Also there are ancillary equipment that are powered post generation, particularly the gas compressor on the Series 1 which is external and this is in contrast to the series which have an internal compressor.

The efficiency is most affected by the ambient temperature of the oxidising air. Increased the air temperature means reducing the air density. Reducing the air density means reducing the mass flow for the same number of turbine revolutions and pressure. This means more work must be done by the turbine in terms of compression and revolutions to generate the same mass flow with the lower ambient air temperature.

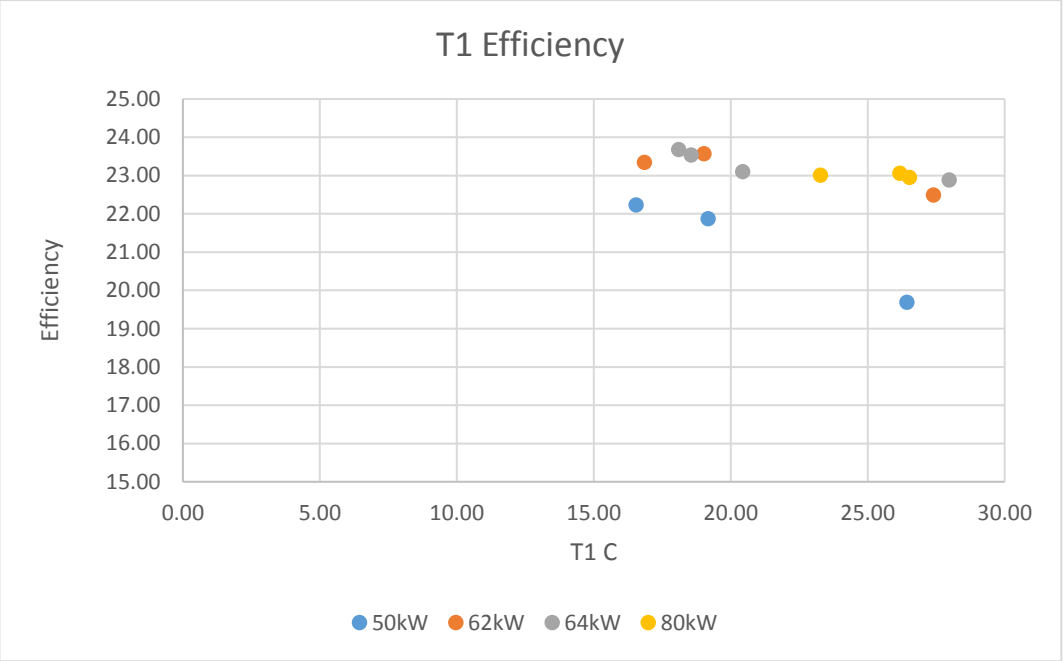

Figure 3-29 Efficiency relationship to ambient temperature.

In Figure 3-29 Efficiency relationship to ambient temperature it can be seen that across all turn down ratios increases in ambient temperature reduce the turbine efficiency. Since it is difficult to gain a spectrum of the ambient temperature results, due to the unpredictable nature of the weather and restrained group testing times, this is the broadest range of results available for the presentation of this temperature relationship from testing.

3.3.3.1 SFC

The specific fuel combustion (SFC) is an indicator of the turbine efficiency. Since changes in the overall turbine efficiency appears relatively small in comparison to the overall efficiency this is the best indicator of the change in turbine performance. Specific fuel consumption is the mass of fuel combusted per kWh generated by the turbine. This is calculated by converting the measured fuel volume flow rate into a mass determined by the fuel composition on the day of testing and this is then divided by the number of kW generated during that test to find the g/kWh specific fuel combustion for the test. An increase in specific fuel consumption is equivalent to a

decrease in efficiency as it means more fuel is being consumed per kWh generated. The Figure 3-30 Specific fuel combustion, is a mirror image of the Figure 3-28 Turbine electrical efficiency, seeing peak efficiency 65-75kW.

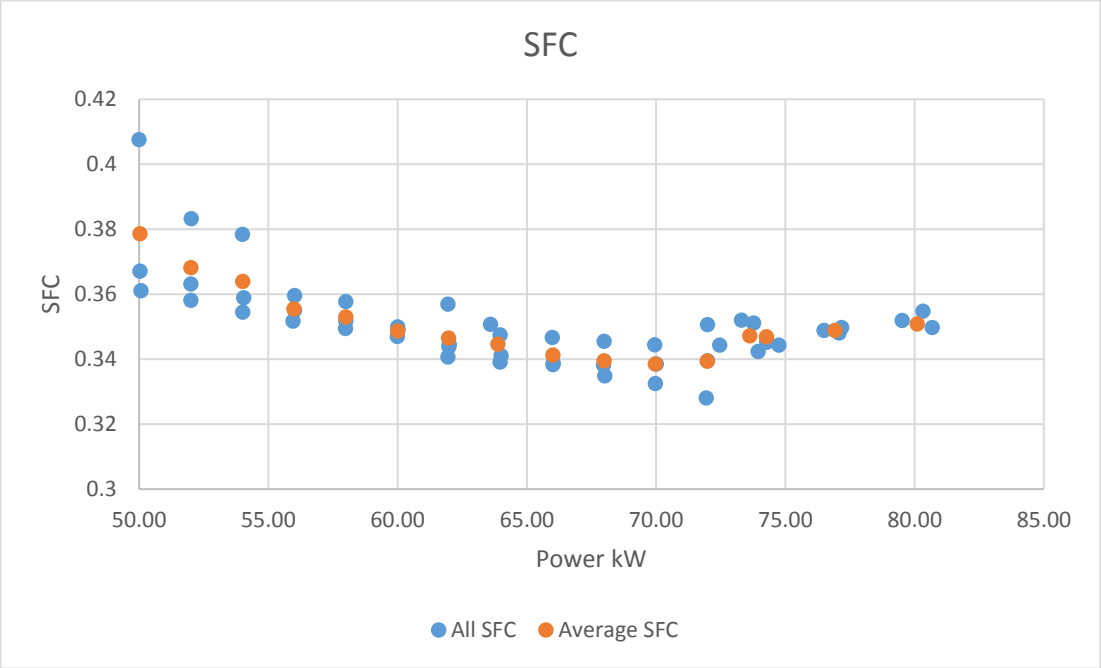

Figure 3-30 Specific fuel combustion.

3.4 Conclusions

In this chapter the baseline performance for the Series 1 Turbec microturbine has been established for comparison to alterations made for both simulated EGR with the addition of CO_2 before the compressor, and HAT with the addition of steam post compression.

It is established that combustion performance is good across most of the power range, but with evidence of some uncombusted fuel at the lowest turn down ratios of 50kW. This occurs at the lowest turbine pressure ratios, and turbine frequency. This will be at the lowest relative mass flow through the turbine, of all power settings.

Normal operating Tubine Outlet Temperature, and calculated Turbine inlet temperatures at 645C and 880C respectively have been established, that are useful indicators of flame temperature and expected efficiency.

Results replicated the well established Brayton trend of increased atmospheric temperature impacting on efficiency, with high temperatures reducing the effectiveness of the compressor, and hence the efficiency of the turbine.

These efficiencies indicated turbine performance to be significantly lower than manufacturers stated at time of production, at only 20 – 24%. For this reason, and the future comparison of emissions, specific fuel consumption is established as a useful metric for efficiency change comparison.

4 Simulation of Exhaust Gas Recirculation with CO_2

4.1 Introduction

The aim of this chapter is to investigate the process of exhaust gas recirculation, by simulating the combustion air composition that will contain more CO_2, by adding CO_2 before compression. The impact that this has on the combustion performance and the gas turbine efficiency is analysed.

Controlled flow rates of CO_2 from external storage were piped into the combustion air before compression. As reviewed in the literature it is expected that 8% CO_2 by volume can be injected into the combustion air without lean blow out and turbine stall occurring, and for a CCGT this represents approximately up to 35% EGR [60]. Tests were designed for CO_2 to be added up to 175kg/h, equivelant to far in excess of 35% EGR. This is since the combustion of the Microturbine series 1 Turbec fuel:air ratio is very lean, the equivalent CO_2 of up to 356% EGR was added. To evaluate the impact of the addition of CO_2, variations in flue gas composition, temperatures and speeds were analysed.

The main focus is to evidence the incomplete combustion in terms of CO, UHC and oxides of nitrogen (NO_x). In addition the mechanical impact on the turbine through variations in frequency, compression pressure and temperatures due to CO_2 addition. The final element of the analysis is the efficiency and specific fuel consumption.

4.2 Modifications to the PACT Core Facilities

4.2.1 Additional Instrumentation and Calibration

After the initial baseline testing of emissions and performance recorded through the WinnApp program, additional instrumentation was planned and implemented. Also after visiting research facilities at which the University of Stavanger use Turbec series 2 turbines for testing, with additional instrumentation. A similar data collection enhancement program was planned.

Key performance indicators for the Turbec turbine is the pressure post compression. This indicates the efficiency of the compressor, and the pressure ratio through the turbine. It is also important for determining how close to the manufacturer performance the turbine may be.

The temperature post compression is also important, this will be particularly so in order to determine the impact of CO_2 on the oxidiser composition, and its thermal capacity.

Figure 4-1 Photograph of the additional instrumentation on the Turbec Series 1.

Most additional instrumentation was added to the existing lug points on the Turbec. As seen in Figure 4-1 Photograph of the additional instrumentation on the Turbec Series 1the locations of the PT and thermocouples were paired and adjacent.

The copper piping seen is the pressure delivery lines to the PT that were mounted externally to the turbine, for reasons of space practicalities, and regular access that is required to the turbine.

Also modification of the housing cabinet could have led to a change in the negative pressure provided by the external pump.

The type K thermocouples generate a thermoelectric voltage, through linearization the voltage output can correspond to a temperature of the total measurable range. The voltages generated by the thermocouples were checked together in warm and hot water to see if they gave the same result and they did. This was also checked in a hot water bath at a set temperature to ensure the voltage reading was correct for the temperature. The voltages where checked against the manufacturers voltage table, and the LabView program was calibrated accordingly. The mV/°C is almost linear for interpretation. It would be preferable to calibrate thermocouples using a calibrated hot block, for accuracy and auditing purposes in future work.

The Rosemount pressure transducers display the pressure reading as both a percentage of the range and the actual pressure as seen in Figure 4-2 Photograph of the Rosemount pressure transducer displaying the pressure and range values and for some transducers it is possible to switch between ranges.

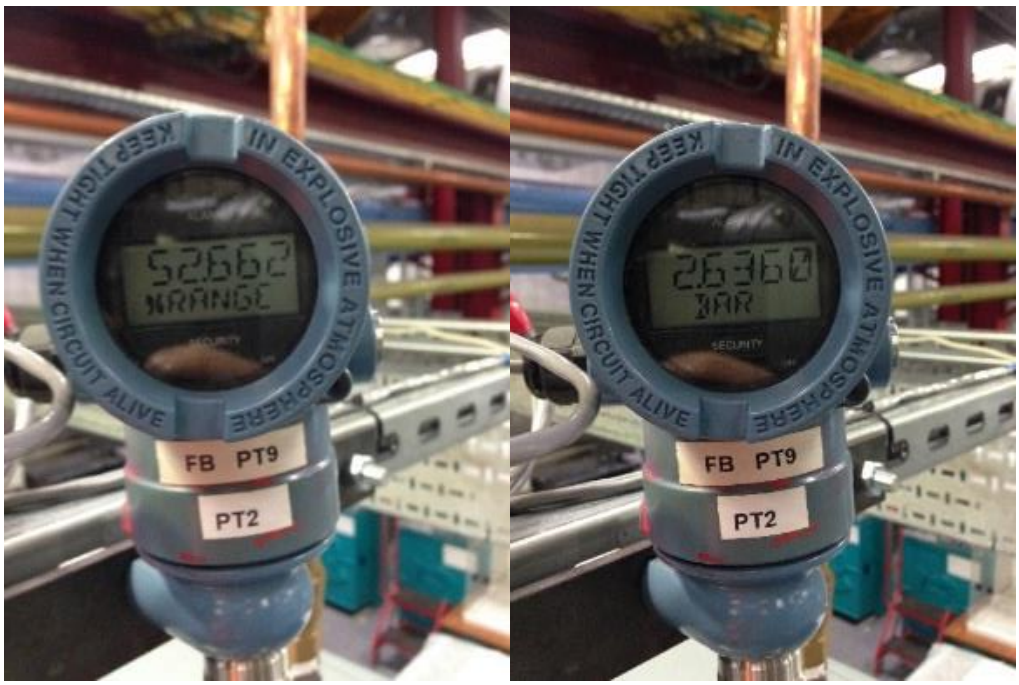

Figure 4-2 Photograph of the Rosemount pressure transducer displaying the pressure and range values.

Pressure transducers were calibrated using a pressure calibration pump. The pressure was set on the device and attached to the inlet of the differential pressure transducers. Where possible this was performed at the sample end of any pressure delivery tube lines in order to check line integrity. The generated pressure was then confirmed on the pressure transducers locally, and the current or voltage generated is wired to a National Instruments Compact RIO-9022 Real-Time Controller, and this is connected to the LAN. The interpreted voltage or current is then calibrated on the LabView program, corresponding to the different pressure readings. These were all validated, and were equal to the locally displayed results, and the set pressures of the calibration pump.

The mass flow was measured by the ValuMass flow meters see Figure 4-3 Photograph is the ValuMass flow meter. One meter measures the inlet mass flow, and the other measures the cooling air mass flow. The idea of this system application was that the difference would be the air mass used for combustion.

Figure 4-3 Photograph is the ValuMass flow meter

However in practical applications, this proved to be an unreliable measurement technique, and the calculated flow provided more realistic estimates of the true mass flow.

Sources of error for the mass flow was that each turbine housing is at a negative pressure maintained by a pump near the exhaust of each turbine from the point of start up, and after the turbine has been switched off for a significant period of time it continues to cool the turbine.

This pump and negative pressure means additional air is drawn into the turbine housing through gaps in the seals and ventilation holes within the turbine cabinet housing. This mass flow is difficult to quantify and offset due to its variance. In addition to this, it was found that the air valves can be shut between the turbines when one is in operation and the other is not, i.e. the change over valves for the inlet air and the exhaust were not sufficiently good to prevent cooling the air pressure pushing through one turbine and leaking through the other to a small extent. Again this is difficult to measure, and quantify.

It was not possible to perform in house calibration of the volumes flow meters. This would require a controllable air mass flow under standard temperature and pressure conditions. For this reason the supplied test certificates were relied upon. This was within -0.19% and 3.53% of the range equivalent 1.2 kg/min, and this was calibrated for 1 bar pressure.

The delivery line integrity was determined through testing to ensure that there was no hazardous CO_2 leaks and that the delivered mass flow to the turbine is as expected.

An additional Servomex analyser was used to analyse the cooling air of the Turbec Series 1 Turbine. This was used to determine how much of the CO_2 was being drawn into the compressor and not escaping. No significant change was monitored. Also, with validation of expected CO_2 appearing in the exhaust gas as monitored by the FTIR.

4.2.2 LabView Program Development

For monitoring and recording of the additional instrumentation as discussed a National Instruments Compact RIO-9022 Real-Time controller was used. This was connected to a LabView program that was specially designed. The LabView program was calibrated to read the appropriate voltage and current readings at the corresponding pressures and temperatures.

This data was then displayed live on the program interface. Graphs plotted the last 1 hour of results for any selected thermocouple, flow meter, or pressure transducer. This helped establish when steady state had been achieved by the instrumentation by observing when consistent readings of the results had been achieved, and also when dynamic or interesting behaviours were occurring. As the testing periods were approximately 20 minutes per condition, it displayed step changes between up to 3 conditions.

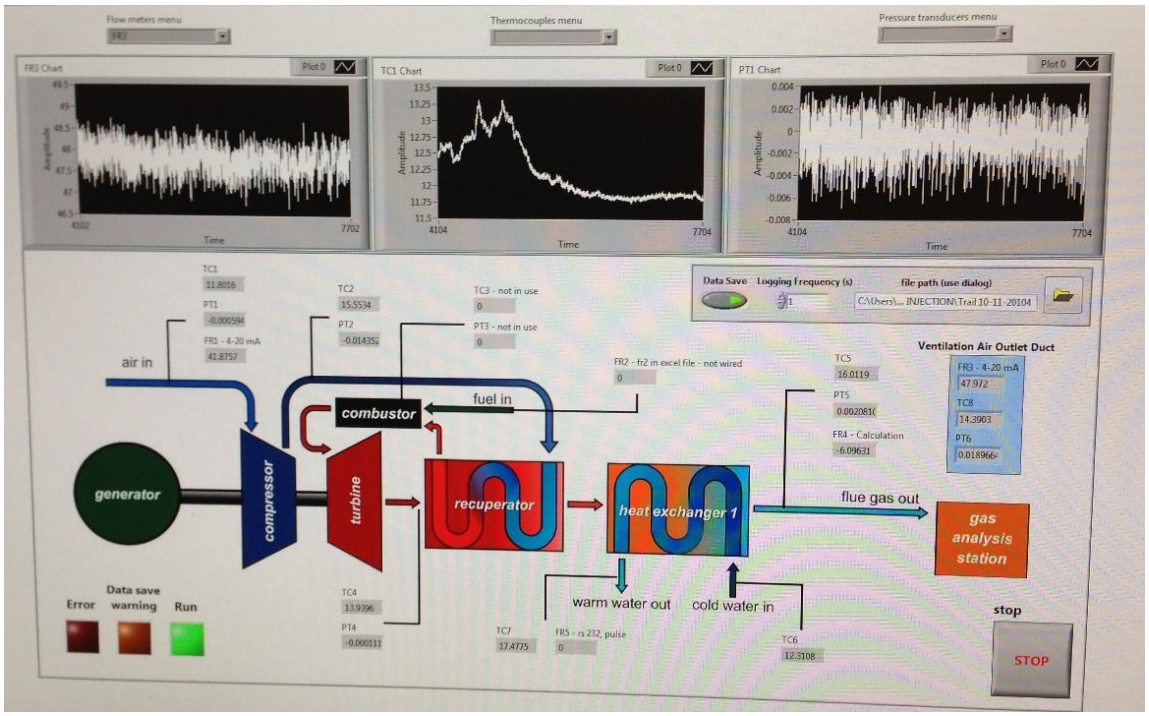

Figure 4-4 The LabView program interface.

Before saving the data, the program sampling frequency could be selected. This was maintained at 1Hz in order to match with the sample frequency of the WinnApp software, so the simultaneous data could be more easily collated and processed.

4.2.3 CO_2 Delivery Process

Before and during each test, the pressure of the external CO_2 tank was checked to ensure it was within norms, and contained enough for a full test run, and to manage the needs of multiple testing parties on the site using the same supply.

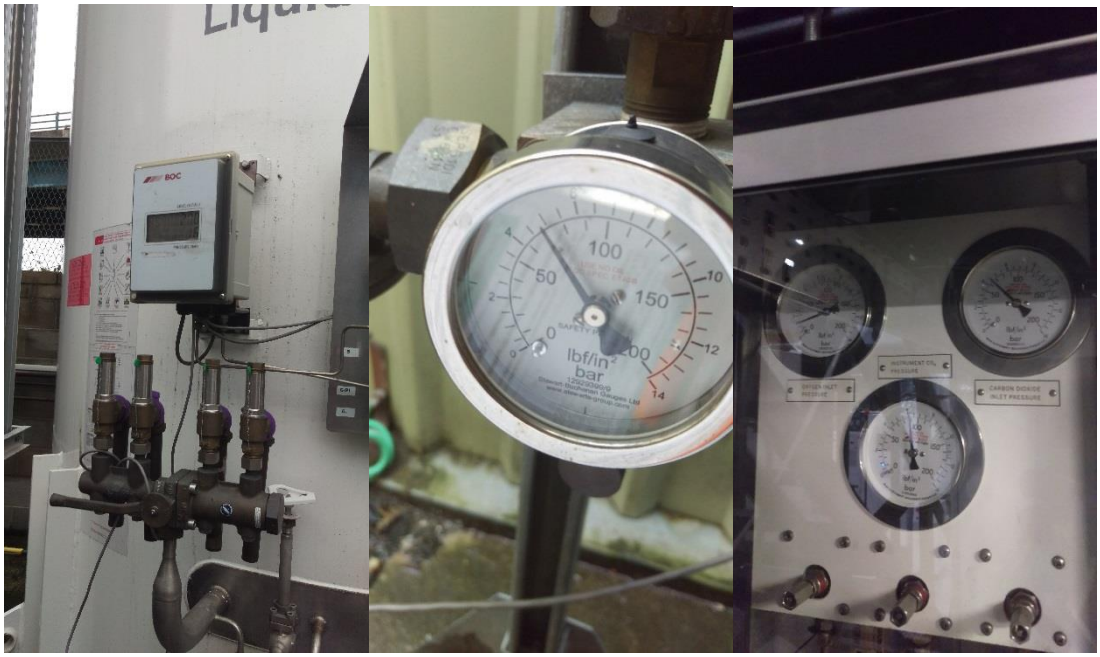

Figure 4-5 Photograph of the CO_2 external storage tank, tank pressure, SKID delivery pressure.

The delivery pressure to the mixer was also monitored to ensure that there were no dangerous spikes in pressure, and to ensure it was close to the external delivery pressure with no significant and potentially dangerous losses occurring during the vapour withdrawal.

The actual line pressure to the turbine injection point was significantly lower after expansion of the gas. This was monitored also to ensure it was within the SKIDS maximum delivery pressure,

over which the valves may become damaged. The corresponding flowrates and openings were recorded to determine the maximum flow available for the testing with CO_2.

Table 4-1 Delivery mass flow, valve position and pressure.

Mass flow kg	% Open	Pressure bar
5.1	10.9	<0.5
13.4	16.8	<0.5
22.8	20.7	<0.5
49.7	33.1	<0.5

This pressure was also used to determine the likely temperature and pressure of the CO_2 entering into the turbine. This pressure is slightly above atmospheric means there will not be a significant temperature drop at the injection point due to expansion of the CO_2.

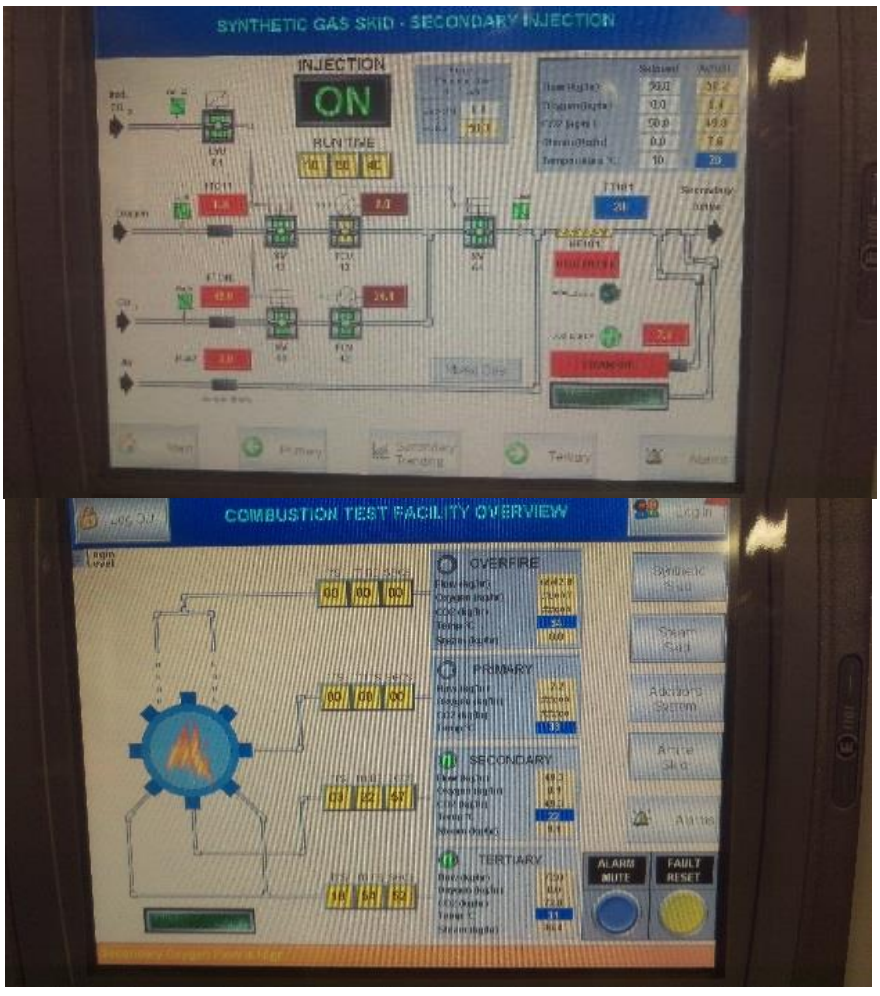

Figure 4-6 Photographs of the CO_2 mixing SKID interface.

The Siemens SKID system was used to control, monitor and record the flow on the SCADA. As the flow was not perfectly consistent then this data was recorded and averaged to ensure that the flow delivery was within experimental boundaries.

4.2.4 CO_2 Addition Point

After the baseline testing, modifications were planned and designed for the addition of CO_2 to the combustion air. This was designed to use externally stored CO_2 from a tonne tank through a gas mixing skid, which can also supply the oxyfuel and capture plant. The mixing skid can control the mass flow rate of delivery over three delivery lines. Within the PACT facility, there are already gas delivery lines with fixed distribution points. It was required for an “off take” to be taken from the nearest distribution point to the gas turbine. This was done above the turbine to reduce the risk of human interference when live, and for the simplest direct route into the turbine housing at the compressor point. It was considered that the ideal injection point would be into the air post compression to ensure 100% of the injected CO_2 got to the combustor, but it was not possible to generate sufficient CO_2 pressure above that of the compressors namely 4.5bar.

The CO_2 could not simply be added directly into the intake air as the intake air is used both for combustion and turbine cooling. This means a significant proportion would not go through the turbine for combustion and this would be an unknown total mass of CO_2 lost, and unknown alteration to the oxidiser mix. In addition to this, it could result in significant CO_2 leakage in the turbine proximity.

The pragmatic solution was to pipe directly into the face of the compressor, to ensure maximum entrainment into the compressor due to the negative pressure in its vicinity. The location was measured and modelled due to the tricky layout, and to ensure adequate flow, temperature and pressure of CO_2 could be calculated.

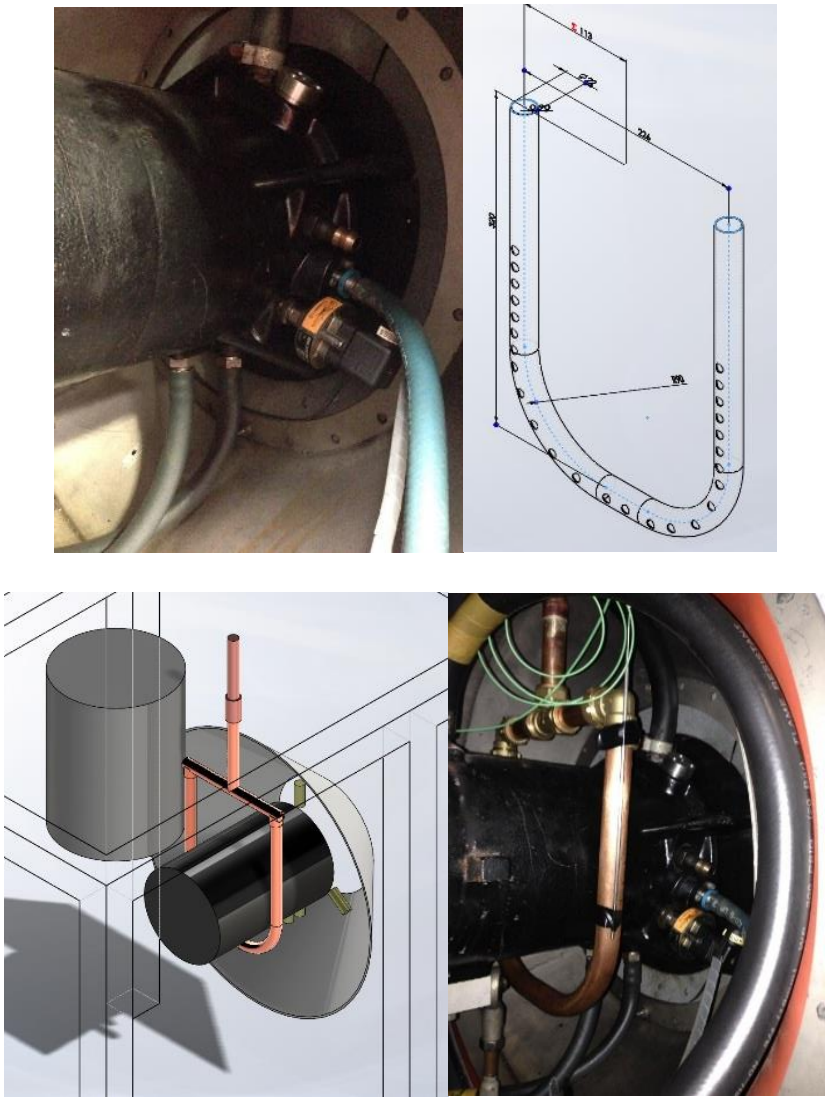

Figure 4-7 Photographs of the CO_2 injection point, design, and location installed.

The 22mm diameter copper design fitted perfectly with the holes facing into the compressor.

Under normal temperature and pressure, CO_2 has a density 1.842kg/m^3. If the maximum flow, including some variance, is considered to be 180kg/h, this is equivalent to 0.05kg/s. Each 16mm diameter drilled hole has an area of 0.0002m^2, with a minimum of 10 holes drilled this is 0.002m^2.

Velocity as a function of mass flow and area

$$V = \frac{\mathrm{m}}{\rho \mathrm{A}}$$

$$V = \frac{0.05}{1.842 * 0.002} \qquad \textbf{4-1}$$

$$V = 13.5 ms^2$$

This is equivalent to a “strong breeze” and is unlikely to cause damage. Due to the expansion of the gas to ambient (or below ambient pressure with the compressor sucking) it can be anticipated that there will be a temperature drop in the CO_2. However after leaving cryogenic storage, the CO_2 passes through an external air heater, and then a trim heater to above 10°C, on leaving the mixing Skid the maximum pressure is 2 bar, so the minimum likely temperature is 5°C, and unlikely to cause damage. As a precaution, a temporary thermocouple was placed at the injection point to ensure that there was no significant temperature drop or variation to the TC1. The thermocouple wire can be seen in Figure 4-7 Photographs of the CO2 injection point, design, and location installed.

4.2.5 CO_2 Health and Safety

The CO_2 sampling lines were used to draw samples from near the turbine to the Crowcon sampling system alarm. This system alternates between sampling lines providing periodic measurement of the O_2 and CO_2 in each location. These sampling lines were set at floor level at four points around the gas turbine due to the higher molecular weight of CO_2 than air meaning any large escape would likely pool at a low point. In addition to this, remote Tetra 3 CO and CO_2 alarms were placed at strategic locations. This was at the point of the exhaust analysis, at the heated mixing cabinet from which CO_2 enters the mixing SKID from the external CO_2 storage tank, and at the mixing SKID control panels where an operator may be stood.

Portable Tetra alarms were also worn to further reduce risk, and cover those going to external regions. Site notifications were displayed during testing, and email notification was given to all site staff of scheduled testing times.

4.3 Calculation of Predicted Results

In preparation for the testing with CO_2, a planned test matrix was developed as shown in Table 4-2 Test matrix, power, expected results, and required CO_2 mass addition 0% - 50% EGR & 50kg enhancement. and Table 4-3 Test matrix, power, expected results, and required CO_2 mass addition 50kg - 175kg. For this it was thought useful to be able to anticipate the approximate CO_2 volume percentage results to ensure CO_2 was not being lost, and as a flag for any potentially anomalous results

Table 4-2 Test matrix, power, expected results, and required CO_2 mass addition 0% - 50% EGR & 50kg enhancement.

CO_2	0%			10%			30%			50%			50kg		
Power Output kW	Mass	EGR %	Expected Exhaust %	Mass	EGR %	Expected Exhaust %	Mass	EGR %	Expected Exhaust %	Mass	EGR %	Expected Exhaust %	Mass	EGR %	Expected Exhaust %
50	0	0	1.56	4.90	10	1.76	13.63	30	2.13	22.62	50	2.50	50	133.00	3.63
55	0	0	1.42	4.01	10	1.56	12.04	30	1.85	20.07	50	2.13	50	124.58	3.19
60	0	0	1.47	4.33	10	1.62	12.99	30	1.91	21.66	50	2.21	50	115.44	3.17
65	0	0	1.50	4.60	10	1.65	13.80	30	1.95	22.99	50	2.25	50	108.72	3.13
70	0	0	1.48	5.61	10	1.63	16.84	30	1.92	28.07	50	2.22	50	89.07	2.80
75	0	0	1.53	5.18	10	1.68	15.53	30	1.99	25.88	50	2.30	50	96.59	3.01
80	0	0	1.60	5.58	10	1.76	16.74	30	2.08	27.91	50	2.40	50	89.58	3.03
85	0	0	1.57	5.61	10	1.73	16.83	30	2.04	28.05	50	2.36	50	89.12	2.97

Table 4-3 Test matrix, power, expected results, and required CO_2 mass addition 50kg - 175kg

CO_2	75kg			100kg			125kg			150kg			175kg		
Power Output kW	Mass	EGR %	Expected Exhaust %	Mass	EGR %	Expected Exhaust %	Mass	EGR %	Expected Exhaust %	Mass	EGR %	Expected Exhaust %	Mass	EGR %	Expected Exhaust %
50	75	199.50	4.67	100	265.99	5.71	125	332.49	6.75	150	398.99	7.78	175	465.49	8.82
55	75	186.87	4.07	100	249.16	4.96	125	311.45	5.84	150	373.74	6.73	175	436.04	7.61
60	75	173.16	4.02	100	230.88	4.86	125	288.60	5.71	150	346.32	6.56	175	404.04	7.41
65	75	163.08	3.95	100	217.44	4.76	125	271.80	5.58	150	326.16	6.39	175	380.52	7.21
70	75	133.60	3.46	100	178.14	4.12	125	222.67	4.78	150	267.21	5.43	175	311.74	6.09
75	75	144.89	3.75	100	193.18	4.49	125	241.48	5.22	150	289.77	5.96	175	338.07	6.70
80	75	134.38	3.75	100	179.17	4.47	125	223.96	5.18	150	268.75	5.90	175	313.54	6.62
85	75	133.68	3.67	100	178.24	4.37	125	222.80	5.07	150	267.36	5.77	175	311.92	6.47

From the fuel composition data it is possible to calculate the moles of oxygen needed, and the moles of CO_2 formed from complete combustion. This calculation was done using excel as Table 4-4 Fuel composition example.

Table 4-4 Fuel composition example.

	Relative DENSITY	NITROGEN	CARBON_DIOXIDE	METHANE	ETHANE	PROPANE	BUTANE	BUTANE	NEO_PENTANE	I_PENTANE	N_PENTANE	HEXANE
	0.622	2.406	1.186	89.440	4.936	1.233	0.192	0.212	0.002	0.057	0.045	0.074
	Typical Analysis (mole %)	**Density g/L**	**Molar Mass g/mol**	**Molecular Weight**	**Litres/ Mole of Natural Gas**	**% Volume Composition**	**Mole/ m3**	**Moles in m3 Gas**	**Std Combustion Enthalpy kJ/mol**	**MJ/mn3**	**Gas Specific Enthalpy HHV MJ/mn3**	**Gas Specific Enthalpy LHV MJ/mn4**
Methane	89.43991548	0.6556	16.04	14.35	20.03	89.44	44.64	39.93	891.56	39.80	35.60	32.08
Ethane	4.935816172	0.5440	30.07	1.48	1.11	4.94	44.64	2.20	1562.14	69.74	3.44	3.15
Propane	1.23270622	2.0090	44.1	0.54	0.28	1.23	44.64	0.55	2221.10	99.16	1.22	1.13
iso-Butane	0.192024516	2.5100	58.12	0.11	0.04	0.19	44.64	0.09	2879.76	128.56	0.25	0.23
Butane	0.212081869	2.4800	58.12	0.12	0.05	0.21	44.64	0.09	2879.76	128.56	0.27	0.25
iso-Pentane	0.12	0.6160	72.15	0.09	0.03	0.12	44.64	0.05	3538.60	157.97	0.19	0.18
Pentane	0	0.6260	72.15	0.00	0.00	0.00	44.64	0.00	3538.60	157.97	0.00	0.00
Hexanes	0.073867748	0.6548	86.18	0.06	0.02	0.07	44.64	0.03	4198.24	187.42	0.14	0.13
Nitrogen	2.406374658	1.2510	14	0.34	0.54	2.41	44.64	1.07			0.00	0.00
Carbon Dioxide	1.186267176	1.5620	44	0.52	0.27	1.19	44.64	0.53			0.00	0.00
Oxygen	0	1.4290	16	0.00	0.00	0.00	44.64	0.00			0.00	0.00
Hydrogen	0	0.07	1	0.00	0.00	0.00	44.64	0.00			0.00	0.00
				17.62	22.35	99.80		44.55		Total	41.11	37.15
			Density kg/m3	**0.79**								

Knowing the fuel composition the Table 4-5 Stoichiometric requirement calculation for complete combustion of fuel. can be calculated.

Table 4-5 Stoichiometric requirement calculation for complete combustion of fuel.

	No Carbon	Molecular Weight Carbon	Molecular Weight Hydrogen	No CO2	Molecular Weight CO2	No H2O	Molecular Weight H2O	O2 Req	Molecular mass of O2 Req	Moles O2 req /m3 fuel	Moles of H2O exhaust/m3 fuel	Moles of Exhaust CO2/ m3 fuel	Volume of Exhaust CO2/m3 fuel	Latent Heat of Vaporistion
Methane	1	12	4	1	44	2	36	2	64	79.86	79.86	39.93	0.89	3.51
Ethane	2	24	6	2	88	3	54	3.5	112	7.71	6.61	4.41	0.10	0.29
Propane	3	36	8	3	132	4	72	5	160	2.75	2.20	1.65	0.04	0.10
iso-Butane	4	48	10	4	176	5	90	6.5	208	0.56	0.43	0.34	0.01	0.02
Butane	4	48	10	4	176	5	90	6.5	208	0.62	0.47	0.38	0.01	0.02
iso-Pentane	5	60	12	5	220	6	108	8	256	0.43	0.32	0.27	0.01	0.01
Pentane	5	60	12	5	220	6	108	8	256	0.00	0.00	0.00	0.00	0.00
Hexanes	6	72	14	6	264	7	126	9.5	304	0.31	0.23	0.20	0.00	0.01
Nitrogen					0			0	0			0.00	0.00	0.00
Carbon Dioxide	1	***12***		1	44			1	32			0.53	0.01	0.00
Oxygen					0			0	0	0.00	0.00	0.00	0.00	0.00
Hydrogen			***1***		0	0.5		0.25	8	0.00	0.00	0.00	0.00	0.00
										92.24	90.12	47.70	1.07	3.97

This data gives the total stoichiometric air requirement as Table 4-6 Total air required for combustion per m^3 of fuel.

Table 4-6 Total air required for combustion per m^3 of fuel.

		Air for combustion	
	Moles	kg o2/m3 fuel	m3 air/ m3 fuel
Total O2 from air (21%)	92.24	2.95	2.07
N2 (79%)	346.98	9.72	7.77
Air total	439.22	12.67	9.83

Using the baseline results of O_2, CO_2, and fuel consumption, and the known moles of CO_2 from complete combustion it is possible to calculate the total air flow through the turbine. It is also possible to do this on an O_2 basis. Both methods were used with very similar estimations given in the results of both. The examples presented in Table 4-7 Calculation of total air through turbine for a specific power output. are on a CO_2 basis.

Table 4-7 Calculation of total air through turbine for a specific power output.

		85kW	
		Exhaust O2 %	Exhaust CO2 %
		18.12	1.57
		Fuel m3/h	34.78
		kg	m3
	O2	102.65	71.84
	N2	337.90	270.11
Total Combustion Air		440.56	341.94
21.00	Compressor O2	695.04	486.38
79.00	Compressor N2	2298.49	1837.32
O2 Exhaust Dry Basis		592.39	414.55
N2 Exhaust Dry Basis		2298.49	1837.32
CO2 Exhaust Dry Basis		56.10	35.92
Total Air flow Exhaust Dry		2946.98	2287.78

From this data it was possible to predict the expected CO_2 exhaust volume percentage for each power output, and the CO_2 enhancement. Also it provided the value for the mass of CO_2 the

addition required for each power output for varying percentages of the exhaust gas recirculation to levels similar to those discussed in the literature, particularly 30 – 50%. This is provided in the Table 4-8 Calculation required CO2 mass addition to simulate 0-50% EGR at 85kW and the expected results for validation and Table 4-9 Calculation of expected results for 85kW with 50 - 125kg/h CO_2 enhancement. for the experimental tests.

Table 4-8 Calculation required CO_2 mass addition to simulate 0-50% EGR at 85kW and the expected results for validation.

85kW CO2 Addition		0% Exhaust Recylce			10% Exhaust Recylce			30% Exhaust Recycle			50% Exhaust Recycle		
		Mass	Volume	Vol %	Mass	Volume	%	Mass	Volume	%	Mass	Volume	%
From Exhaust	O2	102.65	71.84	21.01	59.24	41.45	18.12	177.72	124.36	18.12	296.19	207.27	18.12
	N2	337.90	270.11	78.99	229.85	183.73	80.31	689.55	551.20	80.31	1149.24	918.66	80.31
	CO2			0.00	**5.61**	**3.59**	1.57	**16.83**	**10.78**	1.57	**28.05**	**17.96**	1.57
	Air total	440.56	341.94		294.70	228.78		884.09	686.34		1473.49	1143.89	
Into Compressor	O2	695.04	486.38	20.93		485.631	20.90		484.13	20.83		482.62	20.77
	N2	2298.49	1837.32	79.07		1834.479	78.95		1828.80	78.70		1823.12	78.46
	CO2			0.00	5.61	3.592	**0.15**	16.83	10.78	**0.46**	28.05	17.96	**0.77**
	Air total	2993.53	2323.70			2323.70			2323.70			2323.70	
New Exhaust	O2	592.39	414.55	18.12	591.31	413.79	18.09	589.16	412.29	18.02	587.02	410.79	17.96
	N2	2298.49	1837.32	80.31	2294.93	1834.48	80.19	2287.83	1828.80	79.94	2280.72	1823.12	79.69
	CO2	56.10	35.92	**1.57**	61.71	39.51	**1.73**	72.94	46.69	**2.04**	84.16	53.88	**2.36**
	Air total	2946.98	2287.78		2947.96	2287.78		2949.93	2287.78		2951.89	2287.78	

Table 4-9 Calculation of expected results for 85kW with 50 - 125kg/h CO_2 enhancement.

85kW CO2 Addition		50kg Exhaust Recycle			75kg Exhaust Recycle			100kg Exhaust Recycle			125kg Exhaust Recycle		
		Mass	Volume	%	Mass	Volume	%	Mass	Volume	%	Mass	Volume	%
From Exhaust	O2			0.00			0.00			0.00			0.00
	N2			0.00			0.00			0.00			0.00
	CO2	**50.00**	**32.01**	100.00	**75.00**	**48.02**	100.00	**100.00**	**64.02**	100.00	**125.00**	**80.03**	100.00
	Air total	50.00	32.01		75.00	48.02		100.00	64.02		125.00	80.03	
Into Compressor	O2		479.68	20.64		476.33	20.50		472.98	20.35		469.63	20.21
	N2		1812.01	77.98		1799.35	77.43		1786.70	76.89		1774.04	76.35
	CO2	50.00	32.01	**1.38**	75.00	48.02	**2.07**	100.00	64.02	**2.76**	125.00	80.03	**3.44**
	Air total		2323.70			2323.70			2323.70			2323.70	
New Exhaust	O2	582.81	407.85	17.83	578.03	404.50	17.68	573.24	401.15	17.53	568.45	397.80	17.39
	N2	2266.82	1812.01	79.20	2250.99	1799.35	78.65	2235.16	1786.70	78.10	2219.33	1774.04	77.54
	CO2	106.10	67.93	**2.97**	131.10	83.93	**3.67**	156.10	99.94	**4.37**	181.10	115.94	**5.07**
	Air total	2955.74	2287.78		2960.12	2287.78		2964.50	2287.78		2968.88	2287.78	

These calculations were carried out individually using the baseline O_2, CO_2, and fuel consumption for every power output and CO_2 enhancement individually to improve the accuracy in the estimation.

During testing these estimates proved to be very accurate, to within 0.2% for the majority of results. The only significant disparity was at the highest powers with the highest CO_2 enhancement, where as seen in the baseline performance analysis the turbine speed and total air mass flow increases above what would be linearly expected.

4.3.1 Total Mass Flow Calculation

As discussed air flow was measured for the inlet air and cooling air, with the combustion air assumed to be the difference between the readings of the ValuMass500 flow meters. However there was significant leakage and this gave inaccurate flow measurements.

For this reason in the presented results for the mass and volume flow these are from the calculated values, through a similar methodology used for the prediction of CO_2 concentration results.

The mass of CO_2 injected is known, and this mass is than converted into a volume. It is measure in the FTIR at 180°C and this equates to a volume. The volume at the intake is smaller at a lower temperature, but as a volume % it is consistent as all other gas species volumes will increase linearly with each other in accordance with the Ideal Gas Law.

The exhaust volume is calculated from the measured CO_2 vol% and the calculated corresponding volume knowing the volume of the CO_2 addition. The volume of CO_2 is calculated from the known mass addition of CO_2 to the process.

The total CO_2 mass is the CO_2 from the combustion and enhancement. The enhancement mass is metered and controlled. The combustion mass of CO_2 is calculated from the volume of the fuel combusted during the test.

As the fuel is of a known composition, the moles of CO_2 from the complete combustion can be calculated and hence the mass of CO_2 from that volume can be calculated. When the volume of the fuel combusted during the test is multiplied by the known mass of CO_2 complete combustion produces per hour. This is then added to the known enhancement mass. Each day may have a slightly different fuel composition and hence the calculation is individual for each fuel.

The CO_2 volume is calculated using the ideal gas law. From the mass at 180°C it is as measured in the FTIR at 1 ATM.

Ideal Gas Law:

$$PV = nRT \qquad \textbf{4-2}$$

$$V = \frac{\mathrm{nRT}}{\mathrm{P}}$$

First the mass of CO_2 is converted into grams from kilograms, then moles (n) this is the mass divided by the atomic mass, 44g/mol.

The gas constant R is 0.0821 L atm K mol. The temperature is in Kelvin +273K to deg °C.

For 4.9kg CO_2 enhancement at 50kW 23.82m^3/h fuel on 28/11/2014.

$$= \frac{\left((55.88 * 1000 * \left(\frac{1}{44}\right)\right) * 0.0821 * 453}{1000} \qquad \textbf{4-3}$$

$$CO_2 = 47.23\ m^3/h$$

From the calculations of this reading using the fuel data and enhancement, the dry vol % of CO_2 is calculated to be 1.52%, the reading from the FTIR dry at that time is 1.52%, and the reading results and calculations consistently agree through all the tests and hence the calculation is considered to be reliable.

Taking the dry volume of CO_2 calculated and dividing it by the FTIR measured value of CO_2 gives the total volume for the gas to be 3101 m^3/h. However, as the volume changes throughout the process, the mass can be more important. For the purposes of the calculation of the exhaust mass is considered to only constitute of nitrogen, oxygen, water and carbon dioxide.

Each of these additional masses have been calculated from the measured volume percentage by the FTIR. For oxygen using the Ideal Gas law to calculate the volume and then calculating the mass.

$$O_2 Exhaust\ Volume = Total\ Exhaust\ Volume * O_2\ Fraction\ Measured \quad \textbf{4-4}$$

$$PV = nRT$$

$$n = \frac{\mathrm{PV}}{\mathrm{RT}} \quad \textbf{4-5}$$

$$Total\ Moles\ O_2 = \frac{O_2\ Volume\ at\ 1\ Atm}{RT}$$

$$Mass\ of\ O_2 \text{ in Exhaust} = Moles * Molar\ Mass$$

$$= \frac{3196590 * 0.184}{0.0821 * 453} * 0.032 \quad \textbf{4-6}$$

$$Mass\ of\ O_2 \text{ in Exhaust} = 506.07 kg/h$$

4.4 Methodology

There are two natural gas-fuelled Turbec T100PH microturbines at the PACT Core Facility. Both turbines have a combined heat element capable of generating 165kW of thermal power from hot water delivered at 70-90°C and this is in addition to the 100kW of Electrical power. The combined efficiencies of the turbines are rated by the manufacturer at ~77%, with the maximum electrical generation efficiency quoted as 30% [90].

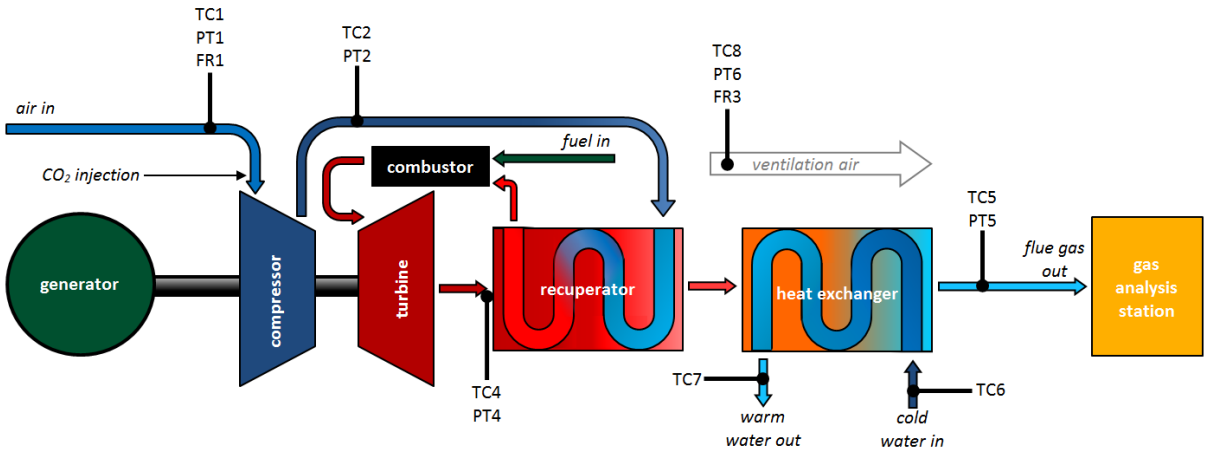

Figure 4-8 Schematic of the components of the Turbec T100 PH combined heat and power gas turbine system, including the modifications made for the CO2 injection and the instrumentation (TC – thermocouples; PT – pressure transducers; FR flowrate meters).

The principle components of the turbine are shown in Figure 4-8 Schematic of the components of the Turbec T100 PH combined heat and power gas turbine system, including the modifications made for the CO2 injection and the instrumentation (TC – thermocouples; PT – pressure transducers; FR flowrate meters)which shows a schematic of the components of the Turbec T100 PH combined heat and power gas turbine system, including the modifications made of the CO_2 injection and the instrumentation (TC – thermocouples; PT – pressure transducers; FR flowrate meters). The gas turbine engine is of a single shaft deign, with the compressor and generator driven by the turbine on the same shaft. The centrifugal

compressor compresses the ambient air for combustion to the optimum pressure ratio for each power output, up to ~4.5:1 for the maximum power output. This compressed air is pre-heated in the recuperator using hot exhaust gases, then it enters the combustion chamber, and this improves the electrical efficiency. Natural gas enters the combustion chamber and is premixed with the hot compressed oxidising air where it is ignited by an electrical spark. There is a fuel lean, oxygen rich mix that helps ensure complete combustion, with low emissions of carbon monoxide, unburned hydrocarbons and NO_x, without further exhaust gas treatment being required, making it adaptable and appropriate for most locations.

A radial turbine drives the compressor and generator. Hot combustion gases at ~950°C, and an elevated pressure of ~4.5 bar leave at the combustor exit and enters the turbine. This gas expands through the turbine, with the pressure decreasing through it to near atmospheric upon exit, the temperature also drops by about 300°C. The hot turbine outlet exhaust gas passes through the recuperator, pre heating the inlet air and further reducing the temperature. This gas then passes through another heat exchanger in the form of a counter current gas-water exchanger that generates hot water for further combined heat recovery.

There are several auxillary systems within each power module, a cooling system, a lubrication system, an air intake and a ventilation system (which includes a coarse external air filter and an internal fine filter), a fuel gas booster and a buffer air system. Manufacturers additional technical information for the gas turbine engine is outlined in Table 4-10 T100 Technical data (Turbec, 2009) .

Table 4-10 T100 Technical data (Turbec, 2009) .

Inlet and Compressor	
Type	centrifugal
Pressure ratio	4.5:1
Maximum inlet air flow at 15°C (kg/s and m^3/s)	1.69 (1.38)

Combustor and Fuel Requirements	
Type of chamber	lean, pre-mix
Pressure in combustion chamber (bar, a)	4.5
Fuel flowrate (m^3/hr)*	31
Lower heating value (LHV) of fuel (MJ/kg)	38-50
Wobble Index (MJ/m^3)**	43-55

Turbine	
Type	radial
Inlet temperature (°C)	950
Normal turbine outlet temperature (°C)	650
Maximum turbine outlet temperature (°C)	710
Outlet pressure	~atmospheric
Nominal shaft speed (RPM)***	70,000

Flue Gas Heat Exchanger	
Type	gas-water
Flow	counter-current
Maximum flue gas flowrate at outlet (kg/s)	0.87
Maximum flue gas temperature at outlet (°C)	325
Minimum and maximum water flowrates (l/s)	1.5-4.0
Minimum water temperature at inlet (°C)	50
Maximum water temperature at outlet (°C)	150

* The fuel flowrate depends on the gas composition – this is specified for a fuel with a LHV of 39 MJ/m^3

** m^3 at 288.15K and 101.325kPa.

*** Revolutions Per Minute

4.4.1 Test Conditions

The two controlled variables for this testing were the power output of the turbine and the level of CO_2 enhancement, simulating EGR ratio with additional mass. 66 different conditions were tested, the CO_2 mass injection was varied from 0kg/h to 175kg/h, and the power outputs from 50kW – 80kW, and this covered the EGR ratios equivelant to 0% up to 356%, with this ratio being calculated on a volume basis. Every test condition was carried out for a minimum of 15 minutes of stable operation to be in compliance with the ISO 2314 recommendations for determining gas turbine emissions. High power, low CO_2 enhancement combinations were ignored due to know expected impact as seen in Table 4-11 Test matrix.

Table 4-11 Test matrix.

	CO_2									
Power Output kW	0%	10%	30%	50%	50kg	75kg	100kg	125kg	150kg	175kg
50										
55										
60										
65										
70										
75										
80										
85										

4.4.2 Data Acquisition

All testing was conducted using the PACT facilities with the T100 PH Series 1 microturbine. The performance of the turbine was measured using its own instrumentation and recorded with the NewEnco vendor WinNap program that monitored and recorded:

- air inlet temperature (T1 °C)
- calculated turbine inlet temperature (TIT °C)
- turbine outlet temperature (TOT °C)

- power generated by the turbine (kW)
- power set point (kW)
- engine speed (Revolutions Per Minute RPM and % of maximum)
- gas pressure (mbar)
- opening of the pilot and main fuel valves (both %)

In addition, further instrumentation was added to the turbine which monitored and recorded a range of flow rates, multiple system temperatures and pressures and, of particular importance, post compression. As discussed, additional instrumentation readings were recorded using a National Instruments Compact RIO-9022 Real-Time controller. Table 4-12 Quantities monitored by the LabView for the Series 1 gas turbine. outlines the additional monitoring.

Table 4-12 Quantities monitored by the LabView for the Series 1 gas turbine.

LabView DESIGNATION	PARAMETER	UNIT OF MEASUREMENT
THERMOCOUPLES		
TC1	system air inlet temperature	°C
TC2	compressed air temperature (compressor outlet)	°C
TC4	flue gas diffusion zone temperature	°C
TC5	flue gas outlet temperature	°C
TC6	cold water temperature (heat exchanger inlet)	°C
TC7	hot water temperature (heat exchanger outlet)	°C
TC8	ventilation air outlet temperature	°C
PRESSURE TRANSDUCERS		
PT1	system air inlet pressure	bar g
PT2	compressed air pressure (compressor outlet)	bar g
PT4	flue gas diffusion zone pressure	bar g
PT5	flue gas outlet pressure	bar g
PT6	ventilation air outlet pressure	bar g
FLOWRATE MEASUREMENTS		
FR1	system air inlet flowrate (total air in) – measured	kg/min
FR3	ventilation air outlet flowrate – measured	kg/min
FR4	flue gas outlet flowrate – calculated	kg/min

As discussed in the baseline performance chapter, two analysers were used for the gas species measurement, a Servomex analyser, and Gasmet FTIR. The Servomex Servoflex MiniMP 5200 analyser monitored O_2 and CO_2 in the exhaust using a non-dispersive infrared sensor for the CO_2 analysis and paramagnetic transducers for O_2 detection.

The FTIR used was a Gasmet DX4000, fourier transform infrared spectroscopy and it measures the absorbance of infra red to determine and differentiate the multiple gas species in a sample. The exhaust gas passed through a conditioning system to the FTIR where the levels of CO_2, CO and various hydrocarbons were measured. In addition, water vapour and the total NO_x were monitored with a number of other species options in the sample library.

The flow rate of the natural gas fuel into the turbine was measured with a Quantometer turbine flow meter. Additional temperature measurements throughout used Type K Thermocouples, and two variations of the Rosemount 2051 pressure transducers were installed. The maximum uncertainty for instrumental error is presented in Table 4-13 Instrumental errors. which shows the instrumental errors. The type K thermocouples error is quoted by the supplier as the greater of either 0.4% of the measurement or 1.5°C.

Measurements of all values were fairly consistent, as the tests began after significant warm up, and stabilisation at each setting. This resulted in low deviations in the results from the mean, that would not be visible in the graphs plotted, the maximum observed deviations are presented in Table 4-14 Standard deviation . It should be noted that the majority of the results fell within a much smaller deviation than the maximums in the table, this indicates consistent reliable results.

Table 4-13 Instrumental errors.

	Instrumental error	
Instrument	**%**	**Unit**
Servomex Servoflex MiniMP	0.10%	
Gasmet DX4000 FTIR	na	na
Quantometer	0.63%	
Type K thermoucouples	0.40%	1.5°C
Rosemount pressure transmitters 2051CDC2A	0.07%	0.8 mbar
Rosemount pressure transmitters 2051TG2A	0.07%	7.5 mbar

Table 4-14 Standard deviation

	Max Standard Deviation	
Gasmet DX4000 FTIR Readings	**Baseline**	**Enhancement**
CO ppm	9.2	17.32
CH_4 ppm	1.45	3.91
CO_2 vol%	0.51	0.03
NO_x ppm	1.88	1.27
Turbec T100 Readings		
RPM	141.65	143.66
kW	1.57	2.19
T1 °C	0.22	0.6
Additional Instrumentation		
PT2 mbar	0.02	0.02
TC2 °C	0.66	0.69

4.5 Results and Discussion

Experiments were carried out at the PACT Core Facilities, and the post processing, normalisation and analysis was carried out at the University of Leeds.

4.5.1 Performance with EGR

4.5.1.1 Mechanical Speed

The evident mechanical performance impact on the turbine is the effect on speed. As discussed, this is dominated by the ambient temperature or the temperature of the oxidiser being compressed. The addition of CO_2 changes the thermal properties of the oxidising air being compressed, and this is due to the higher thermal capacity of the CO_2 that displaces the nitrogen and oxygen in the air. During the test days, that were particularly cold, the CO_2 addition raised the oxidiser temperature, and on warmer test it reduced it. This is due to the relatively constant delivery temperature from the gas mixing facilities. Figure 4-9 The CO2 Mass addition to the oxidiser with turbine frequency shows the CO_2 Mass addition to the oxidiser with turbine frequency and it is observed that the reduction in speed with CO_2 addition at 50kW, the principle driver of which is the ambient temperature.

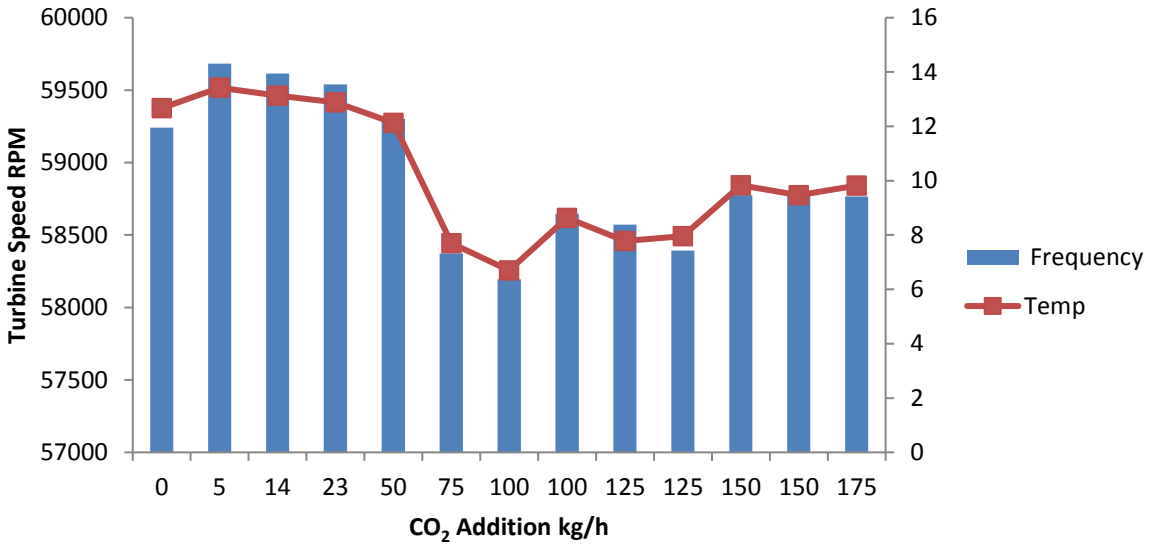

Figure 4-9 The CO2 Mass addition to the oxidiser with turbine frequency and the oxidiser temperature relationship at 50kW.

From Figure 4-9 The CO2 Mass addition to the oxidiser with turbine frequency and the oxidiser temperature relationship at 50kW. it is clear that the higher density and heat capacity CO_2 does reduce the turbine revolutions, and this is due to its displacement of air. However the lowest turbine speeds are still observed on the lowest ambient temperature days, not necessarily with the highest CO_2 mass flow. This trend reinforces the relationship discussed with the ambient temperature as seen in **Error! Reference source not found.** With an increased testing capacity, in terms of the available CO_2 flow to give a higher volume percentage, it could be expected to produce a more significant impact on the turbine speed.

4.5.1.2 Pressure post compressor

The reduction in speed has no impact on the pressure achieved by the turbine, and the RPM with higher CO_2 mass enhancement is well depicted in Figure 4-10 Impact of CO2 on the turbine frequencywhich shows the impact of CO_2 on the turbine frequency across the power range from 50 to 80kW. Replicating the results of those modelled by Mansouri Majoumerd [70], and those experienced in the turbine speed variations of De Paepes EGR microturbine investigations [87].

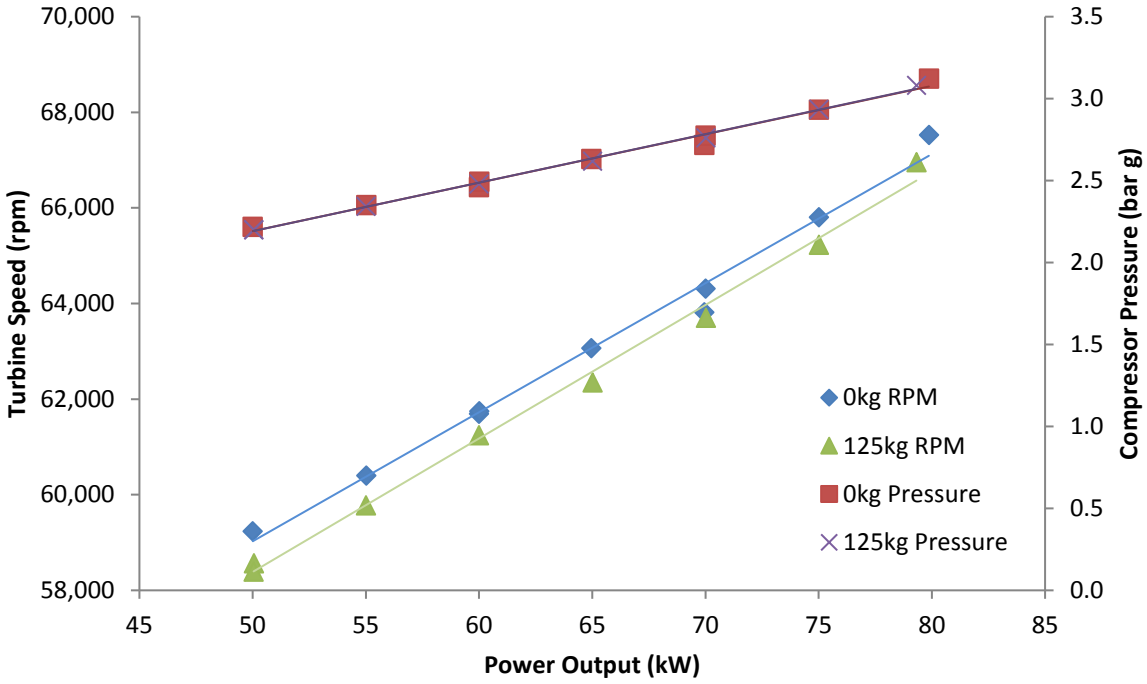

Figure 4-10 Impact of CO2 on the turbine frequency.

After the compression the CO_2 enhancement significantly impacts the oxidiser, altering the heat capacity and density. Figure 4-11 The CO2 addition impact on the post compression temperature (T2shows the CO_2 addition impact on the post compression temperature (T2) depicts the injected CO_2 influence on the compressed working fluid temperature TC2. The lower temperatures achieved is due to the higher heat capacity of CO_2 than that of the air it displaced.

The compressor work input (W_C) is equal to the heat capacity (c_p) of the oxidiser times the output temperature (T_2) of the compressor minus the input temperature (T_1).

$$W_C = c_p\,(T_2 - T_1)$$

Increasing the mass of CO_2 in the oxidiser increases the heat capacity and therefore would require more work for the same compressed combustion air temperature to be achieved. [91]

In addition the effect of the higher ambient temperature reduces the air density and pressure ratios, and total mass flow. To compensate the turbine frequency increases. [57]

4.5.1.3 Temperature Changes

Figure 4-11 The CO2 addition impact on the post compression temperature (T2shows the CO_2 addition impact on the post compression temperature (T2) and it is observed there is a change in the compressed air temperature with CO_2. In addition the plot shows consistently lower temperatures post compression with the only anomalous dip being from the lowest ambient temperature days. There was not available temperature measurement to effectively monitor the impact of this on the heat recovery of the recuperator, or measurement in the combustion chamber. The TC2 reduction in temperature, in combination with the knowledge that the heat capacity has been increased, the radiation and combustion characteristics changed.

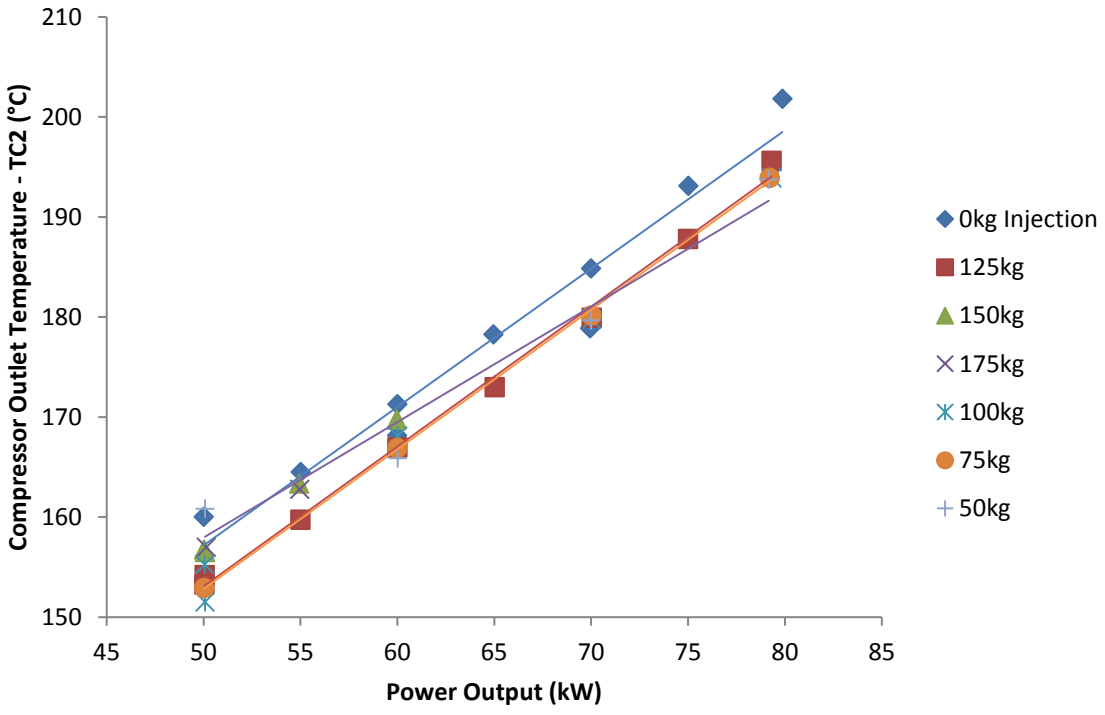

Figure 4-11 The CO_2 addition impact on the post compression temperature (T2).

The contrast in heat capacity between the baseline with no CO_2 injection, and 125kg/h is shown in Figure 4-12 Heat capacity change. In addition the trend also shows the decreasing influence

that CO_2 constant mass injection has on heat capacity at higher power outputs, due to the disproportionately higher turbine speed, and hence mass flow increase making CO_2 a smaller proportion of the oxidiser mix.

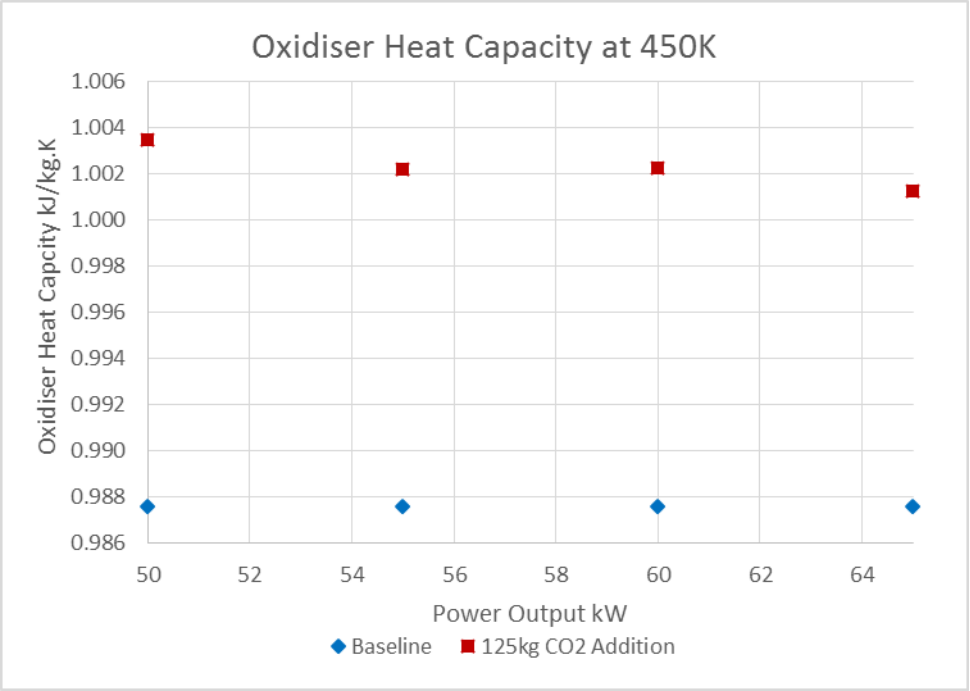

Figure 4-12 Heat capacity change.

4.5.1.4 Emissions Analysis Impact of the EGR

4.5.1.4.1 Emissions Reporting and Correction

As discussed in Chapter 3 the baseline, gas species reported have been corrected to a dry basis, and these have been reported and analysed as such. The standard reporting method for the NO_x emissions from the combustion power plant is corrected to 15% O_2, as mandated by the EU Large Combustion Plants Regulation 2012, requiring data to be reported on a dry basis at 273.15K, 101.3kPa and 15% O_2 for gas turbines [88]. This is discussed in Chapter 3.

However with Exhaust Gas recirculation this may not be an appropriate metric for equal comparison of combustion plant emissions. ElKady et al. [60] correctly suggested that recirculation will cause NO_x emissions to appear higher when corrected to an oxygen basis, in

comparison to non-EGR burners, which is particularly deceptive as the EGR can be used for peak temperature control to reduce NO_x on the basis of fuel consumption.

The skewing of the reported NO_x is due to the reduction of O_2 in the exhaust and this is due to the displacement of air with CO_2, due to the recirculation, or in this case of CO_2 enhancement, simulating it. Hence the smaller denominator in the NO_x the O_2 correction equation will result in a greater multiplication of the uncorrected NO_x volume. If the oxygen levels were known at the entrance to the combustor after recirculation then this may be allowed for. However the inlet oxygen conditions are considered to be 20.9%.

There are more appropriate NO_x reporting metrics. Reporting NO_x in terms of fuel mass consumption, and net power output are more appropriate. ElKady et al. [60] reported emissions on a fuel mass basis, and it was not possible for ElKady et al. [60] to report them on a power basis, as it is within this study, as they were only utilising a combustor. The calculation for the NO_x Emissions Index (g/Kg Fuel) is given by:

NO_x Fuel Emissions Index

$$NO_{x_{EI}} = \frac{NO_{x_{mg/Nm^3}} . Exhaust_{Total\, m^3/h}}{Fuel_{\dot{m}}} \quad \textbf{4-7}$$

The NO_x/kWh, corrected to 15% O_2, can thus be calculated using:

NO_x Reported per kWh:

$$NO_{x_{g/kWh}} = \left(\frac{\left(NO_{x_{mg/Nm^3}} . Exhaust_{Total\, m^3/h} \right)/1000}{Net\ Power_{kWh}} \right) \quad \textbf{4-8}$$

The EU Industrial Emissions Directive (IED) regulation includes a large single cycle gas turbine, those with an efficiency greater than 35%, with NO_x limited to 50η/35 (where η is the turbine efficiency, which would give 34mg/Nm3 for the T100.

The Turbec T100 microturbines do not fall under these regulation definitions and emissions limits [88]. There are other applicable emissions limits for single cycle CHP units from regional air quality guidelines. An example would be the Greater London Authority proposes 5g/kWh for compression ignition gas engines [89]. The Turbec Series 1, under normal operating conditions, is compliant and achieves significantly lower emissions, as detailed in Chapter 3.

4.5.1.4.2 CO_2 Impact

At the PACT, Low Carbon Combustion Centre there is the capacity to enhance the Turbec Series 1 oxidiser with 175kg/h of CO_2.

The CO_2 added to the oxidiser has an almost predictable linear impact on the exhaust concentration found with the FTIR analysis. This is seen in Figure 4-13 CO2 vol% with the addition of CO2 to the oxidiser. which shows the CO_2 Vol% with the addition of CO_2 to the oxidiser. The decrease in the exhaust volume CO_2 % on higher turn down ratios with the same CO_2 mass addition is attributable to the higher turbine speeds required to achieve those powers compressing more air, resulting in a greater total mass flow.

The mass flow is calculated from the measured CO_2 volume percentage, and the known CO_2 addition via the mixing skid for the simulated EGR experiments. This technique exposed the increase of total flow for high powers, and the resultant significantly leaner fuel:air ratios than CCGTs. The microturbines fuel:air ratio is calculated to be 1:105-130, with a CCGT being 1:42-58. [92]

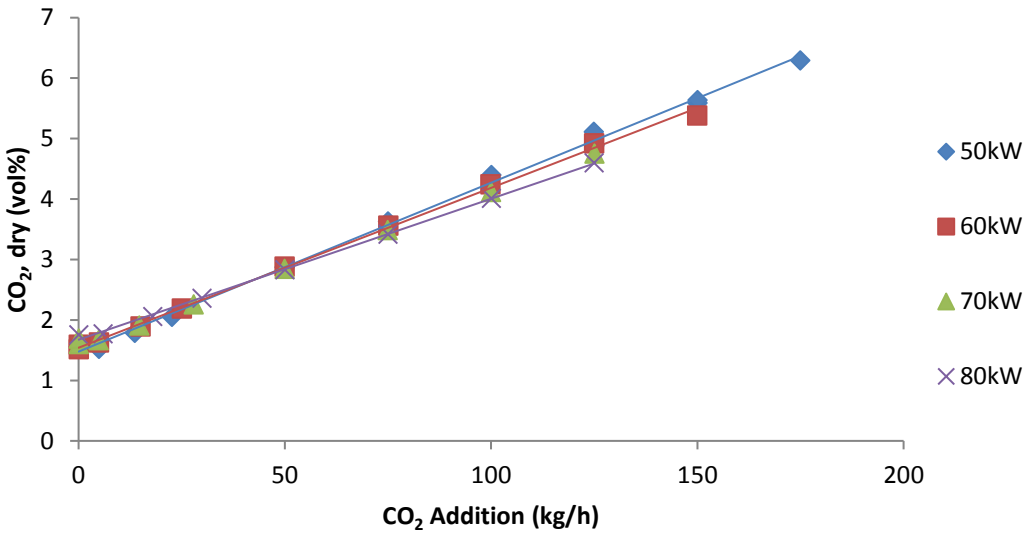

Figure 4-13 CO2 vol% with the addition of CO_2 to the oxidiser.

4.5.1.4.3 Combustion Performance

The reduction of oxygen concentration in the oxidising gas for combustion significantly effects the combustion performance. Insufficient oxygen can prevent combustion, and the oxygen levels only as low as 14-16% cause flame instability. [60]

Exhaust gas recirculation causes the displacement of oxygen, with CO_2 from combustion, and nitrogen as oxygen is consumed for combustion. With the CO_2 enhancement, high levels of CO_2 injection causes the same effect.

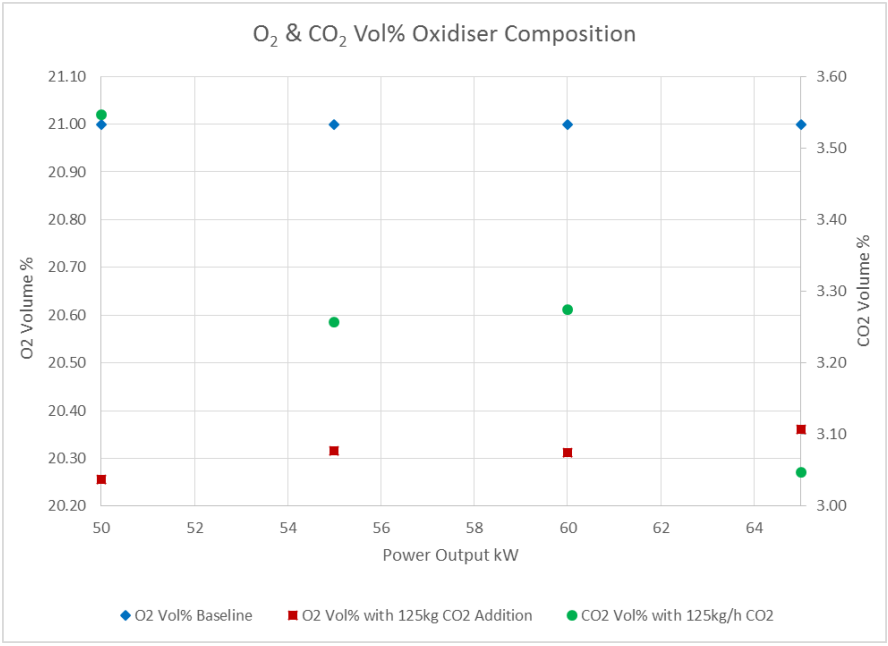

Figure 4-14 Impact of CO_2 addition on O_2 Vol%

With gas, the Turbec gas turbines fuel:air ratio is very lean, in Figure 4-14 Impact of CO_2 addition on O_2 Vol% the impact of constant CO_2 addition on O_2 and CO_2 vol% in oxidiser is depicted at 125kg/h. Though CO_2 increases 3.05 – 3.55% the oxygen displacement is not as significant. With oxygen being calculated to be 19.4% with the maximum CO_2 volume injection possible and lowest turbine power at the Low Carbon Combustion Centre. The plot also shows how the higher turbine speed increases flow rate, hence making CO_2 vol% lower. At such levels, lean blow out is not a significant risk, and the combustion performance would not be expected to significantly suffer as seen in the studies by Elkady et al.

4.5.1.4.4 CO & UHC

The reduction in O_2, and the increased heat capacity from the higher heat capacity of CO_2, do still both have a combined impact on complete combustion. This impact is observed at low powers of 50-55kW, and this is where the fuel:air ratio is at its richest.

As shown in Figure 4-15 The CO & CH4 emissions baseline comparison with 125kg/h CO2 enhancement across the turn down ratios, an elevation in the level of CO is recorded and this is

due to reduction in oxygen availability. The incomplete combustion of the natural gas, results in higher methane and TOC emissions. The increased heat capacity from the addition of CO_2 to the oxidizer also influences the reaction rates, reducing them and hence the flame speed. The combination in this reduction in the reaction rates and the depletion of oxygen is the cause of the increase in the incomplete combustion observed.

The observed poorer combustion performance of the Turbec series 1 gas turbine at low turn down ratios, with and without enhancement with CO_2, is attributable to the turbine combustor design, and the temperature. Continuous operation of the Turbec gas turbine is expected to be over 60kW.

The results follow the trend of the findings presented by Evulet et al [93], with higher levels of exhaust CO at reduced temperatures, with the EGR causing these to rise further. The reduced total mass flow of oxidiser, due to the lower turbine speed and pressure ratio, could be insufficient for full and effective premixing of the fuel in the burner[57].

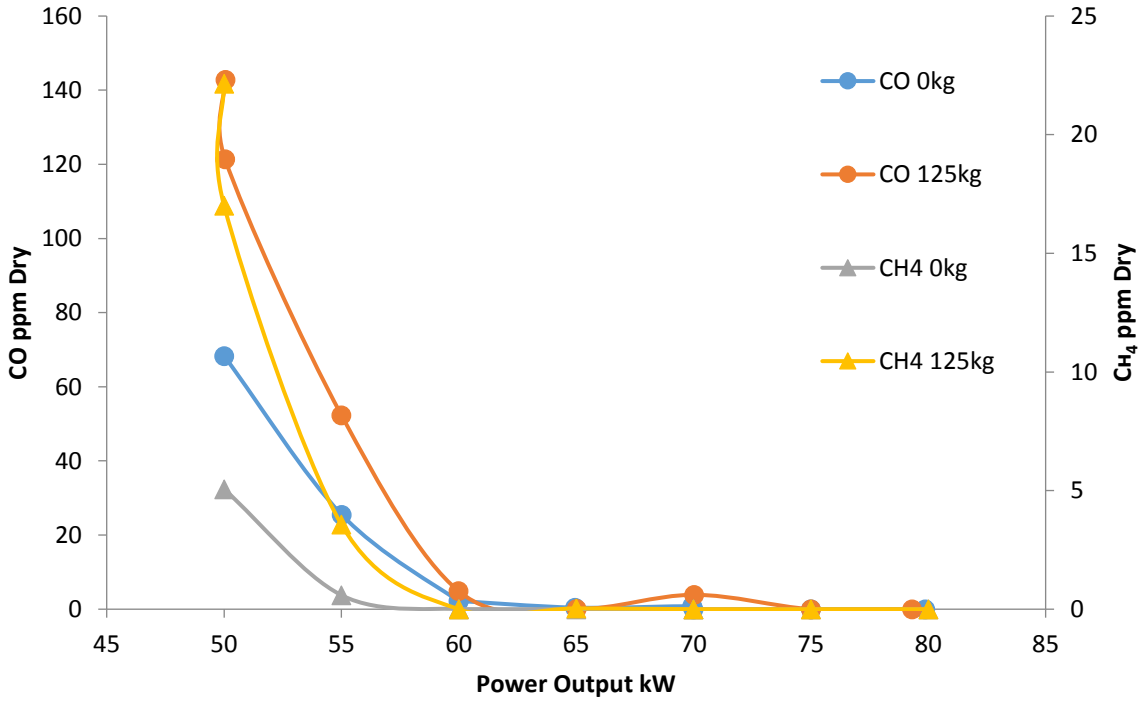

Figure 4-15 The CO & CH_4 emissions baseline comparison with 125kg/h CO_2 enhancement across the turn down ratios.

A significant and clear trend for this was found, with only one anomalous result at 70kW with 125kg/h of CO_2 enhancement for which there wasn't a significant standard deviation in the FTIR results collected. However on the test day all the results for CO were 2-3ppm higher than on any other run. This may be attributable to the fuel source, or more likely to the presence of the ambient CO. Ambient CO levels of this concentration would not be considered unusual with several urban studies finding similar levels, in addition to which it should be considered that the Low Carbon Combustion Centre is on an industrial estate where combustion does take pace, and near a busy road the wind direction could easily cause this raised level [94, 95].

4.5.1.4.5 NO_x

There is significant regulation over NO_x emissions from both stationary, and mobile sources, due to the impact it can have on the environment, and human health. The NO_x was measured during the experiments with FTIR as mg/Nm^3, for the purpose of effective comparison of other emission sources it is converted to g/kWh (kg/MWh) using NOx Fuel Emissions Index & NOx Reported per kWhThe NOx is reported per kWh.[60]

The NO_x levels produced by the series of experiments with CO_2 enhancement simulating the EGR showed consistent reductions. This trend with a reduction in the NO_x species produced is attributable to the increased heat capacity of the oxidiser and combustion mix. The higher heat capacity results in lower temperatures, and thus a reduction in the creation of thermal NO_x, the primary source of the NO_x emissions. [57]

The turbine inlet temperatures reduced in line with CO_2 enhancement as would be expected. Calculated TIT values were 6-13C lower with CO_2 enhancement, although this is just indicative of the temperature change due to the calculation methodology. The NO_x emissions performance was also best during the operation at the turbines optimal 60-70kW range.

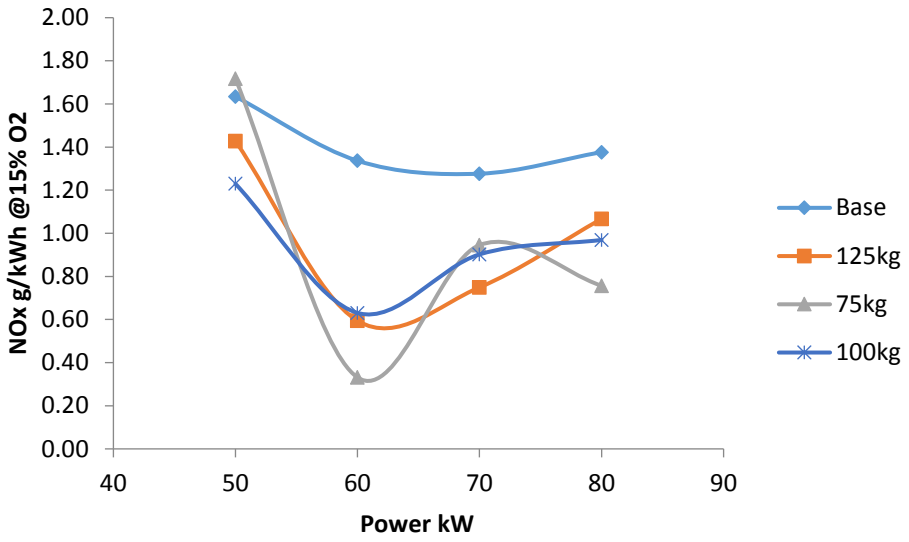

Figure 4-16 The NOx g/kWh at 15% O2, with CO_2 enhancement.

A NO_x reduction was apparent in 11 out of the 12 tests with the addition of CO_2 to the oxidiser simulating the EGR, with only the behaviour of the 75kg/h appearing more erratic. The reason for the varied 75kg/h behaviour has not been discernible, not apparent in fuel consumption, TIT, or the ambient temperature.

4.5.1.5 Efficiency Impact of the EGR

A significant reduction in the combustion efficiency would be expected to result in the fuel consumption increasing for the same power output when the oxidiser is enhanced with CO_2. Changes in the fuel consumption during the testing was in line with the observed combustion species and CO_2 enhancement. Although the efficiency changes did not present a very strong trend, on closer analysis there are nominal increases in terms of the specific fuel consumption (SFC), thus presenting a clear trend, with SFC increasing 1.7 – 2.9% with enhancement of 125kg/h. This shows CO_2 enhancement, which replicated the EGR, and reduced the turbine efficiency of power generation. The efficiency of a CCGT, with significantly higher fuel flow rate and a richer fuel:air mix would be expected to be significantly more impacted on the basis of the findings here.

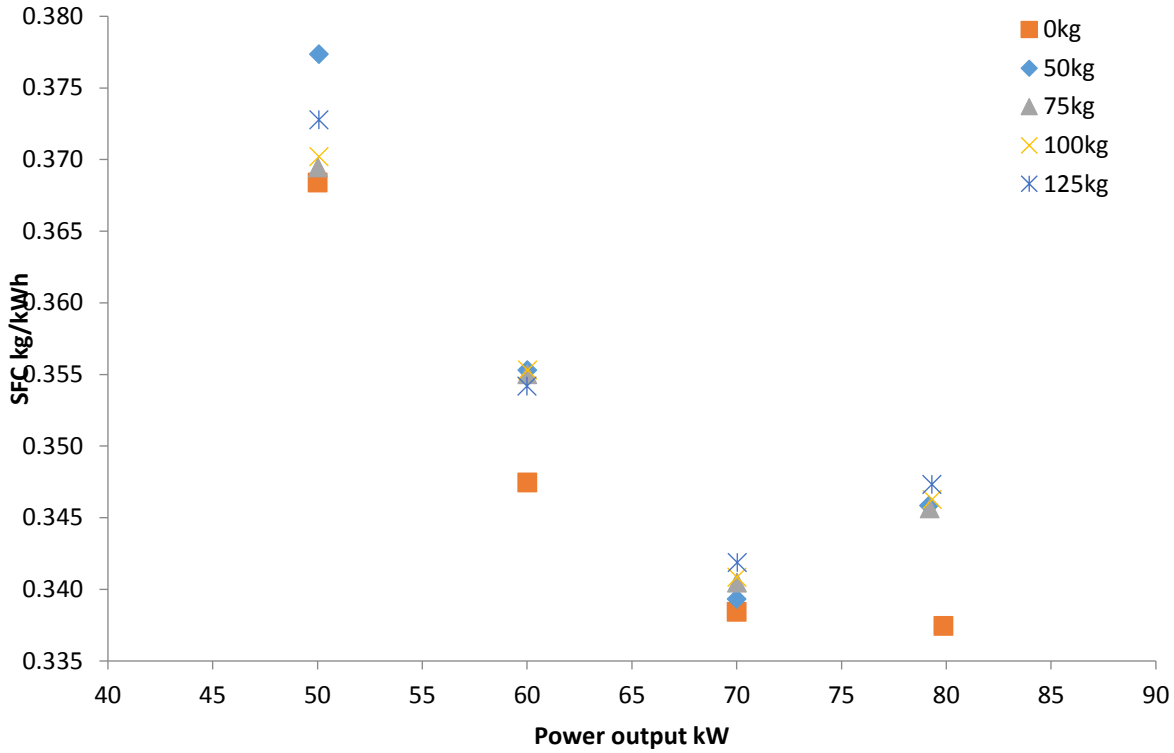

Figure 4-17 Specific fuel consumption with varying CO2 enhancements

Before the testing it was expected that enhancement with CO_2 would have a more significant impact on the combustion and the turbine performance, but this did not occur due to the low fuel:air ratio. For this reason, CO_2 enhancement as a volume % was low, even large CO_2 mass addition, equivalent to over 50% EGR, up to 356% created a relatively small CO_2 increase, displacing less air, and thus leaving sufficient oxygen for combustion, and having a less severe impact on the oxidiser heat capacity and the flame speed.

The mass of the fuel consumed has been calculated from the volumes recorded, and some of the points from this calculation fall within the maximum potential instrumental error. However there is a significant visible trend that is unlikely to be anomalous due to the number of data points over which it is observed. The significant outlier is the 50kW generation with 50kg/h of CO_2 enhancement having a higher than expected SFC, this can be attributed to the highest

ambient temperature on that test day, indicating the dominance of ambient temperature on the efficiency.

4.5.1.6 Energy Intensity of Capture

Regeneration of capture solvent is the most energy intensive process of post combustion capture. By increasing the partial pressure of CO_2 in the exhaust, the relative mass flow of solvent, and hence regeneration required can be reduced[55]. Models have shown an increase in the exhaust concentration from less than 2% to above 5% may reduce the reboiler duty from 7.5MJ/kgCO_2 to below 4.0MJ/kgCO_2, which is an energy saving of over 45%.

The post combustion capture performance at the PACT facility is significantly less than that. Tests were conducted at 4.5% vol CO_2upwards so as to represent the CCGT emissions. Solvent regeneration at 4.5% CO_2 resulted in energy intensity of capture at 8.3MJ/KgCO_2, and at 6.5% CO_2 7MJ/Kg [96]. Comparable exhaust gas concentration numbers to those tested with the gas turbine are 50kW, with 100kg of CO_2 enhancement giving 4.34% CO_2 volume percent in the exhaust emissions, and 125kg giving 5.11 vol% CO_2. Akram et al, 2015, extrapolates the energy consumption to dropping 7.5% per 1 percent unit increase of CO_2, giving an estimated regeneration of 8.4MJ/KgCO_2 at 4.34% exhaust CO_2 and 7.92MJ/KgCO_2 at 5.11% CO_2 exhaust volume. This represents a 5.7% reboiler efficiency gain for the PACT facilities small scale capture plant, and an increase in capture efficiency. When compared to the Turbec Series 1, there is 1.7% to 2.9% increase in the specific fuel consumption. This is a relative overall efficiency gain for the system process with CO_2 enhancement simulating EGR at this pilot scale. On a larger demonstration scale, or even commercial size, significantly larger process efficiency gains can be expected due to more efficient and less CO_2 intensive generation, the higher exhaust volume % of CO_2 with a recirculation up to 50% of the total combustion volume, and the larger more efficient capture and regeneration plant required for larger scale capture per day. In addition to

more efficient built for the purpose design of the plant, rather than modular build up of the PACT test facilities.

4.6 Conclusions

In this chapter we have shown that there is quantifying reduction in combustor performance with the addition of CO_2 that is simulated high levels of the EGR.

The enhancement of the oxidising air with CO_2 resulted in a clear impact on the 3 key performance areas investigated. Affecting the turbine mechanically, having a visible impact on the combustion through exhaust emissions, and reducing the turbine efficiency as shown with increased specific fuel consumption.

The ambient temperature and the resultant temperature of the oxidiser, both with and without CO_2 enhancement, significantly affected the turbine performance. Turbine speeds increased significantly when temperatures were higher to maintain a consistent mass flow. The addition of CO_2 most significantly affected the temperature post compression, which can be seen clearly when in comparison to other 20°C ambient results. This is shown in Figure 4-11 The CO2 addition impact on the post compression temperature (T2), where 125kg/h CO_2 enhancement resulted in temperatures post compression being consistently 5C lower than those without the addition of CO_2.

Increasing the heat capacity of the working fluid may have an increased effect on the heat exchanger efficiency through providing lower temperature air into the cool side of the recuperator. It is expected that the increased heat capacity and radiativity [57] will have resulted in lower exhaust gas temperatures, as seen in TOT, than without the addition of CO_2, and hence a slighter lower temperature in the hot side of the recuperator. This means that there is less energy being available in the exchange. This will have contributed to the lower efficiency of the turbine with CO_2 enhancement simulating exhaust gas recirculation.

The enhancement with CO_2 of the air showed small changes in the emissions trends and this is in line with those expected. Higher CO and methane emissions resulted from the reduced combustion efficiency with increased CO_2 enhancement, which represented higher levels of EGR. Enhancement with 125kgCO_2/h at 50kW showed an increases in the CO emissions of 109%, and methane which accounts for the majority of the fuel composition up 338%. This is due to the displacement of oxygen with CO_2, meaning less availability for complete combustion, and with the extra CO_2 increasing the heat capacity in the combustion mix, thus causing temperatures to be lower and reducing the reaction rates and slowing flame speed.

The changes to the combustion caused an observable difference to the NO_x emissions. Decreases in flame temperature can be expected to result in a reduction in the thermal NO_x created. This trend was observed for 11 of the 12 points plotted in Figure 4-16 The NOx g/kWh at 15% O2, with CO2 enhancement. Although the reduction in thermal NO_x was small, going form 0.20g/kWh to 1.01g/kWh, the trend was consistent. The NO_x emissions produced by the Turbec Series 1, both with and without CO_2 enhancement, are within the Greater Londons, and German air quality emission limits of 5g/kWh and 75mg/m^3 at 15% O_2.

Changes in the efficiency and carbon intensity were observed with the addition of CO_2. There was a small trend of decreasing electrical efficiency, however these changes were within the maximum potential instrumental error. When closely examined in terms of specific fuel consumption, the trend of a reduction in efficiency is consistent, and extremely unlikely to be caused by error. With 125kg/h of CO_2 enhancement specific fuel consumption was seen to rise 1.7 – 2.9% above that of the turbines without CO_2 addition. This is the change in performance that would be expected with exhaust gas recirculation.

Through adding known volumes of CO_2, it was possible to more accurately calculate the total mass flow of the oxidizer through the turbine than before the series of experiments. This showed that the total mass was significantly higher than first anticipated, and that fuel:air ratios were

very lean down to 1:105-130, which is much more so than a CCGT of 1:42-58 [92]. This very fuel lean ratio is the reason that there was less significant impact on the combustion and the turbine performance than was postulated before the experiments were carried out.

5 Simulated EGR with HAT

5.1 Introduction

This chapter explores the possibility of combining both exhaust gas recirculation (via CO_2 injections to the compressor inlet) and HAT (humidification of the cycle through steam injections between the compressor outlet and cold-side recuperator inlet) processes with the purpose of improving post-combustion capture efficiency through the resultant increase in flue gas CO_2 concentrations. These methods will also reduce the volumetric gas flowrate requiring treatment, thus further enhancing the capture performance. The chapter explores the relative impacts on the emissions of each process and in combination. The effects on the emissions as an indicator of incomplete combustion is characterised by CO and UHC emissions, and a range of turbine parameters are also quantified, including engine speed, fuel consumption and thus efficiency. Taimoor et al. [97] and others have simulated the impact of the processes addition on a CCGT. However this is the first experimental work of this kind that investigates the combination of both techniques.

Humidified Air Turbines (HAT), where steam is injected before combustion to improve the turbine efficiency, reduces the NO_x emissions and after being condensed out increases the volume percentage of CO_2 found in the exhaust. Exhaust gas recirculation (EGR), where combusted air is recycled to increase the CO_2 content in the exhaust, is a more efficient capture process.

EGR can increase the capture process efficiency from gas turbine emissions due to the increased partial pressure of CO_2 [55]. However EGR can reduce the combustor performance, this reduces the peak temperatures, and turbine inlet temperature [70]. HAT has been shown to increase turbine efficiency through increased mass flow, and the addition of mass post compression, thus reducing the compressor work. It may be possible to negate some of the reduced turbine

efficiency experienced with EGR by combining it with HAT. However HAT has its own detrimental impact on combustion, and hence all the benefits must be balanced. It may be the case that in the T100 microturbine, due to the lean fuel air mix, that there may be a limited impact on the combustion [98], and hence HAT will provide significant performance and efficiency benefits to the turbine. Simultaneously, as previously seen in experiments at the PACT core facility, the CO_2 enhancements have limited impact on the combustion whilst providing significant capture efficiency gains. However in a CCGT with significantly air leaner mixes, both EGR and the HAT process may have a significantly larger impact on the combustor, and thus cause flame stability and lean blow out issues.

Humidified Air Turbines have been used historically to improve turbine efficiency and reduce emissions. Also it has the benefit that after being condensed out of the exhaust gases that the volume percentage of CO_2 is increased, meaning more efficient capture is possible with higher partial pressure. [63]

In a conventional gas turbine, the pressure ratio and turbine inlet temperature are the biggest factors driving the performance of a turbine. With HAT, the rate of steam injection post compression becomes a strong influencing factor. Steam injection increases the specific power output of the turbine and steam injection reduces NO_x formation. The addition of steam increases the mass flow through the turbine[63]. If this steam is added post compression (as it is in the experimental set up) it means additional mass flow through the turbine for which the compressor has not had to do work for. This is indicated in the experiment by the constant compressor pressure at vary steam injection rates. The addition of steam also increases the specific heat capacity of the oxidising working fluid, implying that a greater heat transfer through the recuperator can be achieved by increasing its efficiency [64]. The steam also cools the flame temperature and reduce NO_x formation. Older lower NOx combustors used water for peak flame temperature control[63].

The residence time and temperature are the factors that influence the thermal NO_x formation. Steam acts as a diluent reducing temperature. Although the addition of steam may appear to augment the power output of the microturbine, this is not taking into account the energy of rendering the steam which is done by an external unit. [65] If water was added instead of steam to the post compression phase then efficiency gains would be reduced due to the energy required to generate that into steam.

The addition of steam to create humidified air can cause combustion instabilities and this would be shown by higher levels of UHC and CO [66]. It is possible to reduce NO_x without increasing CO and incomplete combustion significantly.

However it has been shown when HAT is used the higher concentrations of CO_2 can be achieved in the exhaust gas on condensing out the air [67].

5.2 Modifications to the Beighton Facilities

The PACT centre is constantly increasing in capacity. In particular there have been significant modifications and improvements made to the capture tower, and process, and additional instrumentation since last publication by Akram et al [99].

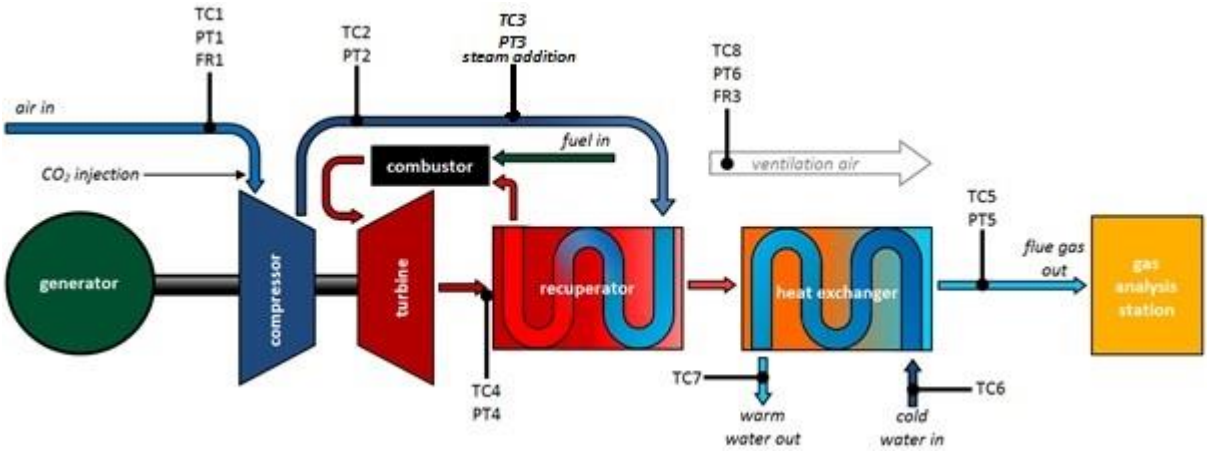

Figure 5-1 Schematic of the components of the Turbec T100 PH combined heat and power gas turbine system, including the modifications made CO_2 injection for HAT and with instrumentation (TC – thermocouples; PT – pressure transducers; FR flowrate meters).

Additional instrumentation was added in house to measure more temperature, pressure and flow rate parameters. As shown in

Table 5-1 Additional Instrumentation, this additional instrumentation data was collected using the Compact RIO-9022 Real–Time controller, and displayed and recorded the custom LabView program developed for the EGR experiments with new additional adaptations in the form of TC3 and PT3.

Table 5-1 Additional Instrumentation for Series 1

LabView DESIGNATION	PARAMETER	UNIT OF MEASUREMENT
THERMOCOUPLES		
TC1	system air inlet temperature	°C
TC2	compressed air temperature (compressor outlet)	°C
TC3	steam inlet temp	°C
TC4	flue gas diffusion zone temperature	°C
TC5	flue gas outlet temperature	°C
TC6	cold water temperature (heat exchanger inlet)	°C
TC7	hot water temperature (heat exchanger outlet)	°C
TC8	ventilation air outlet temperature	°C
PRESSURE TRANSDUCERS		
PT1	system air inlet pressure	bar g
PT2	compressed air pressure (compressor outlet)	bar g
PT3	steam inlet pressure	bar g
PT4	flue gas diffusion zone pressure	bar g
PT5	flue gas outlet pressure	bar g
PT6	ventilation air outlet pressure	bar g
FLOWRATE MEASUREMENTS		
FR1	system air inlet flowrate (total air in) – measured	kg/min
FR3	ventilation air outlet flowrate – measured	kg/min
FR4	flue gas outlet flowrate – calculated	kg/min

All the gas species are measured using a Gasmet DX4000 FTIR, Fourier transform infrared spectroscopy, measuring the absorbance of the infra-red to determine the gas species within a sample. In the previous chapter, oxygen was monitored using a Servomex Servoflex MiniMP 5200 analyser. In this study, oxygen was monitored using a modification to the Gasmet DX4000 FTIR.

5.2.1 Steam Generation and Delivery

For the HAT process, the decision was to use a boiler and add the steam post compression. The boiler available was a Fulton 10J, with a 100kW thermal rating designed to generate up to 160kg/h of steam, however due to its age it was not possible to render this amount. The steam is inserted into the turbine at pressure, post compression. The dew point of the steam must be considered. The dew point is where steam condenses into water and this can occur with a drop in pressure or temperature. The pressure of steam injection ranged from 3.84bar – 5.28 bar, and the pressure of the compressor generated during testing was 3.1bar – 3.76 bar. The temperature of the compressed air was slightly higher than TC3 steam temperature. The temperature and pressure of the compressed oxidiser mix is taken after the point of steam enhancement, and takes account of the effect of its addition.

If water condensate were to be entrained into the combustor then this could lead to flame turbulence and possible blow out.

Therefore the additional injection of steam must be above the pressure of the compressed air.

For this reason the additional pressure transducer and thermocouple is installed to monitor immediately before injection. In the region into which the steam was injected the pressure was monitored also. The maximum expected pressure is 4.5 bar gauge and in practice, during testing, 4.12 bar was achieved by the compressor.

The steam boiler generates a maximum pressure of 7bar, before then travelling to the mixing SKID and then from the mixing SKID to the turbine. When all the valves are open, the boiler does not maintain 7 bar generation consistently.

Steam is generated through the combustion of oil fuel that is dragged into the boiler via a negative pressure.

Figure 5-2 Photograph of the boiler house, water tank, boiler, and pressure.

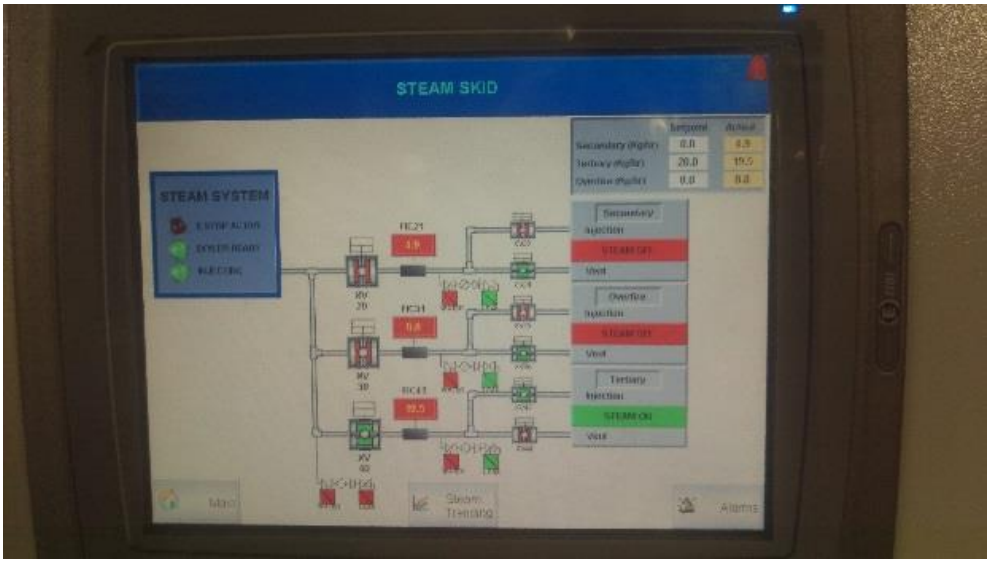

Figure 5-3 Photo of the steam Skid control and monitoring of the tertiary line.

Testing with steam was carried out at 20- 40kg/h, and monitored by the steam skid as shown in Figure 5-3 Photo of the steam Skid control and monitoring of the tertiary line which shows the steam skid control and monitoring of the tertiary line. During testing it was not possible to attain high mass flows of steam planned at the required pressure. This was due to the boiler not being maintained at this pressure. The cause for this was investigated but not resolved. It was thought that the fuel delivery may have been the issue, or the fuel viscosity but inspection of fuel filters

showed that they were free from debris that would restrict flow. The cost of full service was prohibitive particularly in comparison to the cost of replacement.

5.2.2 Steam Addition Point

Figure 5-4 Photograph of the steam Injection point into compressed air line, steam deliver valves, manual and pneumatic.

Steam is injected into the compressed air shown in Figure 5-4 Photograph of the steam Injection point into compressed air line, steam deliver valves, manual and pneumatic the steam line through the top of the turbine. To control the flow there is a manual valve that is opened before start up and then during the operation a pneumatic valve is opened remotely. The valve is not opened until steady steam flow is achieved, and the pressure at injection is steady and above the pressure of the compressed air. The valve was closed by turning off the compressed air supply.

5.3 Power Electronics Failure

After initial successful commissioning runs with steam, on the following test day the turbine would not start, and on inspection there was evidence that water had pooled in a tray below the heat exchanger, Figure 5-5 Photographs showing evidence of steam condensate, and above the power control electronics of the turbine it is probable that the condensed water dripped

onto it, or that the conditions were very humid in the electronics cabinet see Figure 5-6 Photograph of the Turbec power electronics.

Figure 5-5 Photographs showing evidence of steam condensate rust.

The cause of the condensed steam from the heat exchanger was thought to be either due to a leak in the heat exchanger, or possibly from the back flow of condensate in the exhaust, as the exhaust is vertical from the exit.

Figure 5-6 Photograph of the Turbec power electronics.

To tackle this issue the water pumps for the heat exchanger were switched off and the heat exchanger was drained of all water. The entry water valve was closed off and the exit valve was opened to allow expansion and contraction of the air trapped inside. Holes were drilled into the tray and piped out so the formation of any condensate during testing could be monitored whilst the turbine cabinet is shut.

After drainage of the heat exchanger, short steam injection test runs were carried out, then stopped before opening the turbine and allowing it to cool to check for evidence of condensate.

The exhaust gas temperature rose from 130 - 145°C, with the heat exchanger from 230 – 260°C, and no further evidence of condensate was found, with the remaining tests being completed without further turbine breakdown.

5.4 Methodology

5.4.1 Experimental Test Conditions

Both steam and CO_2 addition were varied. Steam at 0, 20, or 40kg/h with addition of CO_2 was added at 0, 50, 75, 100, 125kg/h, and this was done across various turn down ratios.

The experimental set-up involved the Series 1 gas turbine with CO_2 injections to the compressor inlet and steam injection to the compressor outlet, coupled with the extensive monitoring systems for the various gas turbine parameters and flue gas species that were assessed via an FTIR and paramagnetic oxygen transducer. The gas turbine parameters were those that are internally monitored with a winnap program, as well as additional instrumentation that has been integrated into the turbine system to ensure the full systems monitoring and more comprehensive characterisation of the gas turbine cycle. There are 3 variables for the test conducted. The electrical power output of the turbine, the CO_2 mass enhancement that mimics the exhaust gas recirculation, and the mass addition of steam for the HAT simulation. There are 35 permutations of the conditions tested in this study, with 0kg – 40kg steam addition, 0 – 125kg CO_2 enhancement (representing different levels of EGR depending on the power output – EGR ratios of up to 356 % were tested), over turn down ratios 50 – 70kW; a test matrix was designed accordingly, and this is outlined in Table 5-2 HAT & EGR test conditions matrix.

Table 5-2 HAT & EGR test conditions matrix.

	Steam Addition											Reference Total Engine Airflow kg/h
	0kg/h	20kg/h					20kg/h					
CO_2 Addition	0kg/h	0kg/h	50kg/h	75kg/h	100kg/h	125kg/h	0kg/h	50kg/h	75kg/h	100kg/h	125kg/h	
50kW												2738.65
55kW												2902.12
60kW												2982.97
65kW												3178.00
70kW												3222.11

These primary variables were the only ones that were intentionally varied during the course of the experiments; atmospheric/ambient conditions, which have an impact on the results, as considered in Chapter 4, cannot be controlled and therefore the air inlet temperature and relative air humidity varied throughout the test campaign. All the tests were carried out over a minimum of 15 minutes of continuous stable operation as recommended by ISO 2314 for evaluating the mechanical and emissions performance [100]

5.5 Results

The results are presented as in previous chapters without plotting the errors, see Table 5-3 Instrumental error the deviation. As testing was carried out during steady operation, and averaged over 15 minutes, they are too small for meaningful depiction.

Table 5-3 Instrumental error.

	Instrumental error	
Instrument	**%**	**Unit**
Gasmet DX4000 FTIR	na	na
Quantometer	0.63%	
Type K thermoucouples	0.40%	1.5°C
Rosemount pressure transmitters 2051CDC2A	0.07%	0.8 mbar
Rosemount pressure transmitters 2051TG2A	0.07%	7.5 mbar

Table 5-4 Max SD

	Max Standard Deviation	
Gasmet DX4000 FTIR Readings	**Baseline**	**EGR & HAT**
CO ppm	17.32	17.32
CH_4 ppm	3.91	5.96
CO_2 vol%	0.02	0.02
NOx ppm	1.27	1.16
Turbec T100 Readings		
RPM	58.59	139.20
kW	0.464	0.464
T1 °C	0.60	0.60
Additional Instrumentation		
PT2 mbar	0.01	0.01
TC2 °C	0.53	11.63

5.5.1 Mechanical Performance with HAT & EGR

The addition of steam has a significant impact on the turbine frequency. The additional mass reduces the frequency from 1500 to 2000 rpm, and this is about 2.9%, being similar to the SFC savings of 3.2% at 50kW with 40kg steam addition. The lower pressure directly corresponds to the lower rpm that can be seen in Figure 5-7 Impact of steam addition on the turbine speed. This should mean a lower relative expansion change.

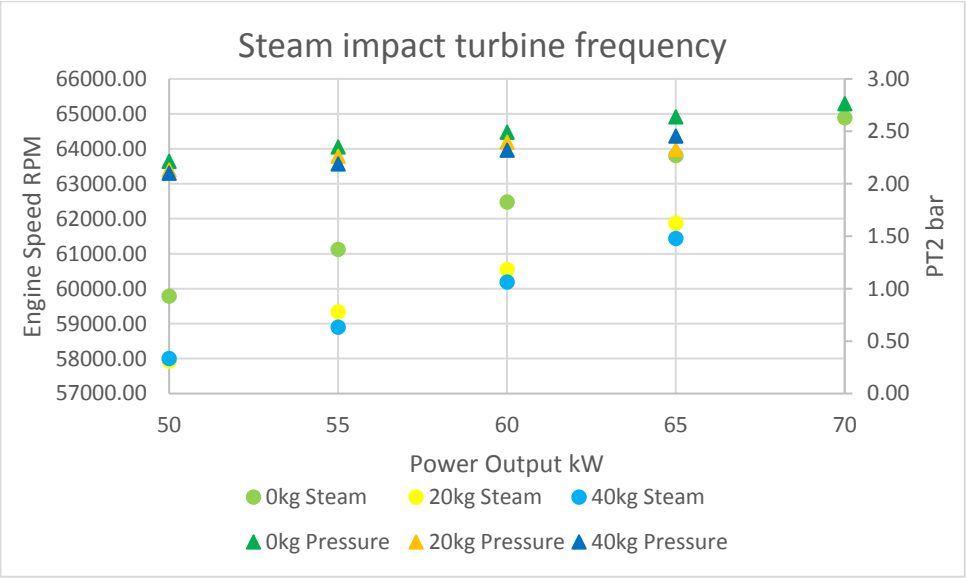

Figure 5-7 Impact of steam addition on the turbine speed.

The injection of the steam lowers the compressed air temperature fed to the recuperator and combustor. This reduction is due to the temperature being higher than that which the steam is injected.

5.5.2 CO_2 & HAT Performance

With the addition of CO_2, the temperature is less affected and it is more consistent, and this is probably because the heat capacity is higher, and the addition of steam produces a more radical change shown in Figure 5-8 Impact of the steam on the temperature post compression.

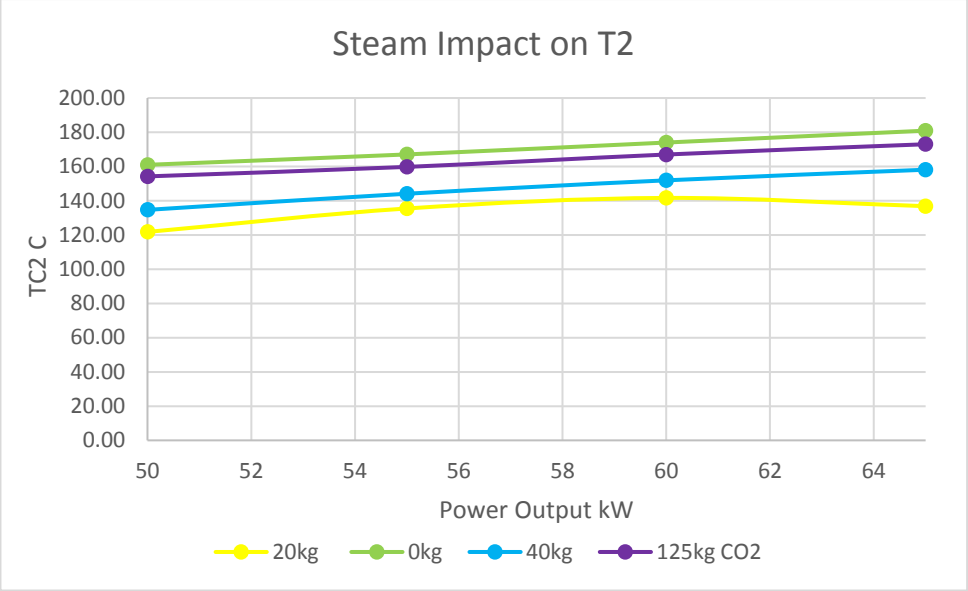

Figure 5-8 Impact of the steam on the temperature post compression.

5.5.2.1 Combined impact of HAT, CO2, & Ambient Temperature

With the addition of steam post compression, there is a change to the relevant impact ambient temperature. From Figure 5-9 Turbine speed and oxidiser temperature relationship with CO2 enhancement and it can be seen that the steam addition has the most significant impact on the turbine frequency, with speeds dropping with the increasing addition of CO_2. After this initial step with the steam addition, as previously observed in chapter 3 and 4, the turbine speed reflects the ambient oxidiser temperature. The lowest RPM for 40kg occurs on a test run with less than half a degree ambient temperature difference to the other test conditions. The RPM appears to be dictated by the mass of the steam addition for the HAT, and the quality and consistency of the steam flow.

This is also mirrored by the 20kg steam injection results, again with all of which with there is a maximum 0.5°C difference in the inlet temperature. There is a consistent trend of reducing the frequency with CO_2 enhancement replicating EGR, and this is in line with previous results published by Best et al [1].

The only anomalous result appears to be that of 40kg steam addition, at 125kg CO_2 injection. It would be expected that this would theoretically provide a lower frequency than it does, and a lower frequency would also be in line with all the other experimental results presented here. This anomaly could well be due to the quality and consistency of the steam delivery.

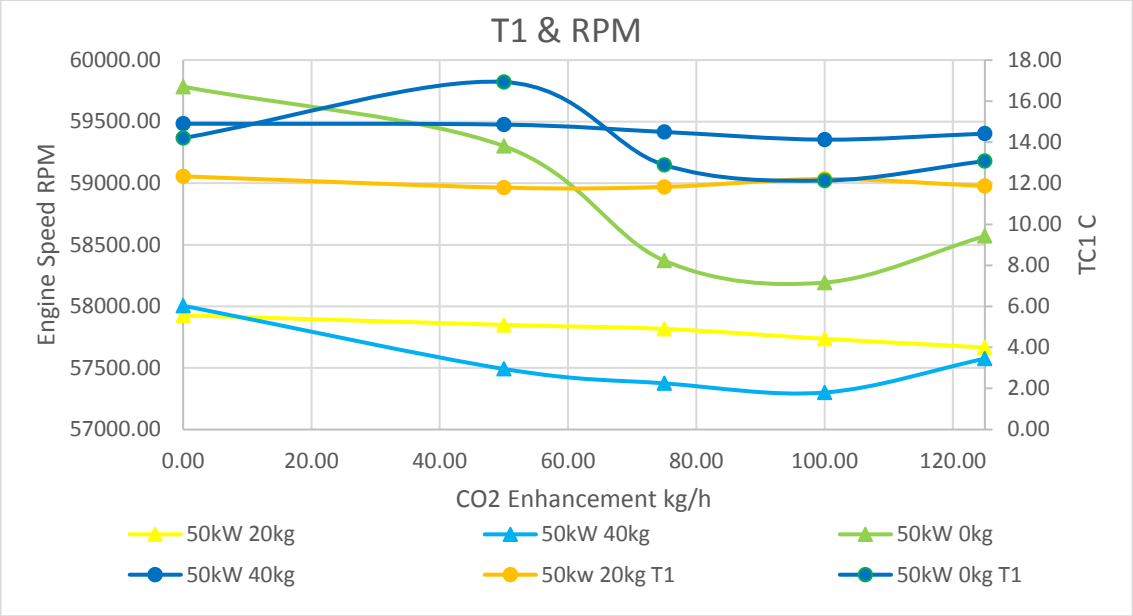

Figure 5-9 Turbine speed and oxidiser temperature relationship with CO_2 enhancement

5.5.2.2 HAT Base Performance

With the addition of steam post compression to simulate the HAT process, it is expected that the CO_2 would increase on a dry basis in the exhaust, above that of the baseline, with steam displacing the air. Although this is observed in **Error! Reference source not found.**, and with this good trend of higher CO_2 with steam addition with the volume percentage fractionally larger due to the HAT process after the water has been condensed out. The higher 40kg steam injection rate is expected to increase the CO_2 vol% more than the 20kg addition, but this is not observed. With 3 of the 4 20kg steam addition results being higher than the 40kg results. This discrepancy is greater than the maximum deviation observed at these conditions of 0.02 vol%.

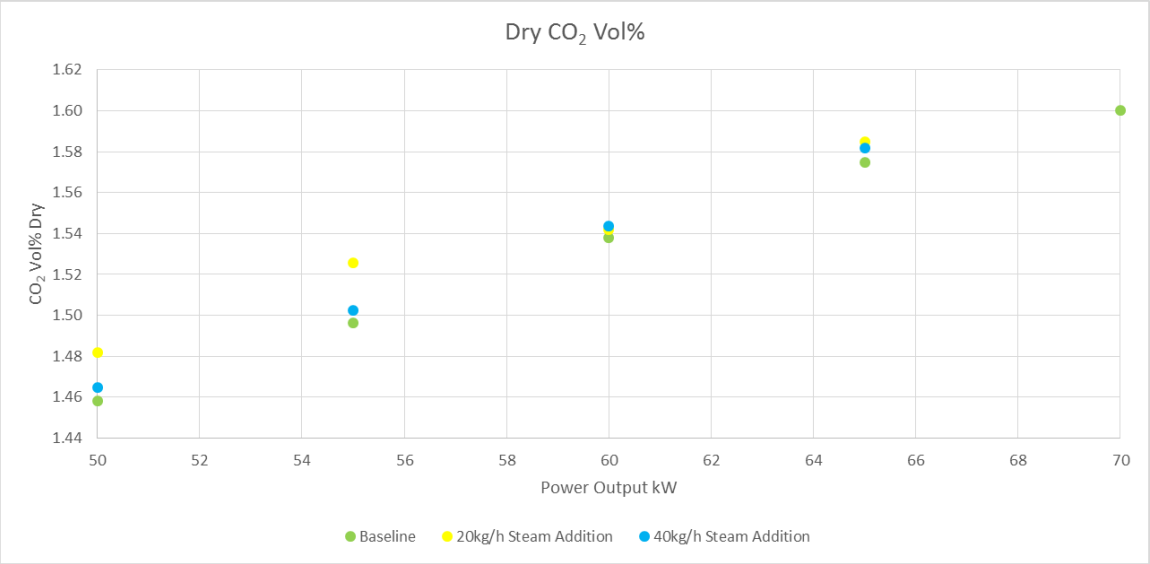

Figure 5-10 HAT CO_2 exhaust emissions across turn down ratios

5.5.2.3 Combustion Performance

5.5.2.3.1 Emissions Impact

With the addition of CO_2 to simulate the EGR with HAT, a linear CO_2 volume percentage increase was present, as previously observed in Best et al [1]. The 40kg steam enhancement with increasing CO_2 injection across the turn down ratios of 50kW and 60kW are particularly strong, thus producing the highest volume percentage of CO_2 in the dry exhaust gases, as would be expected.

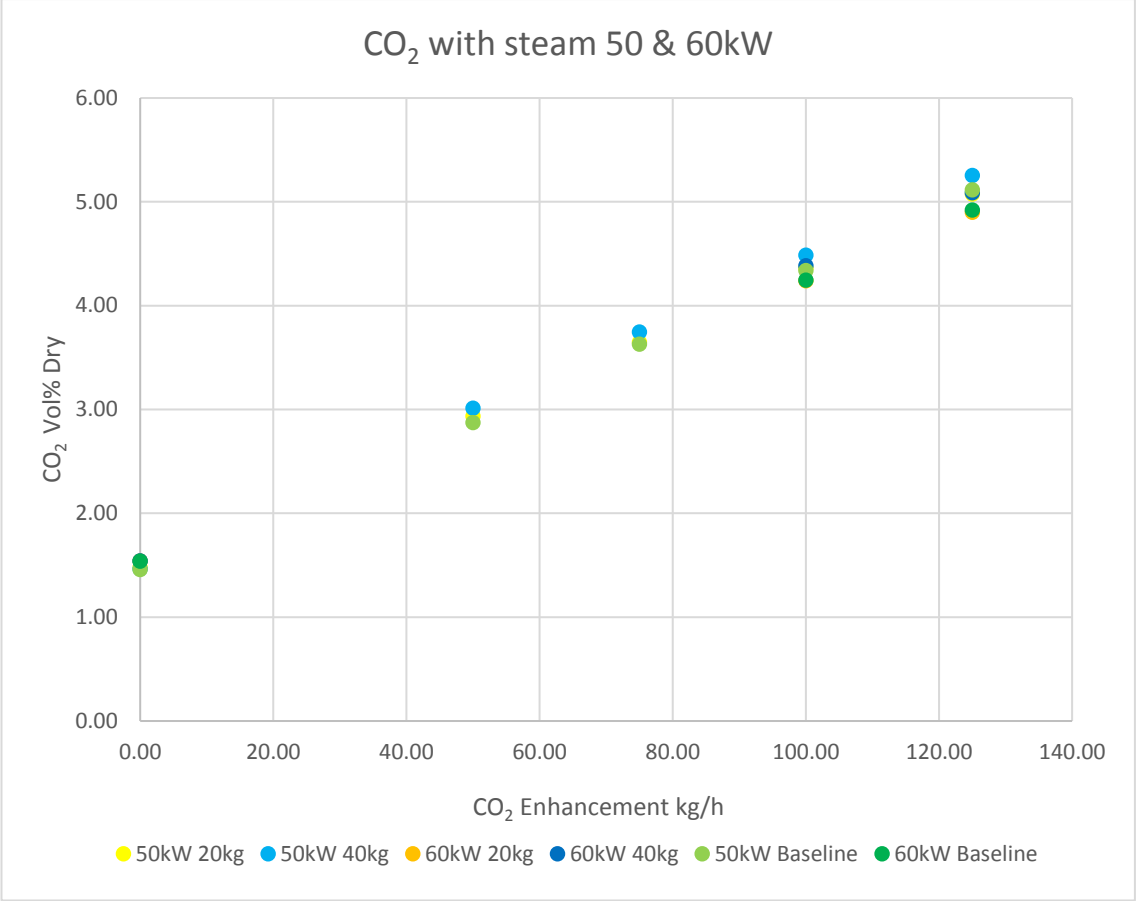

Figure 5-11 CO_2 Emissions of HAT and EGR combined up to 125kg/h CO_2.

Although lower oxygen combustion percentages can cause unstable flames and lean blow out, due to the relatively fuel lean combustion conditions of the Turbec 100, then this is not an issue. However the flame speed and temperature is reduced due to the increased heat capacity. The combination of EGR and HAT further exacerbates this effect. As in Best et al [1] it was shown that the lowest turn down ratios had the most emissions impact, and this was due to the slightly richer fuel air ratio at the bottom of the turbines turn down ratio, with changes in the oxidiser composition having more of an effect and the mixing being more diffuse.

With addition of a small HAT percentage it can be seen in Figure 5-12 Indicators of incomplete combustion with HAT, that the emissions of CO and CH_4, indicators of incomplete combustion are significantly affected beyond that of the simple EGR. With CO going from less than 50ppm to over 200ppm, and CH_4 from less than 2.5ppm to over 50ppm with 40kg steam addition. This

shows increased incomplete combustion and evidence of uncombusted fuel in the increased hydrocarbon volume in the exhaust and this is due to the reduced flame speed.

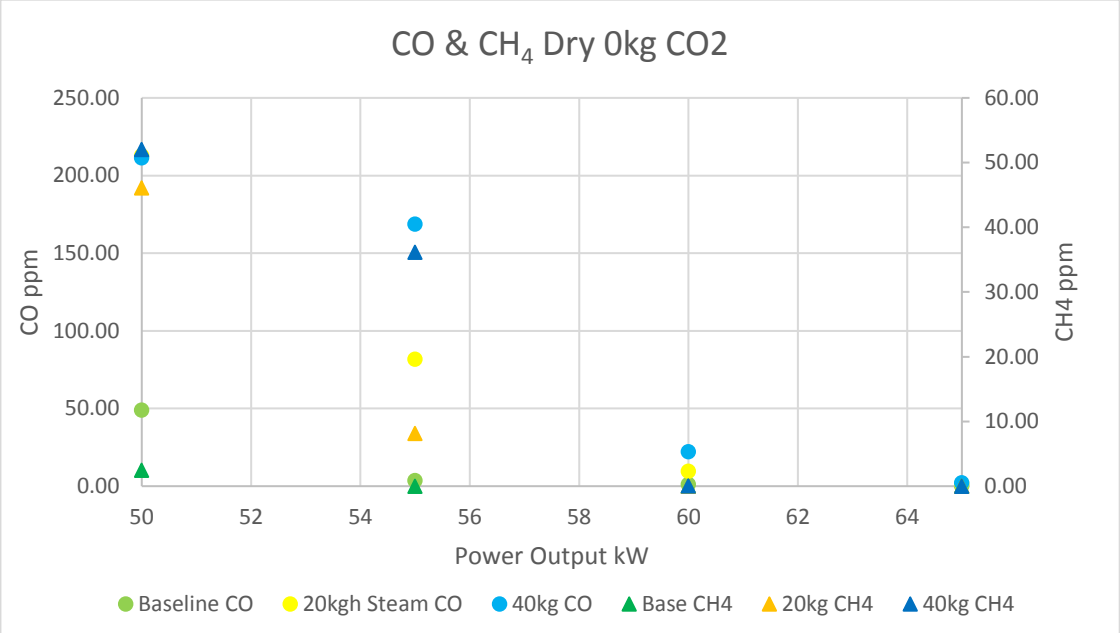

Figure 5-12 Indicators of incomplete combustion with HAT at 50 – 65kW.

With the combination of HAT and EGR, the expected trend is increasing rates of CO and CH_4, due to the increased incomplete combustion. In Figure 5-13 CO Indicators of incomplete combustion with HAT and EGR, and Figure 5-14 CH4 Indicators of incomplete combustion with HAT and EGR, this trend is observed with only one result appearing anomalous at 50kW, for which with CH_4 the SD error is 5.96, and this is slightly larger than the overlap.

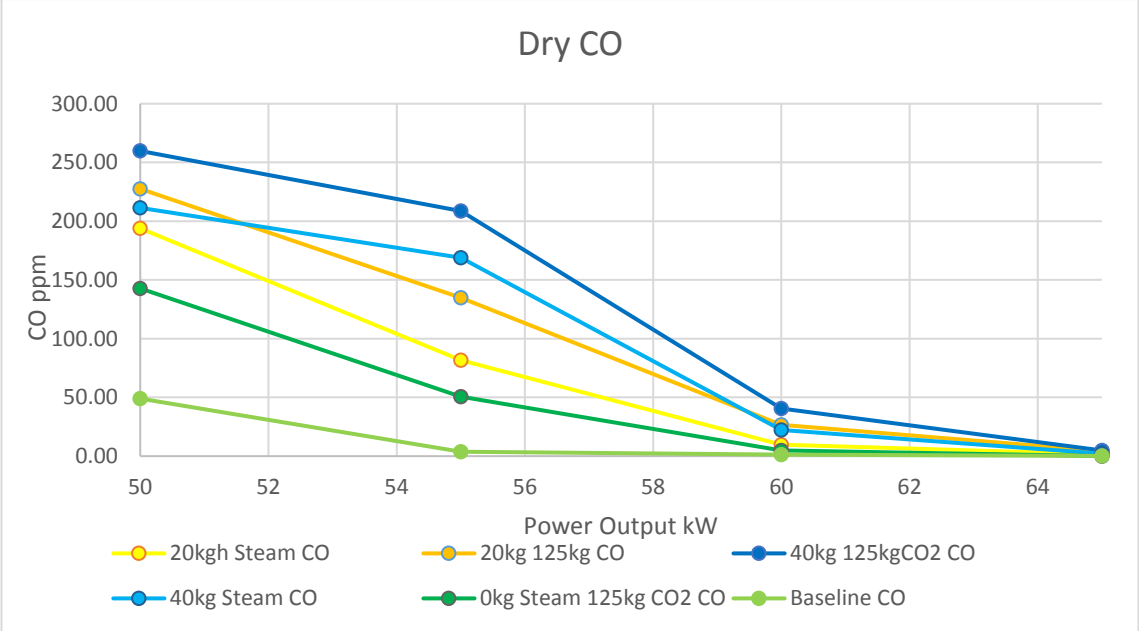

Figure 5-13 CO Indicators of incomplete combustion with HAT and EGR at 50 – 65kW.

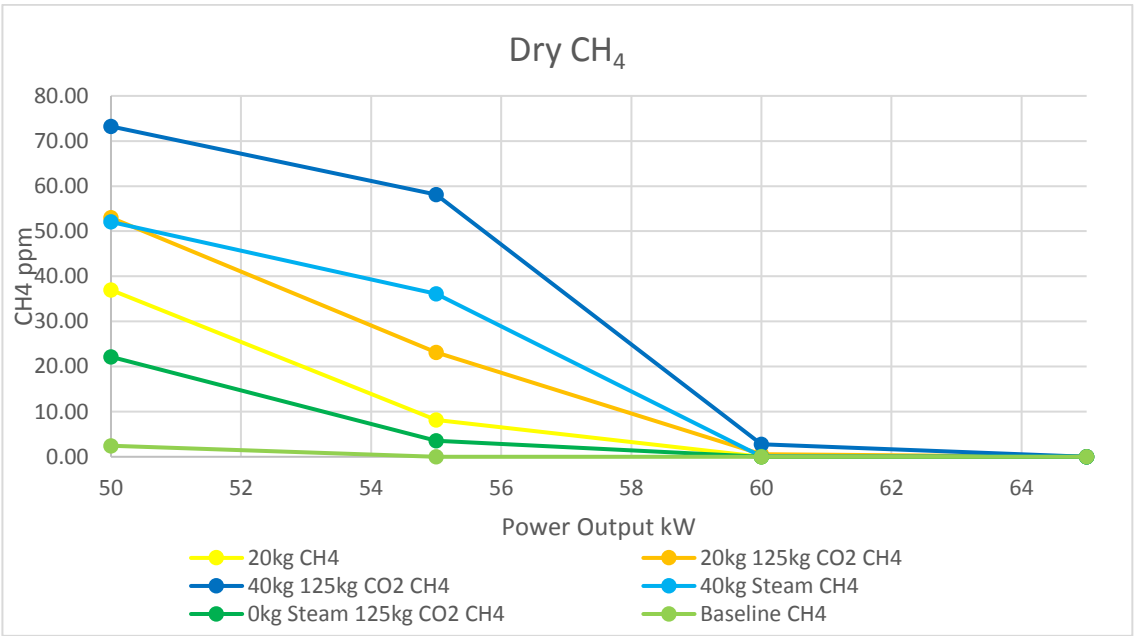

Figure 5-14 CH_4 Indicators of incomplete combustion with HAT and EGR at 50 – 65kW.

5.5.2.3.2 Anomalous NOx Results

As previously investigated in Chapter 4, the NOx can be seen to be reduced by about 60kW, with more efficient combustion occurring.

With the addition of steam simulating humidified air, and in combination with CO_2 representing EGR, it would be expected there would be a further drop in NO_x emissions due to lower combustion temperatures, as also indicated by increased UHC and CO. However with the addition of steam this did not occur.

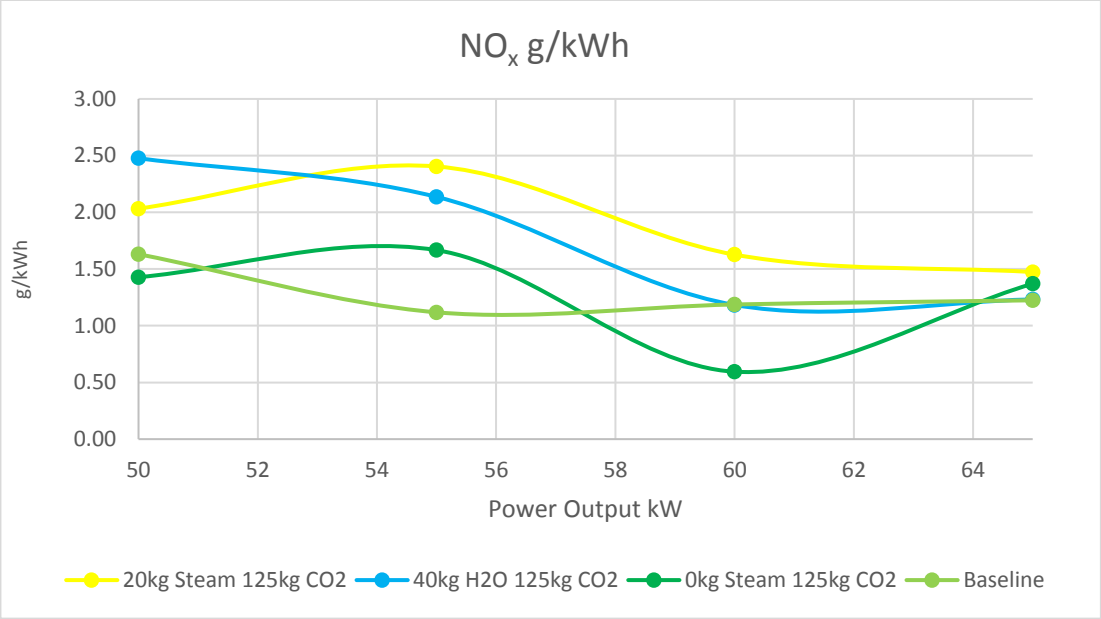

Figure 5-15 NOx Emissions with HAT and EGR at 50 – 65kW.

As the NOx results were above the values expected, it was thought that there was possible NOx formation post combustion with hotter exhaust gas temperatures due to the removal of the draining of the heat exchanger. For this reason, the baseline results for the steam testing conditions were repeated and simulated EGR with 125kG/h of CO2 enhancement. This was done to see if there was a consistent fluctuation in the NOx emissions, to eliminate steam injection being the source of this, when steam would be expected to reduce NOx. However the results showed that the NOx remained lower for the baseline and EGR cases, thus not providing the expected source of the NOx. Increases in CO, and UHC indicate lower combustion temperatures. In addition there is reduced SFC, and turbine speed, and we know that in pre combustion the compressed air temperatures are lower, this would indicate lower peak flame temperatures, and therefore the expected lower thermal NOx creation.

As there is also no NOx reported in the fuel it was not possible to be certain as to the cause of this rise in NOx emissions. It is possible that the burner design is not designed for the steam addition and it is disruptive to the mixing and combustion causing hot spots, but it is difficult to be certain how this would occur.

5.5.2.4 Efficiency impact of the HAT & EGR

With the addition of CO_2 replicating the EGR, it would be expected that the combustor would experience reduced combustion efficiency due to the increased heat capacity and reduced oxygen due to the displacement of the air for the CO_2. In Best et al. [1], and ElKady et al. [60], this is shown to occur and again this is replicated in Figure 5-12 Indicators of incomplete combustion with HAT at 50 – 65kW. As discussed in section 3.3.1 and shown in Figure 5-13 CO Indicators of incomplete combustion with HAT and EGR and Figure 5-14 CH4 Indicators of incomplete combustion with HAT and EGR, the emissions also strongly evidence the reduction in complete combustion and lower flame temperatures. This has a negative impact on SFC, as depicted in the SFC. However with the addition of steam through HAT, an improvement in SFC is observed, and this may be due to the reduced RPM. This outweighs the losses in the combustion performance indicated in the emissions observed in Figure 5-13 CO Indicators of incomplete combustion with HAT and EGR and Figure 5-14 CH4 Indicators of incomplete combustion with HAT and EGR. The impact is so strong that in combination with CO_2 enhancement simulating EGR, HAT improves the SFC beyond that of the baseline turbine performance. The improvement of 20 and 40kg HAT alone is 3-5% better than the baseline case.

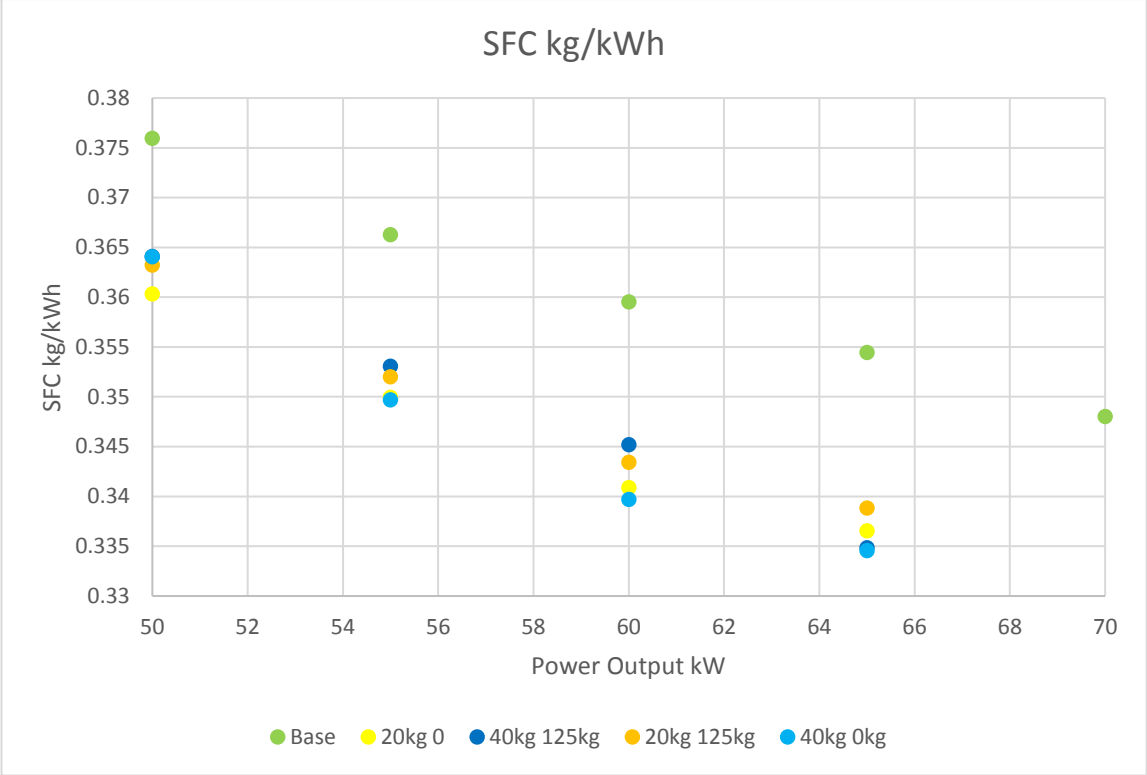

Figure 5-16 SFC with HAT and EGR at 50 – 65kW.

This data on SFC was concluded on cooler days than the previous experiments, and a decrease in efficiency is noted when the lower ambient conditions normally indicate higher turbine efficiency. This may be due to increasing the deterioration of the blades and combustor of the turbine over time, as a number of problems and use has occurred since the previous experiment.

This set of data still illustrates strong efficiency trends, the only apparent anomaly in SFC is the case of 20kg steam 125kg CO_2 @ 65kW.

5.5.2.5 Efficiency losses from steam generation

During this study air was humidified using steam from a stand alone boiler. There are significant inefficiencies from generating the steam with separate process than the combustion of gas for the turbine. On a commercial scale combined cycle gas turbine could generate steam very efficiently through bleeding from either high or low pressure turbine cycles that are already part of the process. In addition a higher quality steam could be rendered from the CCGT, in terms of

both pressure, and temperature. A combined cycle turbine could provide superheated steam that would provide more work in terms of energy from the heat.

The boiler generated saturated steam that was delivered at a pressure of 2.83 – 4.15 Bar gauge at the point of injection.

Using the injection pressure, temperature and flow rate at injection the steam enthalpy has been calculated with ASME steam tables. [101] This embodied energy has then been removed from the electrical energy generated to calculate new generation efficiencies of the process as Figure 5-17 Impact of steam addition on net turbine efficiency.

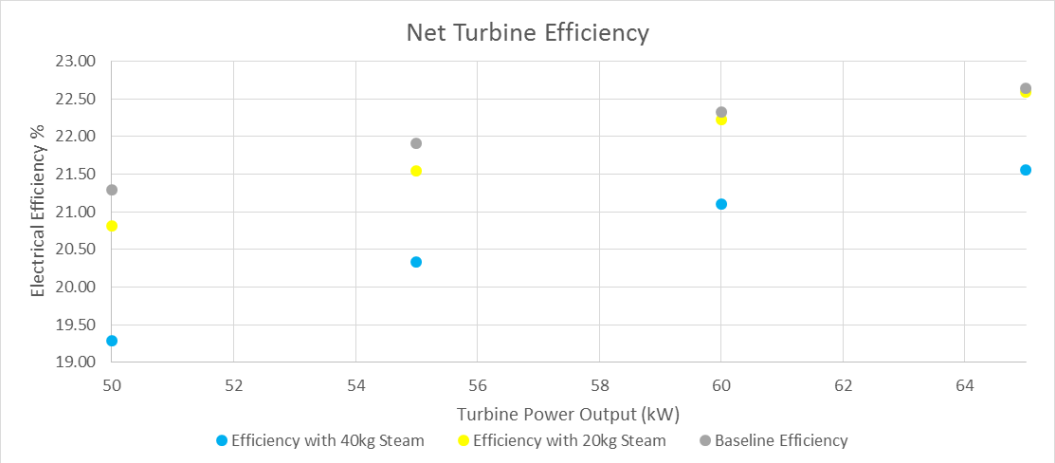

Figure 5-17 Impact of steam addition on net turbine efficiency

It can be seen that the steam addition has net negative impact on the overall generation efficiency in these tests. However s it is not possible to efficiently generate and deliver steam to the turbine at the current test facilities it is not meaningful to energy penalties and input to be represent of a commercial sized CCGT with HAT augmentation.

5.5.2.6 Impact of EGR & HAT on post – combustion capture performance from gas turbines

Post combustion capture is energy intensive due to the regeneration of the capture solvent, thus releasing CO_2 for compression. As gas turbines have a low partial pressure of CO_2, this means

more energy is required per tonne of CO_2 captured. Increasing the partial pressure of CO_2 reduces this and EGR increases the CO_2 partial pressure, through recirculation effectively increasing the CO_2 in the oxidiser. The HAT increases the partial pressure as it maintains a constant mass flow through the turbine, with air being displaced by water. When the water, in the form of steam, is condensed out then the volume % of CO_2 is relatively a larger proportion of the total exhaust volume to be processed for capture. Combining these two options has been shown to increase the CO_2 concentration in the flue gas more than either of these technologies on their own. Increases of CO_2 at 50kW from 5.11% without steam addition to 5.26% with steam addition, equates to a reduction in specific reboiler duty of over 0.1MJ/kgCO_2 captured, a saving of over 1%, and in addition to the reduction in SF of the turbine of 3%. At 60kw, CO_2 goes from 4.92% to 5.09% with 40kg/h steam addition, again reducing the specific reboiler duty by over 0.1MJ/kgCO_2 captured whilst the turbine SFC is reduced by 4%. [96] These reductions in reboiler duty may appear to be modest but on the larger scale they add to significant cost reductions.

5.6 Conclusions

The steam reduces the TC2 in compression, by up to 40°C, and this is due to the higher heat capacity than air, approximately 4 times that or air when the steam is at 100°C. This means that it takes more energy to raise the temperature of the oxidiser by 1°C, but as a total of the mass flow, the water is only approximately 1- 2% of the total mass.

The addition of CO_2 and steam reduces the combustion temperatures, and this is reflected in the lower calculated TIT, up to 9°C lower at 60kW and 65kW.

The addition of steam after condensing did increase the dry CO_2 vol% by up to 0.2%, and this is equivalent to a 4% increase of the total, which would allow for a more efficient post combustion capture.

The specific fuel consumption of the GT markedly improved with the addition of steam. This indicates that not only could HAT possibly be used to increase the CO_2 partial pressure and

increase the capture efficiency and performance for the net process CCS efficiency gains, but also offsets the reduction in the GT turbine efficiency caused by the EGR. The results showed that HAT addition improved on the baseline performance. Without HAT addition, EGR increased SFC above the baseline, thus decreasing the efficiency. When HAT was applied to these EGR cases, the SFC was not as good as HAT alone, but it is still markedly better than the baseline, and hence there is a significant improvement on the EGR SFC performance alone.

6 Particulate Matter Emissions

Particulate matter can have a significant impact on the degradation of amine solvents in post combustion capture CCS. This has been shown to be a significant issue with coal combustion due to the presence of metals in the particulates such as copper, iron and manganese acting as catalysts for oxidative degradation. [102] The presence of volatile elements also found in the emissions from natural gas combustion can contribute to similar degradation pathways occurring. Particulates have been shown to reduce the pH of solvents, increasing degradation products such as heat stable salts and precipitates. [103] This degradation leads to a reduction the capture efficiency and an increase in running expense due to replacement, and less efficient solvent regeneration. The increase in solvent degradation can also have a negative impact resulting in significantly higher ammonia emissions from power plant with post combustion capture systems, than from those without. [104]

There is a lack of research focused on the particulate matter emissions of gas turbines, and the potential impact of the higher number, smaller size distribution emissions from then on post combustion capture solvents. For the reasons of known particulate degradation of solvents, and the knowledge gap with natural gas particulates, the potential for degradation should be investigated. A first step to doing this is to analyse the size distributions of gas turbine exhaust emissions, so this information can be used for further analysis of the solvents. In addition the added processes of exhaust gas recirculation will impact upon the particulate size distribution observed. EGR reduces peak flame temperature and NOx formation, whilst increasing the presence of unburnt hydrocarbons, this will result in a different distribution of volatile organic compounds, and acidic nucleation particles. Similarly the addition of HAT will alter the size distribution of particles, increasing the likelihood for agglomeration and larger accumulation mode particles forming, as well as increasing acidic particles, which could alter amine solvents pH, increasing degradation rates, and decreasing CO_2 loading.

6.1 Experimental set up and methodology

6.1.1 Cambustion Unit

The particulate analyser is a machine that sizes by particle electro mobility.

A tube is charged with rings, each rings has a different charge, as the exhaust gas passes through then the smaller more dynamic particles are attracted to the nearer rings and thus change the current measured on the ring when earthed. The smaller particles travel the further before being attracted to other rings further down the tube. This alters the current reading on those rings. All of this gives an estimate as to the number of particles in a flow and their size distribution. From this it is also possible to estimate the mass of the particles, attributing a density to the sizes, and through this the attribution can be challenging due to the unknown nature and shape of the particles. For the smaller particle size ranges, that are more common in the GDI emissions and natural gas particle mass (mg) = $5.20 \acute{}10^{-16} \times dp^3$ (nm) is suggested. [105, 106]

6.1.1.1 DMS500 Cambustion Unit Set up

The DMS500 Cambustion analyser is a small, mobile unit. At the front, the heated sample line is seen connected in Figure 6-1 Photograph of the DMS500 MKII Cambustion fast particle analyzer, with the sample inflow (a) to being seen splitting off, (b) compressed air for dilution is metered from the DMS500 into the heated line in the centre, and (c) power is the cable on the right side, for the heating of the line.

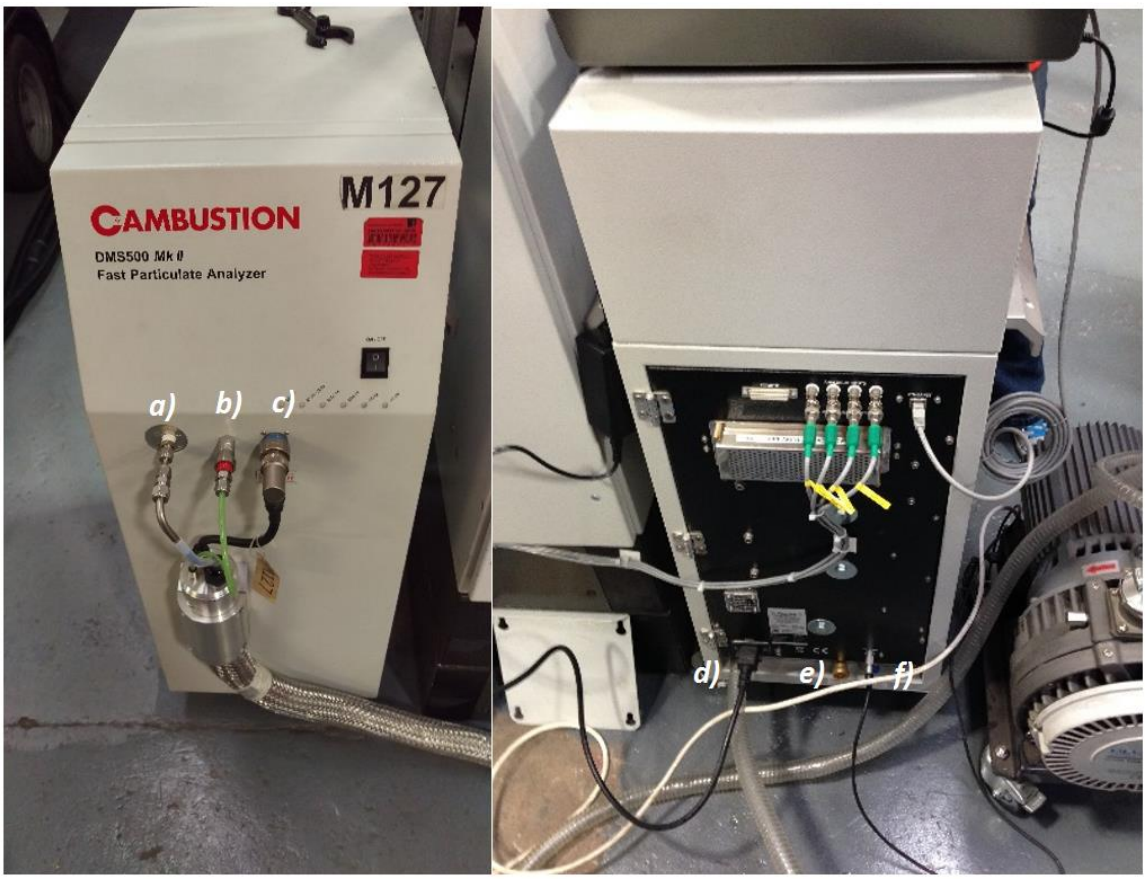

Figure 6-1 Photograph of the DMS500 MKII Cambustion fast particle analyzer.

At the rear of the analyser, compressed air is supplied via the brass fitting seen (e) at the bottom, pressure within the analyser is controlled and reduced by (d) the remote pump seen on the right through, and (f) automatically controlled by a black signal cable.

6.1.2 How the DMS500 Cambustion works

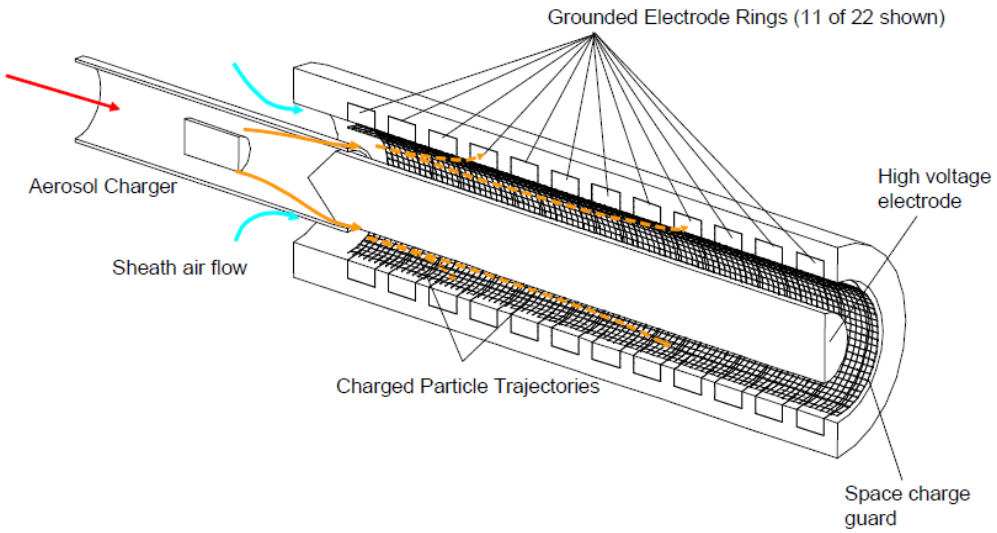

Figure 6-2 A schematic of the DMS500 classifier [107]

The particle detector in Figure 6-2 A schematic of the DMS500 classifier [107] works on the principles of particle charge and drag. The particles enter the classifier and are charged by a fine corona wire that produces positive ions that charge the incoming particles that collide and this charge assists in the sizing of the particles. The particles charge/drag ratio is known as the electrical mobility. With the charged particles then being repelled from the central high voltage rod (Figure 6-3 The DMS classifier, (a) classifier assembled, (b) HT Rod, (c) space charge guard, (d) classifier), and the drag causing them to ground on the electrometer rings, there are multiple rings to detect particles with different electrical mobility, which is related to the particle size where they discharge, and amplifiers detect the particle numbers and size. [107]

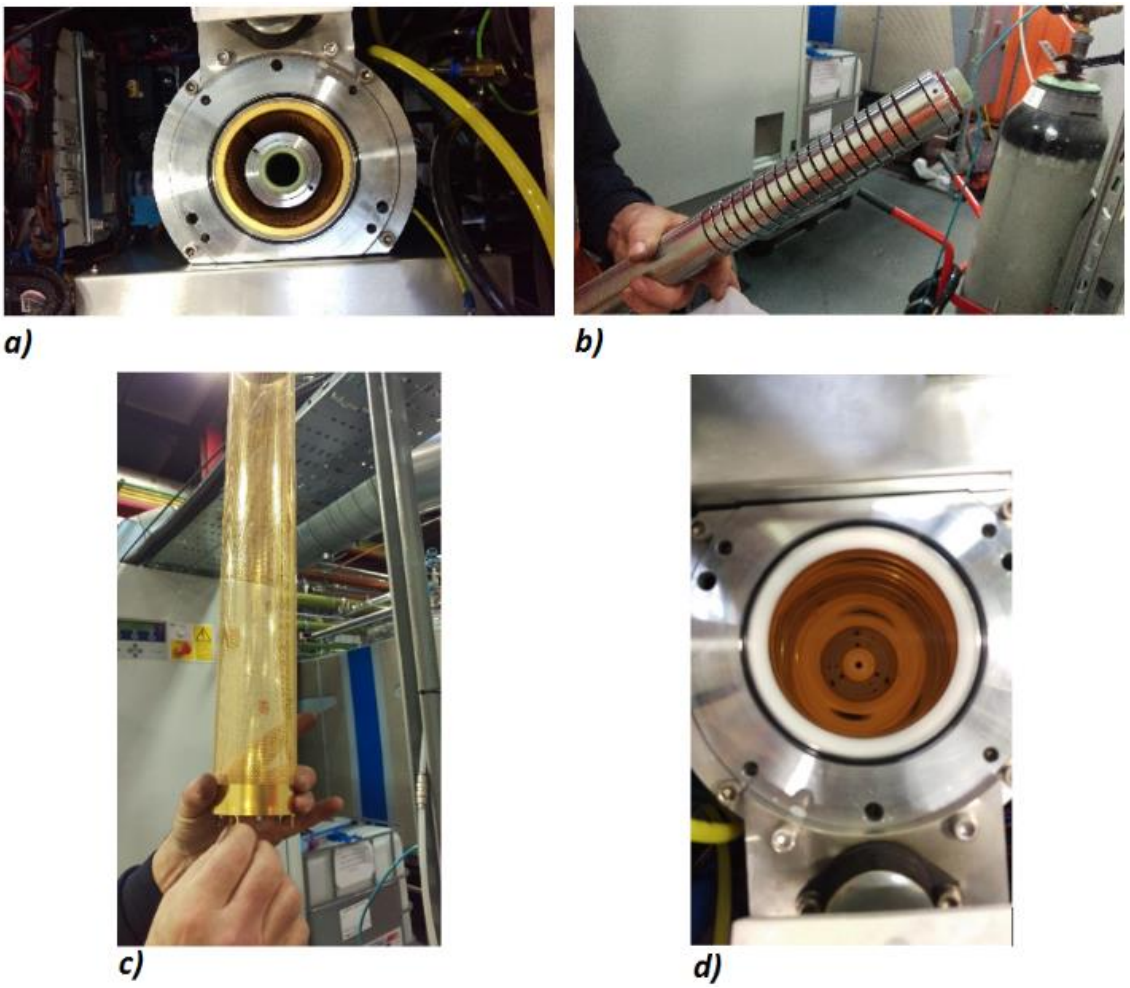

Figure 6-3 The DMS classifier, (a) classifier assembled, (b) HT Rod, (c) space charge guard, (d) classifier

The particles remain within the DMS and attached to the electrometer rings until they are cleaned away, or the analyser is serviced.

Figure 6-4 Schematic of the DMS500 MKII dilution [107].shows the exhaust samples travel through a special heated dilution line. This line is heated to 150°C, at the point of connection it has a remote cyclone and restrictor, and the heated line also incorporates the 1st dilution of the sample with compressed metered air. This dilution helps prevent the formation of condensation which could cause irreparable damage to the DMS500, particularly the mass flow meters.

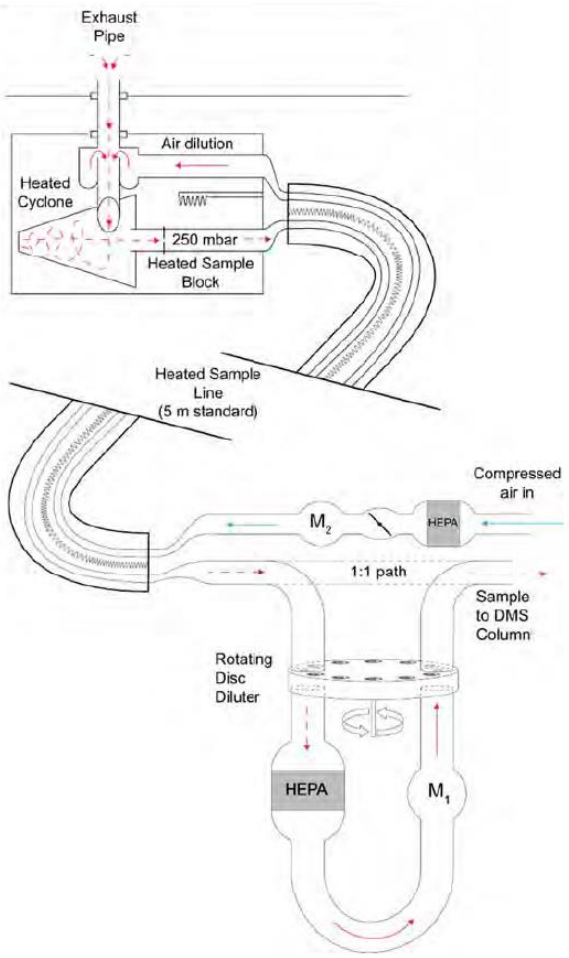

Figure 6-4 Schematic of the DMS500 MKII dilution [107].

The remote cyclone in the heated line removes particles above detectable size of 1um (1000nm).

Figure 6-5 Remote cyclone and restrictor position.

The restrictor (Figure 6-6 Restrictor sizing. controls the flow according to the pressure of the sample exhaust gas. An incorrect selection can result in a too high flow. If flow is restricted then this may be due to particulate debris obstructing the restrictor which may require cleaning.

Figure 6-6 Restrictor sizing.

6.1.3 DMS500 Software and sampling set up

The restrictor in the remote cyclone of the heated line controls the sample flow. This flow should be about 8slpm. If the DMS program warns that the flow is insufficient, the restrictor should be checked for debris, to ensure it is clean and clear, or if necessary, swapped for one with a different orifice size as Figure 6-6 Restrictor sizing..

The compressed air is attached to the rear of the DMS500, and this is used for the first dilution of the sample to drop the dew point of the exhaust emissions. For this reason, it must be dried through refrigeration or from a compressed air or industrial nitrogen cylinder. During the experiments dry cylinder air or industrial grade nitrogen was used, and supplied at a pressure 3-6bar.

A heated sample line is supplied with the DMS and used in conjunction with our own sample line due to the practical length, and possible position of the DMS at the PACT core facilities. The

first sample line collects the emissions directly from the gas turbine exhaust at the same point as the sample for the FTIR and the Servomex are taken. It is 5m long, and heated to a temperature 180°C, and then attached to the heated line supplied by Cambustion with the DMS. The line temperature is controlled to try and prevent significant changes to the particulate size distribution from exhaust point to measurement to increase accuracy. If the temperature is too low condensation and agglomeration of particles may occur. If the temperature is too high VOC may be vapourised, and not measured.[106, 107]

For the test, the restrictor 102 was used as this restrictor is for ambient pressure sampling. For some engine operations this would not be appropriate due to the variable pressure of the exhaust. However our sample is taken from the exhaust where the pressure is near to ambient as the PT5 reading shows 1000.4 - 1000.5 mbar.

The DMS500 is turned on using the front power switch and at this point the user interface program can be loaded, and is connected within a few seconds. In the program it is switched from standby to on, and the flows are checked and the DMS500 starts a 30 minute countdown for the warmup during which time an appropriate inversion matrix can be selected for the emissions source to be sampled. In the case of the Gas Turbines T100 Series 1 and 3, the GDI matrix is selected, this is Gasoline Direct Injection, thus anticipating more particles than ambient conditions and more moisture from the combustion, but less than for diesel. After the warmup is complete the analyser must be autozerod to remove offset voltages that would skew the results, or appear as non existent new particles.

The first dilution reduces the dew point of the exhaust sample, this was set to 4:1. Although the recommendation is 5:1 and above for methane based fuels, which is the primary constituent of the natural gas combusted, the mix is exceptionally fuel lean and hence the moisture content post combustion is relatively low. Due to the low aerosol concentration, the second dilution was not required and set to 1:1.

There is an exhaust pump that lowers the pressure within the unit.

The heated line goes to the exhaust and same sample point at the same location as the FTIR and servomex. The line is connected to another heated line, so total distance of the line is approximately 10m, and not the 5m of the heated line supplied by combustion.

6.1.4 Reducing and accounting for the loss in the lines

During the residence time from the gas turbine exhaust to the DMS sampling unit, particles can form, and also be lost. The transit time for particles in the 5m line is less than 100ms at 5:1 pressure ratio and the total sample time from start to detection is less than 2 seconds. This low residence time helps improve the accuracy of the particulate readings.

Particle size distribution can change due to a number of factors, including electrophoresis – with charged particles collecting this can particularly be a problem in the heated line particle losses, conductive tubing of the DMS line helps reduce static, and this problem. Thermophoresis – the movement of particles due to heat variation can cause agglomeration, however maintaining a heated line temperature helps prevent a heat gradient and limits this effect.

Line losses, particularly important when considering ultrafine particles, Kumar et al [79] found the penetration of 100% of particles over 100nm in diameter, but varying to as low as 20% for particles sub 5nm, however this is outside the range of detection for the DMS500 MKII. 5- 10nm particles penetration rate was found to be up to 70%. [79]

As evaporation is more likely to occur at lower pressures, it is possible for the nanoparticle numbers to be underestimated by the DMS. However in lower pressure environments, heat transfer is less, hence reducing the likely hood of evaporation, and the total residence time is less than 2 seconds from sample point to reading. Different pressures have been tested, showing that the change in particle number to be small when the pressure is dropped from atmospheric to 250mb as the DMS500 operating conditions, there is no change in size distribution. [108]

6.2 Results

This section investigates the particulate emissions that fall into the category of PM1, for the two turbines at Beighton, the Turbec Series 1 and series 3 100kW microturbines. During the gas turbine experiments, data was collected on the particle size distribution in the flue exhaust. This was also done for the experiments with CO_2 addition to see if changing the oxidiser composition altered the particulate size produced. For this a Cambustion DMS 500 analyser has been used to collect the data on the particle size distribution. The particle number distribution gives a very different representation of the data than the mass, or surface area. It is the most appropriate metric for the ultrafine particles generated by gas turbines.

6.2.1 Atmospheric particulate distribution

Measurements were taken on site of ambient readings for comparison to turbine exhaust emissions. These readings were taken through the turbine, before start up, and will include the impact of the turbine filter on particle size distribution.

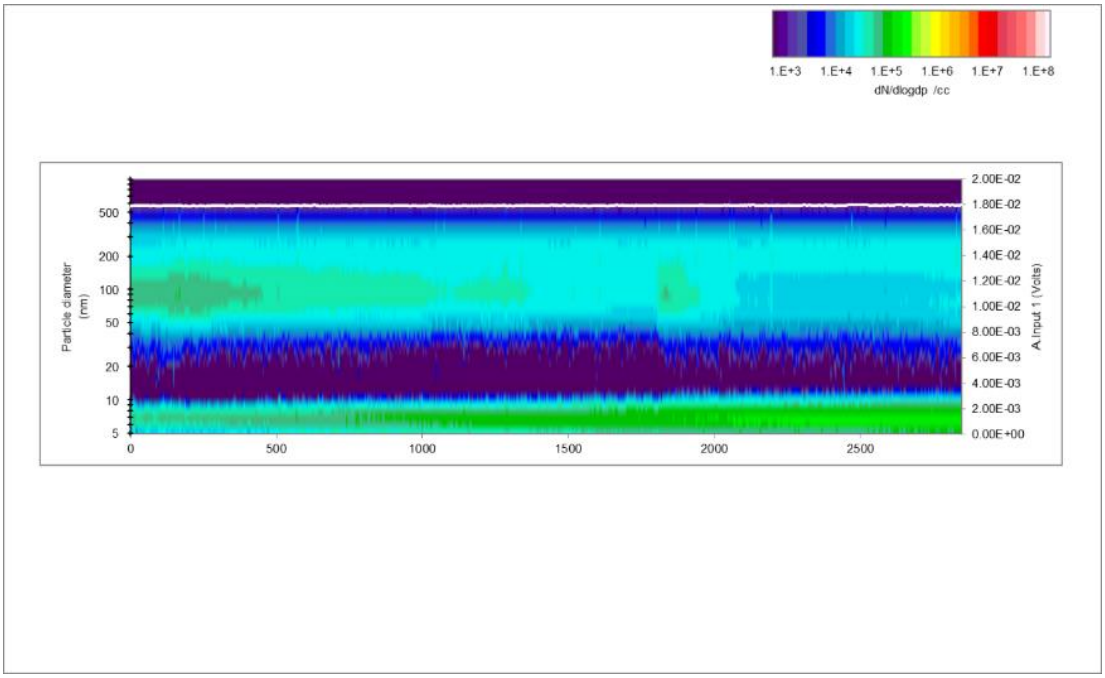

Figure 6-7 Typical ambient particle size distribution concentration voltage

Figure 6-7 Typical ambient particle size distribution concentration voltage seen corresponding to voltage readings from the DMS, and these colourful plots can also show relative concentrations through colour changes. This is a typical atmospheric plot.

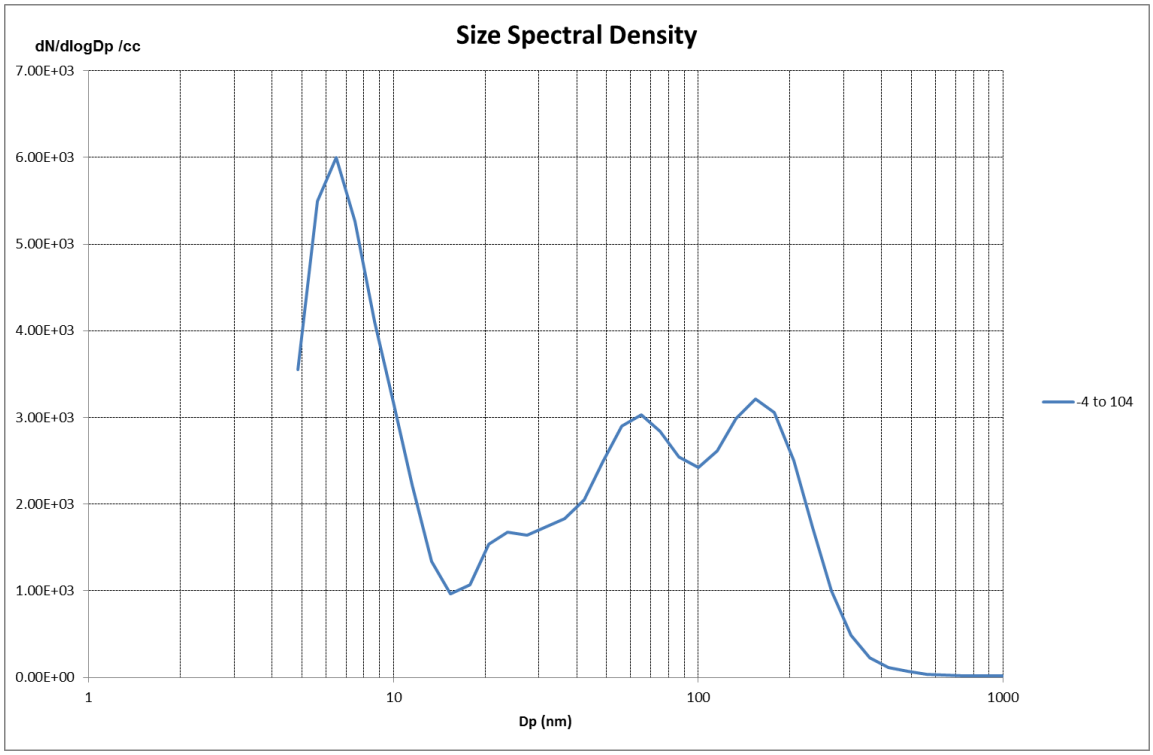

Figure 6-8 Typical ambient particulate measurement

The ambient atmospheric particle readings in Figure 6-8 Typical ambient particulate measurement show peaks in the ultrafine PM1 range at diameter 5- 10 nm, in the nucleation mode, and particularly in the accumulation mode between 30 and 300nm, with slight peaks at approximately 60- 70 nm and 100 – 200nm. In Figure 6-8 Typical ambient particulate measurement, the nucleation mode particles are in the order 3 – 6 $x10^3$, as with the accumulation. However on other days readings have shown nucleation readings going up to 6 x 10^4 and the accumulation 3x 10^4. All of the ambient readings though show the same size distribution, and the corresponding peaks. All the results obtained are similar to those reported by Kumar et al [79].

The variation in concentration could be attributed to the atmospheric conditions, with higher temperatures resulting in less volatile organic compounds, and a slight increase in accumulation mode particles. Humidity increasing accumulation particles such as nitrates and sulphates. Also it may be attributed to the particle numbers for the road adjacent to the PACT facilities, increasing solid particles from diesel and gasoline engines, and nitrates and sulphates.

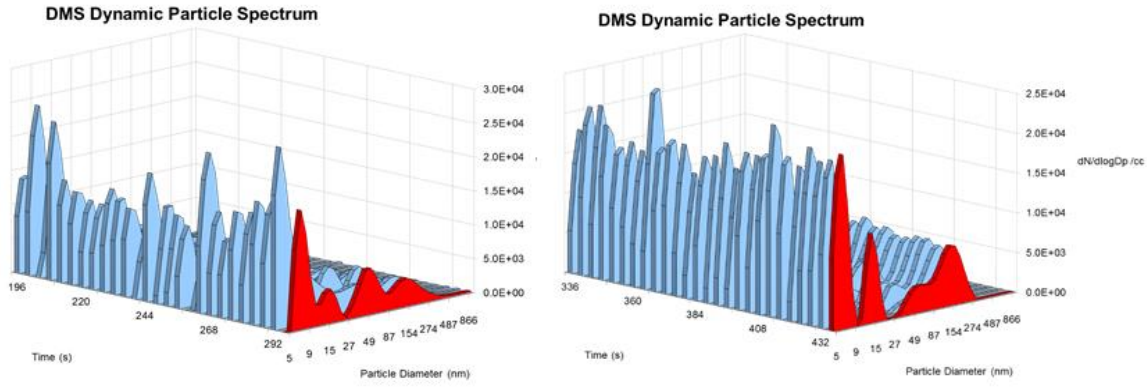

Figure 6-9 Typical ambient particle measurement profiles

The size distributions can be seen over time and interesting variations are observed during transitions of more dynamic operations.

6.2.2 GT3 Results

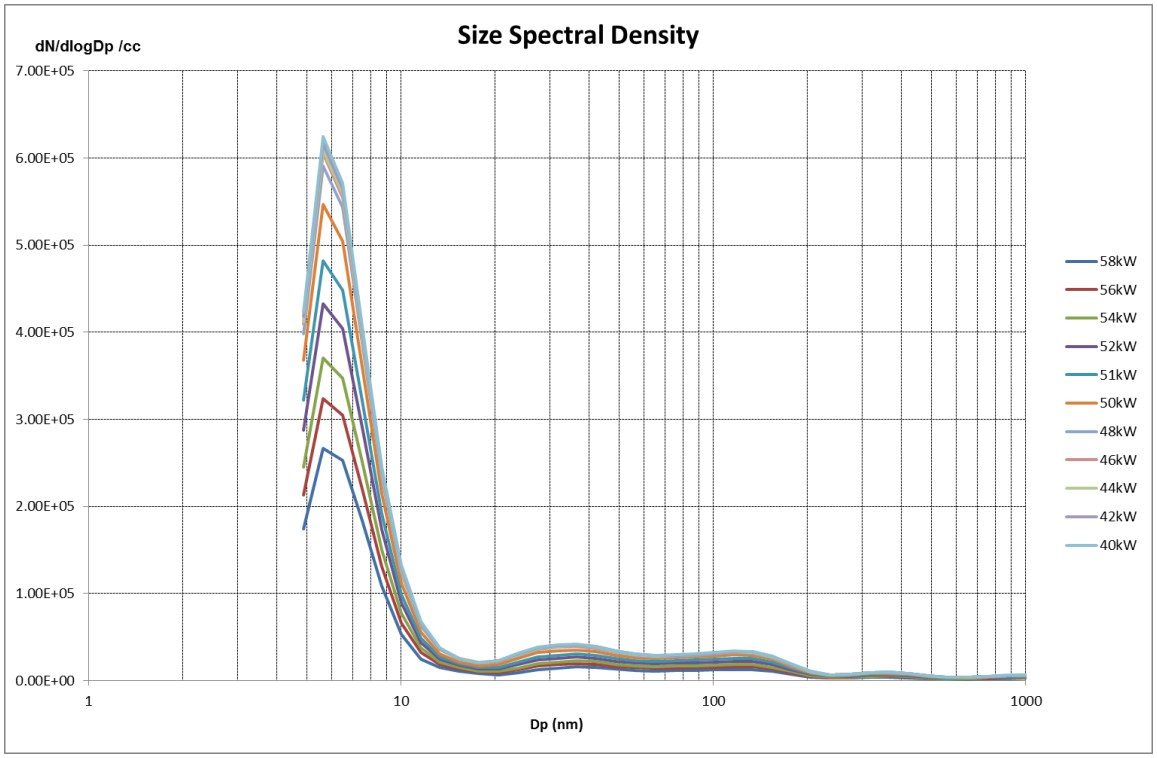

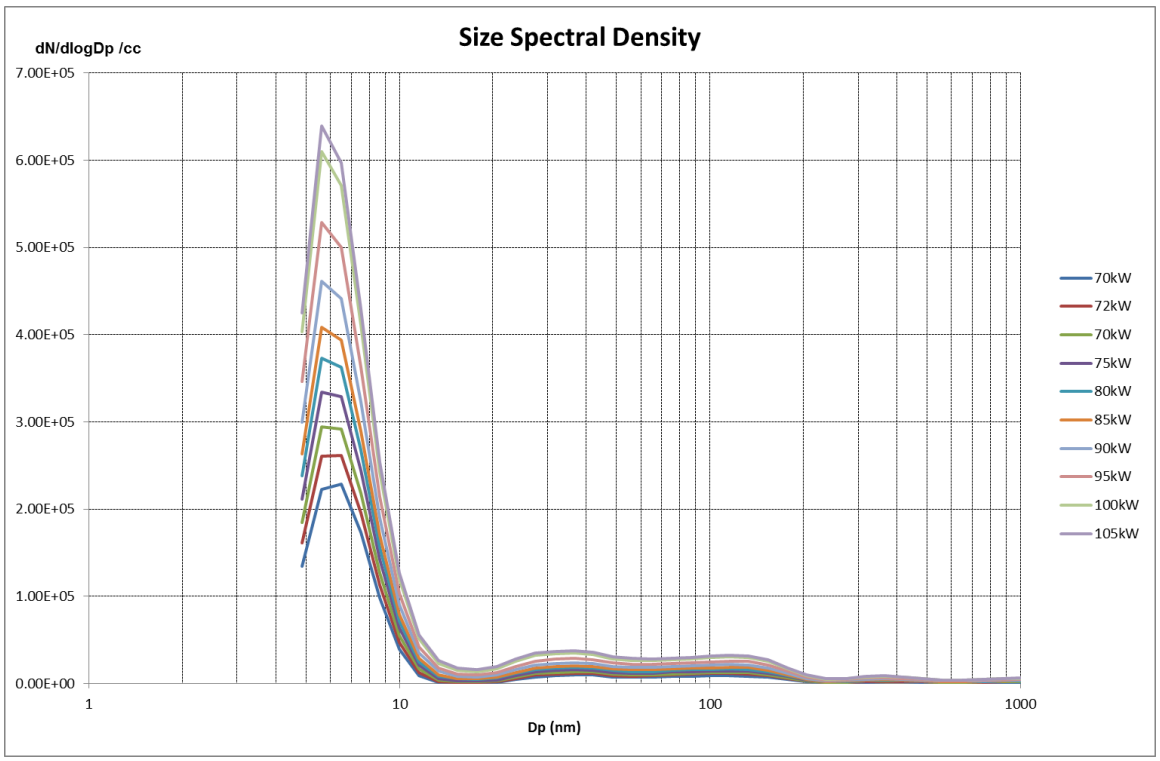

Figure 6-10 Typical GT3 size spectral density 40 -58kW and 70-105kW.

The results in Figure 6-10 Typical GT3 size spectral density shows similar particle size distribution to the ambient readings. The nucleation particles between 6-7nm in diameter being a peak, and the accumulation particles between 30 and 300 nm, but with a slight shift towards smaller nucleation particles and a relative reduction in the particles over 200nm.

Although the particle size distributions are similar, the density of all the particles has increased. The nucleation particles are 2 orders of magnitude higher in concentration, up to 10^5 times rather than from 10^3 times. The accumulation particles have increased by almost 1 order of magnitude to 10^4 times and with the ambient accumulation particles reading of $3x10^3$.

This increase in nucleation particles could well be due to the water from the combustion. The increase in accumulation could be from the agglomeration of VOCs and nitrates formed from the NO_x emissions and H_2O. This corresponds to the highest NOx emissions which are experienced by the GT3 at the highest and lowest turn down ratios of the turbine. This is visible in Figure 6-10 Typical GT3 size spectral density where both the 40kW and 105kW outputs have concentrations close to 4 x 10^4 in the accumulation particles concentration.

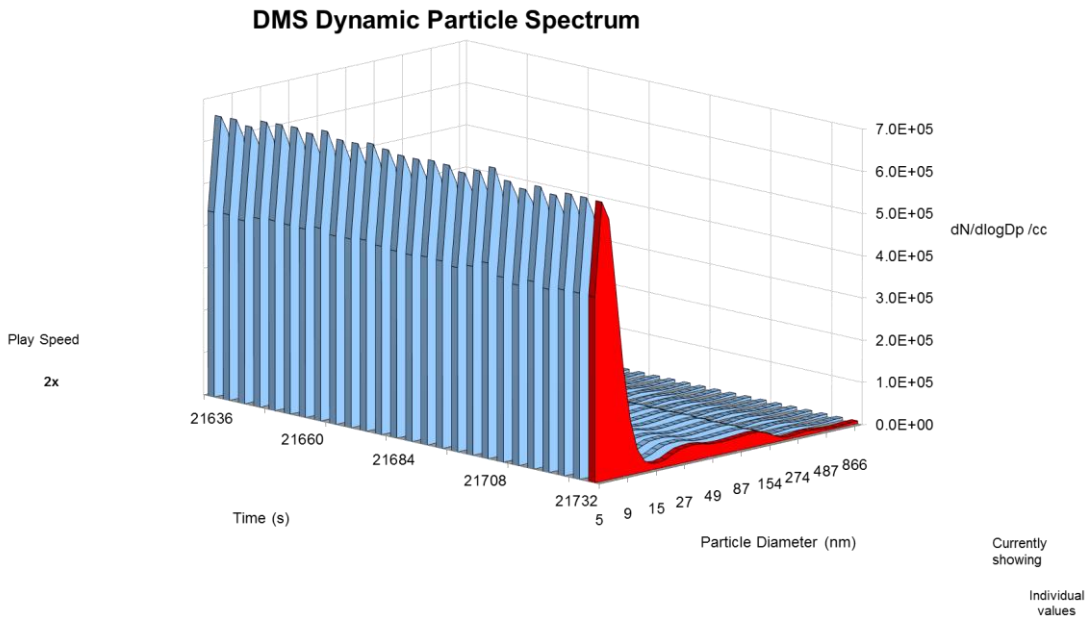

Figure 6-11 GT3 dynamic particle spectrum at 105kW.

From Figure 6-11 GT3 dynamic particle spectrum it can be seen that the performance of the Series 3 GT is quite consistent during the operation and testing, and mirrors the emissions performace. For this reason the high resolution of the sampling times for the DMS 500 is not required.

6.2.3 GT1 Baseline Results

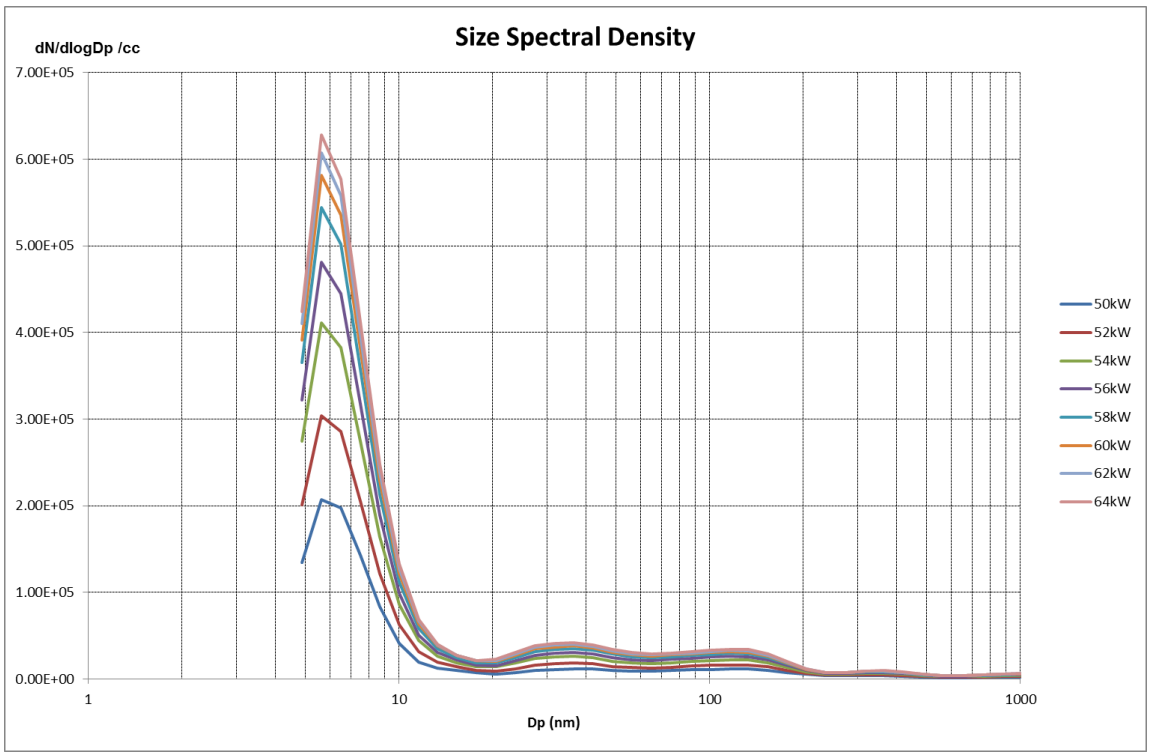

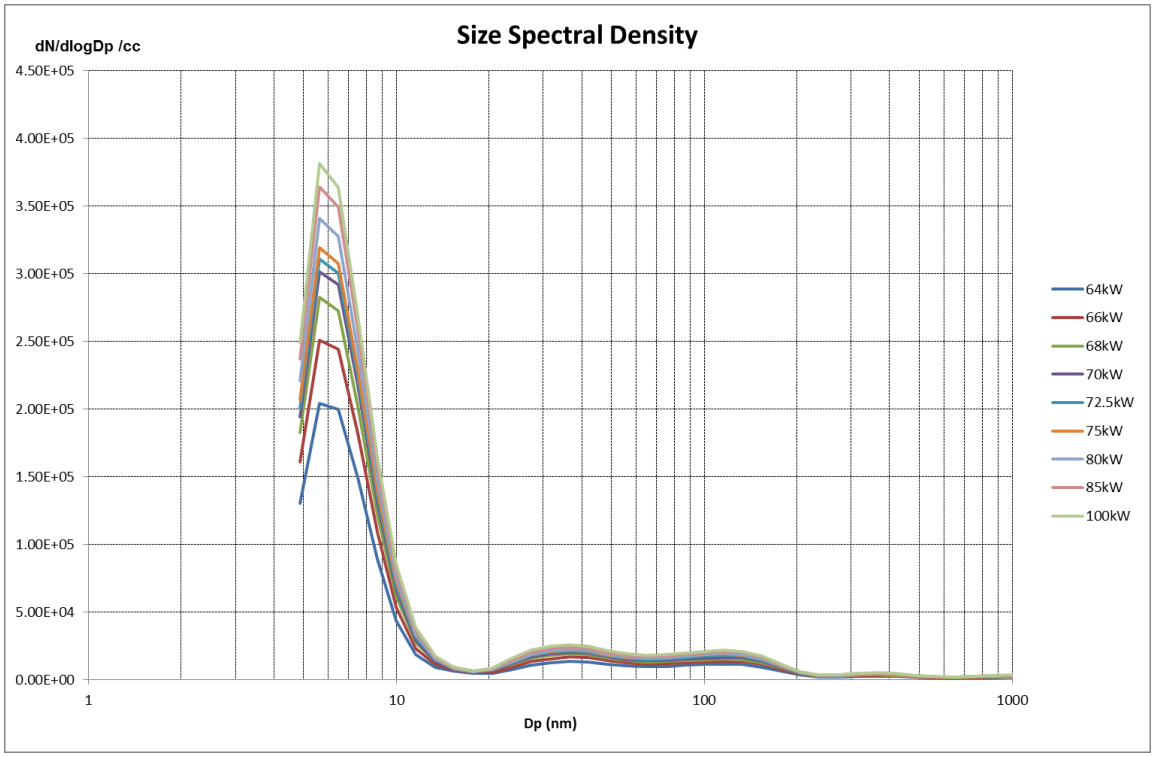

Figure 6-12 The GT1 particle size spectral density for 50 -64kW and 64 – 100kW.

As Figure 6-12 The GT1 particle size spectral density the GT1 particle size distribution is again similar to the ambient as the GT3. However again the particles in the nucleation zone are present in one to two orders of magnitude more than the ambient conditions, and the accumulation mode appears to be about one order of magnitude greater, with a reduction in the relative occurrence of the particles of diameter 200- 300nm, and an increase in the particles of 30-200nm.

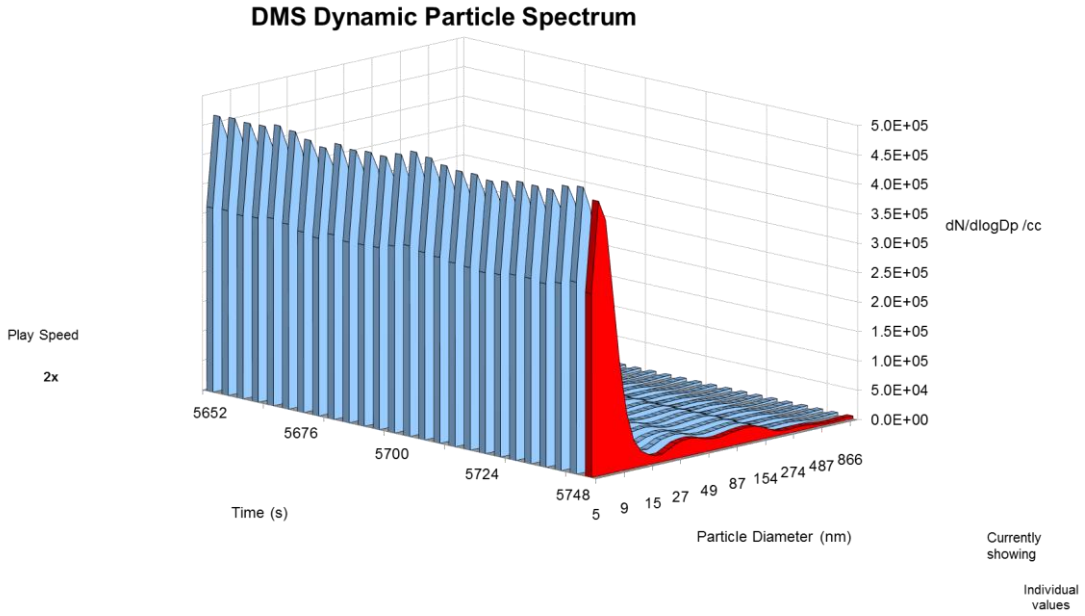

Figure 6-13 The typical GT1 dynamic particle spectrum.

As with the GT3 the GT1 it is seen in Figure 6-13 The typical GT1 dynamic particle spectrum to be fairly consistent in the particles produced in their size distribution and density during each turn down ratio power test.

6.2.4 Faulty GT1 Combustor Results

As discussed in the baseline performance chapter, there was operation with a faulty combustor that resulted in it being burnt out and damaged. This operation resulted in higher temperatures

and higher NO_x levels, and UHC, thus we might expect the formation of increased accumulation particles.

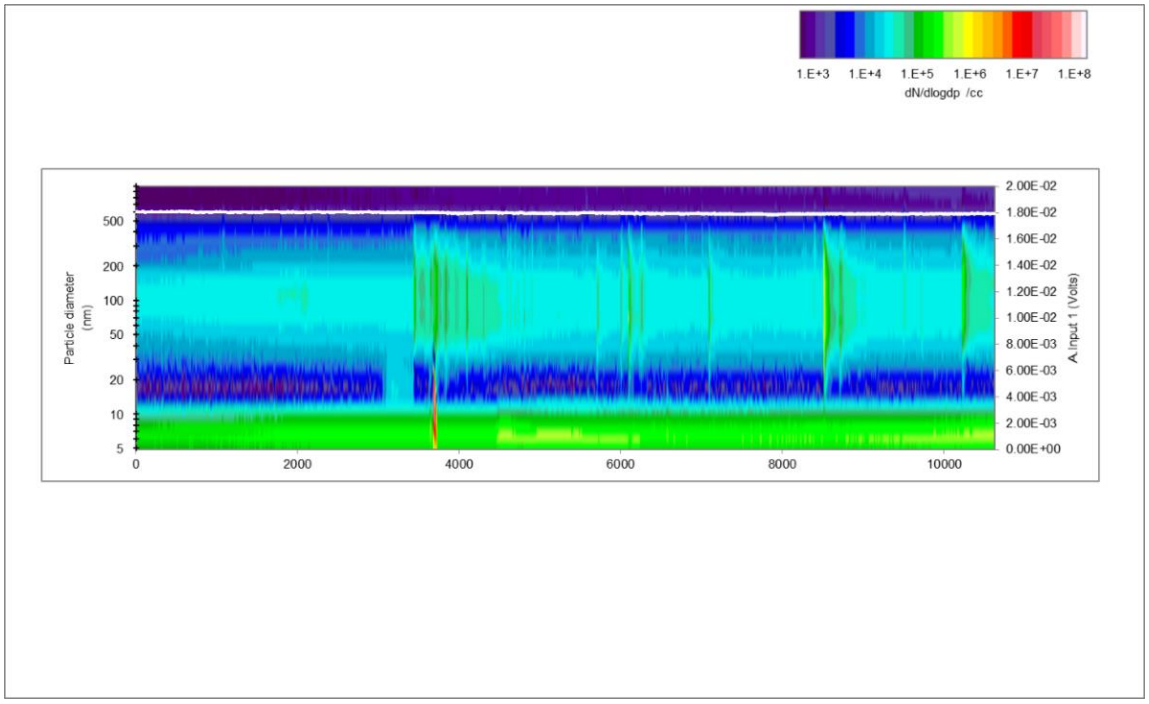

Figure 6-14 Faulty GT1 size distribution concentration voltage, showing voltage spikes from particulate debris.

The voltage readings in Figure 6-14 Faulty GT1 size distribution concentration voltage display interesting results in the spike changes in the particles production.

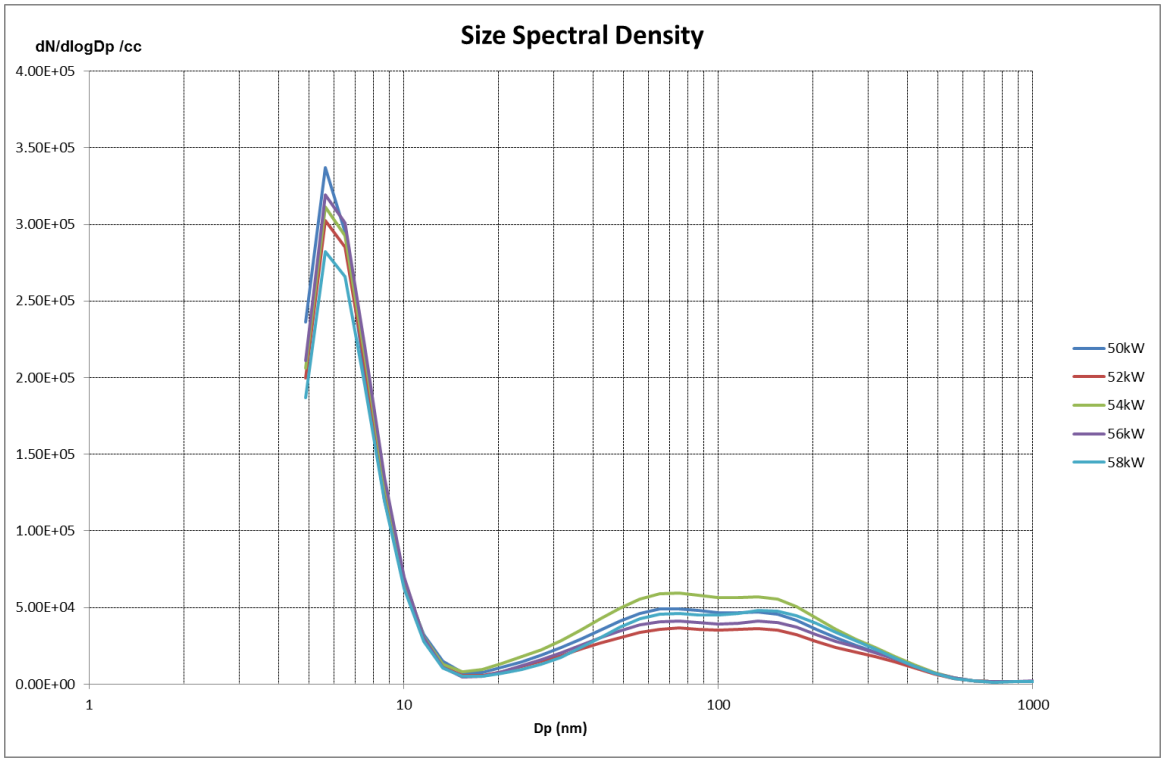

Figure 6-15 Faulty GT1 size spectral density.

The nucleation particle distribution is similar to that of the normal operation, again this is probably due to the H_2O. However the nucleation particles show an increase in the spectrum of particles produced, being broader from diameter 30nm to 400nm, and with less defined peaks across this accumulation zone. These accumulation particles are again likely to be from an increase in the nitrates from the increased NOx emissions, and the agglomeration of VOCs, including UHC. However there will be a significant number of "solid" particles from the damaged combustor, as seen in Figure 6-15 Faulty GT1 size spectral density. Also there have been significant numbers of larger "solid" particles above the ultrafine range monitored by the DMS500 and filtered out by the cyclone and restrictor above a diameter 1000nm.

What is interesting to observe is that the nucleation concentration is not significantly reduced, and hence as one would expect, this is not the agglomeration of smaller nucleation particles, but the formation of new particles that were not present at all in the regular operation baseline tests.

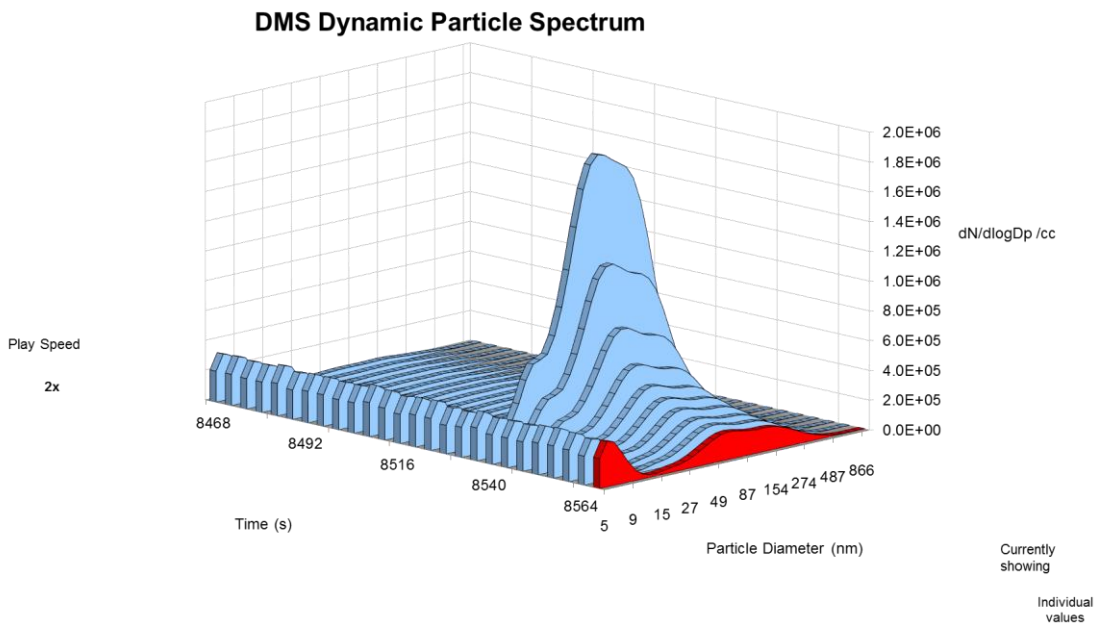

Figure 6-16 Faulty GT1 dynamic particle spectrum showing particulate debris spike

As the performance of the Series 1 was erratic, for such dynamic operation spikes in the size distribution can be seen Figure 6-16 Faulty GT1 dynamic particle spectrum. If it were to be predicted that the performance was continually this transient a higher resolution and an increased sample frequency would be beneficial for analysis.

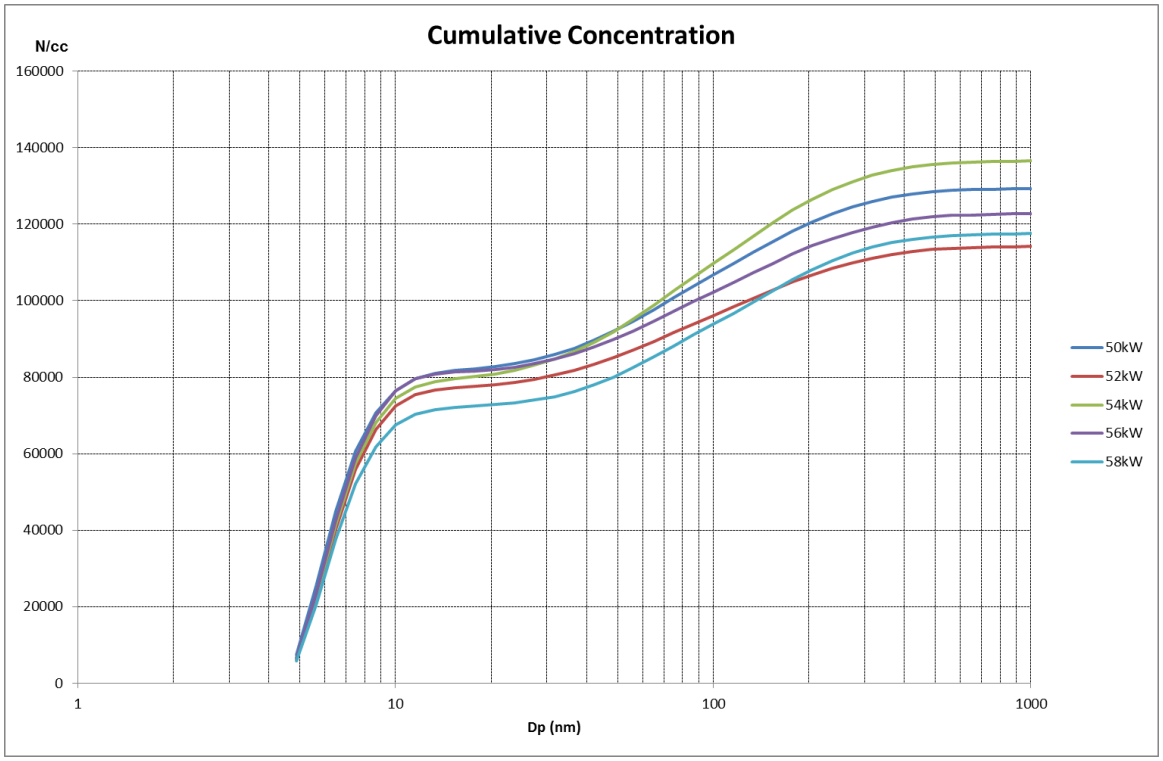

Figure 6-17 Faulty GT1 particle cumulative concentration

The Figure 6-17 Faulty GT1 particle cumulative concentration cumulative concentration of particles shows the shift in the distribution away from the nucleation and into the accumulation zone. In addition there will be a presence of particles greater in diameter than 1µm will not be getting through at all.

It is this kind of dynamic particle size change behaviour that the DMS500 is most appropriate for analysing. Much of the GT emissions distributions are fairly static, and low in concentration.

6.2.5 GT1 CO_2 EGR Results

Particulate analysis of the GT1 with simulated EGR in the form of CO_2 addition shows a small change in the particle distribution for some cases at low turn down ratios with high levels of CO_2 addition, thus representing high levels of EGR.

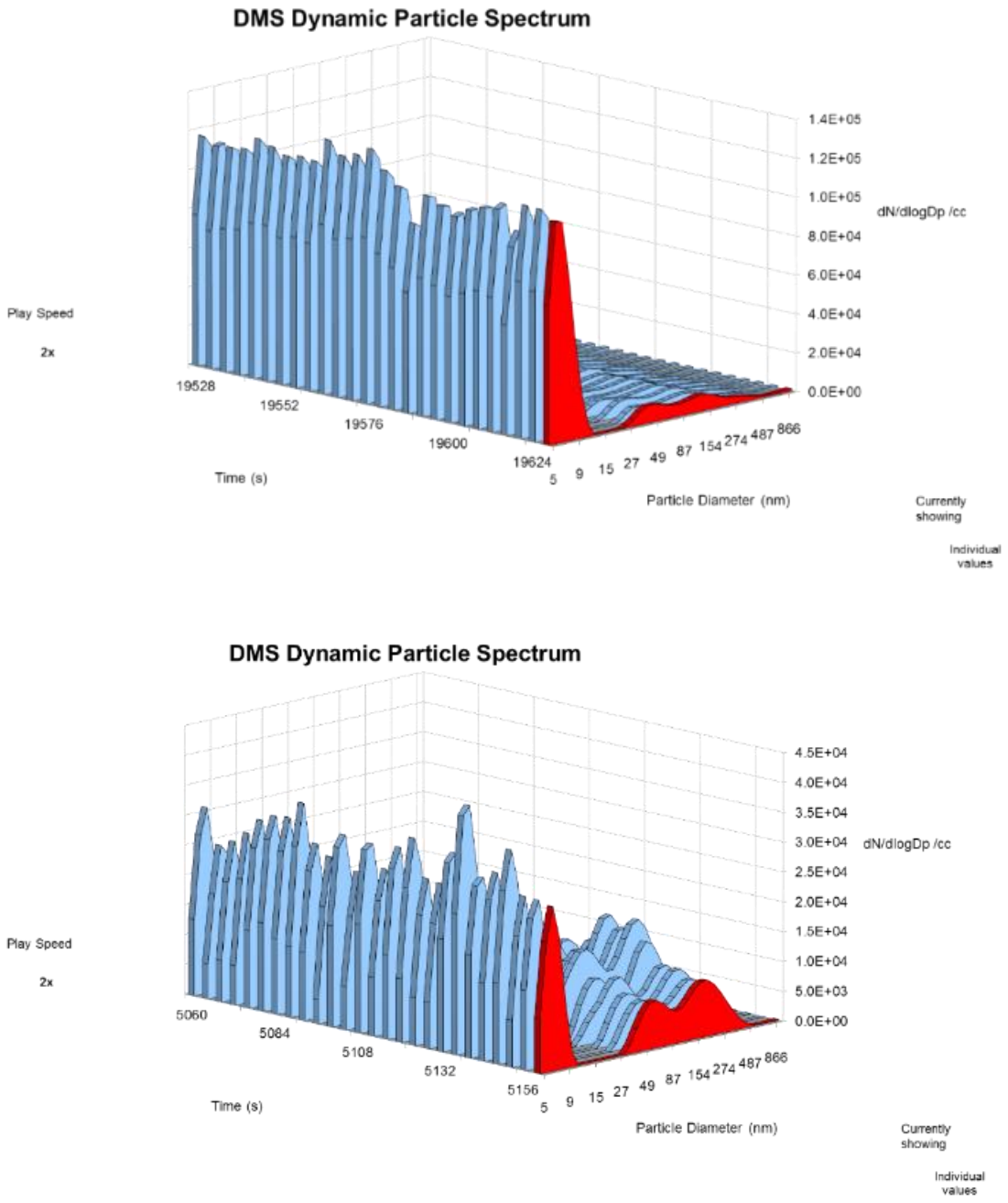

Figure 6-18 The 60kW particulate size distribution change from 15kg/h of CO2 addition to 125kg/h

From Figure 6-18 The 60kW particulate size distribution change from 15kg/h of CO2 addition to 125kg/h it is clearly visible in this 60kW run is a decrease in the nucleation particles and a slight increase in the accumulation particles. This is as since it takes many nucleation particles to form

a single accumulation particle. This is probably due to slight increase in the aromatics in the form of UHC in the exhaust.

From the 60kW simulated EGR tests, it can be seen that there is a clear change in the particle distribution. This is due to a change in the exhaust composition. As discussed in the simulated EGR chapter 4, low CO_2 addition has limited impact on the exhaust composition due to the lean nature of the gas turbine combustion.

Higher levels of CO_2 addition, corresponding to higher levels of EGR, and a change in the oxidiser composition similar to that expected with EGR, produces an increase in the UHC emissions. This increased number of VOC appears to be causing an increase in the accumulation particles from an increase in the agglomeration of nucleation particles. This is evidenced by the reduction in the nucleation particles being mirrored by the increase in accumulation particles.

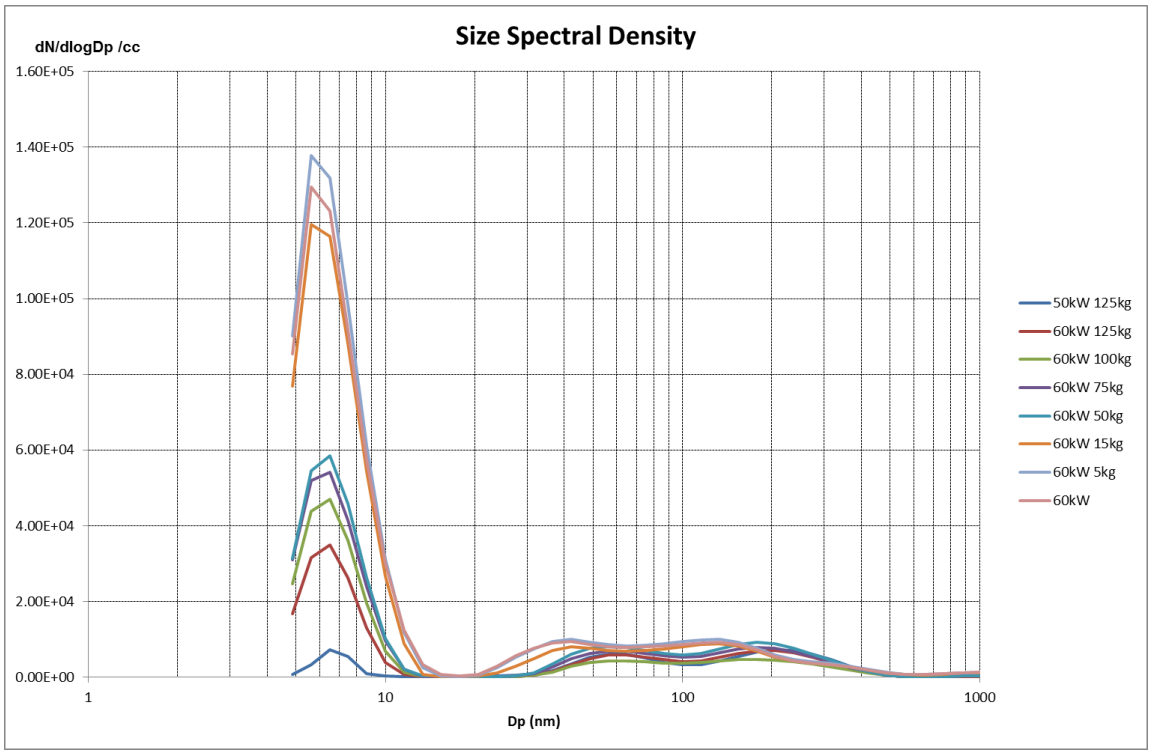

Figure 6-19 Particulate size distribution with CO_2 enhancement at 50 & 60kW

It is clear that there is less nucleation and more accumulation particles with CO_2 in Figure 6-19 Particulate size distribution with CO2 enhancement at 50 & 60kW. There is also a slight shift in the distribution of the accumulation particles, moving away from the smaller "Aitken" mode size to the larger accumulation size though the concentration does not appear to be dramatically increased, again this is due to the multitude of smaller particles required to create the larger particles.

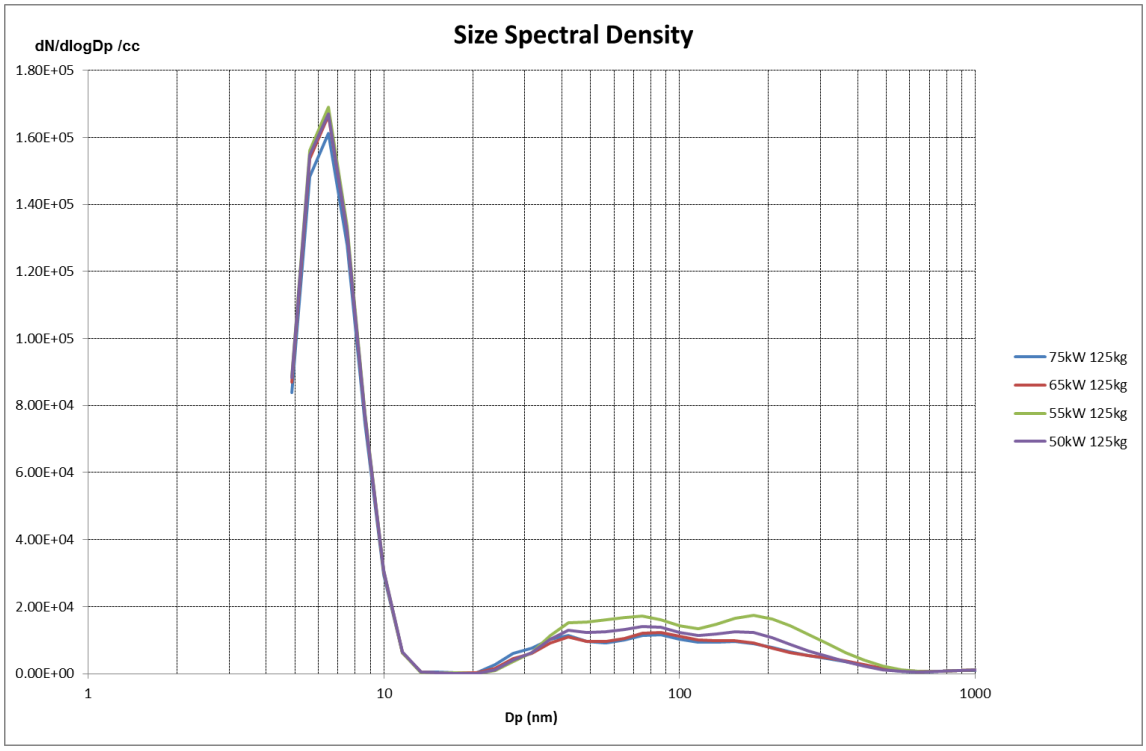

Figure 6-20 50 – 75kW with 125kg/h CO_2 addition particulate size distribution.

The reduction in the total nucleation particles is also evidenced at all turn down ratios. Going from the baseline results of 3 - $5x10^5$ to 1.6 x 10^5, although this reduction is not dramatic, it is consistent.

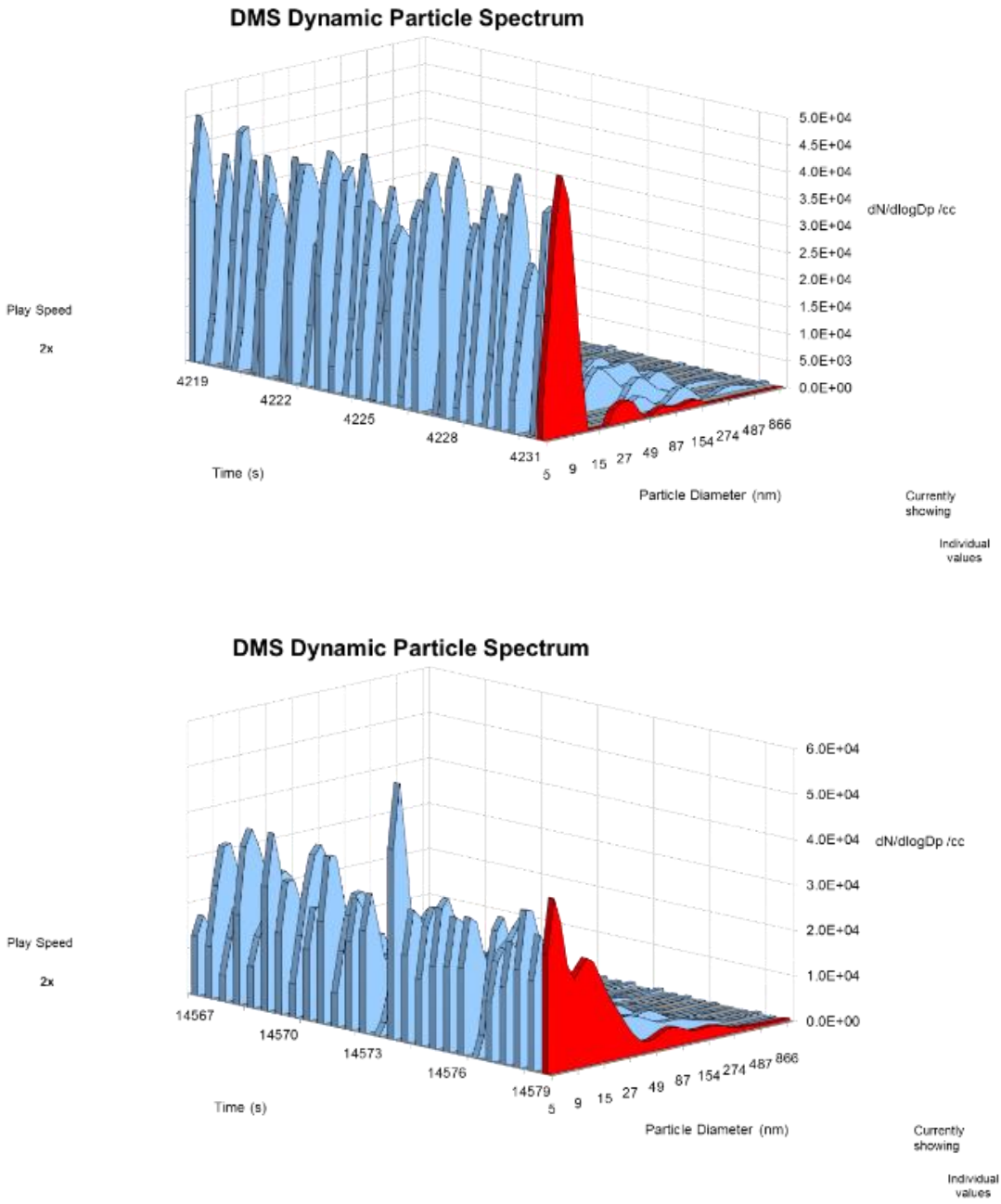

Figure 6-21 Dynamic particle spectrum results with CO_2 addition showing reduced particulate concentration, and altered size distribution

Over shorter periods of time within the 125kg CO_2 addition tests, the trend shows the nucleation particles dropping to 3-5x10^4 in concentration.

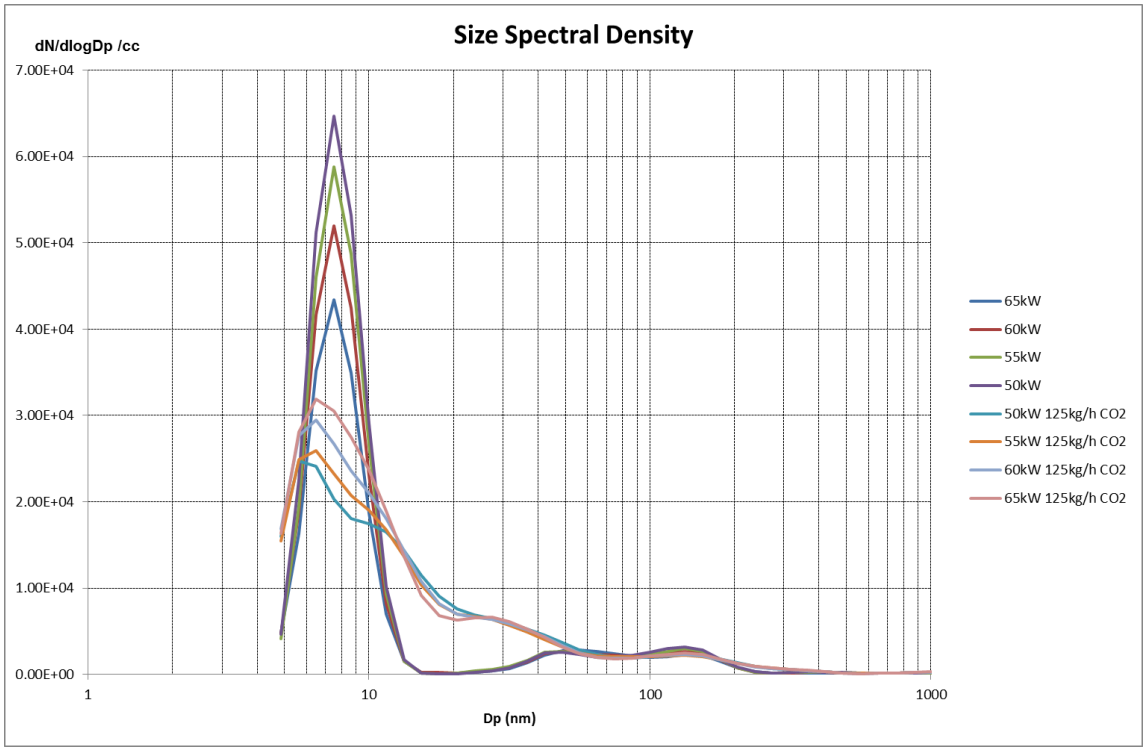

Figure 6-22 Particle size distribution with and without CO_2 addition for 50 - 65kW.

Figure 6-22 Particle size distribution with and without CO2 addition shows that there are more nucleation particles without CO_2, and with CO_2 there is an increase in the accumulation particles and a slight shift in the trend.

6.3 Conclusions

- Both the GT1 and GT3 show an increase in particles in their exhausts above that of ambient air and GT3 appears to have more accumulation particles.
- The size of the particles for both is dominated by the nucleation sized particles, mostly produced from the water from combustion. This is still an issues as nucleation particles can still contribute to climate change.
- There is an increase in the accumulation particles and a decrease in the nucleation particles for larger CO_2 addition, being equivalent to the larger EGR proportions.

- For all the changes in the particle distribution observed, reductions in nucleation particles are matched by slight increases in accumulation particles. The only notable exception being the operation of GT1 with a faulty combustor, when there was an additional solid particulate source from the degradation of the burner.
- The majority of the particles are most likely not to be solid, due to the switch from nucleation to accumulation, and when considering the fuels nature and composition. There are no solid particles to be formed unless they have come from the turbine lubricants, or corrosion. The only increase in both the nucleation and accumulation was from the faulty combustor operation, where there was a source of additional solid particles.
- For some GT3 particles increase in accumulation could be down to the nitrates formed from the NOx emissions. For the EGR simulated particle emissions, the particles are most likely from UHC and aromatics agglomeration, during which time NO_x appears to be lower. This is because there is less excess O_2 to form NO_x, and lower combustion temperatures due to the thermal and conductive impact of CO_2 addition.
- In comparison to coal, biofuel, diesel, and GDI, the particulate emissions are insignificant in number and size distribution. It should be considered that the air passes through a filter before combustion, and although results show an increase in particulate number, some commercial GT have been shown to have less particulates than ambient air.

7 Conclusions

7.1 Introduction

The key issue for CCS, as in all low carbon technologies is to be as economically competitive as possible with conventional generation, reducing the energy demand of the post combustion capture process as much as possible will help reduce the cost. The most energy intensive step is the regeneration of the solvent for capture, reducing this can have the largest impact on improving its competitiveness. Hopefully this study is a contribution to the understanding to help achieve this with EGR and HAT technologies.

7.2 Baseline Conclusions

Baseline testing of the two gas turbines has been performed. This was done to gain familiarity, establish expected performance of both before adaptation, to become familiar with their operation, determines appropriate potential test methodologies and to help develop future planned tests. These tests were carried out over a number of test days with varying ambient conditions. This was also done to establish the gaps in the required potential data to help develop additional instrumentation plans. The base testing allowed the assessment of the accuracy and appropriateness of the current instrumentation.

What was found for both turbines is that important information regarding the performance is the consistency of the turbines output once steady output is achieved. This is useful for providing credible results, and mean anomalous data, or interesting impacts of the EGR or HAT being more easily observable.

The baseline test runs helped establish the achievable turndown ratios for both turbines, without any modifications. Whilst the Series 3 achieved powers up to 106.24kW, the Series 1 performance has been compromised by age, being limited to 80kW actual output.

The baseline testing established the standard emissions performance of the two turbines, showing good combustion across all turn down ratios for both turbines. The only poor combustion observed was at the low powers for both turbines. Lower CO levels were observed for the Series 1 than to the Series 3, being consistently below 5ppm above 60kW. The Series 1 also gave good complete combustion with CH_4 being less than 1ppm.

The data collected showed good levels of complete combustion, and was used to calculate future expected results and form a basis to calculate the total flow rates. This was done using the CO_2 volume percentage collected from the exhaust emissions and the known fuel consumption and composition.

From the baseline testing, it was decided that the Series 1 would be used for adaptation due to the capital value of GT3, and the deteriorating condition of GT1, to make full use of this resource whilst it's still available and to build experience before considering potential adaptations for the S3. It was evident that in order to effectively monitor the turbine performance, and the impact of altering the oxidiser and combustion mix, the pressure and temperature readings post compression would be essential.

The exhaust gas temperature was also not monitored in the Series 1, but was for Series 3 where it was 48°C -75°C, and this would be a consideration for physical recirculation.

The important temperatures are the calculated TIT and TOT. The TOT for both reached ≈645 °C during steady operation above 50kW. However the Series 3 provided no TIT data, and this is another important temperature and a reason to utilise the Series 1.

As might be expected, due to the Series 1 not achieving a full specified turn down range than the efficiency was poor, being below that of the manual stated efficiency, with a peak for the S1 60 -70kW, and S3 75 – 100kW. In general, the SFC of the Series 1 is 15-20% higher than that of the Series 3, with the difference in efficiencies widening as the power output goes up.

7.3 CO_2 Simulated EGR

From the experiments conducted, enhancing the oxidising air with CO_2 to simulate the EGR, a reduction in combustor performance was observed.

The CO_2 enhancement effected the turbine speed, pressure, emissions and the efficiency of generation is visible in the increased specific fuel consumption.

The ambient temperature dominated the performance both with and without CO_2 addition. With the turbine speed increasing to counter the higher temperatures and maintain the mass flow.

The addition of CO_2 impacted on the temperature post compression. The enhancement with 125kg/h of CO_2 resulted in the temperatures post compression being consistently ≈5 °C lower. This is due to the higher heat capacity of the CO_2 than that of the air it displaces. This may have resulted in an increased efficiency in the recuperator, however this will be expected to have reduced the combustion temperatures and hence resulted in the lower exhaust gas temperatures going into the recuperator. Also this would have contributed to the lower turbine efficiency and higher specific fuel consumption, as would be expected with the exhaust gas recirculation.

The enhancement with CO_2 resulted in some changes to the emissions. With the higher levels of CO_2 addition there were observable changes to the incomplete combustion, and CO and CH_4 rising. At 50kW 125kg/h CO_2 enhancement, the CO emissions more than doubled and CH_4 more than trebled. The reduction in the combustion efficiency is attributable to the displacement of oxygen for combustion, thus making conditions slightly more fuel rich. The primary cause will be the increased heat capacity that causes lower flame temperatures, reducing flame speed and reaction rates. This reduction in flame temperatures and speed is also evidenced by the

reduction of the thermal NO_x observed. For 91% of the tests carried out, NO_x was reduced with CO_2 addition.

The simulated EGR had the effect of increasing the specific fuel consumption due to the reduction in efficiency from poorer combustion. Although this increase could be considered within the maximum potential error for the instrumentation, the trend was consistent with all the results and testing days thus giving strong evidence that there was an impact. The CO_2 addition at a rate 125kg/h increased the SFC 1.7 – 2.9%.

As discussed, from the baseline testing it became possibly to more accurately calculate the total mass flow through the gas turbine. This was through the measured changes in the CO_2 volume % concentration, at constant power output with known CO_2 mass addition. These calculations showed significantly leaner combustion conditions than expected, varying from 1:105 – 1:130, and these lean conditions mean excess O_2 for combustion and a less dramatic effect with CO_2

7.4 HAT & CO_2

The combination of synthetic EGR and steam addition had numerous interesting impacts.

The temperature post compression is significantly reduced by up to 40°C. This will be due to another step increase in the heat capacity of the air with both steam and CO_2 displacing the air. Also there is the possibility that the condensate may be entering into the compressed air.

As with the addition of CO_2, there is an expected impact on the combustion temperature with steam addition. This temperature reduction is seen in a reduction in the calculated TIT, when both processes are combined, by up to 9°C at 60 – 65kW.

The combination of the steam with CO_2 enhancement had the impact of increasing the CO_2 volume on a dry basis, due to the displacement of the air mass. This resulted in an increase of 0.2%, which is a 4% increase on the result with CO_2 enhancement alone. Further this increase in

volume % of CO_2 would increase the post combustion capture efficiency through a reduction in the reboiler duty.

The addition of steam to the simulated EGR process also saw an increase in efficiency that was even more significant than the loss in efficiency compared to the baseline results caused by the addition of CO_2. This efficiency gain offset in the loss from the EGR is a tandem benefit to increasing the partial pressure of the CO_2 for capture. Operation of the Series 1 turbine, with both the HAT and EGR processes, resulted in a lower SFC than the baseline operation. This translates to net energy efficiency gains for the complete generation and capture system.

7.5 Particulates Discussion

The particulate emissions of the two turbines are very low, and this is due to the fuel being natural gas, in comparison to heavier fuel combustion.

Due to this particulate distribution being dominated by the nucleation particles for both turbines, then there is a slight shift towards accumulation for the Series 3, and this may be related to the higher NO_x and CO emissions.

With the enhancement of the oxidising air with CO_2 to simulate the EGR, there is an increase in the accumulation of particles and a decrease in the nucleation particles for larger CO_2 addition. This decrease in nucleation and increase in accumulation is due to the increased CO and UHC emissions encouraging the accumulation of slightly larger particles towards the accumulation mode. The significant drop in nucleation number is due to the numbers of particles required to form the accumulation particles.

When considering the fuels nature and composition the majority of the particles formed by the combustion in the gas turbines will not be solid. Any solid particles would have come from the turbine lubricants or corrosion. Such increases in the potential solid accumulation particle

number was observed from faulty combustor operation, where there was a source of additional solid particles.

Although particle numbers are relatively low, the increase in the nucleation particles from gas turbines that may be from water can contribute towards climate change and have a temporary effect if they accumulate. In addition, any significant increase in the accumulation mode may be from nitrates and nitric acid, or carbon monoxide with uncombusted fuel to form carboxylic acids that could have an impact on the rate of decomposition of any post combustion capture solvent.

8 Future Work

There are possibilities to expand testing capacity of Current PACT Core Facilities

8.1 Expanding current capacity

8.1.1 Increased CO_2 flow simulating EGR

Increasing the capacity of the maximum flow of CO_2 achieved by the mixing skid and delivered through the lines to the turbine would allow a greater change to the oxidiser composition at the point of combustion. Currently the maximum flow of CO_2 reduces the O_2 to just over 19% by volume. 35% EGR by volume on a larger CCGT combustor is shown to increase O_2 conditions of 17% by volume, and 50% EGR to 13.2% O_2 by volume. This would produce more interesting and accurate depictions as to the effect on the combustor in terms of unburnt hydrocarbons, carbon monoxide formation and reductions in thermal NO_x creation. This more significant impact on combustion and unburnt hydrocarbons would provide more significant trends for specific fuel consumption increase, and possibly more discernible trends in efficiency as a percentage of power output. This data could then be used to more effectively determine the combined net process efficiency impact of power generation and post combustion capture.

Currently the CO_2 mass injection is limited by the capacity of the secondary line to which it is injected on, and the maximum pressure the valves on that line can effectively control the flow. However there is sufficient CO_2 capacity in the external storage to deliver more. If CO_2 were to be injected by two or more lines of the mixing skid, the total CO_2 injection could double or even triple. This would require further consideration of the speed of the CO_2 leaving the injection point and the temperature at which it is discharged. Both of which could be calculated. Doubling the CO_2 Injection capacity would create O_2 conditions closer to the 35% EGR levels at ≈18.24% and increase the exhaust CO_2 volume by up to ≈16.08% as seen in Table 8-1 Calculation of expected results for 350kg/h CO_2 enhancement.

Table 8-1 Calculation of expected results for 350kg/h CO_2 enhancement

50kW CO2 Addition		350kg Exhaust Recycle		
		Mass	Volume	%
From Exhaust	O2			0.00
	N2			0.00
	CO2	**350.00**	**224.07**	100.00
	Air total	350.00	224.07	
Into Compressor	O2		285.86	18.24
	N2		1056.98	67.46
	CO2	350.00	224.07	**14.30**
	Air total		1566.91	
New Exhaust	O2	339.71	237.73	15.41
	N2	1322.28	1056.98	68.51
	CO2	387.59	248.14	**16.08**
	Air total	2049.58	1542.84	

Also this would mean that there is a greater likelihood of CO_2 leakage to the atmosphere and that not all the injected CO_2 would be entrained into the combustor. This would result in less certainty in the total injected mass and the CO_2 in the cooling air would have to be more effectively monitored. To counter this reduction in uncertainty an analyser with greater accuracy at lower volume percentages would be required for the cooling air flow. In addition to this, a more effective mass flow measurement would also be required due to the inaccuracy in the ValuMass meters. However, the issue with the ValuMass meters is that there is air leakage and this means that the combustion air cannot be calculated as a difference in the two values. However as an individual mass flow for the cooling air it is effective, and hence using TC8 and PT6 it would be possible to calculate the escaped CO_2 with the analyser reading of the CO_2 volume percentage.

8.1.2 Increasing the steam flow for HAT

Currently the maximum reliable steam output for the boiler facilities at PACT is 40kg/h. The mass flow of the turbine is calculated at 50kW minimum to be 2,738kg/h, and at maximum with CO_2 and HAT addition to be 3,291kg/h. This means that the current steam addition mimics 1.46% HAT process by mass, down to 1.22%. Ideally expanding facilities to be able to test up to 5%.

This could be done with the current mixing SKID set up and injection line capacity to inject up to 180kg/h, which would be equivalent to a minimum of 5.45%. This would have an impact on improving the energy efficiency and reduce the specific fuel consumption. There would also have a further detrimental impact on the combustion of the microturbine with expected higher CO and CH_4. What would be interesting is the impact on NO_x, in particular if there would be a continuing trend of NO_x increase anomaly, or if the reduction in NO_x expected would occur with higher levels of HAT having a more significant impact on the combustion temperature, and hence reducing the thermal NO_x creation. Alternatively it may continue to disrupt the combustor mix. It is possible for CO + N2 to react at high temperatures in the presence of hydrogen but these are high energy reactions that are unlikely to be occurring.

Of particular interest for increased steam injection capacity would be the lowest turn down ratio tests at 50-55kW, with the leanest fuel:air mix and with more steam increments tested, every 10kg/h of steam from 0 – 180kg/h.

Although the HAT testing was carried out over several test days and the unusual NO_X emissions were repeated, further duplication would be good for validation phenomena. Further the boiler requires a service to ensure safe operation before further testing is carried out.

The expansion of CO_2 enhancement and the steam addition facilities would also allow for a new broader test campaign for capture at the PACT facilities. Currently there is limited sensitivity to small changes in CO_2 exhaust concentration for capture in terms of the calculation of the reboiler duty. With the increased capacity of CO_2 injection, higher exhaust volumes of CO_2 could be expected to be generated, and using the method for testing the predictions this showed that the CO_2 volume of up to 16.08% at 50kW could then be achieved through a doubling of the CO_2 injection capacity to 350kg/h. This would mean more effective combined generation and capture tests could be carried out simultaneously for additional interesting research possibilities.

With modifications to improve the CO_2 enhancement and steam injection capacity it would also be possible to run a more comprehensive test campaign as to the impacts of combined EGR and HAT.

8.2 Particulates

During the testing with HAT it was not possible to test in combination with the DMS500 particulate analyser. Future work could be done investigating the impact that HAT has on particulate formation. This would be particularly useful due to the expected significant expansion of CCGT power generation, and hence the larger contributor to the particulates that they will become, particular so for their contribution to the PM1, and ultrafine ranges. It might be expected that such an investigation may find an increase in both the accumulation and nucleation particles, with a possible slight shift in distribution towards accumulation growth.

Additional particulate investigations would be good to be performed and to identify the composition of the particulate matter. The simplest start for this procedure would be to clean the classifier before the test runs, and then take samples of the deposited particulate on the classifier rings after testing. These samples could then be looked at with a scanning electron microscope with resolutions comfortably down to 1nm, and this could be used to inspect the morphology of the particulate samples, and accurately measure them. Being able to accurately depict the shape of the particles would also help attribute appropriate densities, and hence total mass of emissions. Further, energy dispersive X-ray analysis could be used to help determine the composition of the particulates from the peaks in the electromagnetic emissions spectrum, and this can also be done using a scanning electron microscope.

8.3 Additional instrumentation

8.3.1 Thermocouples

Currently there is no thermocouple that takes the temperatures in the combustion zone. It was decided that the installation of such a thermocouples would present a risk to the integrity of the combustor due to the required drilling into this region. A thermocouple would also require some shell protection in such zones, which would reduce its sensitivity to changes in the temperature that could experience quite dynamic fluctuations with changes in testing conditions. However longer test run periods may resolve this issue. In addition, the effective placement of a thermocouple for peak temperatures would be difficult to determine and may disrupt the flame. Tests carried out at the University of Stavanger with a probe also did not provide reliable temperature measurements. Now that a testing campaign has been carried out on the turbine, it may beneficial to try and attain this additional data, to at least see the relative changes in the peak temperatures in the combustor, with CO_2 enhancement and steam injection, this may go some way in determining the sources of NO_x. The accurate positioning of the thermocouple may be done through disassembly measurement and accurate modelling of the combustor. A type K thermocouple would also not be appropriate for the measurement due to its peak temperature measurement of up to 1300°C, and therefore a type B thermocouple that measures up to 1800°C may be more appropriate.

8.3.2 Flow meters

As discussed in chapters 33 and 4, accurate measurement of the total mass flow has been a challenging issue. More accurate measurement is possible with higher investment costs in the form of a corona mass flow measurement.

8.4 Inspection

As the turbine does not achieve the maximum rated pressure ratios of 4.5:1 then an inspection of the turbine and compressor blades would be of interest. To do so requires the removal of the turbine housing with a hoist, and for it to be split. Although an endoscope was used to look at the turbine blades, with some pitting evidence being observed, it was not possible to be thorough or conclusive as to the overall condition of the blades. Inspecting the turbine blades for pitting properly requires the opening up of the turbine. It may also be interesting to see if it is possible to reduce the volume of the compressor through adaptation in an attempt to increase the pressure, and reduce the total mass flow.

8.5 With additional investment

8.5.1 Physical recirculation

An interesting area of research may be the physical recirculation of the exhaust gas from the microturbine for EGR, and to investigate the other challenges presented by an EGR system. The recirculation of exhaust gas would require cooling to prevent very inefficient compressor performance, to the detriment of the overall turbine efficiency. Some thought was given to the design of such a system. With calculation of cooling requirement and research into potential heat exchangers.

The flow rate and temperature of the Turbec S1 is ≈ 3,000kg/h (0.83 kg/s) and ≈ 140°C.

The specific heat capacity of the air is 1 kJ/kg.K, and it would be desirable to reduce the temperature of the recirculated air to ≈10°C.

Heat Energy Calculation:

$$Q = \dot{m} C_p \Delta T \quad \textbf{8-1}$$

$$Q = 0.83 * 1 * 130$$

$$Q = 107.9kW$$

That is for 100% of the flow, so for 50% EGR

$$Q = 54kW$$

A water:air plate or shell and tube heat exchanger may be appropriate for this dumping this heat load, and if required it could be used to provide controlled temperature oxidising air for compression, where as previously ambient temperature was the controlling factor. Such heat exchangers could be designed in house or purchased. Also if HAT was not being used it could be used to condense moisture out of the air.

Any off take for EGR in a controlled flow could also be an opportunity for shower HAT system.

8.5.2 Combustor

Of particular interest is the combustor performance. There are currently many facilities at the PACT location that could be used for other CCS experiments. A rig with a CCGT type combustor could produce many interesting results. Using the Skid control and steam boiler for controlled flows into a combustor alone, for which gas could be recycled, the combustion mixes are more easily controlled, and perhaps also the pressure ratios, and this would be just the pressurisation of the oxidising air. Also the fuel control would allow the temperature control of the combustion.

8.5.3 Membranes

Selective EGR using membranes has been discussed as a potential low energy separation technique to try and increase the energy efficiency of capture. A membrane could be used in conjunction with the installation of a full EGR system to the turbine. With physically recirculated

exhaust gas, and with very low CO_2 concentrations, passed through for recycle to increase these concentrations.

9 Appendix A

9.1 Turbine breakdowns

During testing there were numerous issues with the GT1 breaking down and developing a number of faults. However some produced interesting results, in terms of alterations in flame temperature, efficiencies, and emissions.

For example the power electronics failed twice, and required replacement both times. The first occasion was during baseline testing and the cause of the failure was unknown, but it was attributed to age. The second failure was during humidified air testing, when it is believed that the circuitry got wet during the first commissioning tests of the HAT program and required replacement. There were also signal cable failures that prevented communication with the WinNap program, and thus hampered testing and required replacement. The ignitor seen in Figure 9-1 Combustor ignitor also stopped working and after trying cleaning, it was found that it required replacement. This was replaced with a car spark plug after adaptation by NewEnco, as the Turbec ignitors are excessively expensive.

Figure 9-1 Combustor ignitor.

The most significant breakdown was the burning out of the combustor. It is believed that the combustor was not mounted properly in this case, then tightened by a pneumatic or electric drill, thus breaking the small welds on the inside of the combustor. Had the tightening been done by hand, the resistance from the combustor misplacement may have been noticed.

However some results were collected with the combustor misaligned before its total failure, these results are interesting for comparison to the normal turbine operation and speculating on the combustor behaviour during this period of time.

9.1.1 Results of Faulty Combustor for Comparison

The top of the combustor shell was caught and misaligned into the combustor, and turbine housing, and on tightening broke and this changed the direction of the flame angle, projecting the top of the flame to one side. This misalignment can be seen in Figure 9-2 Broken housing combustor angle.

Figure 9-2 Broken housing combustor angle.

Figure 9-3 Heat marked combustor.shows inside that one side of the turbine housing where the combustor sits has been affected by the flame misalignment and discoloured by the additional heat.

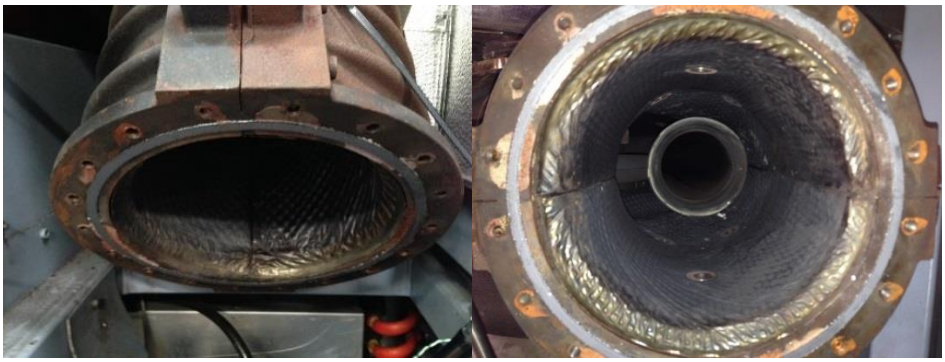

Figure 9-3 Heat marked combustor.

The outer cup of the combustor sits on top of the combustor where the fuel and pilot fuel is added. The veins seen in Figure 9-4 Combustor air veins and channels. direct the air and thus creates a swirl and the mixing for complete combustion. This mixer and veins appeared to be in good condition following the damage.

Figure 9-4 Combustor air veins and channels.

However the combustor was damaged and appeared to have melted. This was most likely due to flame attachment, caused by a change in the air flow from the misalignment. The damage seen appeared quiet significant with the combustor head completely distorted shown in the photographs of Figure 9-5 Heat deformed combustor head..

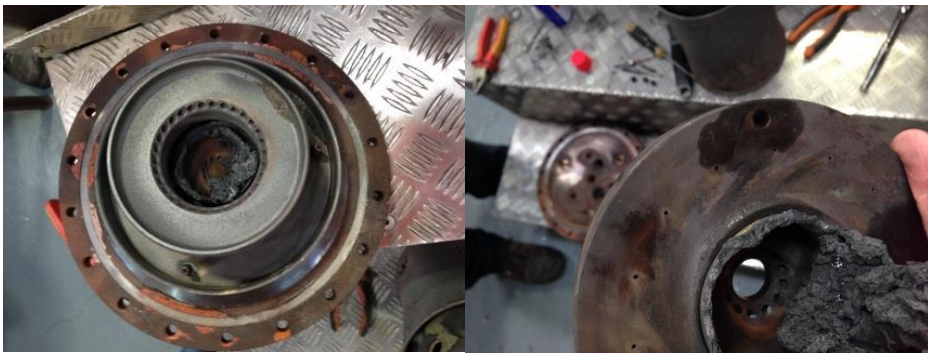

Figure 9-5 Heat deformed combustor head.

The damage to the combustor had almost completely destroyed it, with only part of it remaining undamaged. It is very probable that fragments of this will have been blown out of the combustor and travelled through the turbine and heat exchangers after. This debris most likely impacted on the turbine blades and thus increased the pitting, as some pitting was visible on inspection

with an endoscopic camera. This will have increased the general wear on the turbine, and the pitting gradually reduced the turbine efficiency.

9.1.1.1 Mechanical

When compared to the average performance of the Series 1 turbine, unexpectedly there is a reduction in the turbine speed (RPM) depicted in Figure 9-6 Turbine speed with damaged combustor. This could be partially attributed to the ambient air temperature difference, which is approximately 1°C lower than the average, which would mean increased air density, and the reduction is more significant than seen for similar temperature reductions.

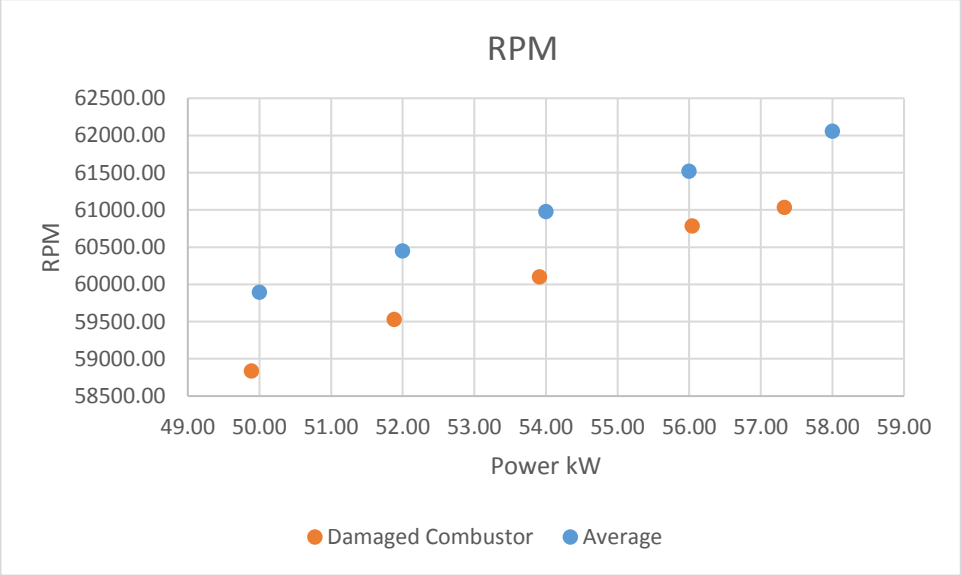

Figure 9-6 Turbine speed with damaged combustor

On review of all the recorded data though, the reduced fuel flow rate was also probably a significant factor, this means that for the turbine to generate the same power for lower speeds, either the compressor efficiency has markedly improved, which from later data is seen not to be the case, or the turbine inlet temperature has increased significantly.

The turbine Inlet temperature is a calculated value from the WInNap software, with the calculation based predominantly on the fuel pressure and valve position for calculating the rate of fuel consumption. Figure 9-7 TIT with damaged combustor, shows the TIT to be lower, which on review of the fuel flow rate being reduced would make sense for the turbine under normal operation. However with the power outputs achieved, it is impossible that the flame temperature was lower and this is further evidenced by the emissions.

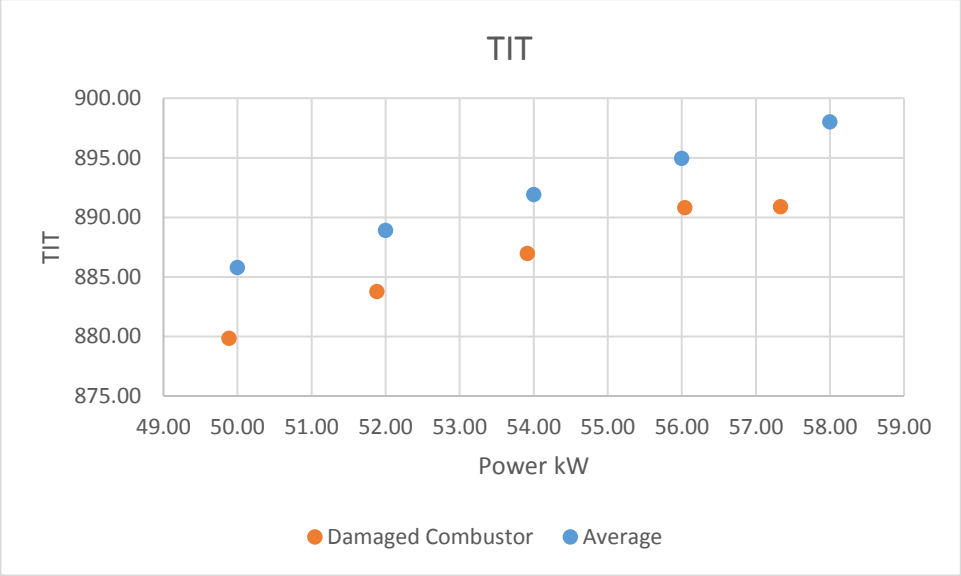

Figure 9-7 TIT with damaged combustor.

As the TIT is calculated from the fuel flow rate, it indicates a lower combustion temperature and inlet temperature than actually occurs, as evidenced by the NO_x emissions. Although the TIT calculated value may produce accurate estimates for the normal operation with the faulty combustor, it is not an appropriate representation of what is occurring. Particularly telling is the drop in TIT past 56kW when a slight spike in the NO_x emissions is observed.

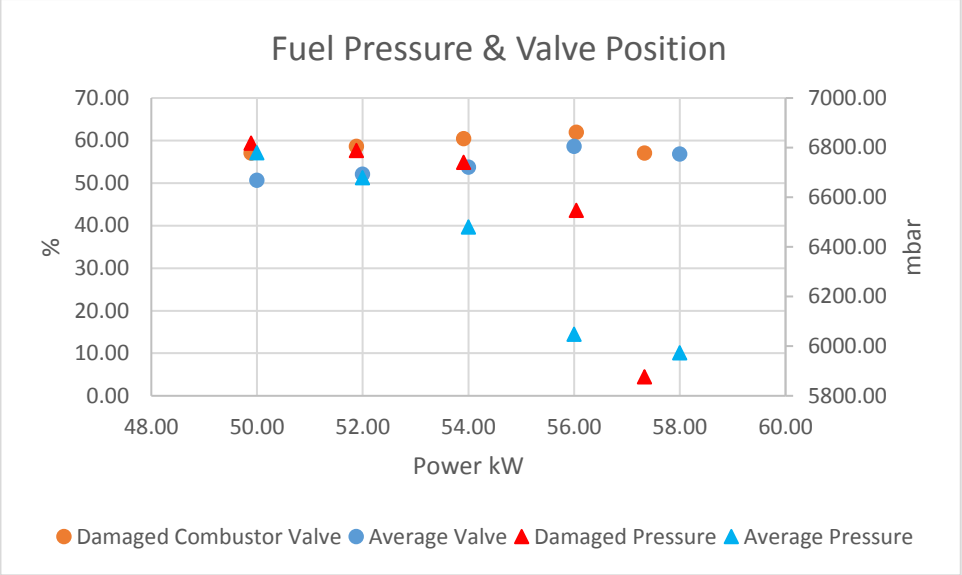

Figure 9-8 Fuel pressure & valve position with damaged combustor.

For 4 out of the 5 plotted test points in Figure 9-8 Fuel pressure & valve position with damaged combustor., the fuel pressure is significantly higher, and the main fuel valve position corresponding to how open is the valve, is also higher. This is due to the lower fuel flow rate and possible restrictions to the fuel flow. It appears the valve has to open significantly more to maintain the same power output that in combination with the higher pressure indicates a restriction in the flow, and this is probably due to deformation at the burner head. The last result at 57.5kW indicates a more significant change to the burner head has occurred in its erosion opening up and relieving some of the previous pressure. This deterioration is also evidenced in the emissions results.

9.1.1.2 Emissions

Although much nitrogen monoxide is observed whilst other emissions remained fairly steady. H_2O appears in Figure 9-9 H2O emissions with damaged combustor. to reduce and the efficiency increase.

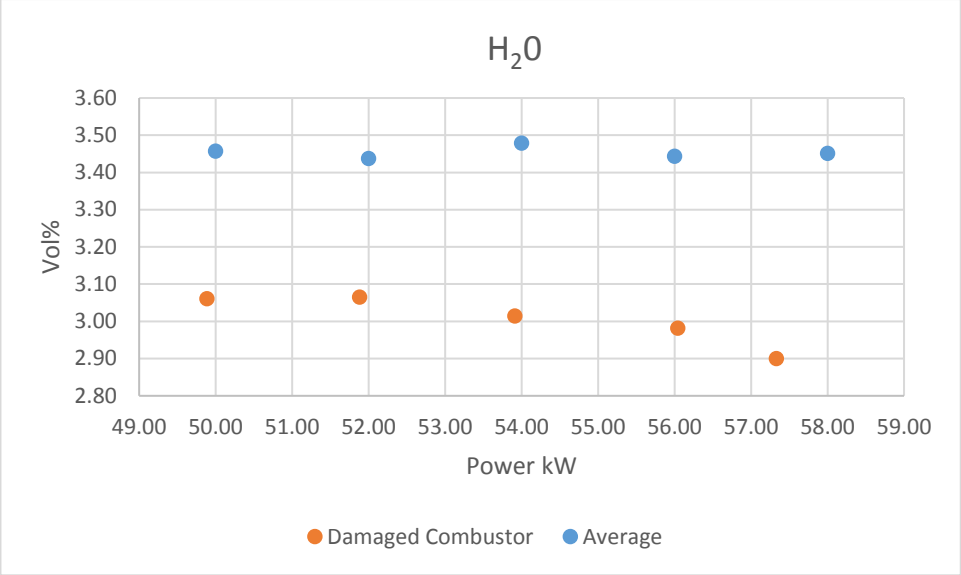

Figure 9-9 H_2O emissions with damaged combustor.

The lower H_2O emissions may be due to the increased turbine efficiency, and the relatively lower fuel consumption. This lower fuel consumption means that less H_2O is formed as a product of complete combustion. The apparent further drop off after 56kW may be further due to the worsening condition of the burner and by this point this also results in relatively higher CO and UHC emissions, that an increasing amount of the fuel is not being fully combusted and forming H_2O, in addition to the higher efficiency running.

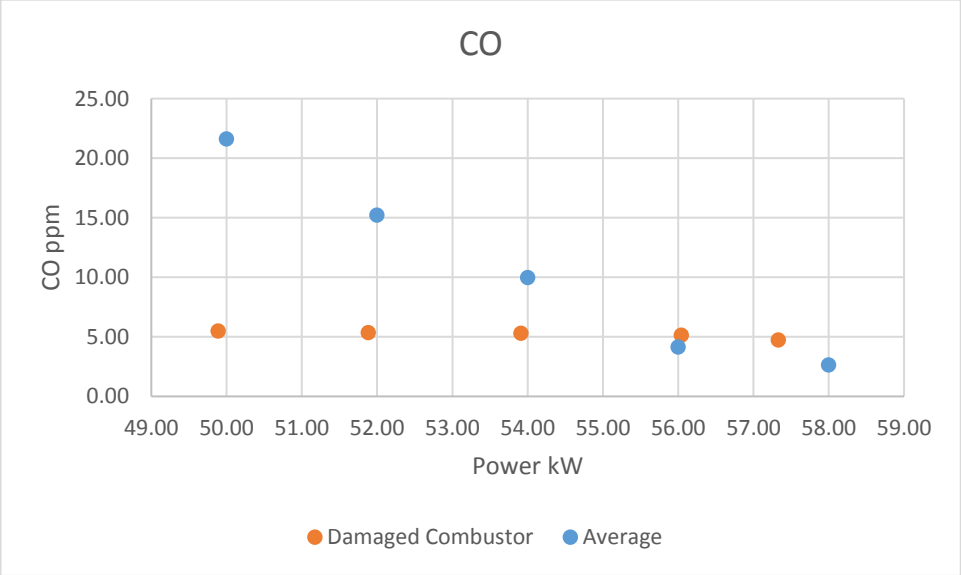

Figure 9-10 CO emissions with damaged combustor.

In Figure 9-10 CO emissions with damaged combustor CO is initially below that of the average combustor performance, and this probably due to a hotter turbulent flame, however as the fuel flow and pressure increases, at higher turn down ratios it would be expected that the CO emissions would drop relatively, however they remain almost constant. This is probably due to an increasing deterioration of the combustors condition and hence, along with other indicators, the combustion becomes less stable.

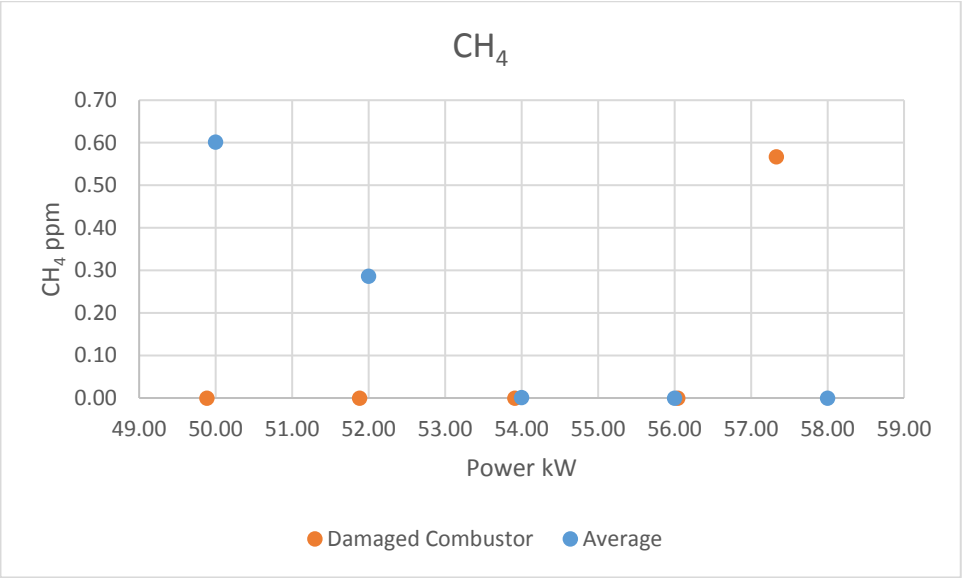

Figure 9-11 CH4 emissions with damaged combustor.

Figure 9-11 CH4 emissions with damaged combustor. indicate less incomplete combustion than with normal operation. This could be due to increased flame turbulence and mixing, and higher combustion temperatures as also indicated by the significantly increased NO_x emissions. The higher temperatures could indicate increased flame kinetics and more complete combustion. This changes with the last CH_4 result, which is opposite to the trend of the faulty combustor operation and to the average emissions trend. This is most likely due to the increasingly bad damage to the combustor head, due to the flame attachment and the deformation of the inner cup of the combustor, due to the longer running time, as the tests were conducted chronologically in ascending power order, with the 58kW experiment was conducted last. There

are other indicators of the damage worsening in terms of CO, fuel pressure, main fuel valve position, NO_x emissions and SFC.

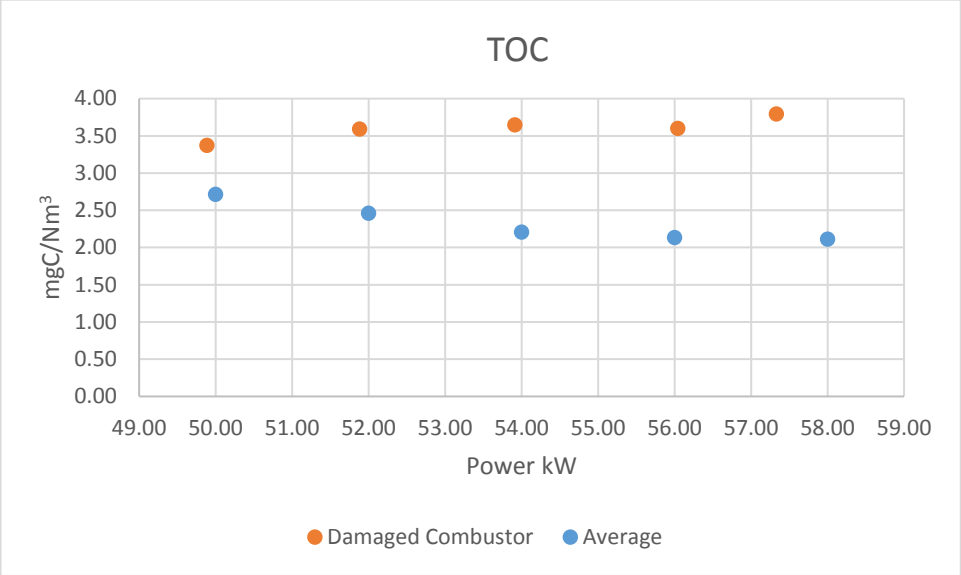

Figure 9-12 TOC emissions with damaged combustor.

The increased TOC of Figure 9-12 TOC emissions with damaged combustorindicates a slight increase in the incomplete combustion of all gas species. Although a small increase in CH_4 is noted, the TOC combines all the unburnt hydrocarbons.

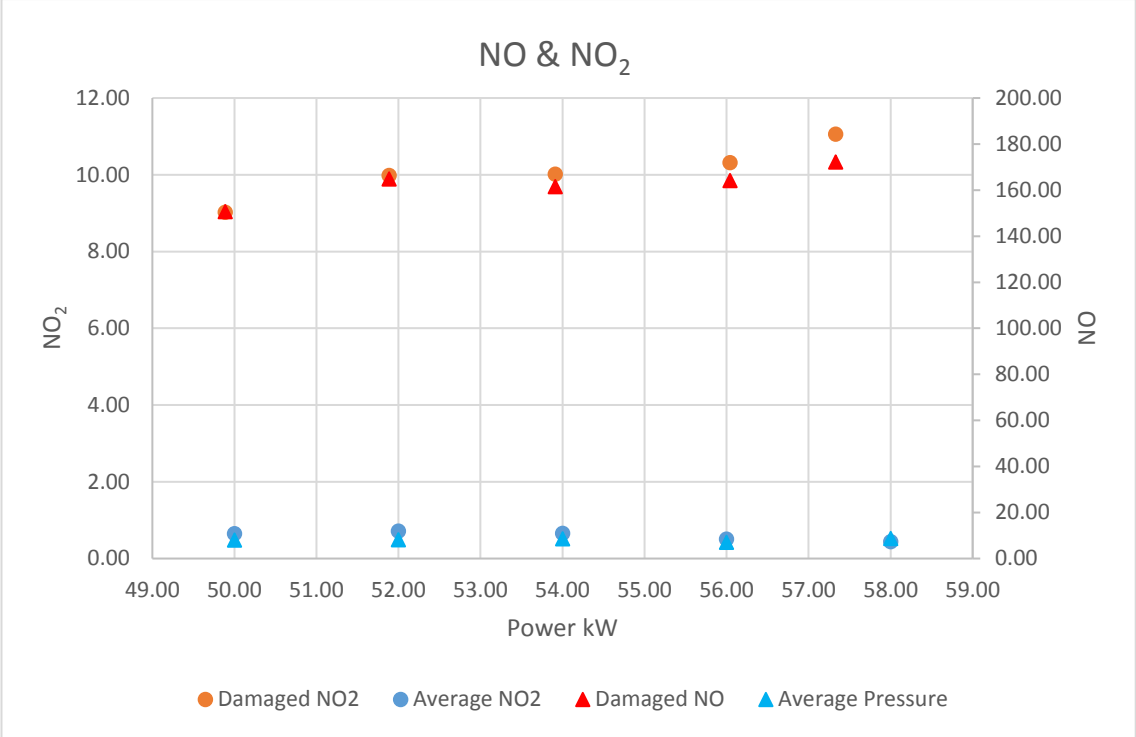

Figure 9-13 NO & NO2 with damaged combustor.

The NO & NO_2 are significantly higher with the damaged combustor. Figure 9-13 NO & NO2 with damaged combustor. indicates a significantly higher combustion temperature than the average combustion temperature, indicated by the lower NO & NO_2 emissions.

The emissions of NO_x also become relatively worse at higher power outputs with higher fuel flows and pressures when it would be expected, and evidenced in the full baseline testing regime, that this would reduce, even comparatively to the initial performance of the damaged combustor. However probably due to the increasing deterioration and fuel flow this does not occur.

9.1.2 Efficiency

As observed by the significantly higher NO_x formation with the damaged combustor, it is reasonable to assume that the combustion temperatures, and turbine inlet temperatures experienced were significantly higher than during standard turbine operation. Significantly increasing TIT is an excellent way to increase the turbine efficiency without increasing the work

required to increase the power as would be required for example with increasing the pressure ratio. However increasing the temperature can damage the turbine, housing, and as seen in the operation of the Turbec Series 1 GT, the combustor itself, and hence normal operation is not at such high temperatures.

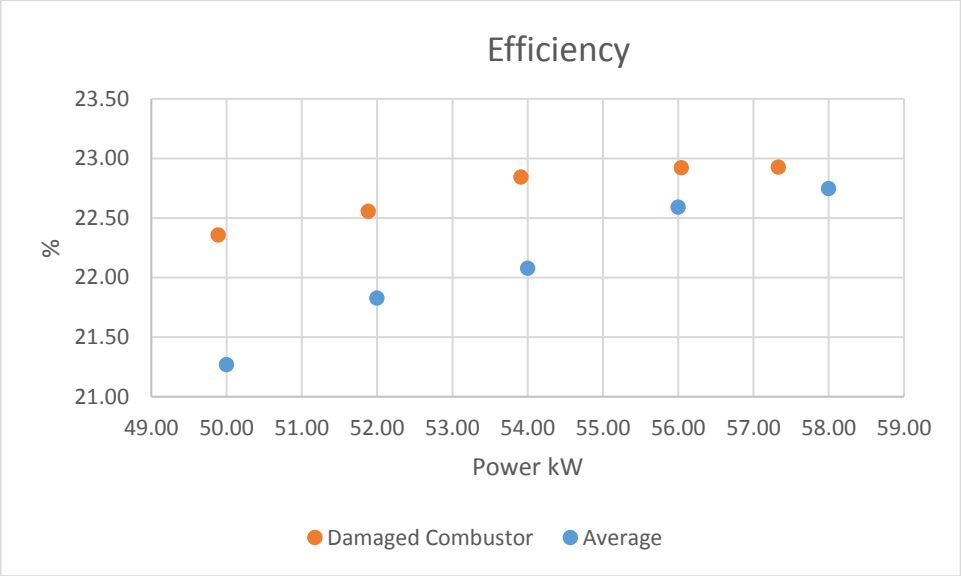

Figure 9-14 Efficiency with damaged combustor

This increase in TIT is the only way to account for the improved turbine efficiency and the reduced RPM observed. The increase in efficiency shown in Figure 9-14 Efficiency with damaged combustor is particularly impressive at the lowest turn down ratio, and this could be because (a) the combustor temperature increases with increasing power, and the relative change may have been smaller, and (b) possibly because the burner head was less damaged at the start up when that experiment was carried out.

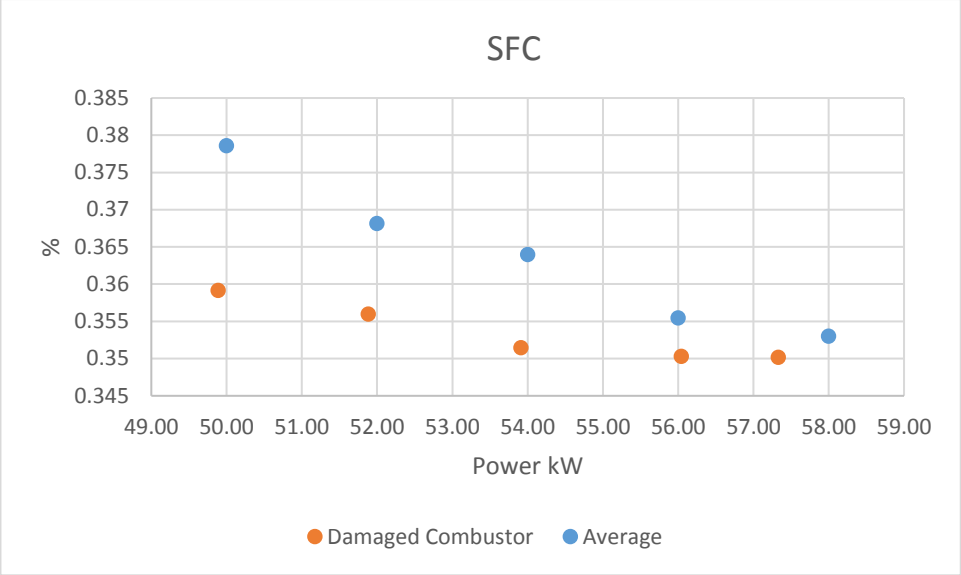

Figure 9-15 SFC with damaged combustor

Naturally the increase in efficiency showed more in the specific fuel consumption as Figure 9-15 SFC with damaged combustor, which is the best measure available for the small changes experienced in the GT1 operation generally.

So the question is why doesn't the turbine always operate at these higher temperatures? – Evidently this is due to the damage observed and the fact it was impossible to restart after and this is probably due to the deformation of the fuel mixing, particularly at the pilot fuel valve the metallurgical limits restrict the higher temperature operation.

In addition to these high NO_x emissions it is not a desirable thing due to environmental and human health concerns and there are domestic and European limits on emissions. Hence high temperatures must be balanced with minimising this.

It is probable that the running with the incorrectly placed combustor housing and corresponding burner damage may have damaged and increased the wear on other elements of the turbine. For example, from the burner photos in Figure 9-5 Heat deformed combustor head. and the complete deformation, it appears that there was also a loss of mass to the burner, which was likely blown in small pieces through the turbine. This probably caused additional pitting to the blades, before passing in to the recuperator, where it may have become lodged, or blown out

through the exhaust. The changes to the turbine blade surface will have an impact on the turbine efficiency, and possibly longevity. Pitting was observed with an endoscopic camera during repair.

9.2 Series 3 Comparison

The Series 3 follows the same pattern of performance as the Series 1, being dominated by the ambient conditions, and this is a well-established relationship that the gas turbines have with performance. In most figures there is a clear split in results, this split is caused by ambient temperature difference, and hence the air density.

Higher emissions of CO, CH_4, H_2O and NO_x occurred on days where testing was at an ambient temperature of 14.5 – 15.5C, where there was also lower RPM, lower SFC, higher fuel efficiency, and lower CO_2 emissions.

The higher emissions ppm on the lower ambient temperature days can be attributed to the lower engine speed, and hence less dilute and more fuel rich combustion, resulting in higher ppm readings.

9.2.1 Mechanical

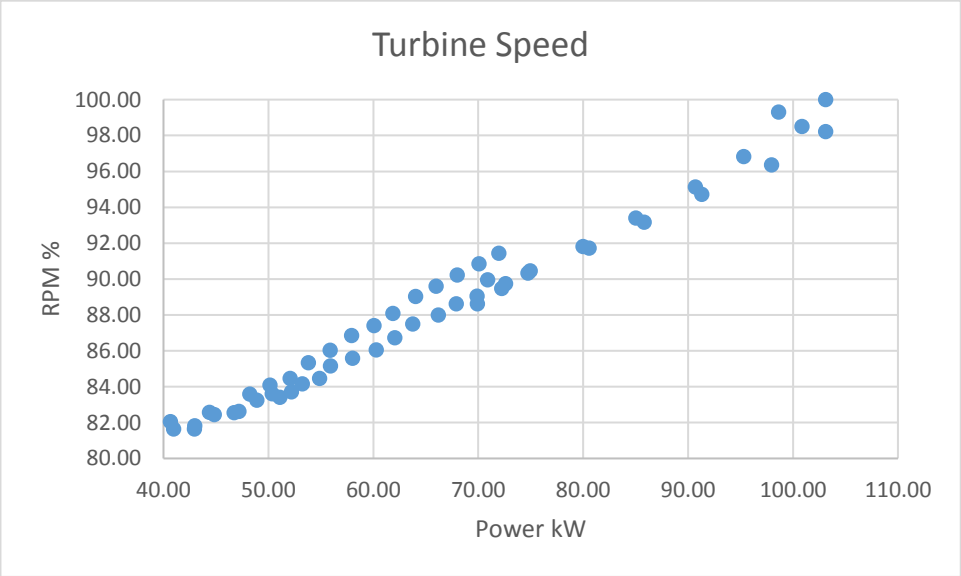

Figure 9-16 S3 Turbine speed and power output.

The lower turbine speed in Figure 9-16 S3 Turbine speed and power output.is on cooler ambient days, with the temperatures in the ranges 14.5°C – 15.5°C. The higher turbine speed results are from days where the ambient temperature was 17.5 – 19.5°C. This is not a huge difference, but results in the frequencies being 2% higher, equivalent to 1,400 rpm.

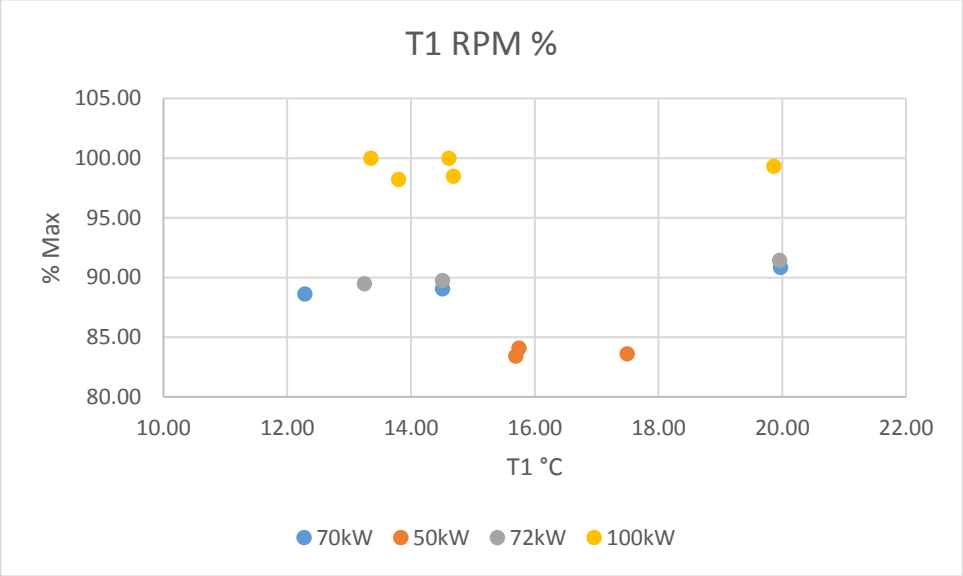

Figure 9-17 S3 turbine speed of 4 power outputs relationship to ambient temperature.

Again the Series 3, as the Series 1, performance is dominated by the ambient air temperature, due to the air density, and the corresponding compressor efficiency and hence turbine efficiency.

It is difficult to get a spectrum of result for the ambient temperature, due to the test day confinements and the natural variability of the ambient conditions, but plotted in Figure 9-17 S3 turbine speed of 4 power outputs relationship to ambient temperature. are a spectrum of results for 50, 70, 72, and 100kW. In the Figure 9-17 S3 turbine speed of 4 power outputs relationship to ambient temperature., the impact of the ambient temperature on the turbine speed, and

Figure 9-18 S3 turbine efficiency and ambient temperature relationshipthe impact this has on efficiency.

In the majority of cases investigated the turbine speed increases with the temperature of the ambient air, and in all cases but one (70kW 15°C) the efficiency is reduced by the ambient temperature increase. This strong trend relating to the efficiency may also be taking into account the improved efficiency gains from the air recuperation possible at the lower temperatures, in addition to the possible more efficient compression.

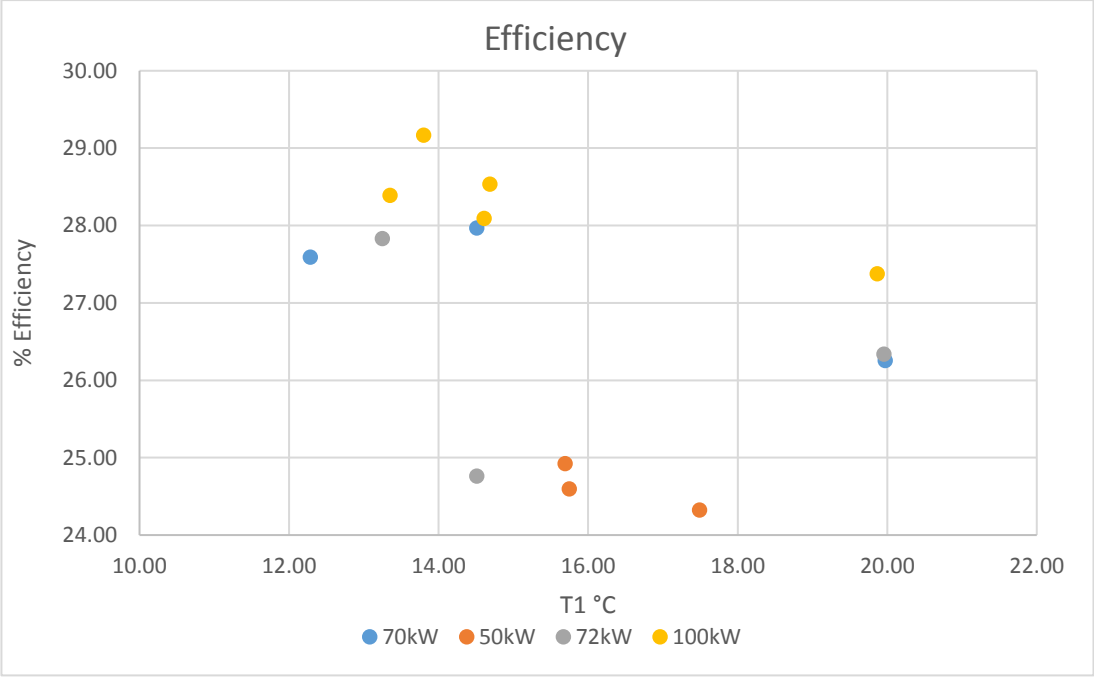

Figure 9-18 S3 turbine efficiency and ambient temperature relationship

9.2.2 Emissions

Interestingly the lower H_2O results in Figure 9-19 Power output and H2O emissionsoccur on hotter days, when the turbine runs less efficiently combusting more fuel, that would otherwise be expected to create more H_2O. This must be due to further dilution, as with other gas species emissions, from the higher RPM of the turbine.

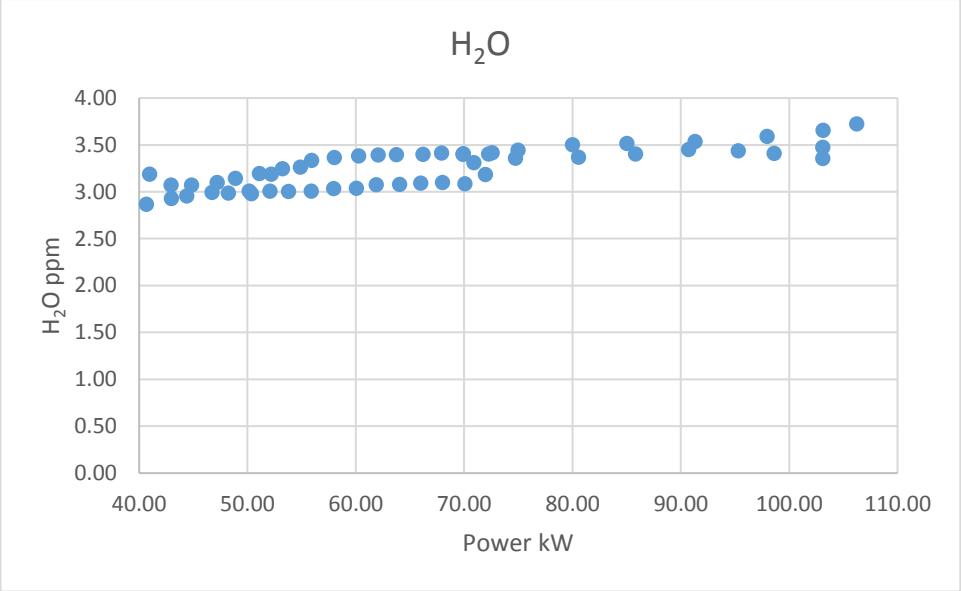

Figure 9-19 Power output and H_2O emissions.

As can be seen in the CO results of Figure 9-20 Power output and CO emissions, there is a split in the emissions patterns, and this split directly corresponds to two different test days.

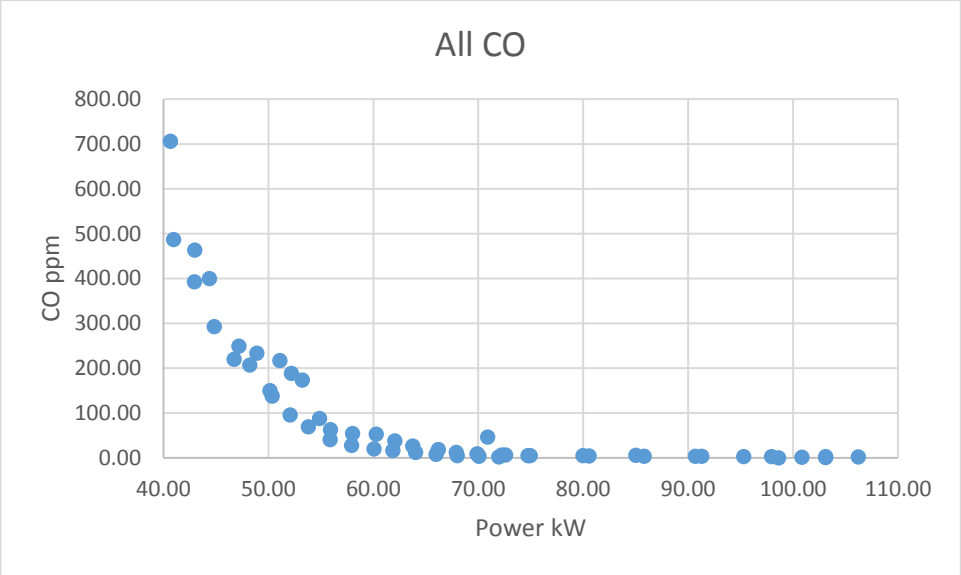

Figure 9-20 Power output and CO emissions.

As with the H_2O higher CO_2 volume % occurs on the hottest days, where increased fuel is combusted seen in Figure 9-21 S3 CO2 emissions.

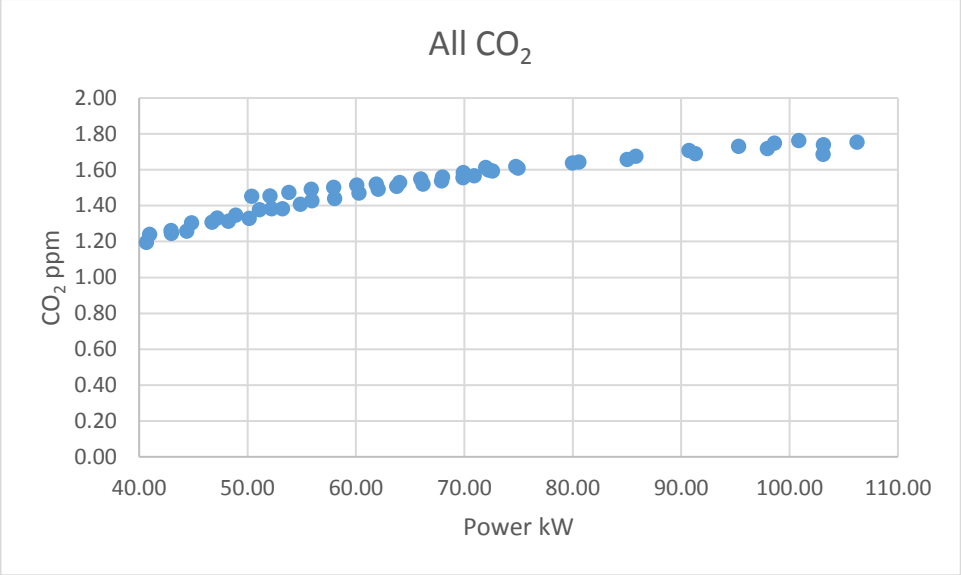

Figure 9-21 S3 CO_2 emissions.

The Series 3 produces a slightly different NO_x relationship than the S1. With the S1, both NO and NO_2 emissions follow a similar trend to each other. With the S3 it is notable that NO_2 is significantly higher at the bottom of the turn down ratio, and then the NO climbs at the higher end. This is due to the higher levels of excess air at the lower end, with the excess O_2 reacting with the NO to form NO_2, and then at higher powers a reduction in excess air, and O_2 relative to the fuel being combusted, and hence there is less opportunity for the NO to react and form NO.

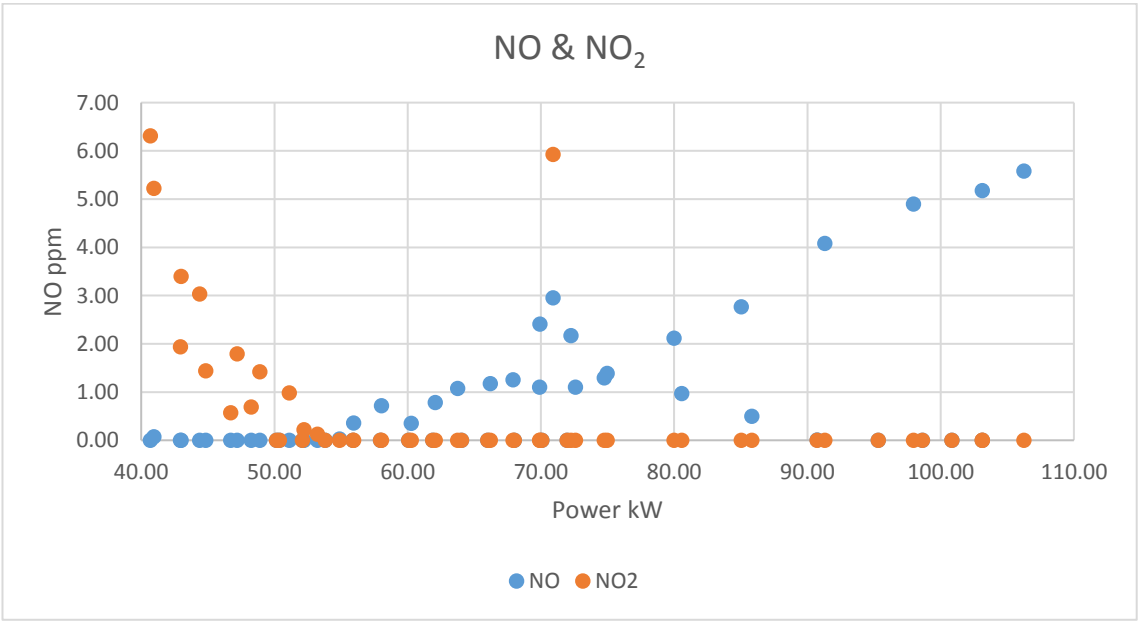

Figure 9-22 S3 NO & NO_2 emissions.

9.2.3 Efficiency

The Series 3 conversely to the Series 1, becomes more efficient after 70kW seen in Figure 9-23 S3 electrical efficiency. dipping after 100kW, and this is beyond what the turbine is rated for, but it can go over power.

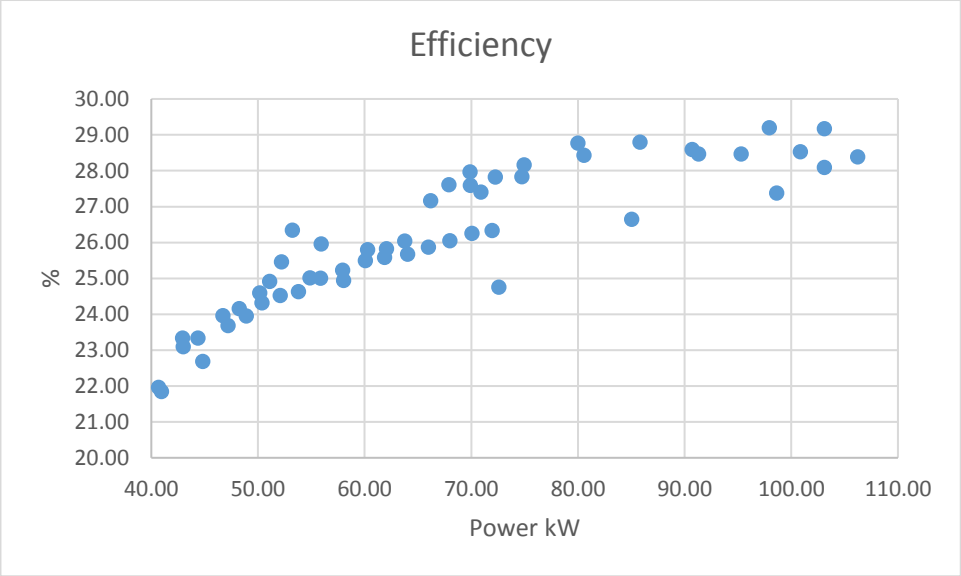

Figure 9-23 S3 electrical efficiency.

The engine speeds of both turbines is relatively similar seen in Figure 9-24 S1 & S3 average engine speed. This is not surprising as they are from the same manufacturer and series of turbine. The older series one consistently runs at a higher speed. This may be due to an inefficient compression, resulting in more work being required to achieve the pressure and mass

flow, or more likely when looking at the emissions species of the Series 3, the Series 1 runs a little more fuel lean than the Series 3.

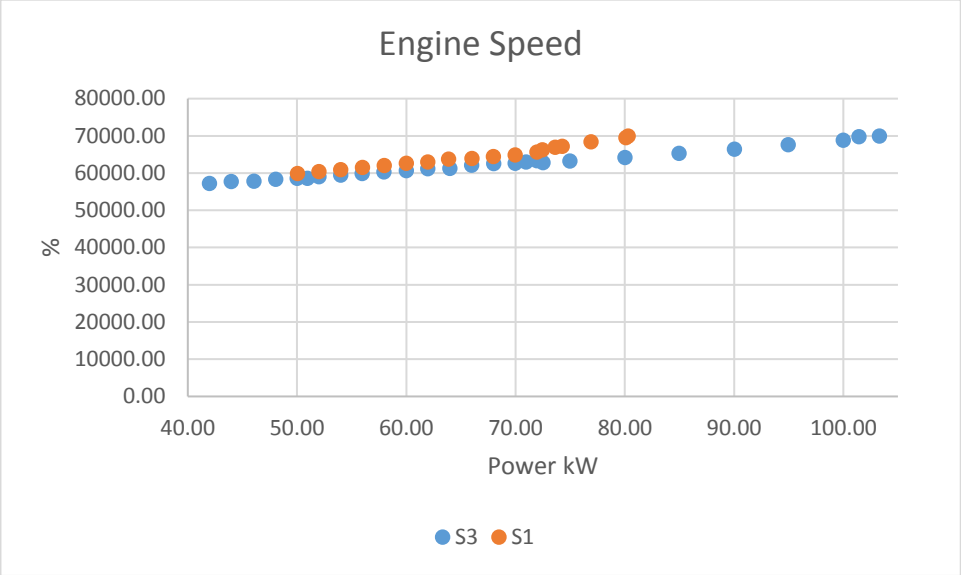

Figure 9-24 S1 & S3 average engine speed.

It is seen in Figure 9-25 S1 & S3 average efficiencyhe S3 is significantly more efficient than the older S1, the efficiency directly corresponds with the engine speed of the two turbines. This is further corroborated by the significant dip in efficiency from 72kW upwards, where the engine speed of the S1 takes a “step” increase.

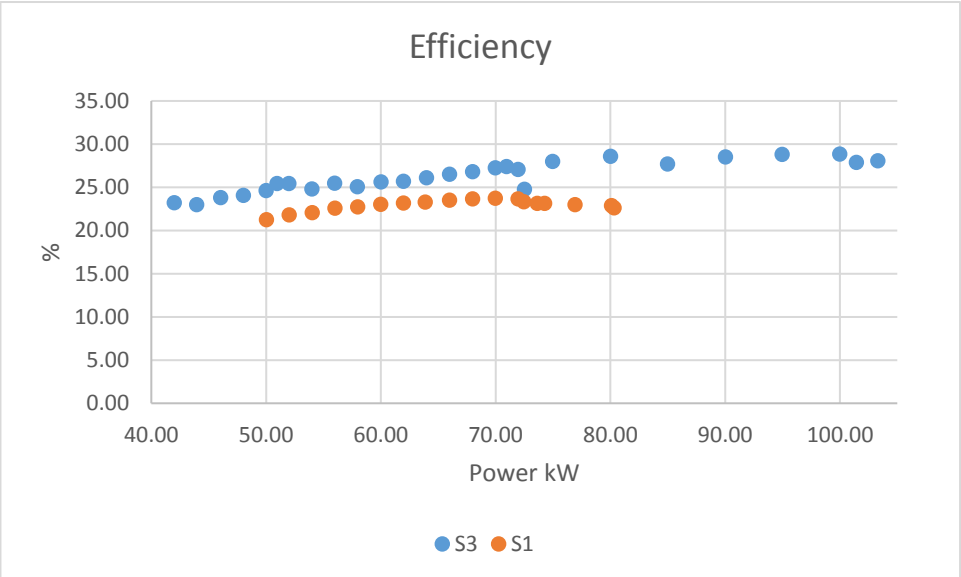

Figure 9-25 S1 & S3 average efficiency

The H_2O comes from the complete combustion of the natural gas. As expected in Figure 9-26 S1 & S3 average H2O. the Series 1 H_2O emissions are higher due to the higher fuel consumption. The SFC shows that the fuel consumption to be 15-20% higher than the S3(Figure 9-31 S1 & S3 average specific fuel consumption. All of these results are within these percentage differences, and actually lower at higher outputs. This indicates that the Series 3 runs more air lean than the Series 1, in fact the highest relative difference in fuel consumption occurs where the H_2O emissions of both turbines are in closest agreement.

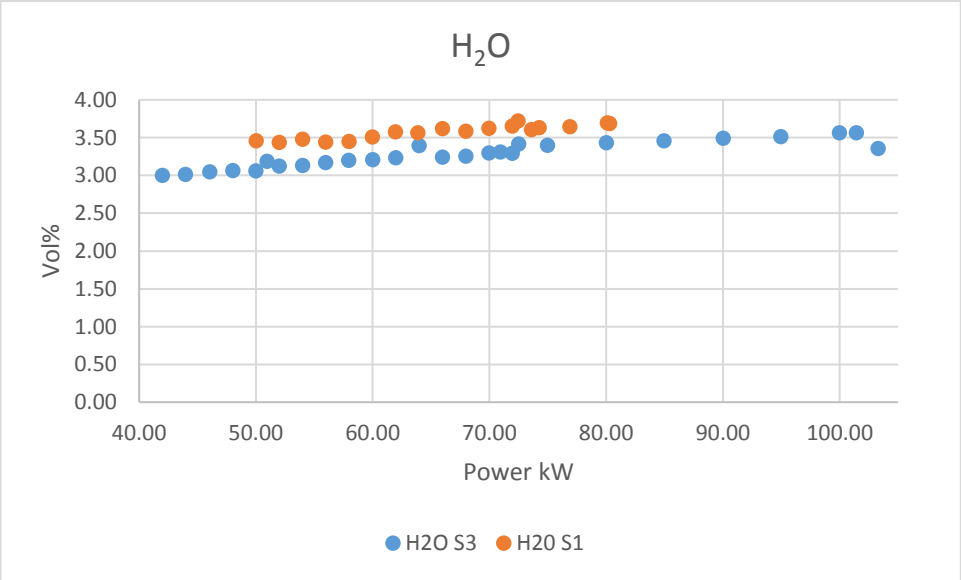

Figure 9-26 S1 & S3 average H_2O.

Both the gas turbines have similar CO_2 emissions levels, with Series 1 consistently higher than that of the Series 3 seen in Figure 9-27 S1 & S3 average CO2. However as the Series 1 runs more air rich and less efficiently by consuming more fuel, this means the Series 1 emissions per kilo watt hour are significantly higher.

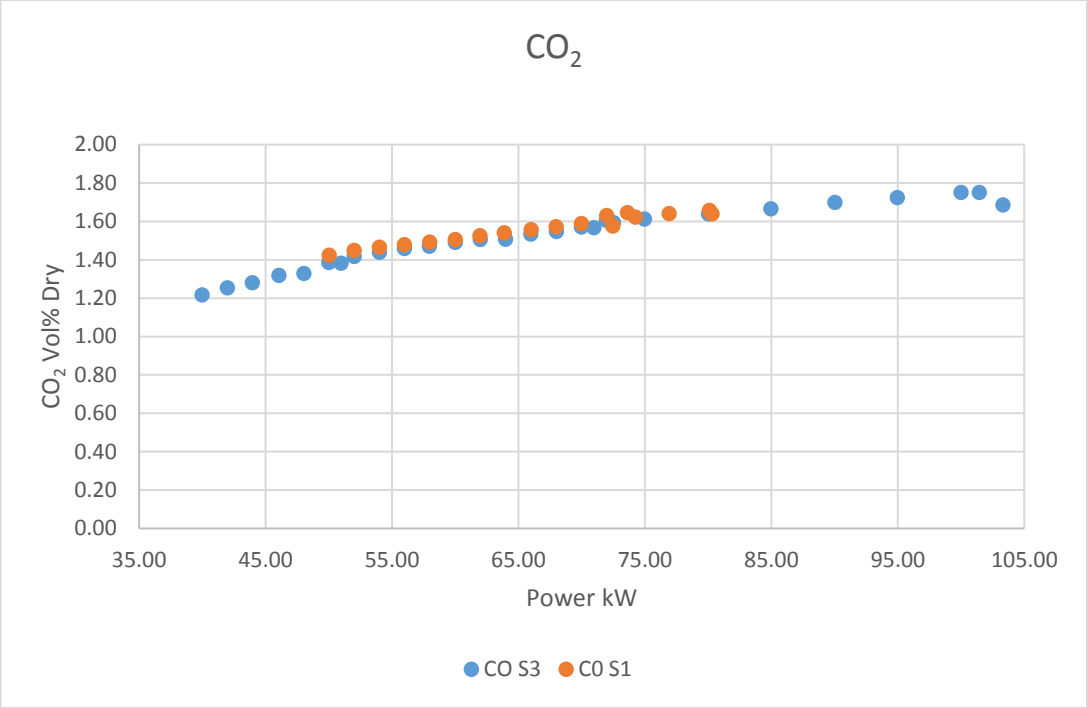

Figure 9-27 S1 & S3 average CO_2.

The carbon monoxide emissions of the Series 3 are consistently higher than those of the Series 1, and the methane emissions follow the same trend in Figure 9-28 S1 & S3 average CO & CH4.. As the readings are parts per million, and the Series 3 is running more air lean, this can be partially attributed to that. However the hugely high CO emissions at the bottom of the Series 3 turn down ratio represents more significant incomplete combustion occurring. This may be due to inadequate mixing, poor flame stability or speed, and insufficient pressure. The emissions do in fact exceed the LCPD for CO emissions of 100 mg/Nm^3, which the Series 1 does not, emissions performance may be why the Series 1 does not permit such low turn down ratios, although depending on the application, the LCPD may or may not be applicable, for example combusting waste or bio gas is exempt.

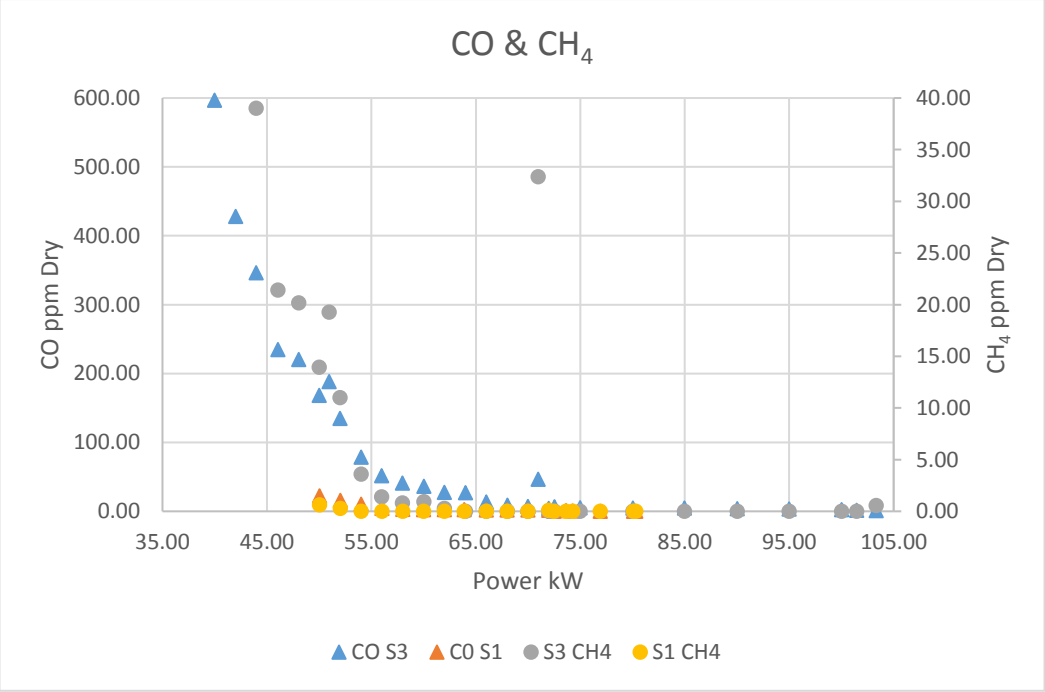

Figure 9-28 S1 & S3 average CO & CH_4.

The high NO_x of the Series 3 at the bottom of the turn down ratio visible in Figure 9-29 S1 & S3 Average NO & NO2 is probably indicative of why the Series 1 turndown range is more limited. With the NO_x emissions being a significant controlled pollutant that can cause acid rain, and smog which is harmful to the lungs. The higher NO_2 at the bottom of the turn down ratio, and the drop off in NO instead, is probably indicative of the more fuel lean conditions, and high levels of excess O_2 at the bottom of the turn down ratio, with O_2 reacting with NO to form NO_2.

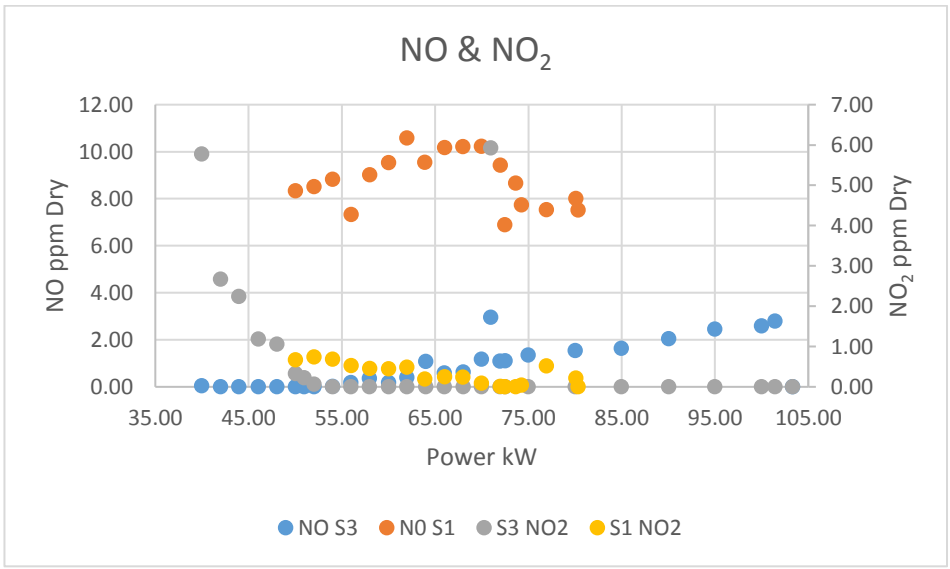

Figure 9-29 S1 & S3 Average NO & NO_2

The higher levels of NO and NO_2 generated by the Series 1 will be due to the increased volume of fuel combusted for each power output, and corresponding to higher flame temperatures. Although as a spike in NO_x is observed at the bottom of the Series 3 turn down ratio, this would probably have been much larger if the Series 1 could operate at the same 40kW – 50kW conditions.

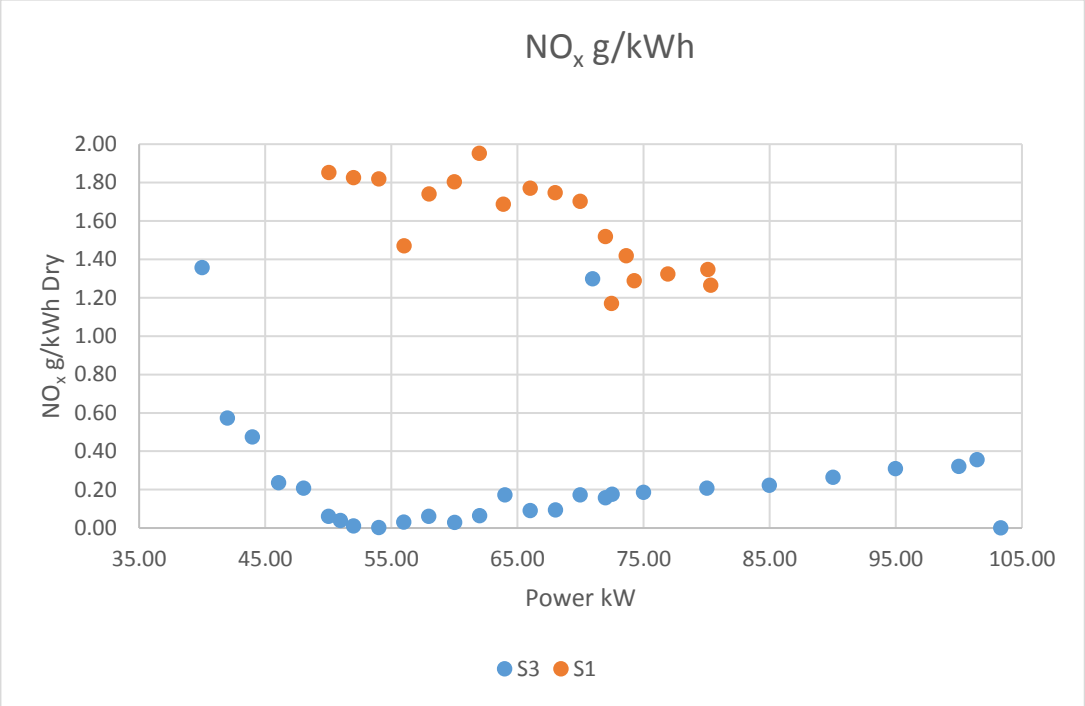

Figure 9-30 S1 & S3 Average NOx g/kWh.

The Figure 9-30 S1 & S3 Average NOx g/kWh.NO g/kWh mirrors the trend seen in the NO_x ppm, but is a better metric for comparison with experiments involving exhaust gas recirculation, or enhanced CO_2 experiments, than results corrected to 15% O_2, due to the altered oxidiser species composition.

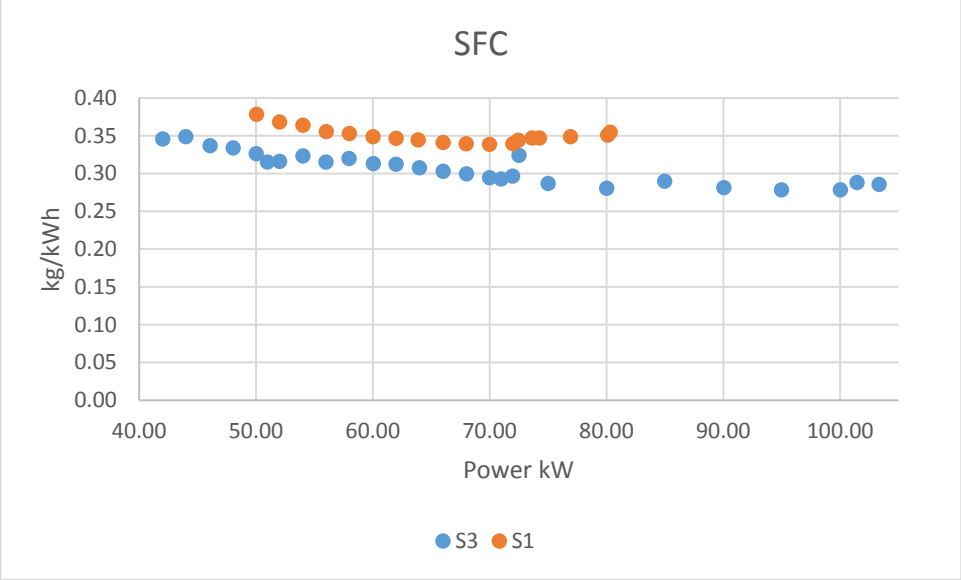

Figure 9-31 S1 & S3 average specific fuel consumption

The specific fuel combustion in Figure 9-31 S1 & S3 average specific fuel consumption is a more effectively depicts the differences in the two turbines relative efficiency, with the higher SFC indicating lower efficiency. In general the SFC of the series 1 is 15-20% higher than that of the Series 3, with the difference in efficiencies widening as the power output goes up. This is because the Series 1 is most efficient between 65kW and 70kW, while the Series 3, is more efficient between 90kW and 100kW, operating at almost full load.

9.3 Energy Intensity of Capture

The key issue with carbon capture from the gas turbines is the lower partial pressure of CO_2 and hence the energy intensity of capture is high. This makes the process inefficient, expensive, and hence uncompetitive.

With the baseline results for the Series 1 and 3 it can be seen that the carbon dioxide intensity is very low at 1.25 – 1.75% in Figure 9-32 All Turbine CO_2 Exhaust Vol%. This is significantly less than the Combined Cycle Gas Turbines which have exhaust emissions of 3-5%, which are already much less than for coal combustion, 10-15%, and this means that the capture will be inefficient.

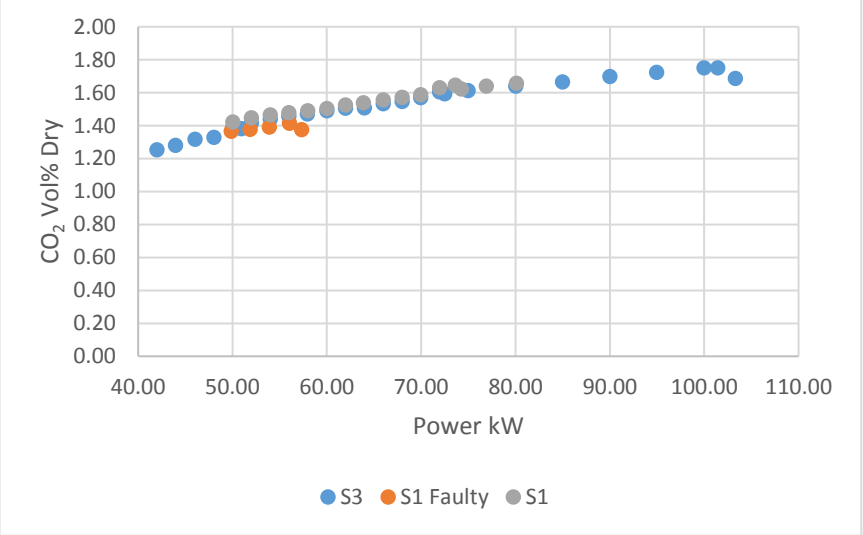

Figure 9-32 All Turbine CO_2 Exhaust Vol%

10 Bibliography

1. Best, T., et al., *Impact of CO2-enriched combustion air on micro-gas turbine performance for carbon capture.* Energy, 2016. **tbc**(Accepted Awaiting Publication date).
2. Best, T., et al., *Exhaust gas recirculation and selective Exhaust gas recirculation on a micro-gas turbine for enhanced CO2 Capture performance.* The Future of Gas Turbine Technology 8th International Gas Turbine Conference, 2016.
3. Agbonghae, E.O., et al., *Experimental and Process Modelling Study of Integration of a Micro-turbine with an Amine Plant.* Energy Procedia, 2014. **63**: p. 1064-1073.
4. Ali, U., et al., *Process Simulation and Thermodynamic Analysis of a Micro Turbine with Post-combustion CO2 Capture and Exhaust Gas Recirculation.* Energy Procedia, 2014. **63**: p. 986-996.
5. Akram, M., et al., *Performance evaluation of PACT Pilot-plant for CO2 capture from gas turbines with Exhaust Gas Recycle.* International Journal of Greenhouse Gas Control, 2016. **47**: p. 137-150.
6. Ali, U., et al., *Benchmarking of a micro gas turbine model integrated with post-combustion CO2 capture.* Energy, 2016. **Submitted In Review**.
7. Finney, K.N., et al., *CFD of Selective Exhaust Gas Recirculation On Micro-Gas Turbines For Enhanced CO2 Capture Performance* ASME, 2016. **Turbo Expo 2017**.
8. Solomon, S., D. Qin, M. Manning, and M.M. Z. Chen, K.B. Averyt, M.Tignor and H.L. Miller, *Summary for Policymakers. In: Climate Change 2007: The Physical Science Basis.* Contribution of Working Group I to the Fourth Assessment Report of the Intergovernmental Panel on Climate Change, 2007.
9. Administration, N.O.a.A., *Monthly Mean CO2 June 2016.* 2016.
10. Morice, C.P., et al., *Quantifying uncertainties in global and regional temperature change using an ensemble of observational estimates: The HadCRUT4 data set.* Journal of Geophysical Research: Atmospheres, 2012. **117**(D8): p. D08101.
11. Lenny Bernstein, P.B., Osvaldo Canziani, Zhenlin Chen, Renate Christ, Ogunlade Davidson, William Hare, Saleemul, et al., *Climate Change 2007: Synthesis Report.* IPCC 4th Report, 2007.
12. Organization, W.H., *Quantitative risk assessment of the effects of climate change on selected causes of death, 2030s and 2050s*. 2014: World Health Organization.
13. Stern, N., *The Stern Review on the Economic Effects of Climate Change.* Population and Development Review, 2006. **32**(4): p. 793-798.
14. DECC, *2012 UK Greenhouse Gas Emissions, Provisional Figures and 2011 UK Greenhouse gas emissions, Final Figures by Fuel Type and End-User.* 2013.
15. DECC, *2014 UK Greenhouse Gas Emissions, Final Figures.* 2016.
16. Richard Smith, D.R., Simon Durk, Edd Wilkinson, *Gone Green 2011.* National Grid, 2011.
17. Committee on Climate Change, *The Fourth Carbon Budget, Reducing emissions through the 2020s.* 2010.
18. NationalGrid, *Electricity Ten Year Statement 2015.* UK electricity transmission, 2015.
19. EC, *Industrial Emissions Directive.* 2016. **Chapter III**.
20. IEA, *CO2 Emissions From Fuel Combustion.* 2012.
21. UN, *United Nations Framework Convention on Climate Change.* 1998.
22. Parliament, A.o., *Climate Change Act 2008.* HM Stationary Office, 2008.
23. IEA, *World Energy Outlook 2012*. 2012: OECD Publishing.
24. IPCC, *Climate Change 2014 Synthesis Report Summary for Policymakers.* https://www.ipcc.ch/pdf/assessment-report/ar5/syr/AR5_SYR_FINAL_SPM.pdf, 2014.

25. Meinshausen, M., et al., *Greenhouse-gas emission targets for limiting global warming to 2[thinsp][deg]C.* Nature, 2009. **458**(7242): p. 1158-1162.
26. DECC, *The Carbon Plan: Delivering our low carbon future.* 2011.
27. Roadmap, U.R.E., *Department of Energy and Climate Change.* UK government, First published, 2011. **12**.
28. EEA, *Europe's onshore and offshore wind energy potential, An assessment of environmental and economic constraints.* Technical report 2009.
29. Boyle, G., *UK offshore wind potential: How offshore wind could supply a quarter of UK electricity by 2024.* Refocus, 2006. **7**(4): p. 26-29.
30. Allan, G., et al., *Levelised costs of Wave and Tidal energy in the UK: Cost competitiveness and the importance of "banded" Renewables Obligation Certificates.* Energy Policy, 2011. **39**(1): p. 23-39.
31. Vazquez, A. and G. Iglesias, *Capital costs in tidal stream energy projects – A spatial approach.* Energy, 2016. **107**: p. 215-226.
32. Carbon Tracker Initiative, *Unburnable Carbon - Are the world's financial markets carrying a carbon bubble? .* 2011.
33. SSE, *Carbon Capture and Storage Project Peterhead* http://www.sse.com/PressReleases2011/CCSPeterhead/, 2011.
34. Element Energy, *One North Sea, , The North Sea Basin Task Force.* 2010.
35. Arup, *Mid CO2 capture 2030, Feasibility Study for Europe-Wide CO2 Infrastructures.* European Commission Directate-General Energy, 2010.
36. Drax Group plc, *Inside Drax, Annual Report and accounts.* 2011.
37. White Rose Carbon Capture & Storage project, *About the White Rose CCS Project* http://www.whiteroseccs.co.uk/about-white-rose, 2013.
38. Nord, L.O., R. Anantharaman, and O. Bolland, *Design and off-design analyses of a pre-combustion CO< sub> 2</sub> capture process in a natural gas combined cycle power plant.* International Journal of Greenhouse Gas Control, 2009. **3**(4): p. 385-392.
39. Simpson, A.P. and A.J. Simon, *Second law comparison of oxy-fuel combustion and post-combustion carbon dioxide separation.* Energy Conversion and Management, 2007. **48**(11): p. 3034-3045.
40. Allam, R.J., *Improved oxygen production technologies.* Energy Procedia, 2009. **1**(1): p. 461-470.
41. Wang, M., et al., *Post-combustion CO2 capture with chemical absorption: A state-of-the-art review.* Chemical Engineering Research and Design, 2011. **89**(9): p. 1609-1624.
42. IEA, *Prospects for CO2 Capture and Storage*. 2004: OECD Publishing.
43. Robert Davidson, *Post combustion carbon capture from coal fired plants - solvent scrubbing.* IEA Clean Coal Centre, 2007(PF 07-07).
44. Kim, S., H. Shi, and J.Y. Lee, *CO2 absorption mechanism in amine solvents and enhancement of CO2 capture capability in blended amine solvent.* International Journal of Greenhouse Gas Control, 2016. **45**: p. 181-188.
45. Bougie, F. and M.C. Iliuta, *Stability of aqueous amine solutions to thermal and oxidative degradation in the absence and the presence of CO2.* International Journal of Greenhouse Gas Control, 2014. **29**: p. 16-21.
46. Liu, H., O.A. Namjoshi, and G.T. Rochelle, *Oxidative Degradation of Amine Solvents for CO2 Capture.* Energy Procedia, 2014. **63**: p. 1546-1557.
47. Davis, J. and G. Rochelle, *Thermal degradation of monoethanolamine at stripper conditions.* Energy Procedia, 2009. **1**(1): p. 327-333.
48. Boyce, M.P., *Gas turbine engineering handbook*. 2012: Access Online via Elsevier.
49. Brooks, F.J., *GE gas turbine performance characteristics.* GE Power Systems, GER-3567H, 2000. **10**(00).

50. Mitsubishi Heavy Industries, *D-series Engine Developed by MHI.* http://www.mhi.co.jp/en/products/expand/f_series_gas_turbine_development_03.html, 2013.
51. Matta, R., G. Mercer, and R. Tuthill, *Power Systems for the 21st Century-" H" Gas Turbine Combined-Cycles*. 2000: GE Power Systems.
52. Fukuizumi, Y., et al., *Application of H Gas Turbine design technology to increase thermal efficiency and output capability of the mitsubishi M701G2 gas turbine.* Journal of engineering for gas turbines and power, 2005. **127**(2): p. 369-374.
53. Kalyanaraman, K., *Breaking the efficiency barrier.* Turbomachinery International, 2009.
54. Li Hailong, et al., *Impacts of exhaust gas recirculation (EGR) on the natural gas combined cycle integrated with chemical absorption CO< sub> 2</sub> capture technology.* Energy Procedia, 2011. **4**: p. 1411-1418.
55. Li, H., et al., *Impacts of exhaust gas recirculation (EGR) on the natural gas combined cycle integrated with chemical absorption CO2 capture technology.* Energy Procedia, 2011. **4**: p. 1411-1418.
56. Li Hailong, M. Ditaranto, and D. Berstad, *Technologies for increasing CO2 concentration in exhaust gas from natural gas-fired power production with post-combustion, amine-based CO2 capture.* Energy, 2011. **36**(2): p. 1124-1133.
57. Lee, K., et al., *CO2 radiation heat loss effects on NOx emissions and combustion instabilities in lean premixed flames.* Fuel, 2013. **106**(0): p. 682-689.
58. Burbano, H.J., J. Pareja, and A.A. Amell, *Laminar burning velocities and flame stability analysis of H2/CO/air mixtures with dilution of N2 and CO2.* International Journal of Hydrogen Energy, 2011. **36**(4): p. 3232-3242.
59. Røkke, P.E. and J.E. Hustad, *Exhaust gas recirculation in gas turbines for reduction of CO2 emissions; combustion testing with focus on stability and emissions.* International Journal of Thermodynamics, 2010. **8**(4): p. 167-173.
60. ElKady, A.M., et al., *Application of Exhaust Gas Recirculation in a DLN F-Class Combustion System for Postcombustion Carbon Capture.* Journal of engineering for gas turbines and power, 2009. **131**(3): p. 034505.
61. ElKady, A.M., et al., *Application of exhaust gas recirculation in a DLN F-class combustion system for postcombustion carbon capture.* Journal of engineering for gas turbines and power, 2009. **131**(3).
62. Soares, C., *Microturbines: applications for distributed energy systems*. 2011: Butterworth-Heinemann.
63. Jonsson, M. and J. Yan, *Humidified gas turbines—a review of proposed and implemented cycles.* Energy, 2005. **30**(7): p. 1013-1078.
64. Horlock, J.H., *Heat exchanger performance with water injection (with relevance to evaporative gas turbine (EGT) cycles).* Energy Conversion and Management, 1998. **39**(16–18): p. 1621-1630.
65. Wan, K., et al., *Performance of humid air turbine with exhaust gas expanded to below ambient pressure based on microturbine.* Energy Conversion and Management, 2010. **51**(11): p. 2127-2133.
66. Day WH, K.D., Knight B, Bhargava A, Sowa W, Colket M, Casleton K, Maloney D, *HAT cycle technology development program.* Advanced Turbine Systems Annual Program Review Meeting, 1999.
67. Rao, A.D. and W.H. Day, *Mitigation of greenhouse gases from gas turbine power plants.* Energy Conversion and Management, 1996. **37**(6–8): p. 909-914.
68. De Paepe, W., et al., *Steam injection experiments in a microturbine – A thermodynamic performance analysis.* Applied Energy, 2012. **97**: p. 569-576.
69. De Paepe, W., et al., *Experimental Characterization of a T100 Micro Gas Turbine Converted to Full Humid Air Operation.* Energy Procedia, 2014. **61**: p. 2083-2088.

70. Mansouri Majoumerd, M., et al., *Micro gas turbine configurations with carbon capture – Performance assessment using a validated thermodynamic model.* Applied Thermal Engineering, 2014. **73**(1): p. 172-184.
71. CO2 Europipe, *Towards a transport infrastructure for large-scale CCS in Europe* 2011.
72. ZEP, *The Costs of CO2 Transport.* ETP, Zero Emissions Platform, 2011.
73. AQEG, *Particulate Matter in the United Kingdom: Summary.* Defra, 2005.
74. Upadhyay, D., et al., *Particulate Matter Induces Alveolar Epithelial Cell DNA Damage and Apoptosis.* American Journal of Respiratory Cell and Molecular Biology, 2003. **29**(2): p. 180-187.
75. Brewer, E., et al., *PM2.5 and ultrafine particulate matter emissions from natural gas-fired turbine for power generation.* Atmospheric Environment, 2016. **131**: p. 141-149.
76. Shilo, M., et al., *The effect of nanoparticle size on the probability to cross the blood-brain barrier: an in-vitro endothelial cell model.* Journal of Nanobiotechnology, 2015. **13**(1): p. 1-7.
77. Ranft, U., et al., *Long-term exposure to traffic-related particulate matter impairs cognitive function in the elderly.* Environmental Research, 2009. **109**(8): p. 1004-1011.
78. González, C.M. and B.H. Aristizábal, *Acid rain and particulate matter dynamics in a mid-sized Andean city: The effect of rain intensity on ion scavenging.* Atmospheric Environment, 2012. **60**: p. 164-171.
79. Kumar, P., et al., *Pseudo-simultaneous measurements for the vertical variation of coarse, fine and ultrafine particles in an urban street canyon.* Atmospheric Environment, 2008. **42**(18): p. 4304-4319.
80. S. Cernuschi, S.C.a.M.G., *Emissions of Fine and Ultrafine Particles from stationary combustion plants.* Final Summary, 2010.
81. Ozgen, S., et al., *Ultrafine particle emissions for municipal waste-to-energy plants and residential heating boilers.* Reviews in Environmental Science and Bio/Technology, 2012. **11**(4): p. 407-415.
82. Minutolo, P., et al., *Ultrafine particle emission from combustion devices burning natural gas.* Chem Eng Trans, 2010. **22**: p. 239-244.
83. D'Anna, A., *Combustion-formed nanoparticles.* Proceedings of the Combustion Institute, 2009. **32**(1): p. 593-613.
84. Ristovski, Z.D., et al., *PARTICLE EMISSIONS FROM COMPRESSED NATURAL GAS ENGINES.* Journal of Aerosol Science, 2000. **31**(4): p. 403-413.
85. Moretti, A.L., C.S. Jones, and P.-G. Asia, *Advanced Emissions Control Technologies for Coal-Fired Power Plants.* Technical Paper BR-1886). Presented to Power-Gen Asia, 2012.
86. Saxena, S.C., R.F. Henry, and W.F. Podolski, *Particulate removal from high-temperature, high-pressure combustion gases.* Progress in Energy and Combustion Science, 1985. **11**(3): p. 193-251.
87. De Paepe, W., et al., *Discussion of the effects of recirculating exhaust air on performance and efficiency of a typical microturbine.* Energy, 2012. **45**(1): p. 456-463.
88. EC, *Large Combustion Plants Directive.* 2001. **http://www.defra.gov.uk/industrial-emissions/eu-international/lcpd/**.
89. Amec, *Greater London Authority Air Quality Support.* Biomass and CHP Emission Standards https://www.london.gov.uk/sites/default/files/old_oak_and_park_royal_air_quality_report_draft_final_issued_new_cover.pdf, 2013.
90. Turbec, *Technical Description T100 Natural Gas.* 2009(3): p. 17.
91. Horlock, J.H., *Chapter 3 - BASIC GAS TURBINE CYCLES*, in *Advanced Gas Turbine Cycles*. 2003, Pergamon: Oxford. p. 27-46.

92. Ibrahim, T.K. and M. Rahman, *Effect of compression ratio on performance of combined cycle gas turbine.* International journal of energy engineering, 2012. **2**(1): p. 9-14.
93. Evulet, A.T., et al., *On the Performance and Operability of GE's Dry Low NOx Combustors utilizing Exhaust Gas Recirculation for PostCombustion Carbon Capture.* Energy Procedia, 2009. **1**(1): p. 3809-3816.
94. Milner, J.T., H.M. ApSimon, and B. Croxford, *Spatial variation of CO concentrations within an office building and outdoor influences.* Atmospheric Environment, 2006. **40**(33): p. 6338-6348.
95. Tian, L., et al., *Carbon monoxide and stroke: A time series study of ambient air pollution and emergency hospitalizations.* International Journal of Cardiology, 2015. **201**: p. 4-9.
96. Muhammad Akram, S.B., Mohamed Pourkashanian, *Influence of gas turbine exhaust CO2 concentration on the performance of post combustion carbon capture plant.* Proceedings of ASME Turbo Expo 2015: Turbine Technical Conference and Exposition, 2015. **GT2015-42454**.
97. Taimoor, A.A., et al., *Humidified exhaust recirculation for efficient combined cycle gas turbines.* Energy, 2016. **106**: p. 356-366.
98. Nikpey, H., et al., *Experimental evaluation and ANN modeling of a recuperative micro gas turbine burning mixtures of natural gas and biogas.* Applied Energy, 2014. **117**(0): p. 30-41.
99. AkramM, A.U.a., Best T, Blakey S, FinneyK.N, PourkashanianM, *Performance evaluation of PACT Pilot-plant for Carbon capture from gas turbines with Exhaust Gas Recycle.* 2015.
100. BSI, *Gas Turbines - Acceptance tests ISO 2314.* BSI Group, 2010.
101. Harvey, A.H., A.P. Peskin, and S.A. Klein, *NIST/ASME steam properties.* NIST Standard Reference Database, 2000. **10**.
102. Schallert, B., et al., *Accumulation of Absorbed Fly Ash Particulate Matter and its Impact on the CC Process.* Energy Procedia, 2016. **86**: p. 150-159.
103. Schallert, B., S. Neuhaus, and C.J. Satterley, *Do we underestimate the impact of particles in coal-derived flue gas on amine-based CO2 capture processes?* Energy Procedia, 2013. **37**: p. 817-825.
104. Koornneef, J., et al., *The impact of CO2 capture in the power and heat sector on the emission of SO2, NOx, particulate matter, volatile organic compounds and NH3 in the European Union.* Atmospheric Environment, 2010. **44**(11): p. 1369-1385.
105. Cambustion, *Particulate Mass Measurement with DMS Series Fast Spectrometers.* Cambustion Application Note (DMS01).
106. Cambustion, *Gasoline Direct Injection Particulate Measurement with the DMS Series.* Cambustion Application Note. **DMS08**.
107. Cambustion, *DMS500 User Manual.* 2015.
108. Cambustion, *Diesel Particulate Filter Measurement with the DMS500.* **DMS05**.